Finn Bjarne Jost

Quantum Field Theoretic and Combinatorial Perspectives on Intersection Numbers on the Moduli Space of Complex Curves

2024

Mathematics

Quantum Field Theoretic and Combinatorial Perspectives on Intersection Numbers on the Moduli Space of Complex Curves:

Explicit calculations in the Quartic Kontsevich Model & logarithmic concavity

Inaugural Dissertation
for the award of a doctoral degree

doctor rerum naturalium

in the field of Mathematics and Computer Science
from the Faculty of Mathematics and Natural Sciences
of the University of Münster

submitted by
Finn Bjarne Jost (né Kohl)

- 2024 -

Dean: Prof. Dr. Arthur Bartels
First assessor: Prof. Dr. Raimar Wulkenhaar
Second assessor: Prof. Dr. Jörg Schürmann
Date of oral examination: 10 December 2024
Date of graduation: 10 December 2024

First, I want to thank Professor Raimar Wulkenhaar for his supervision throughout the course of my PhD. Your effort, support through your openness and approachable attitude as well as your insights have been essential to develop this work. Thank goes also to Professor Jörg Schürmann for his impulses as well as reviewing my thesis as second committee member. Being part of the research training group "Strong and Weak Interactions - from Hadrons to Dark Matter" I am grateful to Professor Kai Schmitz for the valuable scientific interaction about cosmological phenomena as well as discussion of professional issues. I want to extend my gratitude to the members of the geometry, algebra and topology seminar on the "Moduli spaces of complex curves" for a broad and accentuated perspective on different topics within this field of research and the possibility to present my own work. Here, special thanks go to Adam Afandi for the introduction to the topic of Ehrhart theory of intersection numbers on the moduli space of curves and stimulating cunversations. Together with Katharina Harengel and Johannes Branahl, you made the past years a complete experience.

My deepest regards go to my entire family for their support and appreciation during my studies that led me to where I am today. To my sister and especially my parents for their encouragement and commitment in not only my intellectual journey but also for their love and support on all levels. You enabled me to realize this.

This thesis is dedicated to my wife, Finia Penelope Jost.
Your constant and absolute support as well as understanding and loving appreciation are what have made not only this work possible, but my life abundant and complete.

Outline

The moduli space of complex curves, or Riemann surfaces, is endowed with a recursive structure, which has been extensively used in the investigation of the moduli space since its construction in the previous century. Algebro-geometric invariants of this moduli space, which are called intersection numbers, are related correlation functions of matrix models. In this thesis the Quartic Kontsevich Model as well as the LSZ model act as two examples for this. The origin of both matrix models, which in a particular limit are related to quantum field theoretic investigations, can be traced back to the quest of finding a unified physical theory of our universe by constructing a non-trivial interacting model on non-commutative space. It is, however, in the truncated matrix models, where most algebraic structures are evident. These are studied here applying the universal framework of topological recursion to explicitly compute expressions for the correlators of low topological type in terms of intersection numbers on the moduli space of curves. While the LSZ model, a matrix model of complex matrices, can be treated within the original topological recursion, its hermitian counterpart, the Quartic Kontsevich Model requires a generalization to what is called blobbed topological recursion due to its more involved loop equations. The additional data of this framework is provided for the correlators of the Quartic Kontsevich Model for low topological type. These explicit results are set to supply future research towards an understanding of the integrable structure of the Quartic Kontsevich Model (in the sense of the Japanese school) with useful data.
This integrable structure is a consequence of the deep recursive nature of the investigated models. It is, prominently, also shared by the Kontsevich model itself, the cubic analogue of the model studied here, which encodes the intersection numbers on the moduli space. In order to provide a different perspective on this, a relation between intersection numbers and a combinatorial approach to the lattice-point count in polytopes called Ehrhart theory is studied. A restricted setting allows to approach the natural question of the significance of those polytopes corresponding to intersection number. By determining explicit data in the setting of Ehrhart theory this class of polytopes is characterized. Beyond the fact that this data has an interpretation in terms of a specific type of partitions, called order-consecutive partition sequences, in that process interesting patterns are observed. In particular logarithmic concavity is proved for the expansion data by different techniques, which reflect the significant and profound structure of the moduli space of curves.

Der Modulraum komplexer Kurven, beziehungsweise Riemannscher Flächen, weist eine rekursive Struktur auf, welche in der Untersuchung dieses Modulraums weitreichend genutzt wurde. In dieser Thesis werden algebraisch-geometrische Invarianten,

welche aus dem Englischen intersection numbers oder auch Schnittzahlen genannt werden, mit dem quartischen Kontsevich-Modell sowie dem LSZ-Modell in Verbindung gesetzt. Der Ursprung beider Matrixmodelle, welche in einem speziellen Grenzwert quantenfeldtheoretisch betrachtet werden können, sind zumindest bis zu der Suche nach einer vereinheitlichten physikalischen Theorie unseres Universums zurückzuverfolgen, da beide als nicht-triviale, welchselwirkende Modelle auf nicht-kommutativem Raum konstruiert sind. Da die algebraischen Strukturen jedoch in dem Matrixmodell, nicht in dem angesprochenen Grenzprozess, zu beobachten sind, wird hier ersteres untersucht. Mithilfe des universellen Prinzips der Topologischen Rekursion werden explizite Ausdrücke für Korrelationsfunktionen niedrigen topologischen Typs gefunden, welche deren Abhängigkeit zu den Schnittzahlen beschreiben. Während das LSZ Modell, welches ein Matrixmodell komplexer Matrizen ist, im Rahmen der ursprünglichen Topologischen Rekursion betrachtet werden kann, erfordert dessen hermitesches Analogon, das quartische Kontsevich-Modell, aufgrund der komplizierteren Schleifengleichungen eine Verallgemeinerung, welche im Englischen blobbed topological recursion genannt wird. Die zusätzlichen Informationen dieser allgemeineren Formulierung werden für Korrelationsfunktionen niedrigen topologischen Typs explizit im quartischen Kontsevich-Modell hergeleitet und bereitgestellt. Damit kann zukünftige Forschung bezüglich der integrierbaren Struktur des quartischen Kontsevich-Modells (im Sinne der japanischen Schule) auf einem fundierten Verständnis der Verbindung zu Schnittzahlen aufbauen.
Auch dieser zu untersuchenden integrierbaren Struktur liegt die rekursive Natur der untersuchten Systeme zugrunde. Diese wird auch durch das kubische Analogon, das Kontsevich-Modell, geteilt, welches die Schnittzahlen des Modulraums kodiert. Eine weitere Perspektive darauf stellt eine Beziehung zwischen Schnittzahlen des Modulraums und der Ehrhart-Theorie aus der Kombinatorik dar, welche die Zählung von Gitterpunkten in Polytopen beschreibt. In einem eingeschränkten Rahmen können hier natürliche Fragen bezüglich der Bedeutung und Darstellung von den zu Schnittzahlen korrespondierenden Polytopklassen angegangen werden, indem explizite Daten ermittelt werden um, diese zu charakterisieren. Dabei wird nicht nur eine Interpretation der Daten durch einen speziellen Typ von Partitionen gefunden, welche konsekutiv geordnete Partitionsfolgen genannt werden, sondern auch interessante Muster wie logarithmische Konkavität beobachtet. Diese Eigenschaft der Ehrhart-theoretischen Daten, welche auf verschiedene Art und Weisen bewiesen wird, spiegelt die signifikanten und tiefgreifenden Strukturen des Modulraums der Riemannschen Flächen wider.

Introduction

Investigation of natural phenomena has been a human pursuit as it is inherent in evolutionary processes themselves. Documented in texts since antiquity the acquirement of knowledge rested on the element of experimentation through ways of observation, trial and error and reasoning via analogies. Although this can in some sense be regarded an antecedent of the modern experimental quest, the reasoning in ancient text, for which Aristotelian works are pivotal examples, relied rather on philosophical inference than on rigorous data-backed conclusions.

In these days, mathematical considerations mostly arose due to physical problems that were of original interest as opposed to the present when mathematics developed into a discipline of its own interest with a plethora of subfields.

This development can be traced back to the scientific revolution, which had its beginning in the 15th and 16th century, where mathematics became a decisive part of scientific, primarily physical, studies. In various texts authors ascribed different roles to mathematics in scientific inquiry. The plethora of these scholars ranges from Francis Bacon who laid down fundamental ideas developing the scientific method to Galileo Galilei who perceived mathematics as an inherent feature of the universe.

Through various works Bacon, [Bac11], put forward an agenda of scientific method through instrumentation and data collection heralding the beginnings of the scientific revolution. He put forth the idea that† [Bac20]

> « *everything to do with natural phenomena [. . .] should [. . .] be set down, counted, weighed, measured and defined. For we are after works, not speculations, and, indeed, a good marriage of Physics with Mathematics begets practice* »

and further explained the role of *mixed mathematics*, which in the present day might be opposed to pure mathematics, that‡ [Bac05, Bac23]

> « *[it] has for its subject some axioms and parts of natural philosophy, and considers quantity in so far as it assists to explain, demonstrate and actuate these.* »

†from the original « *Illud insuper præcipimus, ut omnia in naturalibus tam corporibus quam virtutibus (quantum fieri potest) numerata, appensa, dimensa, determinata proponantur. Opera enim meditamur, non speculationes. Physica autem et mathematica bene commistægenerant practicam.* » [Bac20]

‡from the English original « *Mixed hath for subject some axioms or parts of natural philosophy, and considereth quantity determined, as it is auxiliary and incident unto them* », [Bac05] or the later Latin version « *Mixta habet pro subjecto Axiomata et portiones physicas; Quantitatem autem considerat, quatenus est ad ea elucidanda et demonstranda et actuanda auxiliaris.* » [Bac23]

In these passages Bacon postulates mathematics as a method for data analysis and interpretation in science, which must be a supplementary but vital part of scientific research. Galileo's perception of the role of mathematics in science reached even further documented in his famous lines[‡] [Dra57, Gal23]

> « *[Science] is written in this grand book – I mean the universe – which stands continually open to our gaze, but it cannot be understood unless one first learns to comprehend the language and interpret the characters in which it is written. It is written in the language of mathematics, and its characters are triangles, circles, and other geometrical figures, without which it is humanly impossible to understand a single word of it; without these, one is wandering around in a dark labyrinth.* »

This passage from *Il Saggiatore*, 1623, describes the nature of mathematics as a language which is not only a convenient tool to describe the universe we live in but referring to it as its intrinsic characteristic.
Today it is obvious that the mathematical description of the world we live in massively facilitates the predictive properties of physics. In that, mathematics acts as a language, being an assignment of meaning to symbols abstracting the world and our thoughts. One that provides appropriate semantics to capture and – in great parts – consistently conceptualize the information gathered through (extended) perception in the observable universe. The consistency of our perception, which is reflected in the mathematical description through abstraction, is not just a curious and fortunate coincidence but rather is due to its formation in an evolutionary process. This illustrates the anthropic principle, as human perception has evolved in a realm of the universe in which it navigates. The mathematical abstraction that we, as humans, use to formulate physical theories can in this sense be seen to be a, not necessarily fated, but direct consequence of the observable universe via the anthropic principle. In this context Galileo's claim pushes even further by describing math as an inevitable constitutional element of the universe.

The quest of abstraction as well as unification, which oftentimes go hand in hand, are inherent features of science as described before. In the modern history of physical theory this can be seen when Isaac Newton used the development of calculus to provide a unified description of gravitation at scales available to observation at that time. Similar in spirit was Paul Dirac when he developed a special relativistic equation for quantum particles rediscovering matrices that were first investigated by William Clifford about half a century earlier. Or Albert Einstein when he built his theory of gravity unifying electromagnetism with gravitation with methods from differential geometry. At

[‡]from the Italian original « *La filosofia è scritta in questo grandissimo libro che continuamente ci sta aperto innanzi a gli occhi (io dico l'universo), ma non si può intendere se prima non s'impara a intender la lingua, e conoscer i caratteri, ne' quali è scritto. Egli è scritto in lingua matematica, e i caratteri son triangoli, cerchi, ed altre figure geometriche, senza i quali mezi è impossibile a intenderne umanamente parola; senza questi è un aggirarsi vanamente per un oscuro laberinto.* » [Gal23]

the present day this quest has a representation in the search of a unified description of quantum and gravitational effects by finding a theory of quantum field theory and general relativity. The various approaches that have been proposed, which not yet have had conclusive success, have in turn stirred far-reaching activities in various areas of mathematics realizing a fruitful interaction of the two disciplines.

The problem of incorporating gravity into a quantum field theoretic model of the universe can be approached at different levels of generality. On the one hand, separating the quantum and gravitational effects one discusses quantum field theoretic objects on an external background, that is described by classical, that is non-quantum, gravity. Here the non-interacting, that is free, field has a satisfying solution. However, once this point in the space of theories is left, there are no constructions of consistent theories tieing to the issue of renormalization. This is exemplified by the proof of triviality of the toy model of quartic scalar fields in four dimensions by Aizenman [Aiz81, AD21]. This shows that one clearly needs to depart from this standard setting to avoid inconsistencies in the interacting theory. On the other hand, as alluded to above, a true theory of quantum gravity that provides a consistent description of gravity and the quantum realm in full generality is right now not available. Future inspirations in the art of mathematics and the curiosity to investigate the physical universe that stir creativity might lead to a yet unwritten theory that achieves this.
At an intermediate level, one might investigate the influence of quantum field theoretical objects on classical gravity via the stress-energy tensor. Described by Heisenberg's relation prescribing the boundedness of the product $\Delta x \Delta p$ from below the measurement uncertainties in position and momentum space in quantum mechanics are correlated introducing a non-commutative structure in the phase-space of quantum mechanics. Equating the momentum uncertainty to one in mass this in turn is responsible for an uncertainty in the Schwarzschild radius of the object that is considered. Thus, the metric is effected by quantum mechanical effects introducing a minimal length which quantum fields can be localised on and thereby a non-commutative structure on space itself. This is related to short-distance singularities in quantum field theories and ultimately to the fact that on small scales geometry might lose its classical meaning, an idea that already Bernhard Riemann speculated about [Rie68]. By consistently handling this issue one constructs a quantum field theory on non-commutative backgrounds resting on the framework of non-commutative geometry [Con94, Con95, Con96]. There have been waves of attention to this subject since the mid of the past century producing literature that ranges from foundational work, renormalizability concerns to connections to string theory amongst others, which will not be discussed here. The interested reader is referred to one of various reviews emphasizing different subjects such as [Sza03, Wul06, Riv07, Wul19].

In this thesis a special limit of one example for a toy model of such a quantum

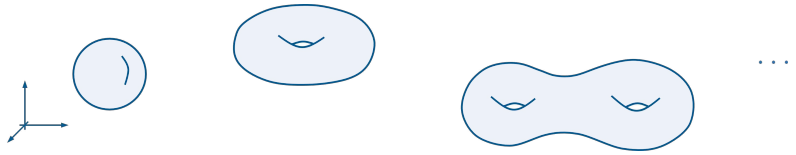

Figure 1: This illustrates Riemann surfaces of increasing genus in $\mathbb{R}^3$.

field theory on non-commutative space is investigated[4] with respect to mathematical structures that it exhibits. Incidentally, in this limit the nature of a quantum field theory is lost and what is studied is a truncated matrix model, while the investigation can still give valuable insights that might apply in the broader context. The gain of this is a wealth of algebraic structure that is, amongst others, related to the moduli space of curves. This entity, which can be seen as the parameter space of a class of surfaces in three-dimensional space that are named Riemann surfaces in honor of Bernhard Riemann, is a classical subject of studies since the past century and can even be traced back at least to Riemann himself [Rie57].

The pursuit of abstraction and generality in mathematics oftentimes leads to programs of classification. A topological classification of Riemann surfaces that is illustrated in Figure 1 is achieved by the integers enumerating what is called the genus. A closer examination of the nature of the space of Riemann surfaces shows that beyond the topological there is a vast range of structures to be discovered by means of complex-analytic, algebro-geometric or combinatorial methods. These lead to the construction of the moduli spaces of Riemann surfaces of fixed genus $\mathcal{M}_g$. A key step in its investigation was the realization that $\mathcal{M}_g$, in fact, has non-trivial boundary. In their seminal work Pierre Deligne and David Mumford and later Finn Knudsen [DM69, Knu83] constructed a compactification $\overline{\mathcal{M}}_g$ of the moduli space of Riemann surfaces as what is today called a Deligne-Mumford stack that allowed for a plethora of new insights. Amongst others, cohomological methods were used to identify invariants of $\overline{\mathcal{M}}_g$. These include intersection numbers of cohomological classes, which are central to this thesis. Intersection numbers are a fascinating object of studies for decades. One crucial property is their recursive structure which is inherited from the boundary of the elements of the collection $\{\overline{\mathcal{M}}_g\}_g$. This structure, which is known by the name of Virasoro constraints can be phrased in terms of a system, or hierarchy, of differential equations, which relate them to the field of partial differential equations as well as matrix models. This remarkable connection was famously first conjectured by Edward Witten [Wit90] and then proved by Maxim Kontsevich [Kon92]. It was later discovered to be an instance of a deep universal framework called topological recursion [CEO06, EO07, Eyn11b, Eyn16], which governs a wide range of problems in different areas of mathematics. As the field of topological recursion, since its initiation by Bertrand Eynard and collaborators more

[4] One can approach the model from various other, certainly more mathematical, directions than the physical approach sketched here. This owes to the author of this thesis deciding to choose that one which is the most natural due to the educational background of the author.

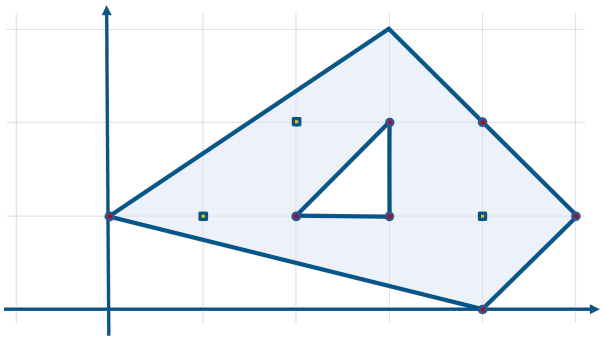

Figure 2: This shows a polygon in $\mathbb{R}^2$. It has area 7 (shaded blue), which can either be deduced classically or by Pick's theorem from the count of its internal (yellow) and half the boundary points (red) as well the number of connected components of its complement minus two.

than 15 years ago, has experienced an incredible growth beyond a tailored introduction a broad discussion will not be attempted here. It will, however, be pointed out that the results presented in this thesis in Chapter 2 are an explicit computation of correlation functions of the physical model described in Chapter 1 in terms of Intersection numbers using an extension of the theory of topological recursion, called blobbed topological recursion. This furthers the understanding of the physical model by the explicit computation of the further parts, called blobs. This will assist a deeper understanding of the implications of the algebraic structures in the model in terms of what is called integrability, which will be the subject of future studies.

As alluded to above, there are various techniques that can shed light on the nature of the moduli space of curves by uncovering new perspectives and interpretations. The analysis in Chapter 2 about its relation to matrix models is accompanied by work on a recent combinatorial interpretation of intersection numbers, to which Chapter 3 is dedicated. In [Afa22], Adam Afandi uncovered that certain polynomials that compute intersection numbers are, in fact, related to the count of integer lattice points in polytopes. The latter is described by a well-developed theory which traces back to Eugène Ehrhart who introduced the theory since the 1960s [Ehr62, Ehr74]. It can be seen as a generalization of a classical theorem by Georg Pick [Pic99]. In his presentation he showed that the area of a polygon in two dimensions can be computed using only combinatorial data about integer lattice point in its interior and boundary. The theorem, illustrated in Figure 2, received, since it was first stated, several different proofs and generalizations that translate the continuous information of the area into discrete data. Ehrhart's work extends Pick's theorem to higher dimensions by considering polytopes. Counting integer lattice points in polytopes, the continuous information is recovered in a certain scaling limit.

By showing that intersection numbers on the moduli space of curves can be computed via Ehrhart theory, Afandi not only gave an interesting new interpretation. He also re-

proved their polynomial asymptotics as relevant information about the Ehrhart theory of polytopes is captured by so-called Ehrhart polynomials. In this thesis the class of polytopes corresponding to evaluations of intersection numbers is investigated. Based on an explicit result about a restricted sector of these, combinatorial properties are conjectured. To be explicit, it is shown that binomial expansions of the Ehrhart polynomials in the restricted sector obey logarithmic concavity. Numerical data as well as the recursive structure of the intersection numbers strongly suggests that this result extends to all Ehrhart polynomials associated to Intersection numbers. This property appears in different contexts in a variety of different fields in mathematics. It, therefore, was subject of studies from numerous different perspectives shedding light on its nature as well as providing different techniques most recently from matroid theory [Huh15, Huh12, HK12]. Due to the rich structures that have been found in the moduli space of curves, the occurrence of logarithmic concavity may not come as a surprise. In this thesis, classical results due to Richard Stanley and others are applied for the proof. Future research will be dedicated to using techniques from topological recursion to verify the intriguing conjecture.

structure

The structure of this thesis is parallel to the order in which the topics were mentioned in this introduction. The thesis is divided into three chapters. The presentation takes the physical point of view on the Quartic Kontsevich Model as well as the LSZ model, which are introduced and defined in Chapter 1. This also includes a discussion of the steps that were taken in the past in approaching a solution of this and related models, which relates through the recursive structures to intersection numbers on the moduli space of curves. As the moduli space of curves acts as a unifying theme, it is the topic of Chapter 2. The latter offers a short presentation of the ideas and definitions that are required to understand intersection numbers on the moduli space of curves. This naturally leads to the structure of topological recursion defined in Section 2.2, which is a reflection of the recursive nature of the moduli space of curves as well as governs the Quartic Kontsevich Model. The relation between physical models such as the latter and intersection numbers is discussed, and the explicit results are laid down. Based on the discussion of the properties of intersection numbers, in Chapter 3 the combinatorial perspective on them through Ehrhart theory is introduced. This includes an exposition of Ehrhart theory results tailored to this thesis as well as its relation to intersection numbers. The discrete data, which this interpretation of intersection numbers generates, is investigated in the following with respect to logarithmic concavity which is discussed in Section 3.4. Two different proofs of this result are provided taking an explicit as well as an abstract approach. The thesis is concluded by highlighting the main results as well as natural avenues to generalize these in future research.

Notation

The notation in this thesis generally follows widely accepted conventions and is for the most part defined where it is first used. For reference some basic notation is laid down here to facilitate comprehension as well as provide transparency and consistency.

The body of this thesis has a layered structure by *chapters*, *sections*, as well as *subsections*.

Numbering of elements in text Throughout the text elements appear such as (i) Definitions, which are illustrated by (ii) Examples, as well as (iii) results stated in Theorems, Propositions, Corollaries and Lemmas. The numbering of these elements, as in

$$c.s.n_g$$

indicates the chapter and the section they are stated in, with numbers c and s, respectively, and enumerates them by n_g within the groups, (i)-(iii), in which they are listed above. The same applies to Figures after the introduction. Results due to the author are contrasted to other work by the fact that these have no description in parentheses after their number.
Equations that are displayed with number

$$(c.n)$$

are enumerated by n in every chapter of number c separately.

In this thesis $\mathbb{N}$, $\mathbb{Z}$, $\mathbb{R}$, and $\mathbb{C}$ denote the natural numbers (starting from zero), the integers, the real and complex numbers, respectively. At various instances the number zero is excluded, which indicated by the symbol '$\times$' in the superscript, that is $\mathbb{N}^\times$ for example.
Furthermore, if not specified otherwise, the letters n, m, and d including their capitals represent natural numbers. These appear for example as numbers of points or the dimension such as in $\{v_1, \dots, v_n\}$, $\mathbb{R}^d$, or $\mathfrak{S}_n$, which denotes the symmetric group on n objects. The imaginary unit, that is the solution to $x^2 + 1 = 0$, is in formulas typeset in an upright, roman-type fashion as i.
The ring of power series in x with real coefficients is denoted by $\mathbb{R}[[x]]$ while $\mathbb{R}[x]$ signifies the corresponding polynomials. The same applies to other domains of the coefficients.

Braces and brackets Curly brackets (or braces) $\{a_1, a_2, \dots\}$ denote sets for some objects a_k, whereas ordinary round brackets (or parentheses) $(a_1, a_2, \dots)$ denote ordered sets. Moreover, for $n \leqslant m$ double square brackets $[\![n, m]\!]$ indicate the set of subsequent

integers $\{n, n+1, \dots, m-1, m\} \subset \mathbb{Z}$, which is not to be confused with the closed interval $[a, b] \subset \mathbb{R}$. Using this, frequent notation is

$$\{a_k\}_{k\in[\![1,n]\!]} \qquad \text{representing} \qquad \{a_1, \dots, a_n\}\,,$$

or $\{a_k\}_k$ if the index set is clear from context. In order to indicate the domain of the elements of some set at various spots in this text the notation $\{a_k\}_k \in X$ is used for some space X, which is to be understood as $\{a_k\}_k \subset X$.

Further peculiar notation include sums in the context of the moduli space of curves $\mathcal{M}_{g,n}$ or its compactified version $\overline{\mathcal{M}}_{g,n}$ (see Chapter 2). Here primed sums, which are typeset as $\sum'$, appear frequently. If not specified otherwise, in these sums terms associated to unstable topological types are excluded.

Combinatorial functions In this thesis $\binom{n}{k}$ for $n, k \in \mathbb{C}$ denotes the binomial coefficient. It has a combinatorial interpretation in terms of counting ways of choosing k objects from a set with n elements in the classical domain defined by $n \in \mathbb{N}$ and $k \in [\![0, n]\!]$ yielding

$$\binom{n}{k} = \frac{n!}{k!(n-k)!}\,,$$

for $n! = n(n-1)\cdots(2)(1)$. Beyond this domain one might either set $\binom{n}{k} \equiv 0$ or analytically continue the binomial coefficients using the Γ-function via the identity $n! = \Gamma(n+1)$. The Γ-function constitutes the natural (and unique up to logarithmic convexity [BM18], see Section 3.4,) extension of the factorial to the complex domain without negative integers. As a variant to the ordinary factorial, the double factorial $n!!$ appears in this text, which signifies the product of all numbers up to n with the same parity as n,

$$n!! = \begin{cases} \prod_{k=1}^{n/2} 2k\,, & k \text{ even}\,, \\ \prod_{k=1}^{(n-1)/2} (2k-1)\,, & k \text{ odd}\,. \end{cases}$$

This should not be confused with the iterated factorial $(n!)!$.

Contents

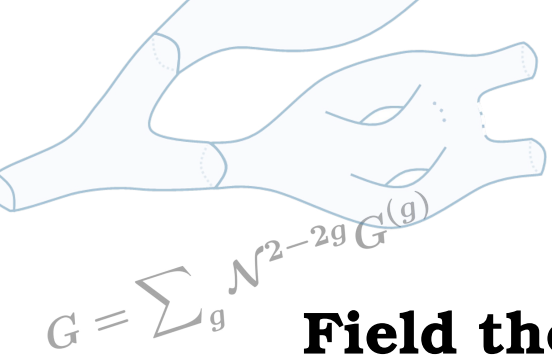

CHAPTER 1

Field theories on non-commutative space

This chapter first introduces the Quartic Kontsevich Model as a matrix field theory, which amongst others draws motivation from quantum field theories on non-commutative space. As such one can see this model as a perturbation of a measure $\mathrm{d}\mathcal{M}$ defined by

$$\exp\left(-\frac{1}{2\mathcal{N}}\sum_{k,l=1}^{N}\frac{J_{kl}J_{lk}}{E_k+E_l}\right)=\int_{H_N'}\mathrm{d}\mathcal{M}(\Phi)\,e^{\mathrm{i}\Phi(J)}\,, \tag{1.1}$$

where the integral is a matrix integral on the space H_N' dual to $N\times N$-matrices and $\{J_{kl}\}_{k,l}$ are the coordinates of some $J\in H_N$ with respect to the standard basis. The non-commutativity of the underlying space is here encoded in the parameter $\mathcal{N}$. Introducing the appropriate notation as well as results that give context to this is the aim of this chapter.

Parallel to toy models in ordinary quantum field theory, this measure is deformed in a quartic manner, here via a non-commutative product parametrized by $\mathcal{N}$. Such deformation away from the free theory is usually – in quantum field theoretical models – the source of interesting models but also ill-defined quantities. This has lead to various attempts to renormalize such models, which had, rigorously speaking, limited success exemplified by the proof of triviality of the quantum field theory with quartic interaction on ordinary four dimensional spacetime by Aizenman and Duminil-Copin in [Aiz81, AD21]. The Quartic Kontsevich Model, as described here, has to be subject to renormalization only in the limit of infinite matrix size $N\to\infty$. This limit will not be investigated here as it is the truncated model which exhibits richer algebraic structures evident in the limit due to the effect of transcendental objects. The reader interested in learning about this sector, which is closer to the quantum field theoretic motivation of the Quartic Kontsevich Model is referred to the dedicated reviews [Wul06, Wul19] as well as a nice presentation in [Bra22].

The main subject of investigation in the subsequent Chapter 2 will be derived from the moments of the partition function $\mathcal{Z}$ associated to the quartically deformed measure

$$\langle e_{p_1q_1}\cdots e_{p_nq_n}\rangle=\int_{H_N'}\mathrm{d}\mathcal{M}_{\mathrm{int}}(\Phi)\,\Phi(e_{p_1q_1})\cdots\Phi(e_{p_nq_n})=\frac{1}{\mathrm{i}^n}\frac{\partial^n\mathcal{Z}(J)}{\partial J_{p_1q_1}\cdots\partial J_{p_nq_n}}\bigg|_{J=0}\,. \tag{1.2}$$

The algebraic structures that these exhibit were first observed in the Kontsevich model, the cubic analogue of the present model. The investigation of the latter by Maxim Kontsevich and its role in the proof of Edward Witten's conjecture about two-dimensional

quantum gravity has crucially led to the formation of the research field this thesis is embedded in. In [Wit90, Wit92], Edward Witten famously conjectured that two-dimensional gravity, or the integrals computing its moments, correspond to intersection numbers on the moduli space of complex curves. Maxim Kontsevich was able to prove this correspondence using so-called Strebel differentials and the language of ribbon graphs [Kon92].
This seminal work stirred a wave of attention for this line of research as well as similar models. Examples for these are the Quartic Kontsevich Model and the LSZ model [LS02, LSZ04] named after Edwin Langmann, Richard Szabo and Konstantin Zarembo, which will briefly be discussed at the end of this chapter in Section 1.4.

The discussion above explains that the investigation of the Quartic Kontsevich Model is inspired by advances in quantum field theory, gravity as well as mathematical disciplines such as algebraic geometry amongst others but can be approached from various other point of view. In the following the quantum field theoretic approach is taken starting with the concept of axiomatic quantum field theories in the Lorentzian and Euclidean setting, Section 1.1. The general theory is accompanied by a running example defining the Quartic Kontsevich Model, which is a central topic of this thesis. In Section 1.3 the solution strategy of this specific quantum field theory is outlined. The exposition in this chapter follows in different parts [Wul19, Wul06, Bra22, BHW22].

1.1 Axiomatic approach to QFTs

A scalar quantum field is, initially, defined on Lorentzian spacetime $\mathbb{R}^{1,d-1}$.

Definition 1.1.1. A *scalar quantum field* φ on $\mathbb{R}^{1,d-1}$ is an unbounded operator-valued distribution acting on a Hilbert space $\mathcal{H}$, that is for any test function[†] $f \in \mathbb{S}(\mathbb{R}^{1,d-1})$ both $\varphi(f)$ and $\varphi^*(f)$ act linearly on a dense set in $\mathcal{H}$.
Furthermore, φ satisfies the axioms of covariance under the Poincare group, a spectrum condition as well as locality.

The Hilbert space associated to a quantum field theory constitutes the space of states. In it one distinguishes the vacuum state $\Omega \in \mathcal{H}$ being a unit vector of the subspace of Poincaré-invariant vectors in the dense set, see above. From these data one can build the essential objects, vacuum expectation values $\mathcal{W}\colon \mathbb{S}(\mathbb{R}^{1,d-1})^N \to \mathbb{C}$ with

$$(f_1, \dots, f_N) \mapsto \langle \Omega, \varphi(f_1) \cdots \varphi(f_N)\Omega \rangle \,, \tag{1.3}$$

which are called Wightman functions in the context of Lorentzian spacetime [Wig56, SW89]. Understanding the axioms of Definition 1.1.1 as properties of Wightman functions leads to the physical implications of covariance, locality as well as spectrum and

[†]The space of Schwartz functions $\mathbb{S}(\mathbb{R}^d)$ on $\mathbb{R}^d$ is defined as a subspace of infinitely differentiable functions as $\mathbb{S}(\mathbb{R}^d) = \{g \in \mathbb{C}^\infty(\mathbb{R}^d)\colon \sup_{x\in\mathbb{R}^d} \left|x^\alpha (D^\beta g)(x)\right| < \infty \quad \forall \alpha, \beta \in \mathbb{N}^d\}$.

cluster properties. Furthermore, it can be shown that these functions enjoy analytic continuation to $\mathbb{C}$ in the time domain, which will be used in the below to define quantum field theories on Euclidean space.
The foundation for the pivotal importance of the Wightman functions, or correlation functions, lies partly in Wightman's theorem stating equivalence of the data contained in the scalar quantum field and the full set of correlation functions, see [SW89].

Euclidean space In order to rigorously define a QFT on a Euclidean space, Osterwalder and Schrader in the 70s of the last century defined axioms building on considerably irrefutable principles of physics [OS73, OS75, GJ87]. These mirror the axioms proposed by Wightman in the context of Lorentzian spacetime.
The fundamental objects subject to these axioms are the vacuum expectation values, or Schwinger functions, see [Sch59b], $\mathcal{S}(x_1, \dots, x_n)$ evaluated at positions $\{x_1, \dots x_n\}$. According to Osterwalder and Schrader the Schwinger functions shall transform in a covariant manner under Euclidean transformations $\mathbb{R}^d \rtimes SO(d)$, obey reflection positivity as well as be symmetric under permutation of their arguments. At this point it is refrained from defining these axioms in more detail and the interested reader is referred the original work as well as the reviews [Wul06, Wul19] for a discussion.
It remains to say that a model, that is constructed satisfying these axioms, can in a mathematically rigorous manner be called a quantum field theory, amongst others being free of spurious divergencies as well as having a proper time evolution [GJ87]. However, completing such a construction beyond non-interacting, that is free, theories required major work [GJ87] in low dimensions and remains elusive in four dimensions and is crucially tied to deep mathematically meaningful insight.

1.2 Non-commutative setting

Expressing the above on *non-commutative space* it is customary to structure the data into a *spectral triple* $(\mathcal{A}, \mathcal{H}, \mathcal{D})$, see [Con94], made of a Hilbert space of states accompanied by an unbounded self-adjoint operator $\mathcal{D}$. The algebra $\mathcal{A}$ acts on $\mathcal{H}$ through a representation. The operator $\mathcal{D}$, which must have a compact resolvent, is usually referred to as the Dirac operator as it behaves like a first-order differential operator due to the boundedness of the commutator $[\mathcal{D}, \mathfrak{a}]$ for all $\mathfrak{a} \in \mathcal{A}$.
In the past it was understood that the correct setup to construct the model, which this thesis investigates, are *nuclear and approximately finite (AF) Fréchet algebras*, see [Wul19]. To understand this, it will first be explained what is meant by the class of algebras referred to. This will be accompanied by a running example pivotal to this thesis, leading to the definition of the Quartic Kontsevich Model.
The algebra acting on $\mathcal{H}$ has the structure of a Fréchet space, which allows for a more general topological structure induced by a family of seminorms compared to Banach spaces, which require a norm.

Definition 1.2.1. A *Fréchet space* is a locally convex vector space X with a topology induced by a countable increasing family (u_n) of seminorms, which make X metrisable and complete.

The Fréchet space X is *nuclear* if

1. for every n there is an inner product $\langle\ ,\ \rangle_n$ which induces u_n,
2. for any u_n there is a larger u_m such that the natural map from the closure of X with respect to u_n to that of u_m is trace-class.

The space obtains its algebraic structure through a product compatible with the topological data.

Definition 1.2.2. A *(nuclear) Fréchet algebra* is an algebra that, as a vector space, is a (nuclear) Fréchet space in which the multiplication associated to the algebra is continuous.

In order to illustrate these definitions, in the following as a running example the *Moyal algebra* will be defined following [Wul19]. This will be the space on which at a later stage the *Quartic Kontsevich Model* is constructed, which is a subject of this thesis.

Example 1.2.1. *In this text the original two-dimensional Moyal space is constructed through double-indexed sequences. This construction can be generalized to any even dimension by mapping indices to tuples acting as indices and using Cantor's bijection. In the two-dimensional case, let $\mathcal{A}_\theta$ be the vector space of double-indexed sequences $(\mathfrak{a}_{k,l})_{k,l\in\mathbb{N}^\times}$, completed with respect to the family of inner products*

$$\langle \mathfrak{a}, \mathfrak{b}\rangle_m := \sum_{k,l} \theta^{2m}(k+1/2)^m(l+1/2)^m\overline{\mathfrak{a}_{k,l}}\mathfrak{b}_{k,l}\,, \tag{1.4}$$

where the notation $\mathfrak{a}^* = (\overline{\mathfrak{a}_{k,l}})_{k,l}$ denotes an involution on $\mathcal{A}_\theta$. To each of these inner products an orthonormal basis of elements of the form $\theta^{-m}(r+1/2)^{-m/2}(s+1/2)^{-m/2}\mathfrak{e}_{r,s}$, with $(\mathfrak{e}_{r,s})_{k,l} = \delta_{rk}\delta_{sl}$, can be associated. Furthermore, a calculation shows that the vector space $\mathcal{A}_\theta$ with the inner products $\langle\ ,\ \rangle_m$ is nuclear.
The vector space $\mathcal{A}_\theta$ receives its algebraic structure by the multiplication defined for $\mathfrak{a}, \mathfrak{b} \in \mathcal{A}_\theta$ by $\mathfrak{a}\mathfrak{b} = \mathfrak{c}$ with

$$\mathfrak{c}_{k,l} := \sum_n \mathfrak{a}_{k,n}\mathfrak{b}_{n,l}\,. \tag{1.5}$$

In that way, the multiplication is compatible with the linear structure as well as is continuous, turning $\mathcal{A}_\theta$ into a nuclear Fréchet algebra with basis elements $\mathfrak{e}_{r,s}$, such that one expands

$$\mathcal{A}_\theta \ni \mathfrak{a} = \sum_{k,l} \mathfrak{a}_{k,l}\mathfrak{e}_{k,l}\,. \tag{1.6}$$

The following theorem, which goes back to Takako and Yukio Kōmura and was later proved for any dimension[‡] d, encodes possible the non-commutative structure in a product of fields, see [KK66, Vog00].

Theorem 1.2.1 (Kōmura-Kōmura)**.** *A Fréchet space is nuclear if and only if it is isomorphic to a closed subspace of* $C^\infty(\mathbb{R}^d)$.

Concretely, the algebra can now be interpreted as a vector space of smooth functions connected via a (deformed) product, denoted by $\star$, which is induced by the isomorphism between $\mathcal{A}$ and a subspace of $C^\infty(\mathbb{R}^d)$. Referring back to the beginning of this paragraph, the construction through Kōmura's theorem allows a consistent interpretation of the coexistence of discreteness and continuity in the theory.

Example 1.2.2. *In the running example of the Moyal algebra, the isomorphism of Kōmura-Kōmura's theorem maps* $\mathcal{A}_\theta$ *to a closed subspace of* $C^\infty(\mathbb{R}^2)$*, which can be linearly extended to the nuclear vector space of Schwartz functions* $\mathbb{S}(\mathbb{R}^2)$*. It can be specified by its action on the basis elements as*

$$\mathfrak{e}_{k+1,l+1} \mapsto f^{(\theta)}_{k,l}(x_1,x_2) \coloneqq 2(-1)^k \sqrt{\frac{k!}{l!}} \left(\frac{x_1+\mathrm{i}x_2}{\sqrt{\theta/2}}\right)^{l-k} \mathscr{L}_k^{l-k}\Big(\frac{\|x\|^2}{\theta/2}\Big) e^{-\frac{\|x\|^2}{\theta}}\,, \tag{1.7}$$

where $\mathscr{L}^\alpha_m$ *are the associated Laguerre polynomials of degree* m *and* $x=(x_1,x_2)$*. This introduces a product on* $\mathbb{S}(\mathbb{R}^2)$*, that is induced by the multiplication on* $\mathcal{A}_\theta$*. One can verify [GBV88] that for* $\phi,\psi\in\mathbb{S}(\mathbb{R}^2)$ *this product takes the form*

$$(\phi\star_\theta\psi)(x) = \int \frac{\mathrm{d}k\,\mathrm{d}y}{(2\pi)^2}\phi(x+\Theta y)\psi(x+y)e^{iyk}\,, \tag{1.8}$$

where $\Theta = \frac{1}{2}\left(\begin{smallmatrix}0 & \theta\\ -\theta & 0\end{smallmatrix}\right)$*. To understand the* $\star_\theta$*-product, it might be noted that in the limit* $\theta\to 0$ *this non-commutative product reduces to the ordinary product of functions. In fact, one can write down an asymptotic expansion, see [Wul06, EGBV89] in the form*

$$(\phi\star_\theta\psi)(z) \sim \exp\left(\mathrm{i}\theta^{\mu\nu}\frac{\partial}{\partial x^\mu}\frac{\partial}{\partial y^\nu}\right)\phi(x)\psi(y)\Big|_{x=y=z}\,. \tag{1.9}$$

In this representation the nature of the product as a deformation of the ordinary product of functions is apparent. It is important to point out that even though in this text the $\star_\theta$*-product was introduced as a way to implement non-commutativity on the level of space, beyond that it has additional, physically-interesting features such as non-locality, see [Wul19].*

A convenient tool to describe a quantum field theory including interacting models as well as their renormalisation is the *partition function* or rather the associated measure. Originating in ideas of statistical models and already applied in the early days of

[‡]Originally the theorem is given for a closed subspace of $C^\infty(U)$ with $U\subseteq\mathbb{R}^d$. Here only $U=\mathbb{R}^d$ will be significant.

quantum mechanics, in this framework vacuum expectation values are calculated via derivations.
In the present context the partition function is constructed via the inner products of the nuclear Fréchet space. On the space $\mathcal{A}_*$ of self-adjoint elements of $\mathcal{A}$ these define a continuous, symmetric, positive-semidefinite bilinear form c, see [Wul19, Section 3.2], called the covariance, as well as associated to it a continuous map

$$\mathcal{Z}_c(\mathfrak{a}) = \exp(-c(\mathfrak{a},\mathfrak{a})/2)\,. \tag{1.10}$$

Using a theorem by Bochner [Boc32] generalised by Minlos [Min59] from this a probability measure is constructed in the context of real Fréchet spaces.

Theorem 1.2.2 (Bohner-Minlos)**.** *Let $\mathcal{Z}$ be a real continuous map on a real nuclear Fréchet space X which is*

- *normalised to $\mathcal{Z}(0) = 1$ and*
- *of positive type, that is for any x_1, ..., $x_n \in X$ and c_1, ..., $c_n \in \mathbb{C}$ one has $\sum_{k,l}^n c_k c_l \mathcal{Z}(x_k - x_l) \geqslant 0$.*

Then there exists a unique probability measure $\mathrm{d}\mathcal{M}$ on the dual space X' with

$$\mathcal{Z}(x) = \int_{X'} \mathrm{d}\mathcal{M}(\varphi)\, e^{\mathrm{i}\varphi(x)} \tag{1.11}$$

As it is familiar from field theories, in general, the moments of the measure due to the theorem above are the Schwinger functions of the theory in consideration

$$\mathcal{S}_N(\mathfrak{a}_1,\ldots,\mathfrak{a}_n) = \int_{(\mathcal{A}_*)'} \mathrm{d}\mathcal{M}_C(\varphi)\,\varphi(\mathfrak{a}_1)\cdots\varphi(\mathfrak{a}_n)\,. \tag{1.12}$$

for elements $a_1,\ldots,a_n$ of the Fréchet space. These Schwinger functions are subject to the axioms by Osterwalder and Schrader.

Example 1.2.3. *For the introduction of fields on the Moyal space different covariances can be defined. One of particular importance here, see [Wul19, Section 4.2] is defined for a sequence of positive real number $(E_k)_{k\in\mathbb{N}}$ by*

$$c_E(\mathfrak{e}_{k,l},\mathfrak{e}_{m,n}) = \frac{\delta_{k,n}\delta_{l,m}}{E_k + E_l}\,. \tag{1.13}$$

The fields associated to this covariance through the Bochner-Minlos theorem can be interpreted to propagate according to this covariance. In that sense the fields carry two indices that are propagated and the positive real numbers $\{E_k\}_k$ can be interpreted as masses carried on the different indices.
Other covariances, that are of relevance for this text[♯], are induced by the action of translations in $\mathbb{R}^2$ or pointwise multiplication of functions in $\mathbb{S}(\mathbb{R}^2)$. For details on these the reader is referred to [Wul06, Wul19] and references therein.

[♯]These play a role in the construction of the Ω-term mentioned in Example 1.2.5, see[Wul19, Section 4.2].

Interacting theories

The physically interesting models arise when the free theory is perturbed by an interaction. The approach that implements such a perturbation is rooted in quantum mechanics and is named after Feynman and Kac [Kac49]. In this spirit the measure of the perturbed theory $\mathrm{d}\mathcal{M}_{\mathrm{int}}$ is proposed as

$$\mathrm{d}\mathcal{M}_{\mathrm{int}}(\varphi) = \frac{\mathrm{d}\mathcal{M}\,(\varphi) e^{-P(\lambda,\varphi)}}{\int_{(A_*)'} \mathrm{d}\mathcal{M}\,(\varphi) e^{-P(\lambda,\varphi)}} \tag{1.14}$$

in terms of the original measure $\mathrm{d}\mathcal{M}$ as well as a polynomial perturbation $P(\lambda, \varphi)$. At this point it was cautiously refrained from making a definition, as naively implementing this approach suffers, in actual quantum field theories, from various issues. Mathematically speaking, the origin of these issues in quantum field theories traces back to the fields in the argument of the polynomial P. Being distributions dual to functions in the Schwartz space, their product constitutes not necessarily a closed operation. This is observed in ill-defined objects such as diverging physical quantities. Solving this requires major work, which is summarized by what is known as the programs of regularisation and renormalisation. For a general discussion it is referred to one of many quantum field theory textbooks [Sch13, Pes18] as well as reviews tailored to the specific setting [Wul06, Wul19] and references therein.

Usually these approaches deal with the theory in a restricted setting and, then, try to lift these restrictions in a careful limiting procedure, which – if successfull – preserves the nice properties. This motivates the additional structure of approximate finiteness which is imposed on the Fréchet space following [Wul19, Definition 3.5].

Definition 1.2.3. A nuclear Fréchet algebra A is called *approximately finite* if there is an increasing sequence of finite-dimensional subalgebras embedded into each other by $*$-homomorphisms

$$A^0 \xhookrightarrow{\iota_0} A^1 \xhookrightarrow{\iota_1} A^2 \xhookrightarrow{\iota_2} \dots\,, \tag{1.15}$$

such that union $\cup_{k\in\mathbb{N}} A^k$ is dense in A with respect to the locally-convex topology induced by the Hilbert seminorms.

Example 1.2.4. *The approximately finite nature of $\mathcal{A}_\theta$ can be seen by identifying truncated double-indexed sequences in $\mathcal{A}_\theta^N := \mathrm{span}(\mathfrak{e}_{k,l} \colon k, l \leqslant N)$ with matrices, that is $\mathcal{A}_\theta^N \equiv M_N(\mathbb{C})$. The $*$-homomorphisms $\iota_N \colon \mathcal{A}_\theta^N \to \mathcal{A}_\theta^{N+1}$ is given by*

$$\iota_N \colon \mathfrak{a} \mapsto \mathfrak{a} \oplus (0)\,, \qquad \text{for } \mathfrak{a} \in M_N(\mathbb{C})\,, \tag{1.16}$$

and a short calculation shows that the infinite union of the finite dimensional algebras $\mathcal{A}_\theta^N$ is dense in $\mathcal{A}_\theta$.

This concludes the definition of the class of nuclear, approximately finite Fréchet algebras, that are used to construct field theories on non-commutative space. In the following the interaction is implemented in the running example.

Example 1.2.5. *The field theory obtained through the Bochner-Minlos theorem in the running example on the Moyal space above can be deformed via the Feynman-Kac approach. It will then be truncated to yield the Quartic Kontsevich Model.*
Although the details of the renormalisation procedure will not be laid down here, as the truncated model in the end does not require it, the resulting action will be quoted [GW05, Bra22] here in $d \in \{0, 2, 4, 6\}$ dimensions

$$S[\varphi] = \int_{\mathbb{R}^d} \frac{\mathrm{d}^d x}{(8\pi)^{d/2}} \left(\frac{1}{2} \varphi \star_\Theta \left(-\Delta + \Omega^2 \left\| 2\Theta^{-1} x \right\|^2 + \mu^2 \right) \varphi + \frac{\lambda}{4} \varphi^{\star_\Theta 4} \right)(x) \,, \tag{1.17}$$

where $\Theta = \mathbb{1}_{d/2} \otimes \left(\begin{smallmatrix} 0 & \theta \\ -\theta & 0 \end{smallmatrix} \right)$. This action can be expanded into matrix base to yield

$$S[\Phi] = \sum_{k,l,r,s} \Phi_{kl} (-\Delta_{kl;rs} + \mu^2) \Phi_{rs} + \frac{\lambda}{4} \sum_{k_1,\ldots,k_4} \Phi_{k_1 k_2} \Phi_{k_2 k_3} \cdots \Phi_{k_4 k_1} \,. \tag{1.18}$$

In the above the interaction polynomial given by the quartic $\star_\Theta$-product of fields expands into a cyclic matrix product. Furthermore, the Laplacian $\Delta = \sum_k \partial_{x_k}^2$ contained in the Gaussian term, which is a well-known part of action functionals in quantum field theories, is accompanied by a harmonic oscillator term weighted by Ω^2. While the precise form of their tensorial representation in $\Delta_{kl;rs}$ is not relevant here, it is interesting to note the motivation for the introduction of the harmonic oscillator term. Although the original reason for its introduction procedure was ad-hoc and rooted in the renormalisation procedure , it was later observed that there is an interplay between the Δ-term and the Ω-term in this model of Equation (1.17). In [LS02] Langmann and Szabo discovered a duality between position and momentum space in this model given by the duality transform

$$S[\Phi; \mu, \{\lambda_k\}_k, \Omega] \;\mapsto\; \Omega^2 \, S[\Phi; \mu/\Omega, \left\{\lambda_k/\Omega^2\right\}_k, 1/\Omega] \,. \tag{1.19}$$

This inverts the roles of the Δ-term and the Ω-term, thus achieving duality-covariance of the model with Ω-term. Furthermore, it is interesting and convenient to study the model at the self-duality point $\Omega = 1$. This is adopted from this point on. In that case

$$(-\Delta_{kl;rs} + \mu^2)/2\big|_{\Omega=1} = \delta_{k,r} \delta_{l,s} \left(\frac{|k| + |l| + d/2}{\theta/4} + \mu^2 \right) /2 =: E_{k,l} \,. \tag{1.20}$$

Additionally, truncating the action at finite N reduces Equation (1.18) to that of an $N \times N$ Hermitian matrix model

$$S[\Phi]|_{\Omega=1} = -(\theta/4)^{d/2} \operatorname{tr} \left(E\Phi^2 + \frac{\lambda}{4} \Phi^4 \right) . \tag{1.21}$$

Finally, it should be pointed out that the dimension of the underlying geometry, which is encoded in the spectral triple and in the case of infinity matrix size also decides renormalizablility, is encoded in the density of eigenvalues of the external matrix (or field) E. Without attempting a rigorous deduction here, this can be seen by following an approach, put forward already by Connes [Wey11, Con94], to look at the trace of

the heat kernel of the unbounded operator $\mathcal{D}$. Relating it by the means of a Mellin transform to the ζ-function of the system, the maximum dimension appearing in its asymptotic expansion decides convergence. Heuristically, the reason for deducing the dimension from a heat kernel is, that the heat kernel, crucially, is sensitive to the dimension of the underlying space. This can already been seen in the fact that the return probability of a random walk radically decreases with dimension [Pól21, Wei]. The quantitative behaviour is dictated by the dimension.

Example 1.2.6. *In the case of the specific model set up here, the geometry is encoded in the coefficients $E_{k,l}$. The notion of dimension given above translates here [Wul19, Bra22] to the smallest d such that for all $\epsilon > 0$ the sum*

$$\sum_{k\geqslant 1}(E_{k,k})^{-d/2-\epsilon} \tag{1.22}$$

converges. Thus, a spectrum truncated at a finite $k = N$ yields a zero dimensional theory, while at $N \to \infty$ the growth-rate of the E_k determine the dimension.

It is important to note at this point, that even in the limit of infinite matrix size the (properly renormalized) model one has obtained is not a consistent quantum field theory. What one achieved in this limit, which goes beyond the structure of the Quartic Kontsevich Model, are physical limits of all relevant quantities, that is all moments, in the sense of a statistical physics model. To obtain an actual quantum field theory a consistent time-evolution is essential, which is a deep consequence of the axioms of Osterwalder-Schrader.

1.3 Solution strategy of Quartic Kontsevich Model

Once the model is set up, referring to the previous section, the objects of study are the *moments and cumulants* [Spe83] of the deformed measure which are obtained from the partition function $\mathcal{Z}(J)$ by derivation with respect to the current

$$\langle \mathfrak{e}_{p_1q_1}\dots\mathfrak{e}_{p_nq_n}\rangle = \frac{1}{\mathrm{i}^n}\frac{\partial^n \mathcal{Z}(J)}{\partial J_{p_1q_1}\cdots\partial J_{p_nq_n}}\,, \quad \text{and} \quad \langle \mathfrak{e}_{p_1q_1}\dots\mathfrak{e}_{p_nq_n}\rangle_c = \frac{1}{\mathrm{i}^n}\frac{\partial^n \log \mathcal{Z}(J)}{\partial J_{p_1q_1}\cdots\partial J_{p_nq_n}}\,. \tag{1.23}$$

These sets of objects carry equivalent information and can be translated into each other computationally. The cumulants are only non-zero if $q_k = p_{\tau(k)}$, where $\tau \in \mathfrak{S}_n$ is a permutation, and then only depend on the cycle-type of τ, which is a result of Wicks theorem. Therefore, let b be the number of cycles of the permutation and n_k, for $k \in [\![1, b]\!]$, their length. Furthermore, they enjoy an expansion

$$\langle(\mathfrak{e}_{p_1^1p_2^1}\mathfrak{e}_{p_2^1p_3^1}\cdots\mathfrak{e}_{p_{n_1}^1p_1^1})\cdots(\mathfrak{e}_{p_1^bp_2^b}\cdots\mathfrak{e}_{p_{n_b}^bp_1^b})\rangle_c = \mathcal{N}^{2-\sum(n_i+1)}\sum_{g=0}^{\infty}\mathcal{N}^{-2g}G^{(g)}_{|p_1^1p_2^1\dots p_{n_1}^1|\cdots|p_1^b\cdots p_{n_b}^b|}\,, \tag{1.24}$$

where the parameter $\mathcal{N}$ can be interpreted as $\mathcal{N} = N = (\theta/4)^{d/2}$ in terms of the setup in the previous section, but is treated as a formal parameter here. This expansion is usually referred to as a *genus expansion*, hence the index g, and was introduced by Gerard 't Hooft [tH74]. This name already suggests a deep connection of the objects $G^{(g)}$ with surfaces of different topological types, which will be discussed below.
The strategy that leads to a solution of the Quartic Kontsevich Model is determined by its *Dyson-Schwinger equations*. These form an infinite system of equations and are also called the equations of motion in the physics literature. Furthermore, the symmetries of the model imply *Ward-Takahashi identities* [DGMR07]. Together these relations imply an intricate structure. In fact, the functions $G^{(g)}$ come with a partial order, encoded in the topological type of the ribbon graphs associated to them. The relations between them, crucially, respect exactly this order, implying that either two functions are independent, or one is smaller and depends on the larger. Therefore, functions depend only on finitely many smaller functions and eventually on the planar two point functions $G^{(0)}_{|pq|}$ and $G^{(0)}_{|p|q|}$. The former is determined by the closed non-linear equation [BHW22, HW21, Bra22]

$$\begin{aligned}(E_p + E_q)G_{|pq|} = 1 + \frac{\lambda}{N}\frac{\partial G_{|pq|}}{\partial E_p} - \frac{\lambda}{N}\sum_{k=1}^{N}\lambda G_{|pq|}G_{|pk|} + \frac{\lambda}{N^2}G_{|pq|}G_{|p|p|} \\ + \frac{\lambda}{N}\sum_{\substack{l=1\\ l\neq p}}^{N}\frac{G_{|lq|} - G_{|pq|}}{E_l - E_p} + \frac{\lambda}{N^2}\frac{G_{|q|q|} - G_{|p|q|}}{E_q - E_p}\,,\end{aligned} \tag{1.25}$$

due to insights by Alexander Hock. In order to solve this equation complex analytic methods turned out to be key, see [SW23, GHW19, Bra22] ascribing meaning to the derivatives with respect to matrix entries of the external field and coinciding matrix indices. Therefore, the correlation functions $G_{|p_1^1\dots p_{n_1}^1|\cdots|p_1^b\cdots p_{n_b}^b|}$ will be holomorphically continued into the complex plain such that

$$G(|E_{p_1^1},\dots E_{p_{n_1}^1}|\cdots|E_{p_1^b}\cdots E_{p_{n_b}^b}|) \equiv G_{|p_1^1\dots p_{n_1}^1|\cdots|p_1^b\cdots p_{n_b}^b|}\,. \tag{1.26}$$

Remark 1.3.0.1. In order to describe this process in more detail, one defines the holomorphic functions G on a neighborhood of the values $E_k \in \mathbb{C}$ according to equation (1.26) and postulates that the Dyson-Schwinger equations carry over to the newly defined functions. This is accompanied by the complexification of the derivative

$$\frac{\partial}{\partial E_q}f(E_q) \mapsto \frac{f(\eta) - f(E_q)}{\eta - E_q} + \left.\frac{\partial}{\partial E_q}\right|_{E_q\mapsto\eta} f(\eta)\,. \tag{1.27}$$

Considering the equation on G in the complement of the $\{E_k\}_k$, one is now also able to define its values at coinciding points by a limit procedure. In that case the spectrum $(E_k)_{k\in[\![1,N]\!]}$ is consisting of pairwise different values $(e_k)_{k\in[\![1,D]\!]}$ with multiplicities r_k for $k \in [\![1, D]\!]$ such that $\sum_{k=1}^{D} r_k = N$.

This results in the non-linear Dyson-Schwinger equation[4]

$$(\zeta+\eta)\,G^{(0)}(\zeta,\eta) = 1 - \frac{\lambda}{N}\sum_{k=1}^{D} r_k \left(G^{(0)}(\zeta,E_k)G^{(0)}(\zeta,\eta) - \frac{G^{(0)}(E_k,\eta)-G^{(0)}(\zeta,\eta)}{E_k-\zeta} \right) \tag{1.28}$$

determining $G^{(0)}(\cdot,\cdot)$, which can be approached by complex analytic methods [SW23]. The authors of [SW23] showed that the central ingredient to the solution of, in fact in all topological sectors, is a variable transformation, denoted R, on $\overline{\mathbb{C}}$.

Theorem 1.3.1 (Schürmann-Wulkenhaar [SW23])**.** *For $\lambda, \{e_k\}_k > 0$, assume that there is a rational function $R\colon \overline{\mathbb{C}} \to \overline{\mathbb{C}}$ such that*

- *R is of degree $(D+1)$, is normalized to $R(\infty)=\infty$ and bi-holomorphically maps a domain $U \subset \mathbb{C}$ to a neighborhood in $\mathbb{C}$ of a real interval that contains $e_1,\dots,e_D$*
- *in terms of $\mathcal{G}^{(0)}(z,w) \coloneqq G^{(0)}(R(z),R(w))$ and $\varepsilon_k = R^{-1}(e_k)$ one has*

$$-R(-z) = R(z) + \frac{\lambda}{N}\sum_{k=1}^{D} r_k \left(\frac{1}{R(\varepsilon_k)-R(z)} + \mathcal{G}^{(0)}(z,e_k) \right), \tag{1.29}$$

for $z,w,\{\varepsilon_k\} \in U$.

Then R and $\mathcal{G}^{(0)}$ are uniquely determined by equation (1.28) *to*

$$R(z) = z - \frac{\lambda}{N}\sum_{k=1}^{D}\frac{\rho_k}{\varepsilon_k+z}, \tag{1.30}$$

$$\mathcal{G}^{(0)}(z,w) = \frac{1-\frac{\lambda}{N}\sum_{k=1}^{D}\frac{r_k}{(R(z)-R(\varepsilon_k))(R(\varepsilon_k)-R(-w))}\prod_{j=1}^{D}\frac{R(w)-R(-\widehat{\varepsilon}_k^{\,j})}{R(w)-R(\varepsilon_j)}}{R(w)-R(-z)}, \tag{1.31}$$

for $R(\varepsilon_k)=e_k$ and $\rho_k R'(\varepsilon_k)=r_k$. In the above, solutions $v\in\mathbb{C}$ of $R(v)=R(z)$ with $z\in U$ are denoted by $v\in\{z,\widehat{z}^1,\dots,\widehat{z}^D\}$. The ansatz (1.29) *is identically satisfied by these R and $\mathcal{G}^{(0)}$.*
Furthermore, the function $\mathcal{G}^{(0)}$ is symmetric and its poles are located at $z+w=0$ and $z,w\in\{\widehat{\varepsilon}_k^{\,j}\}_{k,j\in[\![1,D]\!]}$.

A proof of the theorem will not be given here and the interested reader will be referred to the excellent exposition of this and related results in [Bra22] or the original work [SW23, GHW19]. Nevertheless, it should be pointed out that the variable transform R is introduced such that the Dyson-Schwinger equation for $\mathcal{G}^{(0)}$ reduces to a linear equation which in turn determines the form of R in an involved manner. Considering this, it might be unexpected that one finds R under relatively mild assumptions. This pivotal result now enables to achieve solutions for all higher correlation functions.

[4] The Dyson-Schinger equation in this form already assumes D to be finite. In order to find a $G^{(0)}$ consistent in renormalization for $N,D\to\infty$ requires a more general form of the DSE introducing renormalisation parameters Z,μ_{bare} for the $\{e_k\}$ and $G^{(0)}$ itself. Truncating at finite N,D yields trivial values for these parameters.

To exemplify this, note that there is another two-point correlation function at genus zero of different cycle-type, which is $G^{(0)}(\zeta|\eta)$. The corresponding Dyson-Schwinger equation can be brought to the form

$$\frac{\lambda}{N}\sum_{l=1}^{D}\frac{r_l\mathcal{G}^{(0)}(\varepsilon_l|w)}{R(\alpha_k)-R(\varepsilon_l)}=\lambda\frac{\mathcal{G}^{(0)}(\alpha_k,w)-\mathcal{G}^{(0)}(w,w)}{R(\alpha_k)-R(w)}\,, \tag{1.32}$$

where $\{\alpha_k\}_{k\in[\![1,2D+1]\!]}$ are solutions of $R(z)=R(-z)$, which is solved by the theory of Cauchy matrices [SW23, Sch59a] observing the linearity of this equation in contrast to Equation (1.28). The latter fact will persist for all larger correlation functions as mentioned above.

Proposition 1.3.2 (Schürmann-Wulkenhaar [SW23])**.** *The planar two-point function $G^{(0)}(\zeta|\eta)$ of cycle type $(2,0)$ determined by Equation (1.32) takes the form*

$$\begin{aligned}\mathcal{G}^{(0)}(z|w)=&\frac{\lambda}{(R(z)-R(w))^2}\Bigg(\mathcal{G}^{(0)}(z,w)\\&-\frac{R(z)+R(w)-2R(0)}{(R(z)-R(-z))(R(w)-R(-w))}\prod_{k=1}^{D}\frac{(R(z)-R(\alpha_k))(R(w)-R(\alpha_k))}{(R(z)-R(\varepsilon_k))(R(w)-R(\varepsilon_k))}\Bigg)\,,\end{aligned} \tag{1.33}$$

with $\mathcal{G}^{(0)}(z,w)$, the planar two-point function of cycle-type $(0,1)$, given in Theorem 1.3.1.

These solutions build the basis for the solution in the higher topological sectors, see [BHW22]. In fact to fully capture and utilize the recursive structure due to the Dyson-Schwinger equations and Ward-Takahashi identities, one is compelled to introduce generalized correlation functions

$$T_{q_1,\dots,q_m||p_1^1\dots p_{n_1}^1|\dots|p_1^b\dots p_{n_b}^b|}:=\frac{(-N)^m\partial^m}{\partial E_{q_1}\dots\partial E_{q_m}}G_{|p_1^1\dots p_{n_1}^1|\dots|p_1^b\dots p_{n_b}^b|}\,, \tag{1.34}$$

as well as

$$\Omega_q:=\frac{1}{N}\sum_{k=1}^{N}G_{|qk|}+\frac{1}{N^2}G_{|q|q|}\,,\quad\text{and}\quad\Omega_{q_1,\dots q_m}:=\frac{(-N)^{m-1}\partial^{m-1}\Omega_{q_1}}{\partial E_{q_2}\dots\partial E_{q_m}}+\frac{\delta_{m,2}}{(E_{q_1}-E_{q_2})^2}\,. \tag{1.35}$$

Assuming that Ω_q has a primitive in E_{q_1} it is easy to see that the $\Omega_{q_1,\dots q_m}$ are symmetric in their indices. The primitive, in fact, corresponds to the partition function or the free energies, which will appear later.
On the same lines as discussed above for the ordinary correlators G one can find relations for the generalized correlators which suggest complexification, yielding generalized correlation functions, as well as composition with the variable transform R to arrive at the functions denoted $\mathcal{T}$ and Ω. The components of the genus expansion of these functions, $\mathcal{T}^{(g)}$ and $\Omega^{(g)}$, obey an interwoven web of equations, which is illustrated

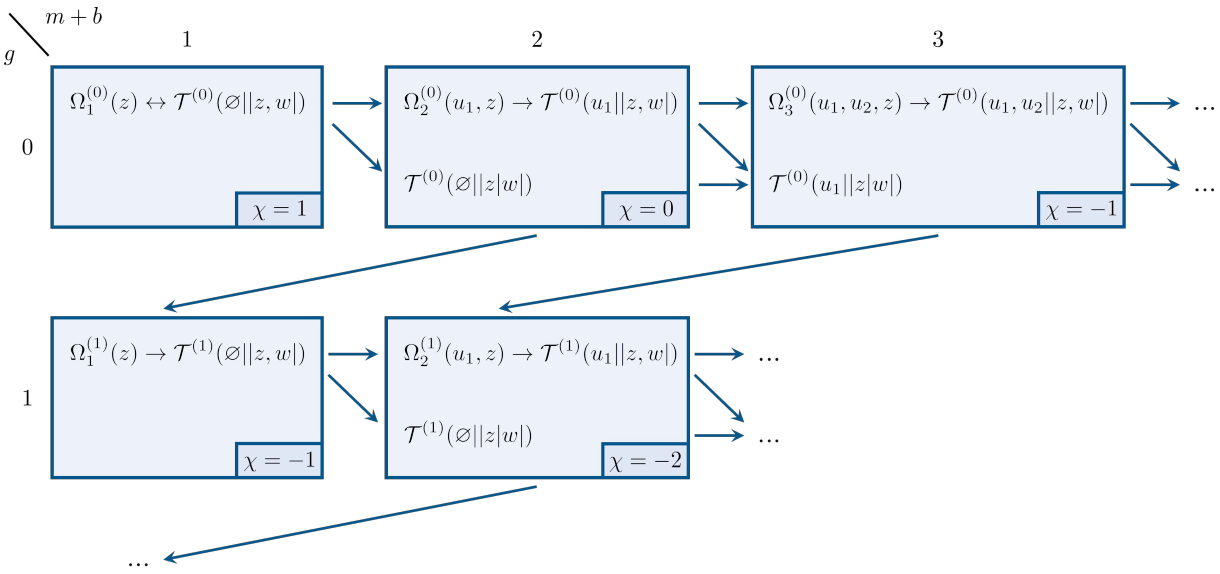

Figure 1.3.1: This graphic, which is borrowed from [BHW22], illustrates the interwoven web of equations determining $\mathcal{T}^g$ and $\Omega^{(g)}$. $\Omega_1^{(0)}(z) = \frac{1}{N}\sum_k r_k \mathcal{G}^{(0)}(\epsilon_k, z)$ and $\mathcal{T}^{(0)}(\varnothing||z,w) = \mathcal{G}^{(0)}(z,w)$ which are determined through the solution of $\mathcal{G}^{(0)}(z,w)$ in Theorem 1.3.1 constitute the initialization.

in Figure 1.3.1 borrowed from [BHW22]. This allows for the recursive construction of the correlation functions of the model starting form the solution of $\mathcal{G}^{(0)}(z,w)$ of Theorem 1.3.1.

In order to get more intuition about the generalized correlation functions it is instructive to take another look at the definition of the cumulants in Equation (1.23) and their genus expansion from the perspective of perturbation theory, see [Bra22, Chapter 6]. The general idea of a perturbative expansion is that one expands the theory around the free theory associated to $\lambda = 0$ and then, crucially exchanges the integral over the configurations with the sum. The latter step is, in general, inherently ill-defined and the resulting series in λ has zero radius of convergence[§]. Instead, one can view the perturbative expansion as a formal expression. For the cumulants one arrives at

$$\langle \mathfrak{e}_{p_1,q_1} \cdots \mathfrak{e}_{p_n,q_n} \rangle_c = \sum_{v=0}^{\infty} \frac{N^v(-\lambda/4)^v}{v!} \Bigg[\int \mathrm{d}\mathcal{M}\, \Phi_{p_1,q_1} \cdots \Phi_{p_n,q_n} \times \sum_{j_i,k_i,l_i,m_i=1}^{N} \prod_{i=1}^{v} (\Phi_{j_i k_i} \Phi_{k_i l_i} \Phi_{l_i m_i} \Phi_{m_i j_i}) \Bigg]_c . \tag{1.36}$$

This expression can be evaluated using ribbon graphs, which are Feynman graphs, with edges that carry two labels such that the vertices obtain a cyclic order of labels. Vertices

[§]It is believed that an expansion at the free theory will generally do not give handleable results. Future research will show, if one should rather expand the theory at the solution to the planar sector instead.

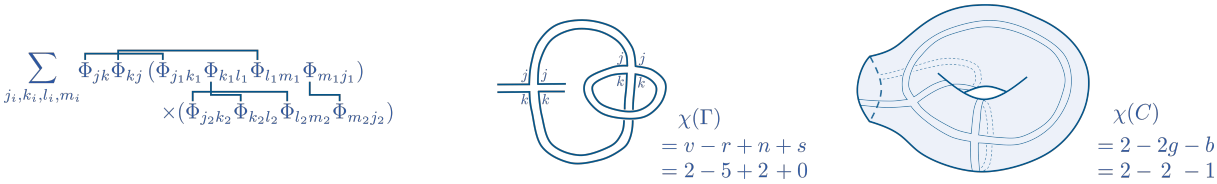

Figure 1.3.2: This illustrates how a cumulant is associated to a ribbon graph (middle) and a Riemann surface with boundary (left). The contractions of fields induce identification of strands, which form the graph Γ. This graph can be drawn on a Riemann surface C, whose topological type is prescribed by the cycle type of the external fields and the topology of the graph encoded in its Euler characteristic.

correspond to cycles of indices with a factor $(-\lambda)$. Fields $\Phi_{jk}\Phi_{lm}$ in the cumulant above are contracted according to the propagator of the free theory, $\frac{\delta_{p\tilde{q}}\delta_{q\tilde{p}}}{N(E_p+E_q)}$, using Wicks theorem.

Note that the number of such contractions is calculated by half the number of involved fields $r = \frac{\#(\text{fields})}{2} = \frac{n+4v}{2} = 2v + n/2$. Using this count and recalling that a cumulant is non-zero if and only if its indices form cycles of a permutation τ one can show that

$$N^n \langle \mathfrak{e}_{p_1,\tau(p_1)} \cdots \mathfrak{e}_{p_n,\tau(p_n)} \rangle_c = \sum_{v=0}^{\infty} \sum_{\Gamma \in \mathfrak{G}^v_{\tau;p_1,\dots,p_n}} N^{v-r+n+s_\Gamma} \varpi_r(\Gamma)\,, \tag{1.37}$$

where s_Γ is the number of loops of Γ. The sum is performed over the set $\mathfrak{G}^v_{\tau;p_1,\dots,p_n}$ of labelled connected ribbon graphs with v four-valent vertices and n one-valent vertices labelled by external indices $((p_k,\tau(p_k)))_{k\in[\![1,n]\!]}$. The weight ϖ_r is obtained from the calculation above and summing over all loop-indices $\{k_i\}_{i\in[\![1,s]\!]}$, i.e. all indices that are not identified with an external index upon contractions, with a factor N^{-s}.
These graphs, with their fixed cyclic order of indices at the vertices that sets them apart from ordinary Feynman graphs, can be embedded into *Riemann surfaces with boundary*. Riemann surfaces are properly introduced in the beginning of next chapter in Section 2.1. Here they can be viewed as surfaces embedded into $\mathbb{R}^3$ with a Riemannian metric on them. As it will be discussed later, closed Riemann surfaces are characterized by a natural number g, which is denoted the genus. For an illustration see Figure 2.1.1 in the next chapter. Riemann surfaces with boundary can be obtained from closed ones by removing open discs and their genus is defined as the genus of the corresponding closed surface. It turns out, that one can show, that the exponent of N in equation (1.37) computes a related invariant of Riemann surfaces

$$v - r + n + s = \chi \equiv 2 - 2g - b\,, \tag{1.38}$$

the Euler characteristic χ, see Section 2.1. This associates a cumulant, or the corresponding correlator $G^{(g)}$, to a Riemann surface of genus g with b boundaries, where

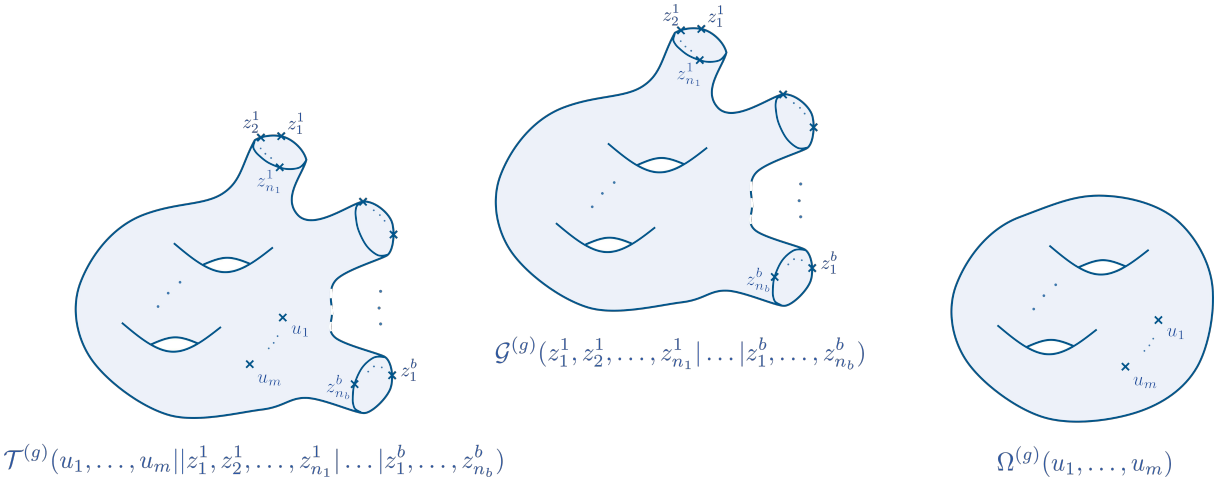

Figure 1.3.3: In this graphic, adapted from [Bra22], the Riemann surfaces associated to the different correlation functions constructed in this section are sketched. Note that the variables $\{z_i^k\}_{i\in[\![1,n_k]\!]}$ are supported on the k-th boundary, for $i \in [\![1,b]\!]$, of the Riemann surface associated to the correlation function while the variables $\{u_i\}_{i\in[\![1,m]\!]}$ are supported on the interior of the surface.

b is the number of cycles of τ, see Figure 1.3.2. By translating this to the functions $\mathcal{G}^{(g)}(z_1^1,\dots z_{n_1}^1|\dots|z_1^b,\dots,z_{n_b}^b)$ the variable z_i^k corresponds to the i-th point on the k-th boundary. Extending this to the generalized correlation functions, the derivatives acting on $\mathcal{G}^{(g)}$ in the definition of $\mathcal{T}^{(g)}(u_1,\dots,u_m||z_1^1,\dots z_{n_1}^1|\dots|z_1^b,\dots,z_{n_b}^b)$ additionally mark m different points on interior of the Riemann surface associated to $\mathcal{G}^{(g)}$. In this language $\Omega^{(g)}(u_1,\dots,u_m)$, then, corresponds to a closed Riemann surface with marked points, see Figure 1.3.3.
The form of the relations for $\Omega^{(g)}$ and their solutions as well as the graphical language suggest [BHW22, HW21, HW23] that these objects, or rather the differential forms

$$\omega_{g,n}^{\text{QKM}}(z_1,\dots,z_n) \coloneqq \lambda^{2-2g-n}\Omega_n^{(g)}(z_1,\dots,z_n)\,\mathrm{d}R(z_1)\cdots\mathrm{d}R(z_n)\ , \tag{1.39}$$

connect the interwoven structure found in the Quartic Kontsevich Model to the universal framework of *topological recursion*. This theory was uncovered by Leonid Chekhov, Bertrand Eynard, and Nicolas Orantin in the years leading to 2007 [CEO06, EO07] and generalized in the following years in a plethora of different ways. One of these, called *blobbed topological recursion*, due to Gaëtan Borot and Sergei Shadrin [BS17] of 2016, is mentioned here as it is believed to be the appropriate framework for the Quartic Kontsevich Model. An exposition of the theory of topological recursion is found in Section 2.2 giving a necessarily incomplete account of it. For a more thorough introduction to the subject the reader may refer to the textbook [Eyn16] as well as the quickly growing literature.

1.4 LSZ model

The model, which is introduced in this chapter, the Quartic Kontsevich Model, is a theory of hermitian matrices with quartic interaction. In that sense it closely resembles the original Kontsevich matrix model, which is its cubic analogue. As it will be discussed in the next chapter the latter model plaid a crucial role in Maxim Kontsevich's proof [Kon92] of the famous Witten conjecture [Wit90] about the generating function of intersection numbers satisfying the differential equations of the KdV hierarchy, which was motivated by considerations of gravity in two dimensions. This has led to a wave of attention for closely related models such as the Quartic Kontsevich Model or the *LSZ model* [LS02, LSZ04] named after Edwin Langmann, Richard Szabo and Konstantin Zarembo. In the form it should be discussed here it is defined by the action

$$S^{\text{LSZ}}[\Phi, \Phi^\dagger] = -N \operatorname{tr}\left(E\Phi\Phi^\dagger + \tilde{E}\Phi\Phi^\dagger + \frac{\lambda}{2}(\Phi^\dagger\Phi)^2 \right). \tag{1.40}$$

In the above E and $\tilde{E}$ are two distinct $N \times N$ hermitian external matrices and λ the coupling constant as described for the Quartic Kontsevich Model. Note that the associated partition function integrates over the space of *complex* $N \times N$ matrices. This distinguishes the LSZ model from the Quartic Kontsevich Model and was believed to by the reason for dramatically different analysis and results in the two different models [ST20]. However, it was recently shown by Johannes Branahl and Alexander Hock in [BH23] using the framework of topological recursion that the models can in fact be treated on a similar footing. In their work their presented a complete solution of the model, which will be used in the subsequent chapter for the explicit investigation of correlators of low (g, n), see Examples 2.2.3 and 2.2.4 and their interpretation in terms of Intersection numbers on the moduli space of curves, see Chapter 2.


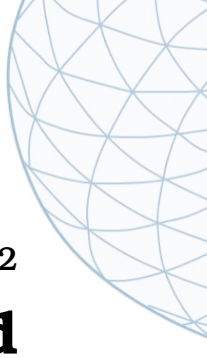

CHAPTER 2

The Moduli Space of Curves and Topological Recursion

In the following chapter the moduli space of complex curves is introduced, mainly following [Zvo12, Sch20]. It constitutes a central and unifying theme of this thesis. For further reading, reference as well as broader context the reader is invited to select from a plethora of textbooks and lecture scripts that goes far beyond [Har77, Hat02, ACG11, Lan82, HM98, Pan16].
As an interesting subject of study by itself and as one of the oldest and most studied moduli problems, it allows for a variety of different perspectives and approaches and thus appears in a wide range of mathematical disciplines. It will be retraced how the Quartic Kontsevich Model as well as the LSZ model, introduced in the previous Chapter 1, relate to the moduli space of curves via the universal framework of topological recursion. This, which is original work due to the author of this thesis, uses a the language of topological recursion, introduced by Chekhov, Eynard and Orantin [CEO06, Eyn11b, Eyn16], in a unified and consistent manner, see Section 2.2.3 as well as Examples 2.2.5 and 2.2.6 and Section 2.2.6. In this process for the Quartic Kontsevich Model explicit novel data is computed that will be helpful in future research in understanding further the deep structures that the model exhibits such as integrability [HB21, Kac90, BCEG23].
In the subsequent Chapter 3 using a combinatorial approach via Ehrhart theory a compelling pattern, logarithmic concavity, is uncovered in intersection numbers on the moduli space of curves.

2.1 Formal introduction to the moduli space of curves

The main object of study are *Riemann surfaces with marked points*, [Rie57, Wey13, Har77]. There are different perspectives on these objects. From a complex point of view, Riemann surfaces are

connected, complex manifolds of complex dimension one.

If one rather approaches these objects from a real setting, one considers Riemannian metrics on smooth real manifolds. These are smooth families of inner products on the tangent spaces, which assign to each point on the manifolds a positive definite symmetric bilinear form. By forming equivalence classes of positive functions on the space of Riemannian metrics, which are denoted conformal structures, angles but not lengths can be measured on these surfaces. Then, Riemann surfaces are

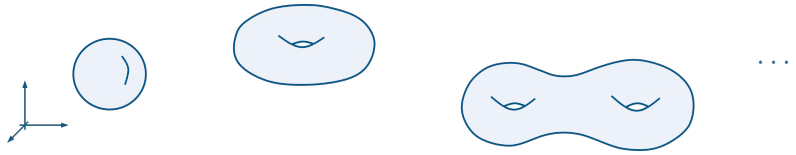

Figure 2.1.1: This illustrates Riemann surfaces of genus $g = 0, 1, 2$ – a sphere, a torus and a surface of genus two – embedded into $\mathbb{R}^3$.

connected, oriented, real manifolds of real dimension two
together with a conformal structure.

More formally, it can be shown that in algebro-geometric terms a Riemann surface X underlies a unique *one-dimensional, smooth and irreducible projective complex algebraic variety* C, also called curve.

Definition 2.1.1. A *projective complex algebraic variety* is given by the set of zeros of finitely many complex homogeneous polynomials in $(n+1)$ variables, viewed as an algebraic subset of the corresponding n-dimensional complex projective space $\mathbb{CP}^n$, for $n \in \mathbb{N}$.

A smooth complex projective algebraic variety is irreducible, if and only if the underlying complex manifold is connected. In the following only compactifiable Riemann surfaces are considered, which are the open complement of a finite subset $S = \{x_1, \ldots, x_n\}$ of labelled points in a uniquely determined compact Riemann surface

$$X = \overline{X} \setminus S\,. \tag{2.1}$$

These are the complex manifolds given by the complex points in smooth, irreducible algebraic curves that are the open complement of the finite subset in a smooth *projective* algebraic curve. On a smooth curve, that is one without any singularities, the Jacobian of the defining functions is required to have full rank in every point. Further below, the requirement of smoothness will actually be relaxed, allowing for nodal singularities. In the neighborhood of a nodal singularity the surface can be described by $\{(x, y) \in \mathbb{C} \colon xy = 0\}$.
Such Riemann surfaces $X = \overline{X} \setminus S$ are topologically classified by their *topological type*, which is encoded in their *Euler characteristic*

$$\chi(X) \coloneqq \textstyle\sum_k (-1)^k \dim H_k(X)\,, \tag{2.2}$$

where $H_k(X)$ denotes the k-th homology group of Riemann surface X or respectively the curve C, see Appendix A.2. In the case of compact Riemann surfaces $\overline{X}$ with n marked points, corresponding to the deleted points $S \subset X$, this calculates to

$$\chi = 2 - 2g - n\,, \tag{2.3}$$

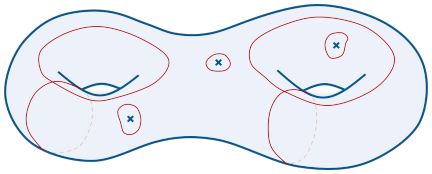

Figure 2.1.2: This depicts a Riemann surface of genus two with three marked points illustrating non-contractible cycles (red).

where g is denoted as the (topological) genus[†]. In Figures 2.1.1 and 2.1.2 this is pictorially explained. Using the Euler characteristic one can define a strict partial order on the topological type (g,n) of Riemann surfaces by calling $(g,n) > (g',n')$ if $\chi_{g,n} < \chi_{g',n'}$.
In order to illustrate the definition further, Riemann surfaces of genus 0 and 1 are examined in the following.

Example 2.1.1. *The orientable manifold of* ***genus zero*** *is the sphere, which has a unique Riemann surface structure being that of* $\mathbb{CP}^1$*. Using its automorphism group,* $PSL(2,\mathbb{C})$*, three of its marked points can be send to a fixed location, making* $(\mathbb{CP}^1;0,1,\infty)$ *the unique Riemann surface of topological type* $(g,n)=(0,3)$ *up to isomorphism.*
At ***genus one*** *the torus obtains its Riemann surface structure by the identification with the quotient of the complex plane by a lattice. The automorphism group of such elliptic curves is harder to describe, containing even the curve itself. From intuition, it is, however, easy to gather that the order of the automorphism group is only infinite if there are no marked points, generated by infinitesimal rotation along one of the two cycles.*

Noting that for $g \geqslant 2$ there is a bound on the order of the automorphism group [Hur93], one realizes that as long as the Euler characteristic is strictly negative, that is

$$2g-2+n>0\,, \tag{2.4}$$

the automorphism group is finite. In that case one can make sense of a moduli space of complex curves $\mathcal{M}_{g,n}$ avoiding the algebro-geometric language of stacks for the most part inferring from this theory only if necessary.
There are different levels to understanding the space of Riemann surfaces with marked points. At a cursory level one can explore the sets of Riemann surfaces of different topologies. However, the use of such inspections is limited. Thus, one tries to investigate the geometry of the space of Riemann surfaces. While explicit computations can serve as useful tools to get intuition at low topologies it has been proven interesting to compute invariants of the geometry of the space of Riemann surfaces. This requires more structure. At a formal level, the precise way to introduce the moduli space is to define it as a Deligne-Mumford stack. This quest will, however, not be undertaken here.

[†]While in the present context, Equation (2.3) can be thought of as a definition, algebro-geometrically it can be defined as the dimension of the space of sections of the cotangent line bundle on the curve. See below Definition 2.1.2

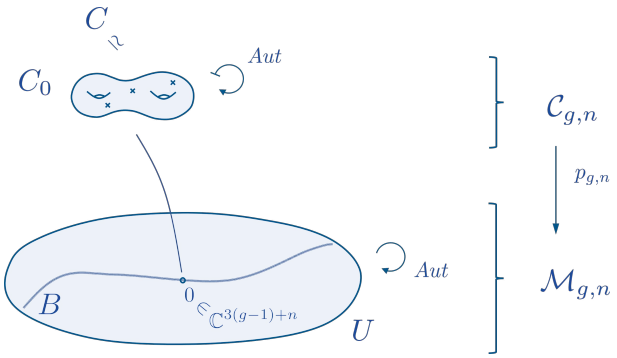

Figure 2.1.3: This illustrates the construction of $\mathcal{M}_{g,n}$ and its universal curve $\mathcal{C}_{g,n}$, given in Theorem 2.1.1.

Instead, most of the structure can be captured by approaching $\mathcal{M}_{g,n}$ as a manifold with local automorphisms, an orbifold.
The tool used to define and investigate the geometry of $\mathcal{M}_{g,n}$ is the idea of a family $p\colon \mathcal{C} \to B$ of genus g curves with n marked points. Every fibre over geometric points of the base scheme B of this family is a (smooth) Riemann surface. Such a family is endowed with n disjoint sections $s_i : B \to \mathcal{C}$ corresponding to the marked points of the curves, such that $p \circ s_i = \mathrm{id}_B$. Furthermore, one can relate two families $p_1\colon \mathcal{C}_1 \to B_1$ and $p_2\colon \mathcal{C}_2 \to B_2$ by pull back along a morphism $\psi\colon \tilde{B}_2 \to B_1$ for $\tilde{B}_2 \subset B_2$ by requiring that $p_2^{-1}(\tilde{B}_2) \subseteq \mathcal{C}_2$ and that the pull back of $\mathcal{C}_1$ under ψ be isomorphic.

Theorem 2.1.1 ([HM98, Zvo12])**.** *Let C be a Riemann surface of topological type (g,n), such that $\chi(C) < 0$, and denote Aut its (finite) isomorphism group. Then there exists*

- *an open bounded simply-connected domain $U \subset \mathbb{C}^{3(g-1)+n}$,*
- *a family $p\colon \mathcal{C} \to U$ of Riemann surfaces of topological type (g,n),*
- *an Aut-action on $\mathcal{C}$ descending to an Aut-action on U such that*
  - *the fibre C_0 over $0 \in U$ is isomorphic to C,*
  - *the action of Aut preserves C_0 and acts as its symmetry group,*
  - *given any family $p_B : \mathcal{C}^B \to B$ such that $p_B^{-1}(b) \simeq C$ for some $b \in B$, there exists an open subset $\tilde{B} \subset B$ containing b and a map $\psi : \tilde{B} \to U$ (unique up to the action of Aut), such that the restriction of the family p_B is the pull-back by ψ of the family p.*

In Figure 2.1.3 the construction of the theorem is illustrated. This theorem achieves a definition of the moduli space $\mathcal{M}_{g,n}$ as the space covered by charts U/Aut as well as its universal curve $p_{g,n}\colon \mathcal{C}_{g,n} \to \mathcal{M}_{g,n}$, where $\mathcal{C}_{g,n}$ is covered by the sets $\mathcal{C}$.
It turns out that $\mathcal{M}_{g,n}$ is in general not compact. This can already be seen extending Example 2.1.1 to Riemann surfaces of topological type $(0,4)$.

Example 2.1.2. *In Example 2.1.1 it was shown that using the automorphism group of $\mathbb{CP}^1$ three marked points can be set to 0, 1, and ∞. This, however, exhausts the ability*

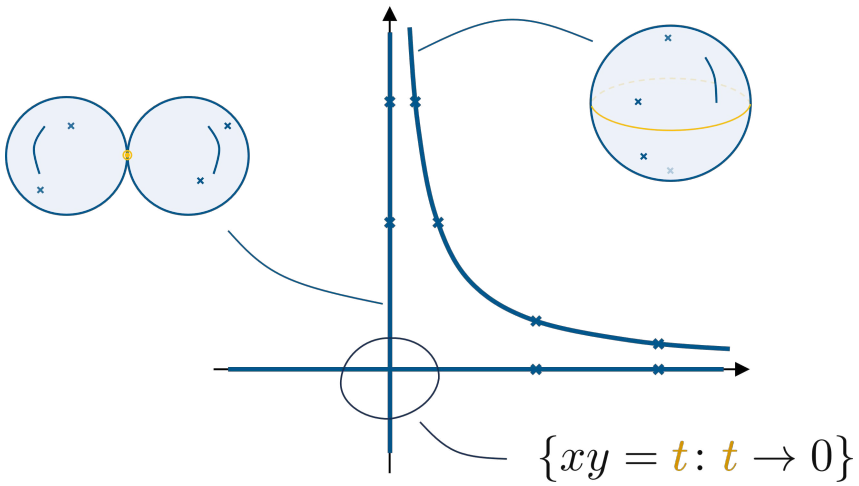

Figure 2.1.4: This illustrates how a smooth Riemann surface with four marked points degenerates into a nodal Riemann surface with two components with each three special points (two marked points and the node). The node is a transverse intersection, such that in local coordinates x, y its neighborhood is described by $xy = t$ in the limit $t \to 0$.

to fix points. The location of any additional point on $\mathbb{CP}^1$ *is a free parameter* t*, also called modulus,*

$$(C, x_1, x_2, x_3, x_4) \simeq (\mathbb{CP}^1, 0, 1, \infty, t)\,. \tag{2.5}$$

Thus, $\mathcal{M}_{0,4} \simeq \mathbb{CP}^1 \setminus \{0, 1, \infty\}$*. In order to see what happens when the modulus approaches the boundary of* $\mathcal{M}_{0,4}$*, one may look at* $t \to 0$*. In that case, naively* x_1 *and* x_4 *collided. However, transforming to another chart by* $x \mapsto x/t$*, one obtains*

$$(C, x_1, x_2, x_3, x_4) \simeq (\mathbb{CP}^1, 0, 1/t, \infty, 1)\,. \tag{2.6}$$

Then, in the limit $t \to 0$ *the points* x_2 *and* x_3 *seem to collide. As none of these perspectives is to be preferred, the geometric picture is, that there are two components with either of the two pairs of points connected by a node. The described situation is pictorially explained in Figure 2.1.4. A different perspective is to describe this degeneration as the limit of a shrinking cycle in the surface. In that case the modulus* t *can be interpreted as the length of the cycle shrinking to zero.*

As constructing geometric invariants via cohomology is not feasible in the non-compact setting, Pierre Deligne and David Mumford in [DM69], generalized by Finn Knudsen [Knu83], constructed a consistent compactification denoted $\overline{\mathcal{M}}_{g,n}$. They introduced the notion of a *stable* nodal curve in order to correctly treat the degeneration behavior illustrated in Example 2.1.1, in that it allows homologically-inequivalent cycles to shrink. Therefore, note that a nodal curve, i.e. curves with only smooth points or nodal singularities, can be de-singularized in two ways. *Smoothening* a node refers to replacing the two discs with identified centers that form its neighborhood with a

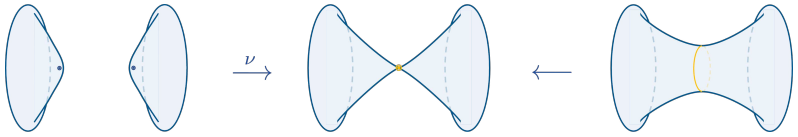

Figure 2.1.5: This illustrates the normalization map ν (left) and the smoothening (right) of a node (middle). Normalizing the surface, the two preimages of the node are marked points of the respective connected components. The node is actually supposed to be a *transverse* intersection of the two components. On the smoothened surface the cycle that is shrunk to obtain the singular surface is indicated.

cylinder. Alternatively, *normalizing* a node describes replacing the same with two disjoint discs, see Figure 2.1.5. Using this notion one observes that starting from the finite setting of smooth Riemann surfaces modulo isomorphism one can construct infinitely many nodal curves. However, this process introduces a series of components with automorphism group of infinite order. This suggests the definition of a stable nodal curve.

Definition 2.1.2. A complete, connected nodal curve is *stable*, if its automorphism group has finite order.

It turns out that in this setting the notion of (topological) genus introduced before is not well-defined anymore. Instead, there are two different ways to define a genus of a nodal surface, which agree in the case of a smooth projective curve with the topological genus of the underlying compact Riemann surface (see also [Hir66]). The geometric genus is given by

$$g_{\mathrm{geo}}(C) \coloneqq \dim H^0(C, \Omega^1_C)\,, \tag{2.7}$$

where Ω^1_C is the dualizing sheaf of C, given as the subsheaf of $\nu_*\Omega^1_C$ characterized by opposite residues in the two points $\nu^{-1}(p)$ for each node p of C. The arithmetic genus is given by $g_{\mathrm{a}}(C) \coloneqq \dim H^1(C, \mathcal{O}_C)$, which agrees with

$$g_{\mathrm{a}}(C) = 1 - \dim H^0(C, \mathcal{O}_C) + \dim H^1(C, \mathcal{O}_C)\,, \tag{2.8}$$

as the considered curves are connected. Interpreting these definitions using the normalization, one finds that when a smooth surface degenerates the geometric genus drops, while the arithmetic genus is constant[‡],

$$\begin{aligned} g_{\mathrm{geo}}(C) &= g_{\mathrm{geo}}(\nu^{-1}C) & g_{\mathrm{a}}(C) &= g_{\mathrm{a}}(\nu^{-1}C) + \#(\text{nodes of } C) \\ &= g(\nu^{-1}C)\,, & &= g(\nu^{-1}C) + \#(\text{nodes of } C)\,, \end{aligned} \tag{2.9}$$

[‡]In this text, when referring to the topological type (g, n), the genus g should be interpreted as the arithmetic genus of the curve. This is because in families of nodal curves the arithmetic genus is constant, referring back to the construction of the moduli space, see Theorem 2.1.1.

see [Zvo12]. This can be used to obtain a description of the stability condition, similar to the smooth setting. In fact, a nodal curve is stable, if for every component $\nu^{-1}(C)_k$ of the normalization of a nodal curve C indexed by k,

$$2g(\nu^{-1}(C)_k) - 2 + \tilde{n}_k > 0\,, \tag{2.10}$$

where $\tilde{n}_k$ is the number of marked points plus the number of preimages of nodes under ν on the respective component.
Later in the text a combinatorial representation of nodal curves in terms of graphs will often be utilized. In this dual description the vertices v of the graph correspond to irreducible components C_v of the curve C and are decorated with the genus of $\nu^{-1}(C_v)$. The vertices v and w are connected by an edge $e_{v,w}$ prescribed by the nodes of C. Half edges, or leaves, attached to a vertex v correspond to the marked points on C_v and obtain a numbering from the marked points of C. In order to work with this dual description the properties of the curves need to be translated to the graphs: The arithmetic genus of the curve translates to the first Betti number b_1 of the graph and the geometric genus to the sum of the decorations of the vertices. Automorphisms $\operatorname{Aut}\Gamma$ of the graph Γ are re-labellings of the edges and vertices that preserve the structure of the graph and are isomorphic to a subgroup of the automorphism group of the curve. In fact, [Sch20], one can construct the short exact sequence

$$0 \longrightarrow \prod_{v \text{ vertex}} \operatorname{Aut}(\nu^{-1}(C_v)) \longrightarrow \operatorname{Aut}(C) \longrightarrow \operatorname{Aut}(\Gamma) \longrightarrow 0\,. \tag{2.11}$$

The stability condition can then be translated to

$$2g(v) - 2 + n(v) > 0 \tag{2.12}$$

for all vertices v, where $n(v)$ is the number of edges and half-edges attached to v.
By allowing *stable* curves Deligne and Mumford and Knudsen showed that the universal curve extends to the compact setting

$$p_{g,n} \colon \bar{\mathcal{C}}_{g,n} \longrightarrow \overline{\mathcal{M}}_{g,n}\,. \tag{2.13}$$

Remark 2.1.1.1. In this setting issues arise when comparing two families $p_1 \colon \mathcal{C}_1 \to U_1$ and $p_2 \colon \mathcal{C}_2 \to U_2$ on the overlap $S = U_1 \cap U_2$. Defining a morphism $\psi \colon S \to M$, it is fully determined in terms of its restriction to U_1 and U_2. The family of curves up to isomorphism, however, is not necessarily uniquely described by its restrictions.
In order to fix this, see [Sch20, Section 5 and 6.2], one can facilitate category-theoretic language. As a stack, $\overline{\mathcal{M}}_{g,n}$ is given by a category with

$$\operatorname{Ob}\overline{\mathcal{M}}_{g,n} = \{(p \colon \mathcal{C} \to U,\ s_1, \dots, s_n \colon U \to \mathcal{C}) \colon \text{family of nodal genus } g \text{ curves}\} \tag{2.14}$$

together with

$$\operatorname{Mor}\left(p' \colon \mathcal{C}' \to U', p \colon \mathcal{C} \to U\right) = \left\{ \begin{array}{ccc} \mathcal{C}' & \xrightarrow{\hat{f}} & \mathcal{C} \\ \downarrow{\scriptstyle p} & & \downarrow{\scriptstyle p} \\ U' & \xrightarrow{f} & U \end{array} \;:\; \begin{array}{l} (\hat{f}, f) \text{ make } \mathcal{C}'/U' \\ \text{a pullback of } \mathcal{C}/U \end{array} \right\}. \tag{2.15}$$

Adding the morphisms to the data, one is able to prescribe the glueing of two families on their overlap.
It turns out that the moduli stack of curves has especially nice structure. In fact, it is smooth as a stack and its charts can be chosen in a way that describes its algebraic structure – it is a smooth Deligne-Mumford stack of dimension

$$d_{g,n} \coloneqq \dim_{\mathbb{C}} \overline{\mathcal{M}}_{g,n} = 3(g-1)+n\,. \tag{2.16}$$

For a short introduction to stacks [Fan01] might serve as a decent start.

Constructed in that manner, $\overline{\mathcal{M}}_{g,n}$ enjoys a *stratified structure* in terms of dual stable graphs with n leaves and genus g. Therefore, associate to a stable graph Γ of topological type (g,n) the set of curves

$$\mathcal{M}_\Gamma \coloneqq \{C \text{ nodal curve of type } (g,n)\colon \Gamma_C \simeq \Gamma\}\,, \tag{2.17}$$

which is an irreducible, locally closed subset of $\overline{\mathcal{M}}_{g,n}$. In particular,

$$\overline{\mathcal{M}}_{g,n} = \coprod\nolimits_\Gamma \mathcal{M}_\Gamma\,, \tag{2.18}$$

where Γ runs through the isomorphism classes of stable graphs. As expected the number of edges of the graph, or the number of nodes of the dual curve gives the co-dimension of $\mathcal{M}_\Gamma$ in $\overline{\mathcal{M}}_{g,n}$. By considering the normalization map one can identify the corresponding closure $\overline{\mathcal{M}}_\Gamma$ of $\mathcal{M}_\Gamma$ as $\prod_{v \text{ vertex}} \overline{\mathcal{M}}_{g(v),n(v)}$ and define the closed inclusion $\iota_\Gamma\colon \overline{\mathcal{M}}_\Gamma \hookrightarrow \overline{\mathcal{M}}_{g,n}$. In particular, restricting to graphs with exactly one edge, that is going to co-dimension one in the boundary of $\overline{\mathcal{M}}_{g,n}$, one finds

$$\coprod_{\Gamma_{(1)}} \overline{\mathcal{M}}_{\Gamma_{(1)}} \simeq \left(\coprod_{(g_1,n_1)+(g_2,n_2)=(g,n)}{}' \overline{\mathcal{M}}_{g_1,n_1} \times \overline{\mathcal{M}}_{g_2,n_2} \right) \coprod \overline{\mathcal{M}}_{g-1,n+2}\,, \tag{2.19}$$

where $\Gamma_{(1)}$ runs through isomorphism classes of stable graphs with one edge and the primed co-product indicates the exclusions of terms containing unstable topologies. This establishes the recursive boundary structure of $\overline{\mathcal{M}}_{g,n}$, which will be key to understanding computations of intersection numbers of cohomological classes in the next section and ultimatively the relation of $\overline{\mathcal{M}}_{g,n}$ to topological recursion, see Section 2.2 as well as Section 2.2.2.

2.1.1 Cohomology on the moduli space of curves

In the previous section the moduli space of complex curves, $\overline{\mathcal{M}}_{g,n}$, is set up including its recursive structure. It is noted that with increasing topological type (g,n), investigating the geometry of $\overline{\mathcal{M}}_{g,n}$ in a naive manner becomes infeasible. A popular tool to obtain information is to construct natural cohomology classes on the moduli space and compute intersection theoretic information from these classes, see [Pan16].
In Appendix A.2 basic notions of singular homology and the associated cohomology

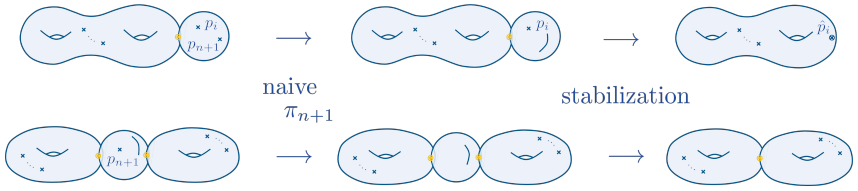

Figure 2.1.6: This illustrates the two cases, in which the stabilization map is not the identity. As the respective component after forgetting the $(n+1)$-st marked point is unstable, it is collapsed. In the upper case collapsing the unstable component, the i-th marked point takes the place of the preimage of the node on the remaining component. In the lower case, the preimages of the nodes on the remaining components connected to the collapsed component are identified.

on varieties over $\mathbb{C}$ are discussed. For a more detailed introduction to this topic the reader is directed to one of many textbooks [Har77, Hat02, ACG11, Lan82, HM98]. In fact, one can construct singular homology and cohomology groups in the setting of stacks [Vis89, Kre99, ACG11]. For the moduli space of curves [Pan16], one is then able to realize an isomorphism between cohomology groups in the stacky description and the language presented here. This is to say that by considering the compactified moduli space as a compact complex manifold with localized quotient singularities, that is an orbifold, Poincaré duality is available between cohomology and homology with rational coefficients. This is why rational coeffients for (co)homology are considered here.
The key tool to constructing the classes that are of interest in this text is the *forgetful map*

$$\pi_{n+1}\colon \overline{\mathcal{M}}_{g,n+1} \longrightarrow \overline{\mathcal{M}}_{g,n}\,, \qquad (C;p_1,\dots,p_n,p_{n+1}) \mapsto (\hat{C};\hat{p}_1,\dots,\hat{p}_n)\,, \tag{2.20}$$

which omits the last marked point of a curve. Here $(\hat{C};\hat{p}_1,\dots,\hat{p}_n)$ denotes the stabilization of $(C;p_1,\dots,p_n)$. This process takes care of the fact that omitting one marked point of a stable curve might return an unstable curve, illustrated in Figure 2.1.6. In fact, one can easily see that as a family over $\overline{\mathcal{M}}_{g,n}$ the forgetful map π_{n+1} is isomorphic to the universal curve and each marked point corresponds to a section $s_i\colon \overline{\mathcal{M}}_{g,n} \to \overline{\mathcal{M}}_{g,n+1}$.
Now, the most natural way to construct cohomology classes on $\overline{\mathcal{M}}_{g,n}$ is using fundamental classes of $\overline{\mathcal{M}}_{g,n}$ itself and its boundary components. Classes obtained in this way, or rather the closure of these under products and pushforwards of forgetful maps and glueing morphisms, form the tautological ring of $\overline{\mathcal{M}}_{g,n}$ and its elements are called *tautological classes* [FP11]. The elements that are of interest here will be introduced in the following.

ψ-classes Let $\Delta \subset \bar{\mathcal{C}}_{g,n}$ be the divisor corresponding to nodes in the singular fibres. On the complement of Δ there is naturally the holomorphic line bundle cotangent to the fibres of the universal curve,

$$\Omega^1_{\pi_{n+1}}\Big|_{\substack{q\in C\\ \text{smooth}}} = T^*_q C\,. \tag{2.21}$$

This line bundle can be extended to the entire $\overline{\mathcal{C}}_{g,n}$ by realizing that locally in Δ the line bundle is generated by the sections $\frac{\mathrm{d}x}{x}$ and $\frac{\mathrm{d}y}{y}$ modulo the relation $\frac{\mathrm{d}(xy)}{xy} = \frac{\mathrm{d}x}{x} + \frac{\mathrm{d}y}{y} = 0$, which is already satisfied on every fibre of $p_{g,n}$. Then,

$$\mathbb{L}_i \coloneqq s_i^*(\omega_{\pi_{n+1}})\,, \tag{2.22}$$

where the line bundle $\omega_{\pi_{n+1}}$ is called the sheaf of relative differentials of the forgetful map, which is isomorphic to the universal curve.

Definition 2.1.3. The *ψ-class* associated to the i-th marked point is defined by the first Chern class

$$\psi_i \coloneqq c_1(\mathbb{L}_i) \in H^2(\overline{\mathcal{M}}_{g,n})\,, \tag{2.23}$$

for $i \in [\![1, n]\!]$.

These classes are the most elementary elements of the tautological ring of $\overline{\mathcal{M}}_{g,n}$ and other elements can be reduced to these. One key property, which will be crucial for determining their intersection numbers using the recursive boundary structure of $\overline{\mathcal{M}}_{g,n}$, is

$$\psi_i - \pi_{n+1}^*(\psi_i) = [\delta_i]\,, \tag{2.24}$$

where the difference class $\delta_i \coloneqq (s_i)_*[\overline{\mathcal{M}}_{g,n}]$ represents for $i \in [\![1, n]\!]$ the divisor on $\overline{\mathcal{M}}_{g,n+1}$ that corresponds to curves on which the respective line bundles do not agree, see [Wit90, Zvo12], equation (2.36). This happens on curves if and only if the stabilization map is not the identity on this curve. These curves are sketched in Figure 2.1.6, where the lower case only happens in co-dimension two not affecting the line bundles. Thus, δ_i is given by curves dual to graphs

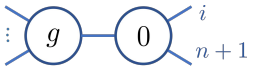

In terms of this divisor one can reinterpret the definition of ψ-classes by writing $\psi_i = -(\pi_{n+1}) * ([\delta_i] \smile [\delta_i])$, verifying its nature as a tautological class, see [Zvo12, Pan16]. This comparison formula is used to prove the important result, called the *string equation*.

Proposition 2.1.2 (String equation)**.** *Let $2g - 2 + n > 0$ and $(d_1, \dots, d_n) \in \mathbb{N}^n$ be such that $\sum_k d_k = d_{g,n+1}$. Then,*

$$\int_{\overline{\mathcal{M}}_{g,n+1}} \psi_1^{d_1} \cdots \psi_n^{d_n} = \sum_{k=1}^{n} \int_{\overline{\mathcal{M}}_{g,n}} \psi_1^{d_1} \cdots \psi_k^{d_k - 1} \cdots \psi_n^{d_n}\,. \tag{2.25}$$

Proof. A nice presentation of a proof can be found in [Wit90], which is recapitulated here.

In order to represent the integral on $\overline{\mathcal{M}}_{g,n+1}$ in terms of integrals on the moduli space with one marked point less, one may use the comparison result (2.24) to write[‡]

$$\psi_i^d = (\pi^*\psi_i)^d + [\delta_i](\pi^*\psi_i)^{d-1}\,. \tag{2.26}$$

Noting that the geometric intersection $\delta_i \cap \delta_j$ for $i \neq j$ is empty, one may deduce

$$\begin{aligned}\int_{\overline{\mathcal{M}}_{g,n+1}} \psi_1^{d_1}\cdots\psi_n^{d_n} = \int_{\overline{\mathcal{M}}_{g,n+1}} (\pi^*\psi_1)^{d_1}\cdots(\pi^*\psi_n)^{d_n} \\ + \sum_{k=1}^{n}\int_{\overline{\mathcal{M}}_{g,n+1}} (\pi^*\psi_1)^{d_1}\cdots[\delta_k](\pi^*\psi_k)^{d_k-1}\cdots(\pi^*\psi_n)^{d_n}\,.\end{aligned} \tag{2.27}$$

Then, the first integral vanishes and the integrals in the sum can be reduced to the desired form using the projection formula. □

Using elementary techniques[ǂ], in low topologies intersection numbers can directly be computed. One finds

$$\int_{\overline{\mathcal{M}}_{0,4}} \psi_1 = 1\,, \qquad \text{and} \qquad \int_{\overline{\mathcal{M}}_{1,1}} \psi_1 = \frac{1}{24}\,, \tag{2.28}$$

as well as, trivially, $\int_{\overline{\mathcal{M}}_{0,3}} 1 = 1$.

κ-classes Another important type of classes in the tautological ring are κ-classes, which are obtained from the pushforward of ψ-classes from moduli spaces of higher topological type [Mum83, AC96, LX09].

Definition 2.1.4. The m-th κ-class is defined by

$$\kappa_m \coloneqq \pi_*\left(\left(c_1(\omega_{\pi_{n+1}}(\delta))\right)^{m+1}\right) = \pi_*\left((\psi_{n+1})^{m+1}\right) \in H^{2m}(\overline{\mathcal{M}}_{g,n})\,, \tag{2.29}$$

where $\delta = \sum_{k=1}^{n}\delta_k$ for $m \in \mathbb{N}$.

Investigating intersection numbers of these κ-classes, one might want to populate the cohomological degree with ψ-classes to obtain a class of top degree. Then, one finds the monomial $\psi_1^{d_1}\cdots\psi_n^{d_n}\psi_{n+1}^{d_{n+1}+1}$. Evaluating this on $\overline{\mathcal{M}}_{g,n}$, one needs to push down inductively the ψ-classes using the comparison result in Equation (2.24) to find

$$(\pi_{n+1})_*\left(\psi_1^{d_1}\cdots\psi_n^{d_n}\psi_{n+1}^{d_{n+1}+1}\right) = \kappa_{d_{n+1}}\psi_1^{d_1}\cdots\psi_n^{d_n}\,, \tag{2.30}$$

and in general

$$(\pi_{n+1}\cdots\pi_{n+k})_*\left(\psi_1^{d_1}\cdots\psi_n^{d_n}\psi_{n+1}^{d_{n+1}+1}\cdots\psi_{n+k}^{d_{n+k}+1}\right) = \left(\sum\nolimits_{\tau\in\mathfrak{S}_k}\kappa_\tau\right)\psi_1^{d_1}\cdots\psi_n^{d_n}\,, \tag{2.31}$$

[‡]Note that $\psi_i[\delta_i] = 0$ because the bundle $\mathcal{L}_i$ is trivial over δ_i. See equation (2.39) of the work [Wit90] that is followed here.

[ǂ]The integral on $\overline{\mathcal{M}}_{0,4}$ can be deduced using Equation (2.24), and the integral $\overline{\mathcal{M}}_{1,1}$ using modular function techniques, see [Zvo12, Pan16], Proposition 2.26.

where $\mathfrak{S}_k$ is the symmetric group of order k, and $\kappa_\tau \coloneqq \kappa_{|\tau_1|} \cdots \kappa_{|\tau_m|}$ for the decomposition of τ into cycles $\{\tau_i\}_{i\in[\![1,m]\!]}$. This might provide insight into the significance of the κ-classes from the physical intuition of moments and cumulants.
To find the general result (2.31) one requires a comparison formula for κ-classes, which is obtained from the comparison relation for ψ-classes by pushing down,

$$\kappa_m - \pi_i^* \kappa_m = (\psi_i)^m \,, \tag{2.32}$$

see for example [Zvo12], Theorem 3.34. As a special case of Equation (2.30), one can show the *dilaton equation*.

Proposition 2.1.3 (Dilaton equation)**.** *In the same setting as Theorem 2.1.2, one has*

$$\int_{\overline{\mathcal{M}}_{g,n+1}} (\psi_1^{d_1} \cdots \psi_n^{d_n}) \psi_{n+1} = (2g-2+n) \int_{\overline{\mathcal{M}}_{g,n}} \psi_1^{d_1} \cdots \psi_n^{d_n} \,. \tag{2.33}$$

Proof. This is a special case of Equation (2.30) for $a_{n+1} = 0$. Noting that

$$\kappa_0 = (2g-2+n)[\overline{\mathcal{M}}_{g,n}] \,, \tag{2.34}$$

one finds the result using the projection formula. □

In the proof above Equation (2.34) was used, see for example [Pan16]. This is a consequence of the Riemann-Roch formula [BS58, Har77, Hir66]. It is intuitive because the degree-zero part of the κ-classes reflects global structure of the moduli space, which is naturally encoded in the Euler characteristic $\chi = 2 - 2g - n$ being a fundamental topological invariant.

2.1.2 Virasoro constraints

In the quest to compute intersection numbers of ψ-classes in the above, see Theorems 2.1.2 and 2.1.3, the recursive structure of $\overline{\mathcal{M}}_{g,n}$ has been used to reduce intersection numbers to moduli spaces of lower (g,n). In order to fully exploit this, it is convenient to collect all intersections of ψ-classes into a generating series

$$F(\{t_i\}_{i\in\mathbb{N}}) \coloneqq \sum_{g\geqslant 0,\, n\geqslant 1}{}' \frac{\hbar^{g-1}}{n!} \sum_{\{d_i\}_i \geqslant 0} \left(\int_{\overline{\mathcal{M}}_{g,n}} \psi_1^{d_1} \cdots \psi_n^{d_n} \right) t_{d_1} \cdots t_{d_n} \,, \tag{2.35}$$

recalling that the notation of intersection numbers prescribes that the integral vanishes as long as $\sum_k d_k \neq d_{g,n} = 3g-3+n$.
The complete set of *Virasoro constraints*, which determine all ψ-class intersection numbers, that is all coefficients of F, are generated by the operators L_m. These operators act on functions in the variables $p_k = t_k/(2k+1)!!$. Therefore, following [Zvo12], Section 4.2, let

$$J_k(f) \coloneqq p_k f \,, \qquad J_{-k}(f) \coloneqq k \frac{\partial}{\partial p_k} f \,, \qquad \text{for } k \in \mathbb{N}^\times \,, \qquad \text{and} \qquad J_0 \coloneqq 0 \,, \tag{2.36}$$

for a function $f = f(\{p_k\})$, and define the series $J(z) := \sum_{k\in\mathbb{Z}} \frac{J_k}{z^{k+1}}$. Then,

$$\sum_{m\in\mathbb{Z}} \frac{L_m}{z^{m+2}} := \frac{1}{2} :J(z)^2: , \tag{2.37}$$

where $:O:$ denotes the normal ordering[§] of the operator O. The operators in $\{L_m\}_{m\in\mathbb{Z}}$ are called *Virasoro* operators as they satisfy the commutation relations

$$[L_n, L_m] = (n-m)L_{n+m} + \frac{n(n^2-1)}{12}\delta_{n+m,0} , \tag{2.38}$$

between each other as well as $[J_k, L_m] = kJ_{k+m}$, with the currents J_k.

Theorem 2.1.4 (Witten-Kontsevich)**.** *For every integer $m \geqslant -1$ one has*

$$(L_{2m} - J_{2m+3} + \delta_{k,0}/8)\, e^{F(((2k-1)!!p_{2k+1})_k)} = 0 . \tag{2.39}$$

In fact, the dilaton and string equation of Theorems 2.1.2 and 2.1.3 are contained in this set of relations. They are equivalent to $m = 0$ and $m = -1$. For $m > 0$ the Virasoro relations translate to

$$\begin{aligned}
&(2m+3)!! \int_{\overline{\mathcal{M}}_{g,n+1}} \left(\prod_{i\in[\![1,n]\!]} \psi_i^{d_i} \right) \psi_{n+1}^{m+1} \\
&= \sum_{j=1}^{n} \frac{(2d_j+2m+1)!!}{(2d_j-1)!!} \int_{\overline{\mathcal{M}}_{g,n}} \left(\prod_{i\in[\![1,n]\!]} \psi_i^{d_i} \right) \psi_j^m \\
&\quad + \frac{1}{2} \sum_{d_{n+1}+d_{n+2}=m-1} (2d_{n+1}+1)!!(2d_{n+2}+1)!! \left[\int_{\overline{\mathcal{M}}_{g-1,n+2}} \left(\prod_{i\in[\![1,n]\!]} \psi_i^{d_i} \right) \psi_{n+1}^{d_{n+1}} \psi_{n+2}^{d_{n+2}} \right. \\
&\qquad \left. + \sum_{\substack{g_1+g_2=g,\\ I_1\sqcup I_2=[\![1,n]\!]}} \int_{\overline{\mathcal{M}}_{g_1,|I_1|+1}} \left(\prod_{i\in I_1} \psi_i^{d_i} \right) \psi_{n+1}^{d_{n+1}} \int_{\overline{\mathcal{M}}_{g_2,|I_2|+1}} \left(\prod_{i\in I_2} \psi_i^{d_i} \right) \psi_{n+2}^{d_{n+2}} \right] .
\end{aligned} \tag{2.40}$$

Note that this actually prescribes a recursive determination, as the Euler characteristic of the moduli spaces on the right-hand side is one less than on the left-hand side.
The theorem was originally conjectured by Edward Witten in [Wit90] and then proved shortly after by Maxim Kontsevich [Kon92]. The proof is a seminal work, which relies on deep results from the theory of the moduli space of curves as well as matrix field theory. It will not be presented here. Rather, in the next section topological recursion will be introduced, which acts as a framework in which not only Kontsevich's proof of Wittens conjecture can be understood but a vast class of mathematical studies ranging from systems in mathematical physics including the Quartic Kontsevich Model introduced in Chapter 1 as a matrix model to problems in combinatorics and enumerative geometry.

[§]The normal ordering describes the process of putting all operators in a product that decrease the degree in p_k to the right and all those that increase it to the left, i.e. for $k, l \in \mathbb{Z}_+$ positive $:a_{-k}a_l:= a_l a_{-k}$

2.2 Topological recursion

The remarkable structures described above that were unvieled in the moduli space of curves were later found to be a pivotal example for a universal mathematical structure, which can be found to describe a plethora of phenomena. Inspired from their research on matrix models, Leonid Chekhov, Betrand Eynard, and Nicolas Orantin described what they called *topological recursion* in their work [CEO06, EO07]. The recursive structures of correlation functions of certain matrix models parallels that of the boundary structure of the moduli space, or more explicitly the Virasoro constrains of its intersection numbers, is what is in their theory called abstract loop equations. These fully determine the respective systems and enable to calculate all higher sectors of invariants from a few base cases.
In the following the theory of topological recursion is briefly introduced with an emphasis on its interrelation to the moduli space of curves as well as the LSZ model and, later, to the Quartic Kontsevich Model. This presentation follows references [EO07, Eyn11b, BCEG23] and does not attempt to give an even or even complete overview of the theory and its application. It should rather serve to provide the neccessary language and perspectives for stating the results. These are comprised of explicit calculations of correlation functions of physically motivated models, that is the LSZ and Quartic Kontsevich Model, in terms of intersection numbers on the moduli space of curves. As the latter is not governed by topological recursion itself but an extension called *blobbed topological recursion*, these calculations also give explicit formulas for the additional data called blobs. This will serve future research in understanding the physical significance of the deep structures in the models, which are reflected by topological recursion, in terms of integrable hierarchies, see [EO07, BCEG23, Kac90, HB21].

2.2.1 Definition of topological recursion

Topological recursion computes an infinite sequence of *admissible correlators* $(\omega_{g,n})_{g,n}$, indexed by the pair $(g,n) \in \mathbb{N} \times \mathbb{N}^\times$. These objects are meromorphic 1-forms in each of their n variables on a Riemann surface and are recursively constructed in $2(g-1)+n$. The significance of the (negative) Euler characteristic here might motivate the association of the correlators $\omega_{g,n}$ with Riemann surfaces of topological type (g,n). This picture is frequently exploited in the following.

The initial data of the recursion is provided by a spectral curve, see Figure 2.2.1.

Definition 2.2.1. A *spectral curve* is the data of a Riemann surface Σ together with two meromorphic functions and a meromorphic symmetric bi-differential of the second kind,

$$x\colon \Sigma \to \mathbb{C}\,, \qquad y\colon \Sigma \to \mathbb{C}\,, \qquad \text{and} \qquad B \in H^0(\Sigma^2, K_\Sigma^{\boxtimes 2})\,. \tag{2.41}$$

The symmetric bi-differential B has a pole with unit residue on the diagonal and no

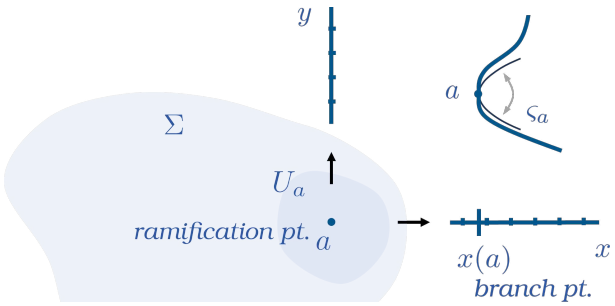

Figure 2.2.1: This illustrates the local behavior of the data of a spectral curve around a ramification point a of the cover x. In this graphic the local Galois-involution ς_β is indicated exchanging the two branches of the curve (top-right).

other pole

$$B(z_1, z_2) \xrightarrow{z_1 \to z_2} \frac{\mathrm{d}z_1\, \mathrm{d}z_2}{(z_1 - z_2)^2} + \text{holo.}\,, \tag{2.42}$$

in local coordinates, where holo. represents possible holomorphic contributions.

Remark 2.2.0.1. The symmetric bi-differential B, which is defined in the definition above as part of a spectral curve is an example for an Abelean differential of the second kind, see [Rie57, Lan82]. In the literature on topological recursion also the term *Bergman kernel* is used for B, which might be misleading, as one is not referring to a so-called reproducing kernel of the Hilbert space of square-integrable holomorphic functions that Stephan Bergman investigated in [BS51].

Depending on the spectral curve data the correlators constructed via topological recursion obey nice properties. The class of spectral curves that is studied the most is regular spectral curves.

Definition 2.2.2. A spectral curve $(\Sigma; x, y; B)$ is called *regular*, if $\mathrm{d}x$ has finitely many simple zeros $\{\beta_i\}_{i\in[\![1,s]\!]}$ and $\mathrm{d}y$ does not vanish there.
The points $\{\beta_i\}_{i\in[\![1,s]\!]} \in \Sigma$ are denoted *ramification points* and their images under x, that is $\{x(\beta_i)\}_{i\in[\![1,s]\!]} \in \mathbb{C}$, *branch points*.

From the spectral curve one constructs the correlators of the unstable topologies, $(g, n) = (0, 1)$ and $(0, 2)$, by setting

$$\omega_{0,1}(z) \coloneqq y(z)\, \mathrm{d}x(z)\,, \qquad \text{and} \qquad \omega_{0,2}(z_1, z_2) \coloneqq B(z_1, z_2)\,. \tag{2.43}$$

The prescription of topological recursion constructing the higher $\omega_{g,n}$, given below, is an inherently local procedure that extracts the information from the spectral curve at the ramification points $\{\beta_i\}_i$ (see Figure 2.2.1) via the *recursion kernel* $\mathcal{K}_i$. It is defined as

$$\mathcal{K}_i(z, q) \coloneqq \frac{\frac{1}{2}\int_{\varsigma_i(q)}^{q} B(z, \bullet)}{\omega_{0,1}(q) - \omega_{0,1}(\varsigma_i(q))}\,, \tag{2.44}$$

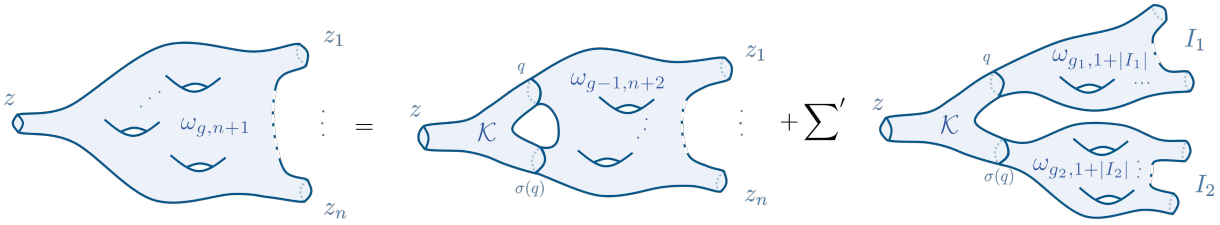

Figure 2.2.2: This illustrates the different terms in the recursion prescription (2.45) using the association of the correlators $\omega_{g,n}$ with Riemann surfaces of genus g with n boundaries corresponding to the n variables. As explained in Remark 2.2.0.2 the recursion is organized as a decomposition of these surfaces into parts of type $(0,3)$.

where ς_i, defined by $x(\varsigma_i(\beta_i)) = x(\beta_i)$, is the local Galois involution of x at the i-th ramification point. Then, the admissible correlators of the stable topological type (g,n), such that $2g-2+n>0$, are given by the recursive prescription

$$\omega_{g,n+1}(z,I) = \sum_{i=1}^{s} \operatorname*{Res}_{q\to\beta_i} \mathcal{K}_i(z,q)\Bigg[\omega_{g-1,n+2}(q,\varsigma_i(q),I) + \sum_{\substack{g_1+g_2=g\\ I_1\sqcup I_2=I}}{}' \omega_{g_1,1+|I_1|}(q,I_1)\,\omega_{g_2,1+|I_2|}(\varsigma_i(q),I_2)\Bigg]. \tag{2.45}$$

In the above $I=\{z_1,\dots,z_n\}$ and in the primed sum terms containing topological types smaller than $(0,1)$ are excluded.

Remark 2.2.0.2. This recursion can be interpreted as a decomposition of a Riemann surface of genus g with $(n+1)$ boundaries into surfaces of genus zero with three boundaries. Therefore, note that using Gauß-Bonnet theorem one can deduce from the Euler characteristic of the surface its mean curvature. In the case $2-2g-n<0$, that is when the recursion applies, the surface associated to $\omega_{g,n}$ is, thus, a hyperbolic surface. This shows that the surface can be glued from hyperbolic polygons or equivalently from surfaces of type $(0,3)$. As this decomposition is not unique the recursion sums over all such possibilities, see Figure 2.2.2.

Basic properties that can be established, which are not manifest in their construction but can be proved using the recursion, for these $\omega_{g,n}$, amongst a vast list, include their symmetry in their variables [EO07] as well as their invariance under symplectic transformations for $2g-2+n>0$, that is such transformations of x and y that preserve the form $\mathrm{d}x\wedge\mathrm{d}y$ [Hoc23b, Hoc23a].
Furthermore, constructed via the recursion (2.45) the $\omega_{g,n}$ constitute a solution to so-called *abstract loop equations*, which is in fact their defining property and holds by construction. The abstract loop equations inherit their name due to their origin in quantum field theoretic methods. In the latter context transformation properties of the measure of the theory can be translated into equations for the correlation functions of the theory. In Chapter 1 these appeared by the name of Dyson-Schwinger equations

and determine the form of the correlation functions $\Omega^{(g)}$. Translating these ideas to the abstract and universal setting of topological recursion one arrives at the *linear and quadratic loop equations*,

$$\omega_{g,n+1}(z, I) + \omega_{g,n+1}(\varsigma_i(z), I) = \mathcal{O}(z - \beta_i)\,, \tag{2.46}$$

and

$$\omega_{g-1,n+2}(z, \varsigma_i(z), I) + \sum_{\substack{I_1 \sqcup I_2 = I \\ g_1+g_2=g}} \omega_{g_1,1+|I_1|}(z, I_1)\omega_{g_2,1+|I_2|}(\varsigma_i(z), I_2) = \mathcal{O}(z - \beta_i)^2\,, \tag{2.47}$$

respectively, for $g \in \mathbb{N}$ and $n \in \mathbb{N}$. It is important to note that although the correlators constructed in this setting are studied the most and behave nicely, they do not provide the complete set of solutions to the abstract loop equations[††]. In fact in order to approach the Quartic Kontsevich Model, defined in Chapter 1 one needs to invoke the more general setting of *blobbed* topological recursion, see Section 2.2.4.
For the sake of completeness and in order to connect to ideas in the previous chapter, note that one can extend the definitions above to $(g, n) = (g, 0)$ by introducing the free energies

$$\mathcal{F}^{(g)} = (2 - 2g)^{-1} \sum_{i=1}^{s} \operatorname*{Res}_{z \to \beta_i} \Phi^{0,1}(z)\omega_{g,1}(z)\,, \qquad \text{for } g \geqslant 2\,, \tag{2.48}$$

where Φ is the primitive of $\omega_{0,1}$ defined by $\mathrm{d}\Phi^{0,1}(z) = \omega_{0,1}(z)$. This relation can be seen as a special case of the dilaton equation for the $\omega_{g,n}$ given by

$$\sum_{i=1}^{s} \operatorname*{Res}_{z \to \beta_i} \Phi^{0,1}(z)\omega_{g,n+1}(z_1, \ldots, z_n, z) = (2 - 2g - n)\omega_{g,n}(z_1, \ldots, z_n)\,. \tag{2.49}$$

The name already suggests a relation of this equation to Equation (2.33). In fact, the upcoming Example 2.2.1 will show that the $\omega_{g,n}$ associated to a basic spectral curve compute intersection numbers of ψ-classes. In that case the dilaton equation above reduces to the result of Theorem 2.1.3.
For $g \in \{0, 1\}$ the free energies are defined using theta functions, which will not be discussed here (see [EO07, Eyn16]). The set $(\mathcal{F}^{(g)})_{g\in\mathbb{N}} \subset \mathbb{C}$ encodes the complete information about the model, which is described by topological recursion as its partition function $\mathcal{Z}$ is given by

$$\log \mathcal{Z} = \sum_{g\in\mathbb{N}} N^{2-2g}\mathcal{F}^{(g)}\,. \tag{2.50}$$

[††]Although at a later stage it is obvious that equations that reduce the most general solution to the abstract loop equations to that special one given in Equation (2.45) is requiring vanishing of all blobs, the author is wondering whether there are more natural relations comparable to the abstract loop equations or a setting in that the vanishing has a natural interpretation in.

Already in the original work Eynard and Orantin were able to show the remarkable connection of topological recursion to integrable hierarchies. These will not be introduced here as both content as well as theoretical and computational machinery would break the scope of this text. It will only be mentioned that these infinite systems of differential equations, which describe different kinds of systems from water waves in shallow water to structures in infinite Grassmannians, constitute a complementary approach to topological recursion, see [BCEG23]. Depending on the genericy of the model there are different generalizations of integrable hierarchies. Important examples for hierarchies are the *KdV*-hierarchy [Bou77, KDV95, SW85], the *KP*-hierarchy [KP70, SW85] or most general the *Toda*-lattice [Tod67] as well as the general formulation by Hirota [Hir71, HB21]. The correlators of topological recursion, constructed via Equation (2.45), obey the KdV equations.

Example 2.2.1. *The pivotal example is the spectral curve with* $\Sigma = \mathbb{CP}^1$ *and*

$$x^{\mathrm{KdV}}(z) = z^2\,, \qquad \textit{and} \qquad y^{\mathrm{KdV}}(z) = z\,, \qquad \textit{and} \qquad B^{\mathrm{KdV}}(z_1,z_2) = \frac{\mathrm{d}z_1\,\mathrm{d}z_2}{(z_1-z_2)^2}\,. \tag{2.51}$$

It can be shown that the correlators generated from this spectral curve by topological recursion reproduce the intersection numbers of ψ*-classes on* $\overline{\mathcal{M}}_{g,n}$*, see [Eyn11b], as*

$$\omega_{g,n}^{\mathrm{KdV}}(z_1,\dots,z_n) = (-2)^{\chi_{g,n}} \sum_{d_1+\dots+d_n=d_{g,n}} \left(\int_{\overline{\mathcal{M}}_{g,n}} \psi_1^{d_1}\cdots\psi_n^{d_n}\right) \prod_{i=1}^{n} \frac{(2d_i+1)!!\,\mathrm{d}z_i}{z_i^{2d_i+2}}\,, \tag{2.52}$$

and $\mathcal{F}_{\mathrm{KdV}}^{(g)} = 0$*, for* $g \geqslant 2$*. This is part of the seminal work by Kontsevich [Kon92] where he used a cell-decomposition of the moduli space of curves induced by Strebel differentials to prove the corresponding conjecture by Witten [Wit90]. A first generalization of this spectral curve can be achieved by allowing higher powers in* y *such that*

$$y(z) = \sum_{k\geqslant 0} t_{k+2}\left(z/\sqrt{2}\right)^k\,, \tag{2.53}$$

introducing $\{t_k\}_{k\geqslant 2}$ *which are widely called KdV-times. Deforming the curve* $f(x,y)=0$ *via these parameters, in the space of families* $\{\omega_{g,n}\}_{g,n}$ *generated by topological recursion one obtains*

$$\omega_{g,n}(z_1,\dots,z_n) = (-2)^{\chi_{g,n}} \sum_{d_1+\dots+d_n\leqslant d_{g,n}} \left(\int_{\overline{\mathcal{M}}_{g,n}} e^{\sum_k \hat{t}_k\kappa_k}\psi_1^{d_1}\cdots\psi_n^{d_n}\right) \prod_{i=1}^{n} \frac{(2d_i+1)!!\,\mathrm{d}z_i}{z_i^{2d_i+2}}\,, \tag{2.54}$$

finding that κ*-classes are appearing, see [Eyn11b]. It is pointed out again that the notation of intersection numbers prescribes that the integral vanishes as long as* $\sum_i d_i \neq d_{g,n}$*. The dual times* $\{\hat{t}_k\}_{k\in\mathbb{N}}$ *are defined by a Laplace transform*

$$e^{\sum_k \hat{t}_k u^{-k}} := \frac{2u^{3/2}}{\sqrt{\pi}} \int_{\gamma_\beta} e^{-u(x(z)-x(\beta))} y(z)\,\mathrm{d}x(z) = 2^{7/2}\sum\nolimits_k (2k+1)!!\,t_{2k+3}u^{-k}\,. \tag{2.55}$$

Observe that in the correlators only the odd times occur, while the even ones completely decouple. This phenomenon as well as the fact that the Laplace transform of the initial data appear in the correlators will generalize to blobbed topological recursion described in Section 2.2.4.
This setup of deformed KdV incorporates celebrated results such as Mirzakhani's computation of Weil-Petersson volumes [Eyn11c, MS06]

$$\mathrm{Vol}_{g,n}(\ell_1,\dots,\ell_n) \coloneqq \frac{1}{d_{g,n}!}\int_{\mathcal{M}_{g,n}(\ell_1,\dots,\ell_n)} w^{d_{g,n}}\,, \tag{2.56}$$

where $w \in H^2(\mathcal{M}_{g,n}(\ell_1,\dots,\ell_n))$ is the Weil-Petersson form on the moduli space of Riemann surfaces of genus g with n boundaries of hyperbolic lengths $\ell_1,\dots,\ell_n$ denoted $\mathcal{M}_{g,n}(\ell_1,\dots,\ell_n)$, which is given by $2\pi^2\kappa_1$, see [Mir07a, Mir07b, Wol11]. The recursion that she found in her work of 2007 can be seen as the Laplace transformation of the equation of topological recursion relating the $(\mathrm{Vol}_{g,n})_{g,n}$ to the correlators of topological recursion with $y(z) = -\frac{\sin(2\pi z)}{4\pi}$ or, equivalently, the deformed dual KdV times $(\hat{t}_k)_{k\in\mathbb{N}} = (\log 2, 2\pi^2, 0, \dots)$.

2.2.2 Topological recursion and intersection numbers

In the example above, it is shown that topological recursion and the moduli space of curves share a deep relation. In the following this is retraced in greater detail.
The mentioned examples share the fact that the spectral curves have only one ramification point. When turning to models that are described by a spectral curve with more than one ramification point, it is convenient to enhance the moduli space $\overline{\mathcal{M}}_{g,n}$ by the information of some continuous *coloring map*

$$\sigma\colon \nu^{-1}C \longrightarrow \{1,\dots,s\}\,, \tag{2.57}$$

denoting the new space $\overline{\mathcal{M}}^s_{g,n}$. Note that continuity of σ implies that it must be constant on each connected component of the normalization of the curve C. In order to illustrate the effect of this additional datum, below the enriched moduli space is decomposed into factors of $\overline{\mathcal{M}}_{g,n}$. This should stress the fact that the colored moduli space is only an auxiliary construction abbreviating notation and structuring the calculations. All computations are equivalently done on (factors of the) ordinary $\overline{\mathcal{M}}_{g,n}$.

Example 2.2.2. *Note that $\overline{\mathcal{M}}^s_{0,3}$ simply gives s factors of $\overline{\mathcal{M}}_{0,3}$ as stable curves of topological type $(0,3)$ cannot degenerate. Therefore, in this and the subsequent examples the focus is on the next higher topological types with $\chi_{g,n} = 1$ and 2.*
Consider first $\overline{\mathcal{M}}^2_{0,4}$. *Points in this space generically are colored curves of genus zero with four marked points. In its boundary there are nodal curves with two components of topological type $(0,3)$. As curves in the bulk only have one component (on which the color is supposed to be constant) and $s = 2$, one finds two copies of $\overline{\mathcal{M}}_{0,4}$. Considering all possible colorings of boundary curves, one finds*

$$\overline{\mathcal{M}}^2_{0,4} \simeq \mathcal{M}_{0,4} \cup \mathcal{M}_{0,4} \cup (\mathcal{M}_{0,3}\times\mathcal{M}_{0,3})^{\cup 12} \simeq \overline{\mathcal{M}}_{0,4} \sqcup \overline{\mathcal{M}}_{0,4} \sqcup (\mathcal{M}_{0,3}\times\mathcal{M}_{0,3})^{\sqcup 6}\,. \tag{2.58}$$

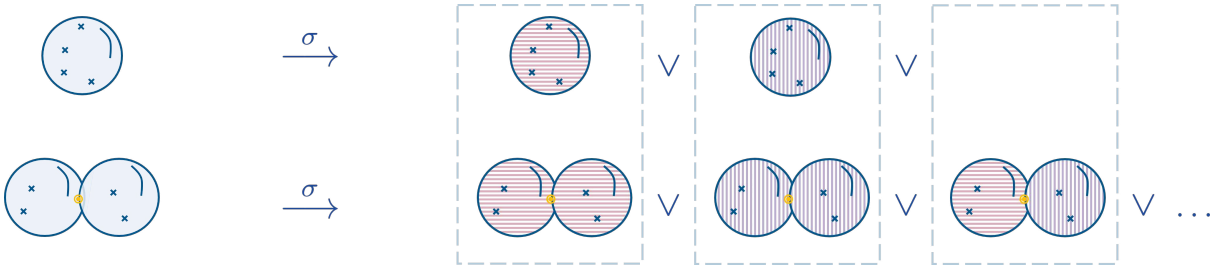

Figure 2.2.3: This depicts different colorings (horizontal red and vertical purple) of curves of topological type $(0,4)$ and its degeneration to a curve with two components of type $(0,3)$. Curves in the same box are in the same compact component (see Equation (2.58)). Note that the labelling of the marked points is omitted here to avoid cluttering.

In the above, unichrome degenerate curves with two components of topological type $(0,3)$ *are parametrized by one of the twelve factors of* $\mathcal{M}_{0,3}\times\mathcal{M}_{0,3}$ *in the decomposition of* $\overline{\mathcal{M}}^2_{0,4}$ *into non-compact moduli spaces. Alternatively due to the inclusion of the boundary strata*

$$\mathcal{M}_{0,3}\times\mathcal{M}_{0,3}\hookrightarrow\overline{\mathcal{M}}_{0,4} \tag{2.59}$$

by one of the two factors of $\overline{\mathcal{M}}_{0,4}$ *in the decomposition in terms of compactified moduli spaces (see Figure 2.2.3).*
Then, consider $\overline{\mathcal{M}}^2_{1,1}$***.*** *Curves of topological type* $(1,1)$ *may degenerate into type* $(0,3)$*. As all curves have only one component, there are no polychrome curves. Thus, one finds*

$$\overline{\mathcal{M}}^2_{1,1}\simeq\mathcal{M}_{1,1}\cup\mathcal{M}_{1,1}\cup\mathcal{M}_{0,3}\cup\mathcal{M}_{0,3}\simeq\overline{\mathcal{M}}_{1,1}\sqcup\overline{\mathcal{M}}_{1,1}\,. \tag{2.60}$$

An illustration can be found in Figure 2.2.4.

As seen in Equation (2.53) the initial data enjoys an expansion at the ramification point $a=0$ in terms of $z\sim\sqrt{x}$, which is what generates KdV times $\{t_k\}_{k\geqslant 2}$. For a

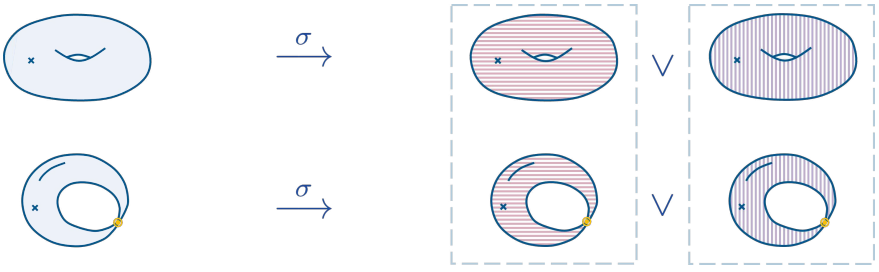

Figure 2.2.4: This depicts different colorings (horizontal red and vertical purple) of curves of topological type $(1,1)$ and its degeneration of type $(0,3)$. Curves in the same box are in the same compact component (see Equation (2.60)). Note that the labelling of the marked points is omitted here to avoid cluttering.

generic ramification point β_i, one can achieve this expansion by a special choice of local coordinates

$$\zeta_i(z) = \sqrt{2(x(z) - x(\beta_i))}\,, \qquad \text{for } z \in U_{\beta_i}\,. \tag{2.61}$$

This yields a collection of KdV times $\{t_{i,k}\}_{k\geqslant 2}$ for each ramification point β_i, with $i = [\![1, s]\!]$.
In order to express the entire space of families generated by topological recursion through intersection numbers on $\overline{\mathcal{M}}_{g,n}$, one wants to allow for a generic bi-differential B. Its holomorphic contributions are parametrized by coefficients $B_{\beta_i,k;\beta_j,l}$ associated to a pair of ramification points (β_i, β_j), with $i \in [\![1, s]\!]$, such that

$$B(z_1, z_2) \overset{\substack{z_1\to\beta_i\\ z_2\to\beta_j}}{\sim} \left(\frac{\delta_{i,j}}{(\zeta_i(z_1) - \zeta_j(z_2))^2} + \sum_{k,l\geqslant 0} B_{\beta_i,k;\beta_j,l}\, \zeta_i(z_1)^k \zeta_j(z_2)^l \right) \mathrm{d}\zeta_i(z_1)\, \mathrm{d}\zeta_j(z_2)\,. \tag{2.62}$$

As for the times, there are dual coefficients $\hat{B}_{\beta_i,k;\beta_j,l}$ defined via Laplace transform by

$$\begin{aligned} \sum_{k,l\geqslant 0} \hat{B}_{\beta_i,k;\beta_j,l} u_1^{-k} u_2^{-l} &:= \delta_{i,j} \frac{u_1 u_2}{u_1 + u_2} \\ &\quad + \frac{(u_1 u_2)^{1/2}}{2\pi} \int_{\gamma_{\beta_i}} e^{-u_1(x(z_1) - x(\beta_i))} \int_{\gamma_{\beta_j}} e^{-u_2(x(z_2) - x(\beta_j))} B(z_1, z_2) \\ &= \sum_{k,l\geqslant 0} (2k-1)!!(2l-1)!! B_{\beta_i,2k;\beta_j,2l} u_1^{-k} u_2^{-l}\,. \end{aligned} \tag{2.63}$$

Theorem 2.2.1 (Eynard [Eyn11a, Theorem 4.1])**.** *Let $(\Sigma; x, y, B)$ be a spectral curve with ramification points $\{\beta_i\}_{i\in[\![1,s]\!]}$ and $\{(U_i, x, y, B^{\mathrm{KdV}})\}_{i\in[\![1,s]\!]}$ the local spectral curves in the vicinities of the ramification points. Then,*

$$\omega_{g,n}(z_1, \dots, z_n) = 2^{d_{g,n}} \int_{\overline{\mathcal{M}}^s_{g,n}} \prod_{m=1}^{k} \hat{\Lambda}_{\beta_m} \prod_{\{q_i,q_j\}} c(q_i, q_j) \prod_{i=1}^{n} \hat{B}_{\beta_{\sigma(\beta_i)}}(z_i; 1/\psi_i)\,, \tag{2.64}$$

where the different contributions are defined below.

In the following the notation of the theorem above is explained.

Integration class

The three factors of the integrand, that is $\prod \hat{\Lambda}_{\beta_m}$, $\prod c(q_i, q_j)$, and $\prod \hat{B}_{\beta_{\sigma(\beta_i)}}(z_i; 1/\psi_i)$, are due to contributions of elements in $\overline{\mathcal{M}}^s_{g,n}$ – the bulk of the different components of a curve, its nodal points as well as the marked points, respectively (see Figure 2.2.5). The product of these factors is integrated over the moduli space of colored complex curves or over the ordinary moduli space accompanied by a sum over colors.

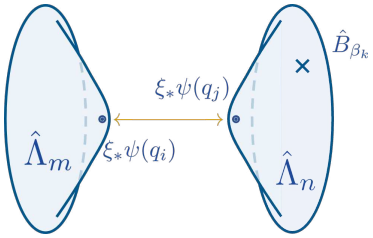

Figure 2.2.5: This sketches the origin of the different contributions to Theorem 2.2.1 associated to the bulk, that is $\hat{\Lambda}$, the nodes, $\xi_*\psi(q)$, and the marked points, $\hat{B}_\beta$.

Bulk contribution: Each component $\nu^{-1}(C)_m$ of a colored curve $C \in \overline{\mathcal{M}}^s_{g,n}$ contributes a factor

$$\hat{\Lambda}_\beta := \exp\left(\sum_k \hat{t}_{\beta,k}\kappa_k + \frac{1}{2}\sum_{\Delta\in\partial\overline{\mathcal{M}}_{g,n}}\sum_{k_1,k_2\geqslant 0}\hat{B}^{\mathrm{KdV}}_{\beta,k_1;\beta,k_2}(\iota_\Delta)_*(\psi^{k_1}\psi^{k_2})\right), \tag{2.65}$$

where the sum $\sum_{\Delta\in\partial\overline{\mathcal{M}}_{g,n}}$ runs over the co-dimension one boundary divisors Δ of $\overline{\mathcal{M}}_{g,n}$, see Equation (2.19). Then for Δ fixed ι_Δ denotes the embedding $\iota_\Delta\colon \Delta \hookrightarrow \overline{\mathcal{M}}_{g,n}$. By that means, the ψ-classes are evaluated on a boundary component at the marked points that make up the node on the respective component. To be precise, for some class $\alpha \in H^\bullet(\overline{\mathcal{M}}_{g,n})$ one evaluates via the projection formula

$$\int_{\overline{\mathcal{M}}_{g,n}} \alpha\,(\iota_\Delta)_*(\psi^{k_1}\psi^{k_2}) = \int_\Delta (\iota_\Delta)_*(\alpha)\,\psi^{k_1}\psi^{k_2}\,. \tag{2.66}$$

Further, if $\Delta \simeq \overline{\mathcal{M}}_{g_1,n_1}\times\overline{\mathcal{M}}_{g_2,n_2}$, one can decompose $(\iota_\Delta)^*(\alpha) = \sum_{i,j}\rho_{1,i}\rho_{2,j}$ into components in $H^i(\overline{\mathcal{M}}_{g_1,n_1})\otimes H^j(\overline{\mathcal{M}}_{g_2,n_2})$, with $i+j = \dim\Delta - (k_1+k_2)$ via the classical theorem by Künneth, see [Kün23, Hat02], and find

$$(2.66) = \sum_{i+j=\dim\Delta-(k_1+k_2)}\int_{\overline{\mathcal{M}}_{g_1,n_1}}\rho_{1,i}\psi^{k_1}\int_{\overline{\mathcal{M}}_{g_2,n_2}}\rho_{2,j}\psi^{k_2}\,. \tag{2.67}$$

Note that $\hat{\Lambda}_\beta$ as well as $\hat{B}^{\mathrm{KdV}}_{\beta,k_1;\beta,k_2}$ is indexed by only one color. This is due to the fact that a one-component curve, to which $\hat{\Lambda}_\beta$ is associated, can be colored in only one single color.

Node contribution: The moduli space of colored curves contains components of polychrome nodal curves. A node p contributes in the integral in Theorem 2.2.1 through

$$c(q_i,q_j) := \sum_{d_1,d_2\geqslant 0}\left(\hat{B}_{\beta_{\sigma(q_i)},k_1;\beta_{\sigma(q_j)},k_2} - \delta_{\beta_{\sigma(q_i)},\beta_{\sigma(q_j)}}\hat{B}^{\mathrm{KdV}}_{\beta_{\sigma(q_i)},k_1;\beta_{\sigma(q_j)},k_2}\right)\iota_*\left(\psi(q_i)^{k_1}\psi(q_j)^{k_2}\right)\,, \tag{2.68}$$

where $\nu^{-1}(p) = \{q_i,q_j\}$. In the above ι embeds the boundary component that the considered nodal curve corresponds to into $\overline{\mathcal{M}}_{g,n}$. Note that if $B_{\beta,k_1;\beta,k_2} = B^{\mathrm{KdV}}_{\beta,k_1;\beta,k_2}$, only

not self-connecting nodes give a non-zero result, that is those with $\sigma(q_i) \neq \sigma(q_j)$. This is also observed when decomposing $\overline{\mathcal{M}}^s_{g,n}$ into components of colored factors of $\overline{\mathcal{M}}_{g,n}$. Only polychrome multi-component curves are due to novel components in $\overline{\mathcal{M}}^s_{g,n}$, while unichrome curves are parametrized by one of the s factors of $\overline{\mathcal{M}}_{g,n}$ in terms of the disjoint decomposition of (see Example 2.2.2).

Contribution of marked points: In terms of graphs, see above Equation (2.11), marked points correspond to half edges or leaves. This is reflected in the way marked points contribute in Theorem 2.2.1. Each marked point contributes by a single sided Laplace transformation

$$\hat{B}_\beta(z;u) \coloneqq -\sqrt{\frac{u}{\pi}} \int_{\gamma_\beta} e^{-u(x(v)-x(\beta))} B(z,v) =: \sum_{k\geqslant 0} \mathrm{d}\xi_{\beta,d}(z)\, u^{-k} \,. \tag{2.69}$$

The expansion coefficients are 1-forms and can be expanded as

$$\mathrm{d}\xi_{\beta,d} \overset{z\to\beta'}{\sim} \delta_{\beta,\beta'}\sqrt{2}(2d+1)!! \frac{\mathrm{d}\zeta_\beta(z)}{\zeta_\beta(z)^{2d+2}} - \frac{(2d-1)!!}{\sqrt{2}} \sum_{k\geqslant 0} B_{\beta,2d;\beta',k}\zeta_{\beta'}(z)^k \,\mathrm{d}\zeta_{\beta'}(z) \,. \tag{2.70}$$

For later reference, note that the Laplace transform can equivalently be expressed as a residue prescription by writing

$$\mathrm{d}\xi_{\beta,d} = -\sqrt{2}(2d-1)!! \operatorname*{Res}_{v\to\beta} B(v,z)\zeta_\beta(v)^{-2d-1} \,. \tag{2.71}$$

The Theorem 2.2.1 as well as the definitions above are illustrated in the following two examples building on Example 2.2.2.

Example 2.2.3. ***Consider*** $\boldsymbol{\omega_{0,4}}$ *for a spectral curve with* $s = 2$ *and* $B = B^{\mathrm{KdV}}$. *As described in Example 2.2.2, the moduli space* $\overline{\mathcal{M}}^2_{0,4}$ *decomposes into two factors of* $\overline{\mathcal{M}}_{0,4}$ *and six factors of* $\overline{\mathcal{M}}_{0,3} \times \overline{\mathcal{M}}_{0,3}$. *Thus, Theorem 2.2.1 expands to*

$$\begin{aligned} 2^{-1}\omega_{0,4}(z_1,\dots,z_4) = {} & \int_{\overline{\mathcal{M}}_{0,4}} \hat{\Lambda}_{\beta_1} \prod_{i=1}^4 \hat{B}_{\beta_1}(z_i;1/\psi_i) + \int_{\overline{\mathcal{M}}_{0,4}} \hat{\Lambda}_{\beta_2} \prod_{i=1}^4 \hat{B}_{\beta_2}(z_i;1/\psi_i) \\ & + \left(\int_{\overline{\mathcal{M}}_{0,3}\times\overline{\mathcal{M}}_{0,3}} \hat{\Lambda}_{\beta_1}\,\hat{\Lambda}_{\beta_2}\, c(q_1,q_2) \prod_{i=1}^2 \hat{B}_{\beta_1}(z_i;1/\psi_i) \prod_{j=3}^4 \hat{B}_{\beta_2}(z_j;1/\psi_j) \right. \\ & \left. + \mathrm{symm}(z_1,\dots,z_4) \right) \,. \end{aligned} \tag{2.72}$$

Noting that $\dim \overline{\mathcal{M}}_{0,3} = 0$ *one expands the integrand in the second line according to the definitions above in Equations (2.65), (2.68) and (2.69) keeping only those parts of degree zero. This yields for the integral over* $\overline{\mathcal{M}}_{0,3} \times \overline{\mathcal{M}}_{0,3}$

$$\begin{aligned} & \int_{\overline{\mathcal{M}}_{0,3}\times\overline{\mathcal{M}}_{0,3}} e^{\hat{t}_{\beta_1,0}\kappa_0} e^{\hat{t}_{\beta_2,0}\kappa_0}\, \hat{B}_{\beta_1,0,\beta_2,0}\, \psi(q_1)^0\psi(q_2)^0 \prod_{j=1}^2 \mathrm{d}\xi_{\beta_1,0}(z_j)\,\psi_j^0 \prod_{j'=3}^4 \mathrm{d}\xi_{\beta_2,0}(z_{j'})\,\psi_{j'}^0 \\ & = e^{(\hat{t}_{\beta_1,0}+\hat{t}_{\beta_2,0})\langle\kappa_0\rangle_{0,3}}\, \hat{B}_{\beta_1,0,\beta_2,0}\, \langle 1\rangle_{0,3}\langle 1\rangle_{0,3}\, \mathrm{d}\xi_{\beta_1,0}(z_1)\,\mathrm{d}\xi_{\beta_1,0}(z_2)\,\mathrm{d}\xi_{\beta_2,0}(z_3)\,\mathrm{d}\xi_{\beta_2,0}(z_4) \,. \end{aligned} \tag{2.73}$$

As $\dim \overline{\mathcal{M}}_{0,4} = 1$*, the integrand of the integral over* $\overline{\mathcal{M}}_{0,4}$ *is expanded to degree one. Furthermore, it is recognized that with every order of* $\hat{B}^{\mathrm{KdV}}$ *in the expansion of the bulk contribution* $\hat{\Lambda}$*, the integral retrieves to a boundary stratum of co-dimension one, see Equation (2.66). This yields*

$$\begin{aligned}
&\int_{\overline{\mathcal{M}}_{0,4}} e^{\hat{t}_{\sigma,0}\kappa_0}(1+\hat{t}_{\sigma,1}\kappa_1)\Big(1+\frac{1}{2}\sum_{\Delta\in\partial\overline{\mathcal{M}}_{0,4}}\hat{B}_{\beta_\sigma,0,\beta_\sigma,0}\psi^0\psi'^0\Big)\prod_{j=1}^{4}\left(\mathrm{d}\xi_{\beta_\sigma,0}(z_j)\,\psi_j^0+\mathrm{d}\xi_{\beta_\sigma,1}(z_j)\,\psi_j^1\right)\\
&=\Big(e^{\hat{t}_{\beta_\sigma,0}\langle\kappa_0\rangle_{0,4}}\hat{t}_{\beta_\sigma,1}\langle\kappa_1\rangle_{0,4}+e^{2\hat{t}_{\beta_\sigma,0}\langle\kappa_0\rangle_{0,3}}(6/2)\hat{B}_{\beta_\sigma,0,\beta_\sigma,0}\,\langle 1\rangle_{0,3}\langle 1\rangle_{0,3}\Big)\prod_{j=1}^{4}\mathrm{d}\xi_{\beta_\sigma,0}(z_j) \qquad (2.74)\\
&\quad+\Big(e^{\hat{t}_{\beta_\sigma,0}\langle\kappa_0\rangle_{0,4}}\,\langle\psi_1\rangle_{0,4}\;\mathrm{d}\xi_{\beta_\sigma,1}(z_1)\,\mathrm{d}\xi_{\beta_\sigma,0}(z_2)\,\mathrm{d}\xi_{\beta_\sigma,0}(z_3)\,\mathrm{d}\xi_{\beta_\sigma,0}(z_4)+\mathrm{symm}(z_1,\dots,z_4)\Big)\,.
\end{aligned}$$

In conclusion

$$\begin{aligned}
2^{-1}\omega_{0,4}=\sum_{\sigma\in\{1,2\}}\Big[&e^{2\hat{t}_{\beta_\sigma,0}}\Big(\hat{t}_{\beta_\sigma,1}+3\hat{B}_{\beta_\sigma,0,\beta_\sigma,0}\Big)\prod_{j=1}^{4}\mathrm{d}\xi_{\beta_\sigma,0}(z_j)\\
&+e^{2\hat{t}_{\beta_\sigma,0}}\sum_{i=1}^{4}\Big(\mathrm{d}\xi_{\beta_\sigma,1}(z_i)\prod_{j\neq i}^{4}\mathrm{d}\xi_{\beta_1,0}(z_j)\Big)\Big]\\
&+e^{(\hat{t}_{\beta_1,0}+\hat{t}_{\beta_2,0})}\;\hat{B}_{\beta_1,0,\beta_2,0}\frac{1}{2}\sum_{i=1}^{4}\sum_{j\neq i}^{4}\mathrm{d}\xi_{\beta_1,0}(z_i)\,\mathrm{d}\xi_{\beta_1,0}(z_j)\prod_{k\neq i,j}^{4}\mathrm{d}\xi_{\beta_2,0}(z_k)\,.
\end{aligned} \qquad (2.75)$$

Now consider $\omega_{1,1}$***.*** *In Example 2.2.2 it is laid down that* $\overline{\mathcal{M}}_{1,1}^2\simeq\overline{\mathcal{M}}_{1,1}\sqcup\overline{\mathcal{M}}_{1,1}$*. Thus, from Theorem 2.2.1 one finds*

$$2^{-1}\omega_{1,1}(z_1)=\int_{\overline{\mathcal{M}}_{1,1}}\hat{\Lambda}_{\beta_1}\;\hat{B}_{\beta_1}(z_1;1/\psi_1)+\int_{\overline{\mathcal{M}}_{1,1}}\hat{\Lambda}_{\beta_2}\;\hat{B}_{\beta_2}(z_2;1/\psi_2)\,. \qquad (2.76)$$

Expanding the integrand and keeping only contributions up to degree one, yields for both summands in the above ($\sigma=1,2$*)*

$$\begin{aligned}
&\int_{\overline{\mathcal{M}}_{1,1}}e^{\hat{t}_{\beta_\sigma,0}\kappa_0}(1+\hat{t}_{i,1}\kappa_1)\left(1+\frac{1}{2}\sum_{\delta\in\partial\overline{\mathcal{M}}_{0,4}}\hat{B}_{\beta_\sigma,0,\beta_\sigma,0}\psi^0\psi'^0\right)\left(\mathrm{d}\xi_{\beta_\sigma,0}(z_1)\,\psi_1^0+\mathrm{d}\xi_{\beta_\sigma,1}(z_1)\,\psi_1^1\right)\\
&=\left(e^{\hat{t}_{\beta_\sigma,0}\langle\kappa_0\rangle_{1,1}}\hat{t}_{\beta_\sigma,1}\langle\kappa_1\rangle_{1,1}+\frac{1}{2}e^{\hat{t}_{\beta_\sigma,0}\langle\kappa_0\rangle_{0,3}}\hat{B}_{\beta_\sigma,0,\beta_\sigma,0}\,\langle 1\rangle_{0,3}\right)\mathrm{d}\xi_{\beta_\sigma,0}(z_1)\\
&\qquad+e^{\hat{t}_{\beta_\sigma,0}\langle\kappa_0\rangle_{1,1}}\,\langle\psi_1\rangle_{1,1}\;\mathrm{d}\xi_{\beta_\sigma,1}(z_1)\\
&=e^{\hat{t}_{\beta_\sigma,0}}\left(\frac{\hat{t}_{\beta_\sigma,1}}{24}+\frac{\hat{B}_{\beta_\sigma,0,\beta_\sigma,0}}{2}\right)\mathrm{d}\xi_{\beta_\sigma,0}(z_1)+e^{\hat{t}_{\beta_\sigma,0}}\;\frac{1}{24}\;\mathrm{d}\xi_{\beta_\sigma,1}(z_1)\,.
\end{aligned} \qquad (2.77)$$

2.2.3 Application to the LSZ model

As it was already mentioned in the definition of the LSZ model, see Section 1.4, the authors of [BH23] were able to solve the model in terms of topological recursion. They

provide the spectral curve

$$x^{\mathrm{LSZ}}(z) = z - \frac{\lambda}{N}\sum_{k=1}^{N}\frac{1}{y'(\tilde{\varepsilon}_k)(z-\tilde{\varepsilon}_k)}\,, \quad \text{and} \quad y^{\mathrm{LSZ}}(z) = -z + \frac{\lambda}{N}\sum_{k=1}^{N}\frac{1}{x'(\varepsilon_k)(z-\varepsilon_k)}\,, \tag{2.78}$$

as well as $B(z_1,z_2) = \frac{\mathrm{d}z_1\mathrm{d}z_1}{(z_1-z_2)^2}$ on $\mathbb{CP}^1$. In the above $\{\varepsilon_k\}_k$ and $\{\tilde{\varepsilon}_k\}_k$ are the preimages of the eigenvalues of the external matrices E and $\tilde{E}$ under x and y, respectively. The correlators due to topological recursion

$$\omega_{g,n}^{\mathrm{LSZ}}(z_1,\dots,z_n) = \Omega_n^{(g),\mathrm{LSZ}}(z_1,\dots,z_n)\,\mathrm{d}x^{\mathrm{LSZ}}(z_1)\cdots\mathrm{d}x^{\mathrm{LSZ}}(z_n) \tag{2.79}$$

give then

$$\begin{aligned}\Omega_n^{(g),\mathrm{LSZ}}(\varepsilon_{p_1},\dots,\varepsilon_{p_n}) = \frac{\delta_{g,0}\delta_{n,1}}{\lambda}V'(x)(E_{p_1}) + \frac{\delta_{g,0}\delta_{n,2}}{(E_{p_1}-E_{p_2})^2} \\ + [N^{2-2g-n}](-1)^n\frac{\partial^n}{\partial E_{p_1}\cdots\partial E_{p_n}}\log\mathcal{Z}^{\mathrm{LSZ}}\,,\end{aligned} \tag{2.80}$$

for $V'(x) = x - \sum_k \frac{1}{x-E_k}$.
Within the investigation of the Quartic Kontsevich Model, the hermitian analogue of the LSZ model, it has proven useful to express the results in terms of parameters $\{x_{\beta,n}\}_{n\in\mathbb{N}^\times}$ and $\{y_{\beta,n}\}_{n\in\mathbb{N}^\times}$ defined as expansion coefficients of the functions x and y by

$$x_{\beta,n} \coloneqq \left.\frac{\partial_z{}^{n+2}x(z)}{\partial_z{}^2x(z)}\right|_{z=\beta}, \qquad \text{and} \qquad y_{\beta,n} \coloneqq \left.\frac{\partial_z{}^{n+1}y(z)}{\partial_z y(z)}\right|_{z=\beta}, \tag{2.81}$$

supplemented with $x_{\beta,0} \coloneqq \partial_z{}^2x(z)\big|_{z=\beta}$ and $y_{\beta,0} \coloneqq \partial_z y(z)|_{z=\beta}$. These are well-defined, as the spectral curve is regular. However, the definitions can be generalized to a larger class of spectral curves.

Times $t_{\beta,k}$ In order to obtain the times $t_{\beta,k}$ in terms of the parameters $x_{\beta,n}$ and $y_{\beta,n}$, one compares the expansion of y parametrized by $x_{\beta,n}$ and $t_{\beta,k}$ to that parametrized by $y_{\beta,n}$ as

$$y(\{x_{\beta,n}\}_n,\{t_{\beta,k}\}_k;z) = y(\{y_{\beta,n}\}_n;z)\,. \tag{2.82}$$

The left-hand side is obtained by expanding first in terms of $\zeta_\beta(z)$, and then in terms of z at the ramification point

$$y(\{x_{\beta,n},t_{\beta,k}\};z) \overset{\zeta_\beta\to 0}{=} \sum_{k\geqslant 0} t_{\beta,k+2}\,\zeta_\beta(z)^k \overset{z\to\beta}{=} \sum_{k\geqslant 0} t_{\beta,k+2}\sum_{l\geqslant k}\mathfrak{z}_{\beta,k,l}(\{x_{\beta,n}\})(z-\beta)^l\,. \tag{2.83}$$

There, for some $k,l\in\mathbb{N}$, $\mathfrak{z}_{\beta,k,l}(\{x_{\beta,n}\})$ is the coefficient of $(z-\beta)^l$ in the expansion of $(\zeta_\beta)^k = (x(z)-x(\beta))^{k/2}$, which depends on the parameters $\{x_{\beta,n}\}$. For the sake of completeness, these are calculated in Appendix B.1.1. The right-hand side is

$$y(\{y_{\beta,n}\};z) \overset{z\to\beta}{=} y(\beta) + y_{\beta,0}(z-\beta) + y_{\beta,0}\sum_{n\geqslant 1} y_{\beta,n}\frac{(z-\beta)^{n+1}}{(n+1)!}\,. \tag{2.84}$$

A comparison of coefficients of the left- and right-hand-side yields relations between the parameters $t_{\beta,k}$ and $x_{\beta,n}$ as well as $y_{\beta,n}$. The expressions for the first few $t_{\beta,k}$ can be found in Appendix B.1 in Tables B.1.1 and B.1.2.

Coefficients $B_{\beta,k;\beta',k'}$ A similar analysis that gave the times in terms of $\{x_{\beta,n}, y_{\beta,n}\}_n$, also gives the expansion coefficients $B_{\beta,k;\beta',k'}$. In particular, one obtains elements of $\{B_{\beta,k;\beta',k'}\}_{k,k'\in\mathbb{N}}$ by expanding the Bergman kernel in the local coordinate $\zeta_\beta(z)$. Again, expanding the appearing powers of $\zeta_\beta(z)$ in z gives

$$\begin{aligned} B(z,z') &\overset{\substack{\zeta_\beta\to 0\\ \zeta_{\beta'}\to 0}}{=} \mathrm{d}\zeta_\beta(z)\,\mathrm{d}\zeta_{\beta'}(z')\left[\frac{\delta_{\beta,\beta'}}{(\zeta_\beta(z)-\zeta_{\beta'}(z'))^2} + \sum_{k,k'\geqslant 0} B_{\beta,k;\beta',k'}\,\zeta_\beta(z)^k\zeta_{\beta'}(z')^{k'}\right] \\ &\overset{\substack{z\to\beta\\ z'\to\beta'}}{=} \mathrm{d}z\,\mathrm{d}z'\left(\sum_{n\geqslant 0}\sum_{n=0}^{m}(n+1)(n-m+1)\mathfrak{z}_{\beta,1,n+1}\mathfrak{z}_{\beta',1,n-m+1}(z-\beta)^n(z'-\beta')^{n-m}\right) \\ &\quad\times\left[\frac{\delta_{\beta,\beta'}}{\left[\sum_{l\geqslant 1}\mathfrak{z}_{\beta,1,l}\left((z-\beta)^l-(z'-\beta)^l\right)\right]^2}\right. \\ &\qquad\left. + \sum_{k,k'\geqslant 0} B_{\beta,k;\beta',k'}\sum_{l\geqslant 0}\sum_{r=0}^{l}\mathfrak{z}_{\beta,k,r}\mathfrak{z}_{\beta',k',l-r}(z-\beta)^r(z'-\beta')^{l-r}\right], \end{aligned} \tag{2.85}$$

with $\mathfrak{z}_{\beta,k,l} = \mathfrak{z}_{\beta,k,l}(\{x_{\beta,n}\})$ as above. This expression is compared with the explicit direct expansion of $B(z,z')$ for $z\to\beta, z'\to\beta'$, yielding relations between $\{B_{\beta,k;\beta',k'}\}_{k,k'\in\mathbb{N}}$ and $\{x_{\beta,n}, x_{\beta',n}\}_{n\in\mathbb{N}}$.

Example 2.2.4. *Using these new parameters, the expressions in the running Example 2.2.3 can be rewritten to*

$$\begin{aligned} 2^{-1}\omega_{0,4} = \sum_{\sigma\in\{1,2\}}\frac{1}{48x_{\beta_\sigma,0}^2y_{\beta_\sigma,0}^2}\Bigg[&\Big((3-5\langle\kappa_1\rangle_{0,4}+20\langle\psi\rangle_{0,4})x_{\sigma,1}^2 - 3(1-\langle\kappa_1\rangle_{0,4}+4\langle\psi\rangle_{0,4})x_{\beta_\sigma,2} \\ &+ 12\langle\kappa_1\rangle_{0,4}x_{\beta_\sigma,1}y_{\beta_\sigma,1} - 12\langle\kappa_1\rangle_{0,4}y_{\beta_\sigma,2}\Big)\prod_{i=1}^4\frac{1}{(z_i-\beta_\sigma)^2} \\ &- 24\langle\psi\rangle_{0,4}x_{\beta_\sigma,1}\sum_{i=1}^4\left(\frac{1}{(z_i-\beta_\sigma)^3}\prod_{j\neq i}^4\frac{1}{(z_j-\beta_\sigma)^2}\right) \\ &+ 72\langle\psi\rangle_{0,4}\sum_{i=1}^4\left(\frac{1}{(z_i-\beta_\sigma)^4}\prod_{j\neq i}^4\frac{1}{(z_j-\beta_\sigma)^2}\right)\Bigg] \\ &+ \frac{1/2}{(\beta_1-\beta_2)^2x_{\beta_1,0}x_{\beta_2,0}y_{\beta_1,0}y_{\beta_2,0}}\left(\frac{1}{(z_1-\beta_1)^2(z_2-\beta_1)^2(z_3-\beta_2)^2(z_4-\beta_2)^2}\right. \\ &\left. + \mathrm{symm}(z_1,\ldots,z_4)\right) \end{aligned} \tag{2.86}$$

as well as

$$2^{-1}\omega_{1,1} = \sum_{\sigma\in\{1,2\}} \frac{1}{x_{\beta_\sigma,0}y_{\beta_\sigma,0}}\Bigg[\Big((-1+10(\langle\kappa_1\rangle_{1,1}-\langle\psi\rangle_{1,1}))x_{\beta_\sigma,1}^2+(1-6(\langle\kappa_1\rangle_{1,1}-\langle\psi\rangle_{1,1}))x_{\beta_\sigma,2}$$
$$-24\langle\kappa_1\rangle_{1,1}x_{\beta_\sigma,1}y_{\beta_\sigma,1}+24\langle\kappa_1\rangle_{1,1}y_{\beta_\sigma,2}\Big)\frac{1}{48(z_1-\beta_\sigma)^2}$$
$$+\frac{\langle\psi\rangle_{1,1}x_{\beta_\sigma,1}}{(z_1-\beta_\sigma)^3}-\frac{3\langle\psi\rangle_{1,1}}{(z_1-\beta_\sigma)^4}\Bigg]. \tag{2.87}$$

Using the parameters $x_{\beta,n}$ and $y_{\beta,n}$ for the spectral curve of the LSZ model one explicitly finds how the intersection numbers on the moduli space of curves are convoluted in the physical model.

In the following a similar result is aspired for the hermitian analogue of the LSZ model – the Quartic Kontsevich Model. Therefore, the framework of topological recursion, introduced here, however, needs to be generalized to include higher order deformation parameters analogous to the times $t_{\beta,k}$ and the parameters $B_{\beta,k;\beta',k'}$. This, more general, blobbed topological recursion will be introduced in the next section.

2.2.4 Blobbed topological recursion

It was already mentioned above that in order to capture the Quartic Kontsevich Model, it is believed that the setup of ordinary topological recursion, which was introduced in the previous section, is too narrow. Nevertheless, on the level of loop equations, the model is supposed to follow a structure close to topological recursion. This less restrictive framework is achieved by considering the most general solutions to the abstract loop equation, denoted $\widetilde{\omega}_{g,n}$, which are constructed via *blobbed topological recursion*. The latter is introduced in the following.

The general solution is obtained by enriching the recursion at each step by a holomorphic contribution $\varphi_{g,n}$, called *blob*, see Figure 2.2.6. Thinking about the system from the perspective of hierarchies of differential equations, the blobs can be interpeted as integration constants, introduced whenever an equation is integrated. Setting all of these integration constants to zero, one retrieves to one special point in the space of solutions. For one specific model which is determined be its loop equations the blobs are constrained in the global picture completely.
These blobs are global sections of the n-th symmetric power of the canonical bundle over Σ symmetric in their arguments. To proceed, define for a meromorphic 1-form η the projection operator $\mathcal{P}$ by

$$\mathcal{P}\eta(z_0) \coloneqq \sum\nolimits_{i=1}^{s} \operatorname*{Res}_{q\to\beta_i} \eta(q)\Phi_i^{0,2}(q,z_0)\,, \qquad \text{for } \Phi_i^{0,2}(q,z_0) \coloneqq \int_{\beta_i}^{q} \widetilde{\omega}_{0,2}(\bullet,z_0)\,. \tag{2.88}$$

If there are multiple variables $(z_i)_i$, the corresponding projections are denoted $(\mathcal{P}_i)_i$. As the divergent part of $\mathcal{P}\eta$ at the points $\{\beta_i\}_i$ agrees with that of η, $\mathcal{P}$ is called the

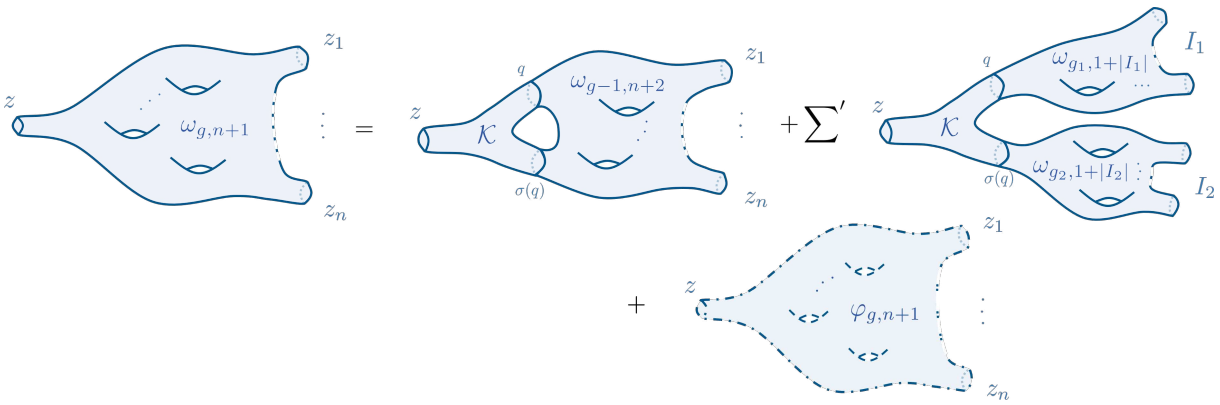

Figure 2.2.6: This illustrates the different terms in the recursion prescription (2.94) using the association of the correlators with Riemann surfaces, similar to Figure 2.2.2. Compared to the latter, here in the case of blobbed topological recursion, there appear the holomorphic blobs $\varphi_{g,n}$, which represent the terms in the second to fifth line of Equation (2.94).

projection on the polar part. The remainder

$$\mathcal{H}\eta \coloneqq \eta - \mathcal{P}\eta \tag{2.89}$$

is accordingly the holomorphic part. Note that these projections are well-defined as for $2g-2+n>0$ the $\widetilde{\omega}_{g,n}$ do not have poles on the diagonals and thus $[\mathcal{P},\mathcal{H}]=0$. For the unstable topologies the polar part vanishes as $\widetilde{\omega}_{0,1}$ and $\widetilde{\omega}_{0,2}$ do not have poles at the β_i. Furthermore, it should be stressed that the exact forms obtained by the projections depends on $\widetilde{\omega}_{0,2}$.

Theorem 2.2.2 (Borot-Shadrin [BS17])**.** *Let $(\widetilde{\omega}_{g,n})_{g,n}$ be a solution to the abstract loop equations, then*

$$\mathcal{P}_1\widetilde{\omega}_{g,n}(z_1,I) = \sum_{i=1}^{s} \operatorname*{Res}_{z\to\beta_i} \mathcal{K}_i(z_1,q)\Bigg[\widetilde{\omega}_{g-1,n+2}(q,\varsigma_i(q),I) + {\sum_{\substack{g_1+g_2=g\\ I_1\sqcup I_2=I}}}' \widetilde{\omega}_{g_1,1+|I_1|}(q,I_1)\,\widetilde{\omega}_{g_2,1+|I_2|}(\varsigma_i(q),I_2)\Bigg]. \tag{2.90}$$

This theorem shows that the solution to ordinary topological recursion ω is convoluted in the $\widetilde{\omega}$, but cannot easily be extracted, as the blobs φ enter the recursion at each individual step. This induces a short exact sequence of solutions to ordinary and blobbed topological recursion, $\mathcal{M}$ and $\widetilde{\mathcal{M}}$, respectively,

$$0 \longrightarrow \mathcal{M} \longrightarrow \widetilde{\mathcal{M}} \longrightarrow \bigoplus_{2g-2+n>0} \mathcal{B}_{g,n} \longrightarrow 0\,, \tag{2.91}$$

where $\mathcal{B}_{g,n}$ consists of global sections of the n-th symmetric power of the canonical bundle over Σ symmetric in their arguments, yielding the stable holomorphic blobs.

Trivially, the $(\omega_{g,n})_{g,n} \in \mathcal{M}$ correspond to the solution of blobbed topological recursion for $(\varphi_{g,n})_{g,n} = (y\,\mathrm{d}x\,, B, 0, \dots)$.

In the general case Borot and Shadrin showed that the polar and holomorphic parts of $\widetilde{\omega}$ can be decomposed according to bipartite graphs (see below).

Theorem 2.2.3 (Borot-Shadrin [BS17])**.** *If $(\widetilde{\omega}_{g,n})_{g,n}$ is a solution to the abstract loop equations and $I_h \sqcup I_p = [\![1,n]\!]$, then*

$$\mathcal{H}_{I_h}\mathcal{P}_{I_p}\widetilde{\omega}_{g,n} = \sum_{\Gamma\in \mathrm{Bip}_{g,n}(I_h,I_p)} \frac{\varpi_\Gamma}{|\#\mathrm{Aut}\,\Gamma|}\,, \qquad \text{for } 2g-2+n>0\,, \tag{2.92}$$

where the set of graphs $\mathrm{Bip}_{g,n}$ and their weights ϖ_Γ are described below.

In the theorem above, the set of graphs $\mathrm{Bip}_{g,n}(I_h, I_p)$ is given by bipartite graphs Γ that satisfy the following conditions.

- The *vertices* are of type φ or ω. They are decorated with a label $h(v)$ which together with their valency $d(v)$ satisfy stability $2h(v) - 2 + d(v) > 0$. [♯]
- The *edges* connect only φ to ω vertices.
- The unbounded edges, also called leaves, are labelled by $[\![1,n]\!]$. The partition $I_h \sqcup I_p = [\![1,n]\!]$, of Theorem 2.2.3, prescribes the type of vertices to which the leaves are connected, where I_h corresponds to φ and I_p to ω vertices.
- The ω vertices must be incident to at least one leaf.
- The *graph* is connected and its first Betti number b_1 satisfies $b_1 + \sum_v h(v) = g$.

Such graphs can be associated with a weight as follows.

- One assigns external variables $\{z_i\}_{i\in[\![1,n]\!]} \in \Sigma$ to leaves according to their labelling. An internal edge e obtains integration variables z_e.
- A vertex v contributes a local weight $\omega_{h(v),d(v)}(Z(v))$ or $\varphi_{h(v),d(v)}(Z(v))$ according to its type, where $Z(v)$ is the set of variables assigned to the edges incident to v.
- Then local weights are multiplied and internal variables $\{z_e\}_e$ are integrated out via the prescription

$$\langle \omega(z_e, I)\varphi(z_e, J)\rangle \quad\longmapsto\quad \sum_{i=1}^{s} \operatorname*{Res}_{q\to\beta_i} \omega(q, I) \int_{\beta_i}^{q} \varphi(\bullet, J)\,. \tag{2.93}$$

Example 2.2.5. *The progress within the Quartic Kontsevich Model over the past decades has lead to the belief, that the model can be described by the general setup of blobbed topological recursion. First and foremost, its solution in the planar and genus one sector provide compelling evidence for this.*
In [BHW22, HW21, HW23], the authors showed that for $g \in \{0,1\}$ its correlators, which

[♯] This allows for $h(v)$ to be interpreted as a local genus

are constructed in Chapter 1, follow the recursion

$$\begin{aligned}\omega_{g,n+1}^{\mathfrak{QKM}}(z,I) = \sum_{\beta_i} \operatorname*{Res}_{q\to\beta_i} \mathcal{K}_i(z,q)\Bigg[\omega_{g-1,n+2}^{\mathfrak{QKM}}(q,q,I) + {\sum_{\substack{I_1\sqcup I_2=I\\ g_1+g_2=g}}}' \omega_{g_1,|I_1|+1}^{\mathfrak{QKM}}(q,I_1)\omega_{g_2,|I_2|+1}^{\mathfrak{QKM}}(q,I_2)\Bigg] \\ + \sum_{j=1}^{|I|} \mathrm{d}_{z_j} \operatorname*{Res}_{q\to -z_j} \mathcal{K}_{z_j}(z,q)\Bigg[{\sum_{\substack{I_1\sqcup I_2=I\\ g_1+g_2=g}}}' \mathrm{d}_{z_j}^{-1}\omega_{g_1,|I_1|+1}^{\mathfrak{QKM}}(q,I_1)\omega_{g_2,|I_2|+1}^{\mathfrak{QKM}}(q,I_2) \\ + \mathrm{d}_{z_j}^{-1}\omega_{g-1,n+2}^{\mathfrak{QKM}}(q,q,I) + \frac{(\mathrm{d}x(q))^2}{6}\frac{\partial^2}{\partial(x(q))^2}\left(\frac{\omega_{g-1,n+1}^{\mathfrak{QKM}}(q,I)}{\mathrm{d}x(q)\,\mathrm{d}x(z_j)}\right)\Bigg] \\ + \operatorname*{Res}_{q\to 0} \mathcal{K}_0(z,q)\Bigg[\omega_{g-1,n+2}^{\mathfrak{QKM}}(q,q,I) + {\sum_{\substack{I_1\sqcup I_2=I\\ g_1+g_2=g}}}' \mathrm{d}_{u_j}^{-1}\omega_{g_1,|I_1|+1}^{\mathfrak{QKM}}(q,I_1)\omega_{g_2,|I_2|+1}^{\mathfrak{QKM}}(q,I_2) \\ + \frac{(\mathrm{d}x(q))^2}{2}\frac{\partial}{\partial x(q)}\left(\frac{\mathrm{d}_{q'}^{-1}\omega_{g-1,n+2}^{\mathfrak{QKM}}(q,q',I)}{\mathrm{d}x(q)}\right)\Bigg], \end{aligned} \tag{2.94}$$

where the primed sum $\sum'$ *excludes terms containing correlators of topological type* $(0,0)$*, with the initial data*

$$x^{\mathfrak{QKM}}(z) = R(z)\,,\quad y^{\mathfrak{QKM}}(z) = -R(-z)\,,\quad \textit{and}\quad \omega_{0,2}^{\mathfrak{QKM}}(z_1,z_2) = \frac{\mathrm{d}z_1\,\mathrm{d}z_2}{(z_1-z_2)^2} + \frac{\mathrm{d}z_1\,\mathrm{d}z_2}{(z_1+z_2)^2}\,, \tag{2.95}$$

referring to the function R*, defined in Equation (1.30) in Chapter 1. In the recursion above,* $\omega_{0,2}^{\mathfrak{QKM}}(q,q)$*, which contains a double pole, should be replaced by its holomorphic part, that is* $\lim_{q'\to q}(\omega_{0,2}^{\mathfrak{QKM}}(q,q') - \frac{\mathrm{d}x(q)\mathrm{d}x(q')}{(x(q)-x(q'))^2})$*. Furthermore, the standard kernel*

$$\mathcal{K}_i(z,q) \coloneqq \frac{-\frac{\mathrm{d}z}{2}\left(\frac{1}{z-q} - \frac{1}{z-\varsigma_i(q)}\right)}{(y(q)-y(\varsigma_i(q)))\,\mathrm{d}x(q)}\,, \tag{2.96}$$

is accompanied by kernels due to the contributions of the reflected part of $\omega_{0,2}^{\mathfrak{QKM}}$ *and zero*

$$\mathcal{K}_u \coloneqq \frac{-\frac{\mathrm{d}z}{2}\left(\frac{1}{z-q} - \frac{1}{z+u}\right)}{(y(q)+x(q))\,\mathrm{d}x(q)}\,, \qquad \mathcal{K}_0 \coloneqq \frac{-\frac{\mathrm{d}z}{2}\left(\frac{1}{z-q} - \frac{1}{z}\right)}{(y(q)+x(q))\,\mathrm{d}x(q)}\,. \tag{2.97}$$

Note, in the correlator of topological type $(0,2)$ *there are two contributions. The first is familiar from Example 2.2.1 and often referred to as the Bergmann kernel in literature on topological recursion. The second term is novel and is a reflected,* $z_2 \mapsto -z_2$*, version of the former. This additional term is also reflected in all higher correlators as can be seen in the subsequent examples.*

The technically involved proof given in the original work amounts to a careful analysis of the pole structure of different functions related to the $\omega^{\mathfrak{QKM}}$ *in order to find globally defined loop equations. The interested reader is referred to the original work as a presentation is*

beyond the scope of this thesis.
Instead, it is pointed out that in Equation (2.94) the contributions entering each step of the recursion that are holomorphic at the ramification points have a structure similar to the polar contributions. Even more, they are expressed in terms of correlators of lower topological type[♯]*. It is currently unknown to what effect or structure within the Quartic Kontsevich Model this relates, but it certainly shows that the exploration and understanding holds a variety of different avenues.*

Using the explicit recursion from the correlators associated to the unstable topologies all higher correlators can be constructed. In order to give an example as well as for later reference the correlators associated to the lowest topological types are provided in the variables $\zeta_i \mapsto \zeta_i/\sqrt{x_{i,0}}$, for $i \in [\![1,s]\!]$, expanded up zeroth order in all variables. First, the different sectors of $\omega_{0,3}^{\mathrm{QKM}}$, that is the various combinations of expansion points, expand according to

$$
\begin{aligned}
&\frac{(\omega_{0,3}^{\mathrm{QKM}})^{(i,i,i)}(z_1,z_2,z_3)}{\mathrm{d}\zeta_i(z_1)\,\mathrm{d}\zeta_i(z_2)\,\mathrm{d}\zeta_i(z_3)}\\
&=\frac{1}{y_{i,0}x_{i,0}}\left[\frac{-1}{\zeta_i^2(z_1)\zeta_i^2(z_2)\zeta_i^2(z_3)}\right.\\
&\quad-\left(\frac{1}{4\beta_i^2}+\frac{1}{24}(x_{i,1}^2-x_{i,2})\right)\left(\frac{1}{\zeta_i^2(z_2)\zeta_i^2(z_3)}+\frac{1}{\zeta_i^2(z_1)\zeta_i^2(z_3)}+\frac{1}{\zeta_i^2(z_1)\zeta_i^2(z_2)}\right)\\
&\quad-\left(\frac{1}{16\beta_i^4}+\frac{1}{48\beta_i^2}(x_{i,1}^2-x_{i,2})+\frac{1}{576}(x_{i,1}^2-x_{i,2})^2\right)\left(\frac{1}{\zeta_i^2(z_1)}+\frac{1}{\zeta_i^2(z_2)}+\frac{1}{\zeta_i^2(z_3)}\right)\\
&\quad+\left(\frac{15}{32\beta_i^6}\frac{3(x_{i,1}-2y_{i,1})}{16\beta_i^5}+\frac{5x_{i,1}^2-3x_{i,2}-12x_{i,1}y_{i,1}+24y_{i,1^2}+12y_{i,2}}{128\beta_i^4}-\frac{(x_{i,1}^2-x_{i,2})^2}{192\beta_i^2}\right.\\
&\qquad\left.\left.-\frac{(x_{i,1}^2-x_{i,2})^3}{3456}\right)\right]\\
&\quad-\sum_{t\neq i}\frac{1}{y_{t,0}x_{t,0}}\left[\frac{1}{(\beta_i-\beta_t)^6}+\frac{3}{(\beta_i-\beta_t)^4(\beta_i+\beta_t)^2}\right]+\mathcal{O}(\zeta_i(z_1),\zeta_i(z_2),\zeta_i(z_3))\,,
\end{aligned}
\tag{2.98}
$$

and

$$
\begin{aligned}
&\frac{(\omega_{0,3}^{\mathrm{QKM}})^{(i,j,j)}(z_1,z_2,z_3)}{\mathrm{d}\zeta_i(z_1)\,\mathrm{d}\zeta_j(z_2)\,\mathrm{d}\zeta_j(z_3)}\\
&=-\frac{1}{y_{j,0}x_{j,0}}\left[\frac{1}{(\beta_i-\beta_j)^2}+\frac{1}{(\beta_i+\beta_j)^2}\right]\frac{1}{\zeta_j^2(z_2)\zeta_j^2(z_2)}\\
&\quad-\frac{1}{y_{i,0}x_{i,0}}\left[\frac{1}{(\beta_i-\beta_j)^4}+\frac{1}{(\beta_i+\beta_j)^4}+\frac{2}{(\beta_i-\beta_j)^2(\beta_i+\beta_j)^2}\right]\frac{1}{\zeta_i^2(z_1)}\\
&\quad-\frac{1}{y_{j,0}x_{j,0}}\left[\frac{1}{2\beta_j^2}+\frac{x_{i,1}^2-x_{i,2}}{12}\right]\left(\frac{1}{\zeta_j^2(z_2)}+\frac{1}{\zeta_j^2(z_3)}\right)\\
&\quad+\frac{1}{y_{j,0}x_{j,0}}\left[\frac{3/2}{\beta_j^2(\beta_i+\beta_j)^4}+\frac{1}{(\beta_i+\beta_j)^3}\left(\frac{1}{\beta_j^3}+\frac{(x_{j,1}-y_{j,1})}{2\beta_j^2}\right)\right.
\end{aligned}
$$

[♯] in terms of the strict partial order induced by the negative Euler characteristic

$$
\begin{aligned}
&-\frac{1}{(\beta_i-\beta_j)^2}\left(\frac{x_{j,1}^2-x_{j,2}}{48\beta_j^2}+\frac{(x_{j,1}^2-x_{j,2})^2}{576}\right)+\frac{1}{(\beta_i+\beta_j)^2}\left(\frac{3}{8\beta_j^4}-\frac{x_{j,1}-2y_{j,1}}{4\beta_j^3}\right.\\
&\left.+\frac{5x_{j,1}^2-3x_{j,2}-12x_{j,1}y_{j,1}+24y_{j,1}^2+12y_{j,2}}{48\beta_j^2}-\frac{(x_{j,1}^2-x_{j,2})^4}{576}\right)\Bigg]\\
&+\frac{1}{y_{i,0}x_{i,0}}\left[\frac{10}{(\beta_i+\beta_j)^6}+\frac{2x_{i,1}-4y_{i,1}}{(\beta_i+\beta_j)^5}-\frac{1}{(\beta_i-\beta_j)^4}\left(\frac{1}{4\beta_i^2}+\frac{x_{i,1}^2-\beta_{i,2}}{24}\right)\right.\\
&+\frac{1}{(\beta_i+\beta_j)^4}\left(\frac{5x_{i,1}^2}{48}-\frac{x_{i,2}}{8}-\frac{x_{i,1}y_{i,1}}{2}+y_{i,1}^2+\frac{y_{i,2}}{2}\right)-\frac{1}{(\beta_i-\beta_j)^2(\beta_i+\beta_j)^2}\frac{x_{i,1}^2-x_{i,2}}{12}\Bigg]\\
&-\sum_{t\notin\{i,j\}}\frac{1}{y_{t,0}x_{t,0}}\left[\frac{1}{(\beta_i-\beta_t)^2(\beta_j-\beta_t)^4}+\frac{1}{(\beta_i-\beta_t)^2(\beta_j+\beta_t)^4}\right.\\
&\left.+\frac{2}{(\beta_i-\beta_t)^2(\beta_j-\beta_t)^2(\beta_j+\beta_t)^2}\right]+\mathcal{O}(\zeta_i(z_1),\zeta_i(z_2),\zeta_i(z_3))\,,
\end{aligned}
\tag{2.99}
$$

and

$$
\begin{aligned}
&\frac{(\omega_{0,3}^{\text{QKM}})^{(i,j,h)}(z_1,z_2,z_3)}{\mathrm{d}\zeta_i(z_1)\,\mathrm{d}\zeta_j(z_2)\,\mathrm{d}\zeta_h(z_3)}\\
&=-\frac{1}{y_{i,0}x_{i,0}}\left[\frac{1}{(\beta_i-\beta_j)^2(\beta_i-\beta_h)^2}+\frac{1}{(\beta_i+\beta_j)^2(\beta_i-\beta_h)^2}+\frac{1}{(\beta_i-\beta_j)^2(\beta_i+\beta_h)^2}\right.\\
&\left.+\frac{1}{(\beta_i+\beta_j)^2(\beta_i+\beta_h)^2}\right]\frac{1}{\zeta_i^2(z_1)}+\mathrm{symm}((z_1,i),(z_2,j),(z_3,h))\\
&+\frac{1}{y_{i,0}x_{i,0}}\left[\frac{3}{(\beta_i+\beta_h)^2(\beta_i+\beta_j)^4}+\frac{3}{(\beta_i+\beta_h)^4(\beta_i+\beta_j)^2}+\frac{4}{(\beta_i+\beta_h)^3(\beta_i+\beta_j)^3}\right.\\
&+(x_{i,1}-2y_{i,1})\left(\frac{1}{(\beta_i+\beta_h)^2(\beta_i+\beta_j)^3}+\frac{1}{(\beta_i+\beta_h)^3(\beta_i+\beta_j)^2}\right)\\
&-\frac{1}{4\beta_i^2(\beta_i-\beta_h)^2(\beta_i-\beta_j)^2}-\frac{x_{i,1}^2-x_{i,2}}{24}\left(\frac{1}{(\beta_i-\beta_h)^2(\beta_i-\beta_j)^2}+\frac{1}{(\beta_i+\beta_h)^2(\beta_i-\beta_j)^2}\right.\\
&\left.+\frac{1}{(\beta_i-\beta_h)^2(\beta_i+\beta_j)^2}+\frac{1}{(\beta_i+\beta_h)^2(\beta_i+\beta_j)^2}\right)+\frac{1}{(\beta_i+\beta_h)^2(\beta_i+\beta_j)^2}\left(\frac{x_{i,1}^2}{4}-\frac{x_{i,2}}{6}\right.\\
&\left.\left.-\frac{x_{i,1}y_{i,1}}{2}+y_{i,1}^2+\frac{y_{i,2}}{2}\right)\right]+\mathrm{symm}((z_1,i),(z_2,j),(z_3,h))\\
&-\sum_{t\notin\{i,j,h\}}\frac{1}{y_{t,0}x_{t,0}}\left[\frac{1}{(\beta_i-\beta_t)^2(\beta_j-\beta_t)^2(\beta_h-\beta_t)^2}+\frac{1}{(\beta_i+\beta_t)^2(\beta_j-\beta_t)^2(\beta_h-\beta_t)^2}\right.\\
&\left.+\frac{1}{(\beta_i-\beta_t)^2(\beta_j+\beta_t)^2(\beta_h-\beta_t)^2}+\frac{1}{(\beta_i-\beta_t)^2(\beta_j-\beta_t)^2(\beta_h+\beta_t)^2}\right]\\
&+\mathcal{O}(\zeta_i(z_1),\zeta_i(z_2),\zeta_i(z_3))\,.
\end{aligned}
\tag{2.100}
$$

It should be noted, that the corresponding sectors only exist if the number of ramification

points is sufficiently large. For $\omega_{1,1}^{\text{QKM}}$ *there is only one sector for which one finds*

$$\begin{aligned}
&\frac{(\omega_{1,1}^{\text{QKM}})^i(z_1)}{\mathrm{d}\zeta_i(z_1)} \\
&= \frac{1}{y_{i,0}x_{i,0}}\left[-\frac{1}{8}\frac{1}{\zeta_i^4(z_1)} + \left(\frac{x_{i,2}}{64} - \frac{7x_{i,1}^2}{576} - \frac{x_{i,1}y_{i,1}}{48} + \frac{y_{i,2}}{48} - \frac{1}{6\beta_i^2}\right)\frac{1}{\zeta_i^2(z_1)}\right. \\
&\quad + \left(-\frac{49x_{i,1}^4}{27648} + \frac{17x_{i,2}x_{i,1}^2}{4608} - \frac{x_{i,3}x_{i,1}}{1152} - \frac{11x_{i,2}^2}{9216} + \frac{x_{i,4}}{5760} - \frac{x_{i,1}^3y_{i,1}}{1152} + \frac{x_{i,1}x_{i,2}y_{i,1}}{1152} + \frac{x_{i,1}^2y_{i,2}}{1152}\right. \\
&\quad \left.\left. - \frac{x_{i,2}y_{i,2}}{1152} + \frac{1}{\beta_i^2}\left(\frac{x_{i,2}}{144} - \frac{x_{i,1}^2}{144}\right)\right] + \frac{1}{(x_0^{[0]})^2}\left[\frac{x_1^{[0]}}{16a_i^2} - \frac{1}{8\beta_i^3}\right]\right. \\
&\quad + \sum_{t\neq i}\frac{1}{y_{t,0}x_{t,0}}\left[-\frac{1}{8(\beta_t-\beta_i)^4} - \frac{x_{t,1}}{24(\beta_t-\beta_i)^3} + \frac{1}{(\beta_t-\beta_i)^2}\left(-\frac{x_{t,1}^2}{48} + \frac{x_{t,2}}{48} + \frac{y_{t,2}}{48}\right.\right. \\
&\quad \left.\left.\left. - \frac{x_{t,1}y_{t,1}}{48} - \frac{1}{6\beta_t^2}\right)\right] + \mathcal{O}(\zeta_i(z_1))
\end{aligned} \tag{2.101}$$

These follow directly by expanding the expressions found from the recursion (2.94)*, for which [Bra22, Section 2] can serve as a reference. In the above additional data* $\{x_k^{[0]}\}_k$ *is used. That is similarly to Equation (2.81) defined as*

$$x_k^{[0]} = \left.\frac{\partial_z{}^{n+1}x(z)}{\partial_z x(z)}\right|_{z=0}, \qquad \textit{and} \qquad x_0^{[0]} = \partial_z x(z)|_{z=0}\,, \tag{2.102}$$

with $x \equiv R$ *here, evaluated at zero instead of at the ramification points.*

The expansion in the KdV-variables in the previous example suggests, that – as in ordinary topological recursion – there is a relation to intersection numbers on the moduli space of curves. This is introduced in the next section together with an associated graphical language. Using the latter from the explicit expressions given in the previous example the form of the blobs can be deduced.

2.2.5 Blobbed topological recursion and intersection numbers

Parallel to the expansion of ordinary topological recursion at the ramification points to find coefficients encoding intersection numbers on the moduli space of complex curves, see Section 2.2.2 one can expand the solutions to blobbed topological recursion. In that case the additional data of the blobs is convoluted in the expansion.
Again, one introduces in neighborhoods $\{U_i\}_{i\in[\![1,s]\!]}$ for the ramification points $\{\beta_i\}_{i\in[\![1,s]\!]}$ the local variables $\zeta_i(z)^2/2 = x(z) - x(\beta_i)$ and the standard bi-differential

$$\widetilde{\omega}_{0,2}|_{\text{KdV}} \coloneqq \delta_{ij}\frac{\mathrm{d}\zeta_{i,1}\,\mathrm{d}\zeta_{j,2}}{(\zeta_{i,1}-\zeta_{j,2})^2}\,, \tag{2.103}$$

where $\zeta_{i,k} \equiv \zeta_i(z_k)$ for $z_k \in U_k$, omitting all holomorphic contributions of $\widetilde{\omega}_{0,2}$ at the ramification points. Using this restricted form one defines $\mathcal{P}^{\text{KdV}}$ and $\mathcal{H}^{\text{KdV}}$ analogously

to Equation (2.88) as with $\Phi_i^{0,2}$ replaced with

$$\Phi_i^{0,2}|_{\mathrm{KdV}}(q, z_0) = \int_{\beta_i}^{q} \widetilde{\omega}_{0,2}|_{\mathrm{KdV}}(\bullet, z_0)\,. \tag{2.104}$$

This yields the KdV-blobs for $2g-2+n>0$ via

$$\phi_{g,n} \coloneqq \mathcal{H}_1^{\mathrm{KdV}} \cdots \mathcal{H}_n^{\mathrm{KdV}} \widetilde{\omega}_{g,n}\,, \qquad \text{and} \qquad \phi_{0,1} \coloneqq \widetilde{\omega}_{0,1}\,, \qquad \phi_{0,2} \coloneqq \widetilde{\omega}_{0,2} - \widetilde{\omega}_{0,2}|_{\mathrm{KdV}} \tag{2.105}$$

is set. One finds the contributions from the different ramification points by expanding

$$\phi_{g,n}(z_1,\dots,z_n) \overset{z_\bullet \to i_\bullet}{\sim} \phi_{g,n}^{(i_1,\dots,i_n)} \coloneqq \sum_{d_1,\dots,d_n \geqslant 0} \phi_{g,n}\left[\begin{smallmatrix} i_1,\dots,i_n \\ d_1,\dots,d_n \end{smallmatrix}\right] \prod_{l=1}^{n} (\zeta_{i_l,l})^{d_l} \mathrm{d}\zeta_{i_l,l}\,. \tag{2.106}$$

The following theorem due to Borot and Shadrin (in [BS17]) shows how the intersection numbers are convoluted in the general framework of blobbed topological recursion.

Theorem 2.2.4 (Borot-Shadrin [BS17, Section 3])**.** *The partition function associated to the solution $(\widetilde{\omega}_{g,n})_{g,n}$ to the abstract loop equations is given by*

$$\widetilde{\mathcal{Z}} = \exp\left(\sum_{g,n} \widehat{\phi}_{g,n}\right) \prod_{i=1}^{s} \mathcal{Z}_i\,, \tag{2.107}$$

where $\mathcal{Z}_i$ is an extended KdV partition function at the i-th ramification point and $\widehat{\phi}$ is a family of operators associated to the KdV blobs defined below in Equation (2.110).

A solution to the abstract loop equations $(\widetilde{\omega}_{g,n})_{g,n}$ is associated to the partition function $\widetilde{\mathcal{Z}}$ in the usual way through a formal expansion

$$\ln \widetilde{\mathcal{Z}} = \sum_{g,n} \frac{\hbar^{g-1}}{n!} \sum_{i_1,\dots,i_n=1}^{s} \sum_{d_1,\dots,d_n \in \mathbb{Z}} \mathrm{IN}\left[\begin{smallmatrix} i_1,\dots,i_n \\ d_1,\dots,d_n \end{smallmatrix}\right] \prod_{k=1}^{n} t_{i_k,d_k} \tag{2.108}$$

$$\overset{t_{i,d} \leftrightarrow \frac{(2d+1)!!\mathrm{d}\zeta_i}{\zeta_i^{2d+2}}}{\longleftrightarrow} \quad \widetilde{\omega}_{g,n}^{\mathrm{odd}}(z_1,\dots,z_n) \overset{z_\bullet \to i_\bullet}{\sim} \widetilde{\omega}_{g,n}^{(i_1,\dots,i_n)} \coloneqq \sum_{d_1,\dots,d_n \in \mathbb{Z}} \mathrm{IN}\left[\begin{smallmatrix} i_1,\dots,i_n \\ d_1,\dots,d_n \end{smallmatrix}\right] \prod_{k=1}^{n} \frac{(2d_k+1)!!\,\mathrm{d}\zeta_{i_k}}{\zeta_{i_k}^{2d_k+2}}\,,$$

where the superscript odd denotes the odd part in each variable and $\mathrm{IN}\left[\begin{smallmatrix} i_1,\dots,i_n \\ d_1,\dots,d_n \end{smallmatrix}\right]$ is a linear combination of intersection numbers of ψ-classes on $\overline{\mathcal{M}}_{g,n}$.
The theorem above can be proved by deforming the KdV partition function. In order to explain this, first note that for intersection numbers the moduli space of genus zero one can find the closed expression $\int_{\overline{\mathcal{M}}_{0,n}} \psi_1^{d_1} \cdots \psi_n^{d_n} = \binom{n-3}{d_1,\dots,d_n}$ as long as $n \geqslant 3$ using the string equation in Theorem 2.1.2. Referring to the analytic continuation of the binomial coefficients beyond their combinatorial domain, one can add terms for the

unstable $\overline{\mathcal{M}}_{0,1}$ and $\overline{\mathcal{M}}_{0,2}$ to the KdV partition function in order to define

$$\begin{aligned}\mathcal{Z}_i &\coloneqq \exp\left(\frac{t_{-2}}{\hbar}+\frac{1}{\hbar}\sum_{d\geqslant 0}(-1)^d t_d t_{-1-d}\right)\mathcal{Z}^{\mathrm{KdV}}\Big|_{\substack{t_d\mapsto -t_{i,d}/\alpha_i\\ \hbar\mapsto\hbar/\alpha_i^2}}\\ &=\exp\left(\frac{t_{-2}}{\hbar}+\frac{1}{\hbar}\sum_{d\geqslant 0}(-1)^d t_d t_{-1-d}\right.\\ &\qquad\left.+\sum_{g\geqslant 0,n\geqslant 1}{}'\frac{\hbar^{g-1}}{n!}\sum_{d_1,\dots,d_n\geqslant 0}\left(\int_{\overline{\mathcal{M}}_{g,n}}\psi_1^{d_1}\cdots\psi_n^{d_n}\right)\prod_{k=1}^n t_{d_k}\right)\Big|_{\substack{t_d\mapsto -t_{i,d}/\alpha_i\\ \hbar\mapsto\hbar/\alpha_i^2}},\end{aligned}\tag{2.109}$$

where $t_{i,d}$ is the d-th KdV time at the i-th ramification point and $\alpha_i \coloneqq \phi_{g,n}\left[\begin{smallmatrix} i\\ 2\end{smallmatrix}\right]$. These partition functions are deformed by the KdV blobs via the operators

$$\widehat{\phi}_{g,n}^{(i_1,\dots,i_n)} \coloneqq \hbar^{g-1+n}\sum_{d_1,\dots,d_n\geqslant 0}\phi_{g,n}\left[\begin{smallmatrix} i_1,\dots,i_n\\ 2d_1,\dots,2d_n\end{smallmatrix}\right]\prod_{l=1}^n(2d_l-1)!!\frac{\partial}{\partial t_{i_l,d_l}},\tag{2.110}$$

for $(g,n)\neq(0,1)$, and

$$\widehat{\phi}_{0,1}^{(i)} \coloneqq \sum_{d\geqslant 2}\phi_{0,1}\left[\begin{smallmatrix} i\\ 2d\end{smallmatrix}\right](2d-1)!!\frac{\partial}{\partial t_{i,d}}.\tag{2.111}$$

Remark two details here. The family of operators $\widehat{\phi}$ only depends on the purely odd part of the $(\phi_{g,n})_{g,n}$. Furthermore, the operator of type $(g,n)=(0,1)$ constitutes an exception due to the fact that $\phi_{0,1}\left[\begin{smallmatrix} i\\ 0\end{smallmatrix}\right]=y\,\mathrm{d}x\,|_{\beta_i}=0$ and the exclusion of $\phi_{0,1}\left[\begin{smallmatrix} i\\ 2\end{smallmatrix}\right]=\alpha_i$. The latter is required to make the action of $\widehat{\phi}_{0,1}$ on $\mathcal{Z}_i$ well-defined. The exclusion of $d=1$ makes sure that the operator respects the structure of $\mathcal{Z}_i$ as a formal power series in the variables $t_{i,d}$ for, $d\leqslant 1$,with coefficients being polynomials in $t_{i,d}$, for $d\geqslant 2$.

Graphical expansion at KdV-solution

It is possible to express the coefficients $\mathrm{IN}\left[\begin{smallmatrix} i_1,\dots,i_n\\ d_1,\dots,d_n\end{smallmatrix}\right]$ graphically as sums of contributions due to connected bipartite graphs. This was described in [BS17] generalizing the graphical language of ordinary topological recursion of [Eyn11b]. These graphs $\Gamma\in\mathrm{Bip}_{g,n}^{\mathrm{KdV}}$ will be defined below and are different from $\mathrm{Bip}_{g,n}$ introduced above. Later, it will be noticed that the set $\mathrm{Bip}_{g,n}^{\mathrm{KdV}}$ is infinite, which limits its significance, but can be renormalized to yield $\mathrm{Bip}_{g,n}^{\boxed{\mathrm{KdV}}}$, following [BS17]. It is both computationally and conceptually important that one can re-sum graphs in $\mathrm{Bip}_{g,n}^{\mathrm{KdV}}$. While finite calculations can only deal with a limited number of graphs, unbounded contributions would signal divergent rendering the theory ill-defined.
Graphs in $\mathrm{Bip}_{g,n}^{\mathrm{KdV}}$ satisfy the following rules.

- There are KdV- and Φ-*vertices*. They are decorated with a label $h(v)$ corresponding to the genus as well their valency $d(v)$ such that $d(v)\geqslant 1$.
- The *edges* connect only KdV- to Φ-vertices.
- The half-edges, leaves, are labelled by $[\![1,n]\!]$ and are incident to KdV-vertices.

– The *graph* is connected and its first Betti number b_1 satisfies $b_1 + \sum_v h(v) = g$.

Remark 2.2.4.1. In the original work [BS17], the third rule is more strict as it also requires leaves to be connected to a KdV-vertex of type $(h(v), d(v)) = (0, 2)$ with one exception given by $(g, n) = (0, 1)$ (in that case the graph consists of only one vertex that is of KdV-type). This is, however, contradictory. Assuming every leaf be connected to a $(0, 2)$-KdV-type vertex, the next vertex *must* be a Φ-vertex. If, however, the theory is specified such that all $\phi_{g,n}$ for $(g, n) \neq (0, 1), (0, 2)$ vanish, this theory would yield $\widetilde{\omega}_{g,n} = 0$ for $(g, n) \neq (0, 1), (0, 2)$, contrary to $\omega_{g,n}$ as would be expected.

According to [BS17], a graph $\Gamma \in \mathrm{Bip}^{\mathrm{KdV}}_{g,n}$ can be associated with a weight as follows.

– One assigns external variables $\{z_i\}_{i\in[\![1,n]\!]} \in \Sigma$ to leaves according to their labelling and an internal edge e obtains integration variables z_e. The set of internal edges is denoted E and the subset of primary internal edges E_0, which are incident to the same KdV-vertex of topological type $(0, 2)$ as the leaves.

– A vertex v contributes a local weight $\widetilde{\omega}_{h(v),d(v)}|_{\mathrm{KdV}}(Z(v))$ or $\Phi_{h(v),d(v)}(Z(v))$ according to its type, where $Z(v)$ is the set of variables corresponding to the edges incident to v and

$$\widetilde{\omega}_{h,d}|_{\mathrm{KdV}}(Z(v)) \coloneqq (-\alpha_i)^{2-2g-n} \sum_{d_1+\cdots+d_n=d_{g,n}} \left(\int_{\overline{\mathcal{M}}_{g,n}} \psi_1^{d_1} \cdots \psi_n^{d_n} \right) \prod_{l=1}^{n} \frac{(2d_l+1)!!\, \mathrm{d}\zeta_{i,l}}{\zeta_{i,l}^{2d_l+2}}\,, \tag{2.112}$$

for $2g - 2 + n > 0$, for $(h, d) = (0, 2)$ by the standard bi-differential of Equation (2.103), and for $(h, d) = (0, 1)$ by $\widetilde{\omega}_{0,1} \coloneqq -\alpha_i \zeta_i^2\, \mathrm{d}\zeta_i$ as well as

$$\Phi_{h,d}(Z(v)) = \int_{a_{i_{e(1)}}}^{z_{e(1)}} \cdots \int_{a_{i_{e(d)}}}^{z_{e(d)}} \left(\phi_{h,d} - \delta_{(h,d)=(0,1)} \alpha_i \zeta_i^2\, \mathrm{d}\zeta_i \right)\,. \tag{2.113}$$

– Then local weights are multiplied and the total weight is given by

$$\varpi_{\Gamma}^{\mathrm{KdV}} = \Big[\prod_{e_i \in E_0} \operatorname*{Res}_{z_{e_i} \to z_i} \Big] \Big[\prod_{e \in E \setminus E_0} \sum_{i_e} \operatorname*{Res}_{z_e \to a_{i_e}} \Big] \frac{\prod_v D[v]}{\#\mathrm{Aut}(\Gamma)}\,, \tag{2.114}$$

where $D(v)$ are the local weights using a pairing similar to Equation (2.93).

Remark 2.2.4.2. At this point a few remarks will be made regarding the prescriptions above.

It was pointed out previously, see Remark 2.2.4.1, that the third rule to construct graphs in $\mathrm{Bip}^{\mathrm{KdV}}_{g,n}$ was modified. This affects the calculation of the corresponding weights. In the original work primary internal edges, that is those edges in E_0, are defined as *all* edges incident to the same KdV-vertex as leaves. In the original formulation then a one-to-one correspondence between these edges and the leaves is claimed, which allowed to write down the residue prescription as in Equation (2.114). Modifying the rules of the graphs, this one-to-one correspondence only applies for those edges that are incident to the same KdV-vertex *of topological type* $(0, 2)$ as leaves. Hence, in

order to be consistent the rule for computing the weights given in by Borot and Shadrin had to be modified.

The local weights of the KdV-vertices correspond to the correlators of the KdV partition function, which encodes the ψ-class intersection numbers, or, in the language of blobbed topological recursion, the solution to the abstract loop equations for $\widehat{\phi}_{g,n} \equiv 0$ for all (g,n). These are already computed in Example 2.2.1 of Section 2.2.2 restricting to $B_{\beta,k;\beta',k'} = 0$ for all $\beta, \beta' \in \{\beta_i\}_{i\in[\![1,s]\!]}$ and $k, k' \in \mathbb{N}$. This illustrates how the blobs of higher topological type in the graphical language connect KdV-sectors, given by ψ-class intersection numbers, in the same way as the holomorphic contributions to $\omega_{0,2} = B$ in ordinary topological recursion do.

Regarding expression (2.114) it may be pointed out that the residue prescription can more easily be understood in the local variables $\zeta_i(z)$ near the i-th marked point.

Describing the same objects, it is possible to relate the two graphical expressions in terms of graphs $\mathrm{Bip}_{g,n}(I_h, I_p)$ and $\mathrm{Bip}^{\mathrm{KdV}}_{g,n}$. Therefore, one needs to associate the leaves to the sets I_h and I_p. This is done by noting that there are three possibilities for the vertices incident to a leaf according to the rules given above. If the leaf is incident to a stable KdV-vertex or a KdV-vertex of type $(0,2)$ that is further attached to a Φ-vertex of type $(0,2)$, then the leaf is said to be of $\mathcal{P}$-type. Otherwise, that is if it is incident to a KdV-vertex of type $(0,2)$ that is further attached to a stable Φ-vertex, then it is called of $\mathcal{H}$-type. This associates leaves of a given type to the corresponding projectors, $\mathcal{H}$ or $\mathcal{P}$, in the representation of correlators in terms of $\mathrm{Bip}_{g,n}(I_h, I_p)$.
Using this knowledge, one obtains the elements of $\mathrm{Bip}_{g,n}(I_h, I_p)$ from the ones constructed here by considering the maximal connected subgraphs that only contain KdV-vertices and unstable Φ-vertices and that are incident to at least one leaf of $\mathcal{P}$-type. These subgraphs are the ω vertices of $\mathrm{Bip}_{g,n}(I_h, I_p)$, while the connected components of the complement give, with one caveat, the φ vertices. At the leaves incident to these φ vertices one needs to remove the KdV-vertex of topological type $(0,2)$ turning the form into a actual function.
Investigating a set $\mathrm{Bip}^{\mathrm{KdV}}_{g,n}$ one constructs graphs used to evaluate solutions to the abstract loop equations by the association of weights to these graphs. This sum over graphs is only well-defined, if there are only finitely many contributions, which is true here. However, this is not manifest from the set $\mathrm{Bip}^{\mathrm{KdV}}_{g,n}$, which is infinite. Without changing topological type one can extend a graph by attaching any vertices of type $(0,1)$, referred to as *blossoming*, or pairs of KdV- and Φ-vertices of type $(0,2)$ arbitrarily often (see Figure 2.2.7). Nevertheless, the sum over contributions is finite because the weights of almost all of these graphs vanish, as it was shown in the original work, see [BS17] Lemma 3.14 and 3.15. This can be incorporated into the graphical language constructing the restricted set $\mathrm{Bip}^{\boxed{\mathrm{KdV}}}_{g,n}$ by requiring

- there is no internal KdV-vertex of type $(0,2)$ and no KdV-vertex of type $(0,1)$ incident to an internal edge,
- if there is a stable KdV-vertex of type $(g, n+k)$ attached to k Φ-vertices of type $(0,1)$ such that $g \geqslant 0$, $n \geqslant 0$ and $k \geqslant 1$, then $k \leqslant d_{g,n}$, where $d_{g,n} = \dim \mathcal{M}_{g,n}$.

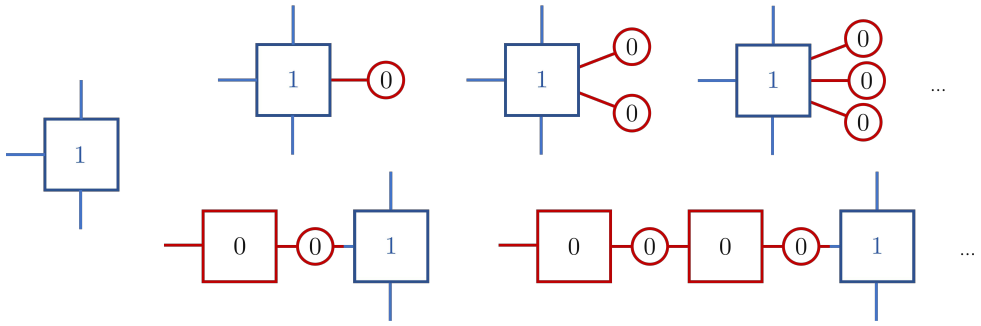

Figure 2.2.7: This depicts graphs of topological type $(g,n)=(1,3)$, where boxes represent KdV- and circles Φ-vertices. This illustrates the fact that the set $\mathrm{Bip}^{\mathrm{KdV}}_{1,3}$ is infinite as vertices (here Φ, but in fact any) of type $(0,1)$ (upper side) and pairs of Φ- and KdV-vertices of type $(0,2)$ can be attached to any graph without changing its topological type.

Remark 2.2.4.3. Note that the fact that internal KdV-vertices of type $(0,2)$ are forbidden for graphs in $\mathrm{Bip}^{\boxed{\mathrm{KdV}}}_{g,n}$ allows for an alternative way to resolve the inconsistency mentioned in Remark 2.2.4.2. Then graphs can be constructed according to the rules $\mathrm{Bip}^{\mathrm{KdV}}_{g,n}$, except for (a) only stable KdV-vertices are allowed, (b) the $(0,1)$-blobs renormalize the (all) KdV-vertices as described above and (c) leaves can be incident to (any) KdV-vertices. For these graphs, which form a finite set, weights can be computed in the same way as for $\mathrm{Bip}^{\boxed{\mathrm{KdV}}}_{g,n}$ only that at leaves incident to a KdV-vertex one replaces correspondingly

$$\sqrt{2}(2d_e+1)!!\,\mathrm{d}\zeta_i(z_e)\,/\zeta_i^{2d_e+2}(z_e) \quad\longmapsto\quad \mathrm{d}\xi_{i,d_e}(z_e)$$

and at leaves incident to a Φ-vertex the residue prescription

$$\operatorname*{Res}_{z_i\to\tilde{z}_i}\frac{\mathrm{d}\zeta_i(\tilde{z}_i)\,\mathrm{d}\zeta_i(z_i)}{(\zeta_i(\tilde{z}_i)-\zeta_i(z_i))^2}$$

is inserted. Then, by ommitting the tilde one obtains the usual symbols of the variables.

Before giving examples for this expansion it should be pointed out that there is in fact nothing special about the graphical expansion of the general solutions $(\widetilde{\omega}_{g,n})$ encoded in blobs $(\phi_{g,n})_{g,n}$ via the KdV solution $(\widetilde{\omega}_{g,n}|_{\mathrm{KdV}})_{g,n}$, which is specified by the vanishing of all $\widehat{\phi}_{g,n}$. By choosing a different special solution as reference point, a similar kind of expansion would be obtained with a similar translation back to ϕ-blobs as described above for φ-blobs.

Example 2.2.6. *In this example the expansion of the correlators $\widetilde{\omega}_{g,n}$ of types $(0,3)$, $(1,1)$, and $(0,4)$ will be explicitly calculated. To that end the graphical language is used. This illustrates not only the reconstruction of the correlators from the graphical language in that it illustrates various effects that occur in this process. It also shows at different instances how blobbed topological recursion is a natural extension of the ordinary theory of Section 2.2. Furthermore, the results of this example can then be compared with the explicit computations in the Quartic Kontsevich Model of Example 2.2.5 yielding the form of the blobs in this model, see Section 2.2.6.*

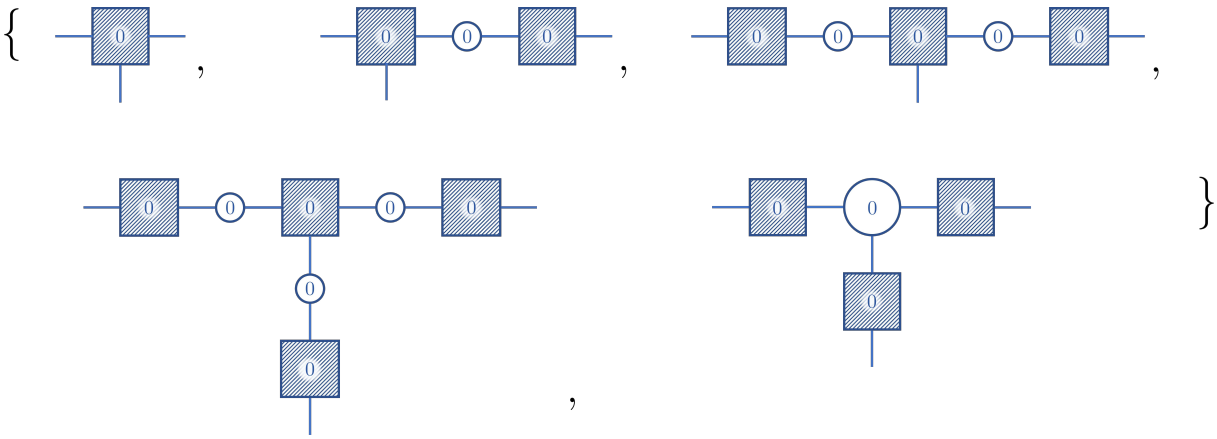

Figure 2.2.8: A list of the graphs present in $\mathrm{Bip}_{0,3}^{\boxed{\text{KdV}}}$. The hatched squares represent blossomed KdV-vertices and the circles represent Φ-vertices. Note that each graph in this list represents one class consisting of a linear combination of labelled graphs, which is symmetric in the leaves.

First construct the set $\mathrm{Bip}_{0,3}^{\boxed{\text{KdV}}}$, *see Figure 2.2.8. As depicted there, the first graph is the pure KdV contribution with only one KdV vertex of topological type* $(0,3)$. *Without creating loops and changing the topological type of the graph only a blob of type* $(0,3)$ *can replace the KdV vertex or blobs of type* $(0,2)$ *can be attached to the leaves of the first graph. In order to obey the rule that leaves can only be incident to KdV vertices additionally a KdV vertex of type* $(0,2)$ *has to be attached. The pair of KdV and* Φ *vertices resulting in the latter case can be attached to either of the leaves of the KdV vertex of type* $(0,3)$. *This gives the graphs in the list in Figure 2.2.8 modulo symmetrization.*

In the following the weights of these graphs are exemplary constructed. Therefore, one first considers the graphs in Figure 2.2.8 with the renormalised KdV-vertices replaced by their not-renormalized counterpart. The weight of the first graph Γ_0, *that is*

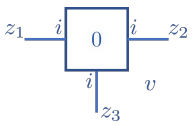

is given by the local weight $D[v] = \omega_{0,3}(z_1,z_2,z_3)|_{\text{KdV}}$ *of the only vertex* v. *Thus, going back to Equation (2.112) this gives*

$$(\varpi_{\Gamma_0}^{\text{KdV}})^{(i,i,i)}(z_1,z_2,z_3) = -\frac{1}{\alpha_i}\langle 1\rangle_{0,3}\frac{\mathrm{d}\zeta_i(z_1)\,\mathrm{d}\zeta_i(z_2)\,\mathrm{d}\zeta_i(z_2)}{(\zeta_i(z_1))^2(\zeta_i(z_2))^2(\zeta_i(z_3))^2}\,. \tag{2.115}$$

Following the structure of attaching a pair of vertices of topological type $(0,2)$ *first at one of the leaves, one computes the weight of a graph of as*

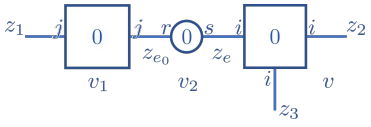

denoted Γ_1. The local weights of the additional vertices is given by

$$D[v_1] = \frac{\mathrm{d}\zeta_j(z_1)\,\mathrm{d}\zeta_j(z_{e_0})}{(\zeta_j(z_1)-\zeta_j(z_{e_0}))^2}\,, \quad D[v_2] = \sum_{k,l\geqslant 0} \frac{\phi_{0,2}\left[\begin{smallmatrix} r,s \\ 2k,2l \end{smallmatrix}\right]}{(2k+1)(2l+1)} \zeta_r^{2k+1}(z_{e_0})\zeta_s^{2l+1}(z_e)\,. \tag{2.116}$$

The set of internal edges is $E = \{e_0, e\}$, while the set of primary internal edges is $E_0 = \{e_0\}$. Using the residue prescription for combining the local weights, see Equation (2.114), one computes

$$\begin{aligned}
&(\varpi_{\Gamma_1}^{\mathrm{KdV}})^{(j,i,i)}(z_1,z_2,z_3) \\
&= \operatorname*{Res}_{z_{e_0}\to z_1}\left(\sum_{i_e}\operatorname*{Res}_{z_e\to\beta_{i_e}}\right)\left[\left(\frac{-\langle 1\rangle_{0,3}}{\alpha_i}\right)\frac{\mathrm{d}\zeta_j(z_1)\,\mathrm{d}\zeta_i(z_2)\,\mathrm{d}\zeta_i(z_2)}{(\zeta_i(z_2))^2(\zeta_i(z_3))^2}\right. \\
&\qquad\left.\sum_{k,l\geqslant 0}\frac{\phi_{0,2}\left[\begin{smallmatrix} r,s \\ 2k,2l \end{smallmatrix}\right]}{(2k+1)(2l+1)}\frac{\zeta_r^{2k+1}(z_{e_0})\,\mathrm{d}\zeta_j(z_{e_0})}{(\zeta_j(z_1)-\zeta_j(z_{e_0}))^2}\frac{\zeta_s^{2l+1}(z_e)\,\mathrm{d}\zeta_j(z_e)}{(\zeta_j(z_e))^2}\right] \\
&= -\frac{\langle 1\rangle_{0,3}}{\alpha_i}\frac{\mathrm{d}\zeta_j(z_1)\,\mathrm{d}\zeta_i(z_2)\,\mathrm{d}\zeta_i(z_2)}{(\zeta_i(z_2))^2(\zeta_i(z_3))^2}\sum_{k,l\geqslant 0}\frac{\phi_{0,2}\left[\begin{smallmatrix} r,s \\ 2k,2l \end{smallmatrix}\right]}{(2k+1)(2l+1)}(2k+1)\zeta_j^{2k}(z_1)\delta_{j,r}\delta_{s,i}\delta_{l,0} \\
&= -\frac{\langle 1\rangle_{0,3}}{\alpha_i}\frac{\mathrm{d}\zeta_j(z_1)\,\mathrm{d}\zeta_i(z_2)\,\mathrm{d}\zeta_i(z_2)}{(\zeta_i(z_2))^2(\zeta_i(z_3))^2}\sum_{k\geqslant 0}\phi_{0,2}\left[\begin{smallmatrix} j,i \\ 2k,0 \end{smallmatrix}\right]\zeta_j^{2k}(z_1)\,.
\end{aligned} \tag{2.117}$$

Comparing this to the weight of the graph Γ_0 above one observes that in addition to a more general index structure (the structure here (j,i,i) includes $j=i$ as well as $j\neq i$) a replacement of the polar contribution $(\zeta_i(z_1))^{-2}$ at the leaf by the holomorphic ones $\sum_k \phi_{0,2}\left[\begin{smallmatrix} j,i \\ 2k,0 \end{smallmatrix}\right]\zeta_j^{2k}(z_1)$ parametrized by the blobs.
This pattern continues in the computation of Γ_2, that is

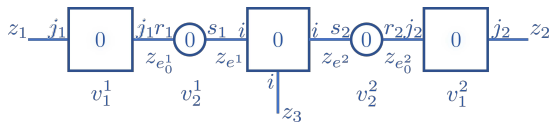

The local weights of the vertices attached at the leaves are

$$\begin{aligned}
D[v_1^1] &= \frac{\mathrm{d}\zeta_{j_1}(z_1)\,\mathrm{d}\zeta_{j_1}(z_{e_0^1})}{(\zeta_{j_1}(z_1)-\zeta_{j_1}(z_{e_0^1}))^2} \quad D[v_2^1] = \sum_{k_1,l_1\geqslant 0}\frac{\phi_{0,2}\left[\begin{smallmatrix} r_1,s_1 \\ 2k_1,2l_1 \end{smallmatrix}\right]}{(2k_1+1)(2l_1+1)}\zeta_{r_1}^{2k_1+1}(z_{e_0^1})\zeta_{s_1}^{2l_1+1}(z_{e^1})\,, \\
D[v_1^2] &= \frac{\mathrm{d}\zeta_{j_2}(z_2)\,\mathrm{d}\zeta_{j_2}(z_{e_0^2})}{(\zeta_{j_2}(z_2)-\zeta_{j_2}(z_{e_0^2}))^2} \quad D[v_2^2] = \sum_{k_2,l_2\geqslant 0}\frac{\phi_{0,2}\left[\begin{smallmatrix} r_2,s_2 \\ 2k_2,2l_2 \end{smallmatrix}\right]}{(2k_2+1)(2l_2+1)}\zeta_{r_2}^{2k_2+1}(z_{e_0^2})\zeta_{s_2}^{2l_2+1}(z_{e^2})\,.
\end{aligned} \tag{2.118}$$

The global weight follows from the residue prescription, Equation (2.114), as

$$
\begin{aligned}
&(\varpi_{\Gamma_2}^{\mathrm{KdV}})^{(j_1,j_2,i)}(z_1,z_2,z_3)\\
&= \operatorname*{Res}_{z_{e_0^1}\to z_1}\operatorname*{Res}_{z_{e_0^2}\to z_2}\left(\sum_{i_{e^1}}\operatorname*{Res}_{z_{e^1}\to\beta_{i_{e^1}}}\right)\left(\sum_{i_{e^2}}\operatorname*{Res}_{z_{e^2}\to\beta_{i_{e^2}}}\right)\left[\left(\frac{-\langle 1\rangle_{0,3}}{\alpha_i}\right)\frac{\mathrm{d}\zeta_j(z_1)\,\mathrm{d}\zeta_h(z_2)\,\mathrm{d}\zeta_i(z_2)}{(\zeta_i(z_3))^2}\right.\\
&\qquad\sum_{k_1,l_1,k_2,l_2\geqslant 0}\frac{\phi_{0,2}\left[\begin{smallmatrix}r_1,s_1\\2k_1,2l_1\end{smallmatrix}\right]}{(2k_1+1)(2l_1+1)}\frac{\phi_{0,2}\left[\begin{smallmatrix}r_2,s_2\\2k_2,2l_2\end{smallmatrix}\right]}{(2k_2+1)(2l_2+1)}\\
&\qquad\qquad\times\frac{\zeta_{r_1}^{2k_1+1}(z_{e_0^1})\,\mathrm{d}\zeta_{j_1}(z_{e_0^1})}{(\zeta_{j_1}(z_1)-\zeta_{j_1}(z_{e_0^1}))^2}\frac{\zeta_{s_1}^{2l_1+1}(z_{e^1})\,\mathrm{d}\zeta_{j_1}(z_{e^1})}{(\zeta_{j_1}(z_{e^1}))^2}\\
&\qquad\qquad\left.\times\frac{\zeta_{r_2}^{2k_2+1}(z_{e_0^2})\,\mathrm{d}\zeta_{j_2}(z_{e_0^2})}{(\zeta_{j_2}(z_2)-\zeta_{j_2}(z_{e_0^2}))^2}\frac{\zeta_{s_2}^{2l_2+1}(z_{e^2})\,\mathrm{d}\zeta_{j_2}(z_{e^2})}{(\zeta_{j_2}(z_{e^2}))^2}\right]. \qquad (2.119)
\end{aligned}
$$

Note that the contributions of both attached leaf structures are completely independent. This is a general phenomenon, which is due to the fact that the computation of the global weight is a local procedure via residue prescriptions. Re-using the computation of the weight of Γ_1*, one finds*

$$
\begin{aligned}
(\varpi_{\Gamma_2}^{\mathrm{KdV}})^{(j_1,j_2,i)}(z_1,z_2,z_3) &= -\frac{\langle 1\rangle_{0,3}}{\alpha_i}\frac{\mathrm{d}\zeta_{j_1}(z_1)\,\mathrm{d}\zeta_{j_2}(z_2)\,\mathrm{d}\zeta_i(z_3)}{(\zeta_i(z_3))^2}\\
&\qquad\sum_{k_1,k_2}\phi_{0,2}\left[\begin{smallmatrix}j_1,i\\2k_1,0\end{smallmatrix}\right]\phi_{0,2}\left[\begin{smallmatrix}j_2,i\\2k_2,0\end{smallmatrix}\right]\zeta_{j_1}(z_1)^{2k_1}\zeta_{j_2}(z_2)^{2k_2}. \qquad (2.120)
\end{aligned}
$$

Continuing to attach a pair of $(0,2)$ *vertices at the last remaining leaf on finds graph* Γ_3*, that is*

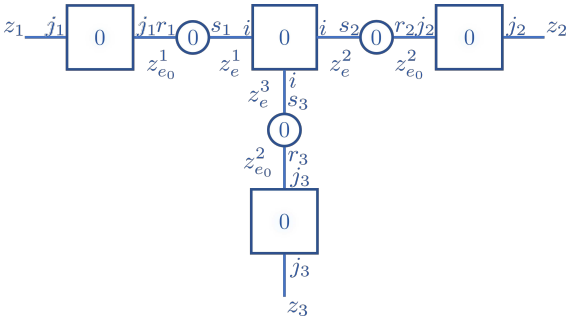

,

the computation is analogously to the above and arrives at

$$
\begin{aligned}
&(\varpi_{\Gamma_3}^{\mathrm{KdV}})^{(j_1,j_2,j_3)}(z_1,z_2,z_3)\\
&= -\sum_i\frac{\langle 1\rangle_{0,3}}{\alpha_i}\,\mathrm{d}\zeta_{j_1}(z_1)\,\mathrm{d}\zeta_{j_2}(z_2)\,\mathrm{d}\zeta_{j_3}(z_3)\\
&\qquad\sum_{k_1,k_2,k_3}\phi_{0,2}\left[\begin{smallmatrix}j_1,i\\2k_1,0\end{smallmatrix}\right]\phi_{0,2}\left[\begin{smallmatrix}j_2,i\\2k_2,0\end{smallmatrix}\right]\phi_{0,2}\left[\begin{smallmatrix}j_3,i\\2k_3,0\end{smallmatrix}\right]\zeta_{j_1}(z_1)^{2k_1}\zeta_{j_2}(z_2)^{2k_2}\zeta_{j_3}(z_3)^{2k_3}. \qquad (2.121)
\end{aligned}
$$

Note that structure of the external index here does not fix the index at the vertex v *of topological type* $(0,3)$*. In order to find a complete result, this index is summed over all*

ramification points.
The last graph $\tilde{\Gamma}$*,*

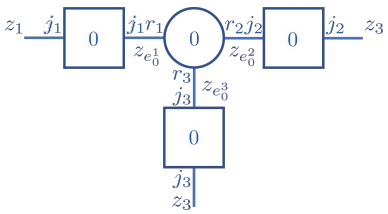

,

is given by the blob of topological type $(0,3)$ *with local weight*

$$D[v] = \sum_{k_1,k_2,k_3\geqslant 0} \frac{\phi_{0,3}\left[\begin{smallmatrix} r_1,r_2,r_3 \\ 2k_1,2k_2,2k_3 \end{smallmatrix}\right]}{(2k_1+1)(2k_2+1)(2k_3+1)} \zeta_{r_1}^{2k_1+1}(z_{e_0^1})\zeta_{r_2}^{2k_2+1}(z_{e_0^2})\zeta_{r_3}^{2k_3+1}(z_{e_0^3}) \tag{2.122}$$

and KdV vertices of type $(0,2)$ *at the leaves. This yields*

$$\begin{aligned}
&(\varpi_{\tilde{\Gamma}}^{\mathrm{KdV}})^{(j_1,j_2,j_3)}(z_1,z_2,z_3) \\
&= \operatorname*{Res}_{z_{e_0^1}\to z_1} \operatorname*{Res}_{z_{e_0^2}\to z_2} \operatorname*{Res}_{z_{e_0^3}\to z_3} \left[\sum_{k_1,k_2,k_3\geqslant 0} \frac{\phi_{0,3}\left[\begin{smallmatrix} r_1,r_2,r_3 \\ 2k_1,2k_2,2k_3 \end{smallmatrix}\right]}{(2k_1+1)(2k_2+1)(2k_3+1)} \right. \\
&\qquad \left. \frac{\zeta_{r_1}^{2k_1+1}(z_{e_0^1})\,\mathrm{d}\zeta_{j_1}(z_{e_0^1})}{(\zeta_{j_1}(z_1)-\zeta_{j_1}(z_{e_0^1}))^2} \frac{\zeta_{r_2}^{2k_2+1}(z_{e_0^2})\,\mathrm{d}\zeta_{j_2}(z_{e_0^2})}{(\zeta_{j_2}(z_2)-\zeta_{j_2}(z_{e_0^2}))^2} \frac{\zeta_{r_3}^{2k_3+1}(z_{e_0^3})\,\mathrm{d}\zeta_{j_3}(z_{e_0^3})}{(\zeta_{j_3}(z_3)-\zeta_{j_3}(z_{e_0^3}))^2} \right] \\
&= \mathrm{d}\zeta_{j_1}(z_1)\,\mathrm{d}\zeta_{j_2}(z_2)\,\mathrm{d}\zeta_{j_3}(z_3) \sum_{k_1,k_2,k_3\geqslant 0} \phi_{0,3}\left[\begin{smallmatrix} r_1,r_2,r_3 \\ 2k_1,2k_2,2k_3 \end{smallmatrix}\right] \zeta_{r_1}^{2k_1}(z_1)\zeta_{r_2}^{2k_2}(z_2)\zeta_{r_3}^{2k_3}(z_3)\,.
\end{aligned} \tag{2.123}$$

To conclude the computation of $\widetilde{\omega}_{0,3}$ *expanded in the KdV variables, one needs to take care of the renormalization of the KdV vertices by blobs of topological type* $(0,1)$*. This step is trivial here as*

$$\chi_{0,3+k} < 0\,, \qquad\qquad k \leqslant d_{0,3} \tag{2.124}$$

has no solution for $k>0$*, referring to the construction of* $\mathrm{Bip}_{g,n}^{\boxed{\mathrm{KdV}}}$*. Collecting the contributions of all graphs one finds* $\widetilde{\omega}_{0,3}^{(i,j,h)}$*. Excluding the last graph the result is equivalent to what one finds using the framework of ordinary topological recursion as the blobs* $\phi_{0,2}\left[\begin{smallmatrix} i,j \\ k,l \end{smallmatrix}\right]$ *can be translated to the coefficients* $B_{\beta_i,k;\beta_j,l}$*. This is reflected in the expansion of* $\mathrm{d}\xi$*, which already includes a polar as well as a sum over holomorphic contributions.*
Then the set $\mathrm{Bip}_{\mathbf{1,1}}^{\boxed{\mathrm{KdV}}}$ ***is considered.*** *It consists of five graphs depicted in Figure 2.2.9. Note the structure here. There is the first graph, which is also there in pure KdV, and the third graph, which is the degeneration of the torus to a three punctured sphere having a self-connecting node represented by a* $(0,2)$*-blob. The second and third graph is obtained from the first and third by the insertion of a* $(0,2)$*-blob at the leaf, respectively. This accounts for a polar and a holomorphic contribution at the leaves, which, as described in the discussion of* $\mathrm{Bip}_{0,3}^{\boxed{\mathrm{KdV}}}$ *above, can already be found in ordinary topological recursion.*
The fifth graph cannot be found in ordinary topological recursion because it contains

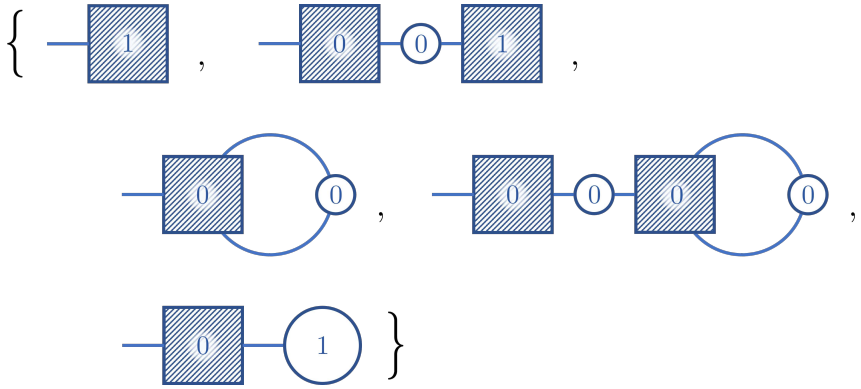

Figure 2.2.9: A list of the graphs present in $\mathrm{Bip}_{1,1}^{\boxed{\mathrm{KdV}}}$. The hatched squares represent blossomed KdV-vertices and the circles represent Φ-vertices.

a $(1,1)$-blob. Here, a $(0,2)$-blob cannot be inserted at the leaf as this would yield an internal $(0,2)$-KdV vertex.
In the construction of the weights, one first considers the graphs in Figure 2.2.10 with the renormalised KdV-vertices replaced by their not-renormalized counterpart.
Starting with the first graph, Γ_1, in Figure 2.2.10,

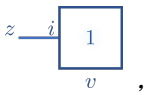

there is only one vertex, which is of KdV-type and has local weight $D[v] = \omega_{1,1}(z)|_{\mathrm{KdV}}$ and no internal edges. Furthermore, the automorphism-group is trivial. Thus, the weight of the graphs evaluates to

$$(\varpi_{\Gamma_1}^{\mathrm{KdV}})^{(i)}(z) = 1D[v] = -\frac{1}{\alpha_i}\langle\psi\rangle_{1,1}(3)!!\frac{\mathrm{d}\zeta_i(z)}{\zeta_i^4(z)}\,. \tag{2.125}$$

Insertion of a $(0,2)$-blob at the leaf yields the graph

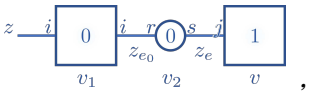

which corresponds to the second element in $\mathrm{Bip}_{1,1}^{\boxed{\mathrm{KdV}}}$. The local weights of the vertices are

$$\begin{aligned} D[v] &= \omega_{1,1}(z)|_{\mathrm{KdV}}\,, & D[v_1] &= \frac{\mathrm{d}\zeta_i(z)\,\mathrm{d}\zeta_i\,(z_{e_0})}{(\zeta_i(z)-\zeta_i(z_{e_0}))^2}\,,\\ D[v_2] &= \sum_{k,l\geqslant 0}\frac{\phi_{0,2}\left[{r,s \atop 2k,2l}\right]}{(2k+1)(2l+1)}\zeta_r^{2k+1}(z_{e_0})\zeta_s^{2l+1}(z_e)\,, \end{aligned} \tag{2.126}$$

and the sets of edges are $E = \{e_0, e\}$ and $E_0 = \{e_0\}$. Using Equation (2.114), the weight

of the entire graph evaluates to

$$
\begin{aligned}
(\varpi_{\Gamma_2}^{\text{KdV}})^{(i)}(z) &= \operatorname*{Res}_{z_{e_0}\to z}\left(\sum_{i_e}\operatorname*{Res}_{z_e\to\beta_{i_e}}\right)\Bigg[\mathrm{d}\zeta_i(z)\left(\frac{-3}{\alpha_i}\right)\langle\psi\rangle_{1,1} \\
&\qquad\qquad \sum_{k,l\geqslant 0}\frac{\phi_{0,2}\left[\begin{smallmatrix}r,s\\2k,2l\end{smallmatrix}\right]}{(2k+1)(2l+1)}\frac{\zeta_r^{2k+1}(z_{e_0})\,\mathrm{d}\zeta_i(z_{e_0})\zeta_s^{2l+1}(z_e)\,\mathrm{d}\zeta_i(z_e)}{(\zeta_i(z)-\zeta_i(z_{e_0}))^2\zeta_j^4(z_e)}\Bigg] \\
&= \mathrm{d}\zeta_i(z)\left(\frac{-3}{\alpha_i}\right)\langle\psi\rangle_{1,1}\sum_j\sum_{k,l\geqslant 0}\frac{\phi_{0,2}\left[\begin{smallmatrix}r,s\\2k,2l\end{smallmatrix}\right]}{(2k+1)(2l+1)}(2k+1)\zeta_i^{2k}(z)\delta_{i,r}\delta_{s,j}\delta_{l,1} \\
&= -\frac{\langle\psi\rangle_{1,1}}{\alpha_i}\sum_j\sum_{k\geqslant 0}\phi_{0,2}\left[\begin{smallmatrix}i,j\\2k,2\end{smallmatrix}\right]\zeta_i^{2k}(z)\,\mathrm{d}\zeta_i(z)\ . \qquad (2.127)
\end{aligned}
$$

The third element in the set $\mathrm{Bip}_{1,1}^{\boxed{\text{KdV}}}$ *is*

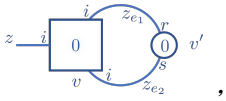

with local weights of the vertices

$$
\begin{aligned}
D[v] &= \omega_{0,3}(z,z_{e_1},z_{e_2})|_{\text{KdV}}\ , \\
D[v'] &= \sum_{k,l\geqslant 0}\frac{\phi_{0,2}\left[\begin{smallmatrix}r,s\\2k,2l\end{smallmatrix}\right]}{(2k+1)(2l+1)}\zeta_r^{2k+1}(z_{e_1})\zeta_s^{2l+1}(z_{e_2})\,. \qquad (2.128)
\end{aligned}
$$

Here, a problem with the modified third rule of graphs in $\mathrm{Bip}_{g,n}^{\text{KdV}}$ *occurs, which the original formulation did not show, see Remarks 2.2.4.1 and 2.2.4.2. As the first vertex after the leaf is not of topological type* $(0,2)$ *there is no one-to-one correspondence between leaves and primary internal edges. Thus, it is initially unclear how the residues should be evaluated. A close examination of the graphical language yields, however, that*

$$
\begin{aligned}
(\varpi_{\Gamma_3}^{\text{KdV}})^{(i)}(z) &= \frac{1}{2}\left(\sum_{i_{e_1}}\operatorname*{Res}_{z_{e_1}\to\beta_{i_{e_1}}}\right)\left(\sum_{i_{e_2}}\operatorname*{Res}_{z_{e_2}\to\beta_{i_{e_2}}}\right)\Bigg[\frac{\mathrm{d}\zeta_i(z)}{\zeta_i^2(z)}\left(-\frac{\langle 1\rangle_{0,3}}{\alpha_i}\right) \\
&\qquad\qquad \times\sum_{k,l\geqslant 0}\frac{\phi_{0,2}\left[\begin{smallmatrix}r,s\\2k,2l\end{smallmatrix}\right]}{(2k+1)(2l+1)}\frac{\zeta_r^{2k+1}(z_{e_1})\,\mathrm{d}\zeta_i(z_{e_1})}{\zeta_i^2(z_{e_1})}\frac{\zeta_s^{2l+1}(z_{e_2})\,\mathrm{d}\zeta_i(z_{e_2})}{\zeta_i^2(z_{e_2})}\Bigg] \\
&= -\frac{\langle 1\rangle_{0,3}}{\alpha_i}\frac{\mathrm{d}\zeta_i(z)}{\zeta_i^2(z)}\sum_{k,l\geqslant 0}\frac{\phi_{0,2}\left[\begin{smallmatrix}r,s\\2k,2l\end{smallmatrix}\right]}{(2k+1)(2l+1)}[\delta_{i,r}\delta_{k,0}][\delta_{i,s}\delta_{l,0}] \\
&= -\frac{\langle 1\rangle_{0,3}}{\alpha_i}\phi_{0,2}\left[\begin{smallmatrix}i,i\\0,0\end{smallmatrix}\right]\frac{\mathrm{d}\zeta_i(z)}{\zeta_i^2(z)}\,. \qquad (2.129)
\end{aligned}
$$

Attaching a $(0,2)$*-blob at the leave of* Γ_3 *one obtains the graph* Γ_4 *as*

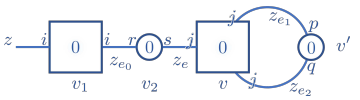

In analogy with the calculation of $\varpi_{\Gamma_2}^{\mathrm{KdV}}$*, see also Remark 2.2.4.2, one finds*

$$(\varpi_{\Gamma_4}^{\mathrm{KdV}})^{(i)}(z) = -\frac{\langle 1\rangle_{0,3}}{\alpha_i}\phi_{0,2}\left[\begin{smallmatrix} i,i \\ 0,0\end{smallmatrix}\right]\sum_j\sum_{k\geqslant 0}\phi_{0,2}\left[\begin{smallmatrix} j,i \\ 2k,0\end{smallmatrix}\right]\zeta_j^{2k}(z)\,\mathrm{d}\zeta_j\,(z) \tag{2.130}$$

The last graph Γ_5 *in* $\mathrm{Bip}_{1,1}^{\boxed{\mathrm{KdV}}}$ *corresponds to*

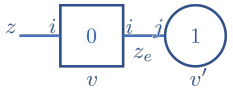

The local weights here are

$$D[v] = \frac{\mathrm{d}\zeta_i(z)\,\mathrm{d}\zeta_i\,(z_e)}{(\zeta_i(z)-\zeta_i(z_e))^2}\,, \qquad \textit{and} \qquad D[v'] = \sum_{k\geqslant 0}\frac{\phi_{1,1}\left[\begin{smallmatrix} j \\ 2k\end{smallmatrix}\right]}{(2k+1)}\zeta_r^{2k+1}(z_e)\,, \tag{2.131}$$

and the sets of edges are $E = E_0 = \{e\}$*. From this one calculates*

$$\begin{aligned}(\varpi_{\Gamma_5}^{\mathrm{KdV}})^{(i)}(z) &= \operatorname*{Res}_{z_e\to z}\left[\mathrm{d}\zeta_i(z)\sum_{k\geqslant 0}\frac{\phi_{1,1}\left[\begin{smallmatrix} j \\ 2k\end{smallmatrix}\right]}{(2k+1)}\frac{\zeta_j^{2k+1}(z_e)\,\mathrm{d}\zeta_i\,(z_e)}{(\zeta_i(z)-\zeta_i(z_e))^2}\right]\\ &= \mathrm{d}\zeta_i(z)\sum_{k\geqslant 0}\frac{\phi_{1,1}\left[\begin{smallmatrix} j \\ 2k\end{smallmatrix}\right]}{(2k+1)}(2k+1)\zeta_i^{2k}(z)\delta_{i,j} = \sum_{k\geqslant 0}\phi_{1,1}\left[\begin{smallmatrix} i \\ 2k\end{smallmatrix}\right]\zeta_i^{2k}(z)\,\mathrm{d}\zeta_i(z)\,.\end{aligned} \tag{2.132}$$

In order to find the true weights of the graphs in $\mathrm{Bip}_{1,1}^{\boxed{\mathrm{KdV}}}$*, the renormalisation by blossomed KdV-vertices needs to be re-installed. Therefore, going back to the definition of* $\mathrm{Bip}^{\boxed{\mathrm{KdV}}}$*, one realizes that amongst those that appear here only KdV-vertices of topological type* $(1,1)$ *are modified. In that case only* $k=1$ *blob of type* $(0,1)$ *needs to be attached. Thus, the weight of subgraphs* $\tilde{\Gamma}$ *of the form*

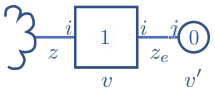

is calculated. The two vertices have the local weights

$$\begin{aligned}D[v] &= \omega_{1,2}(z,z_e)|_{\mathrm{KdV}}\\ &= \frac{\mathrm{d}\zeta_i(z)\,\mathrm{d}\zeta_i(z_e)}{(\alpha_i)^2}\left\{\frac{\langle\psi_1^2\rangle_{1,2}(5)!!(1)!!}{\zeta_i^6(z)\zeta_i^2(z_e)}+\frac{\langle\psi_1\psi_2\rangle_{1,2}(3)!!(3)!!}{\zeta_i^4(z)\zeta_i^4(z_e)}+\frac{\langle\psi_2^2\rangle_{1,2}(1)!!(5)!!}{\zeta_i^2(z)\zeta_i^6(z_e)}\right\}\\ D[v'] &= \int_{\beta_j}^{z_e}\sum_{d\geqslant 0}\left[\phi_{0,1}\left[\begin{smallmatrix} j \\ 2d\end{smallmatrix}\right]-\delta_{d,1}\alpha_j\right]\zeta_j^{2d}\,\mathrm{d}\zeta_j = \sum_{d\geqslant 2}\frac{\phi_{0,1}\left[\begin{smallmatrix} j \\ 2d\end{smallmatrix}\right]}{2d+1}\zeta_j^{2d+1}(z_e)\,.\end{aligned} \tag{2.133}$$

Computing the weight of the subgraph then yields

$$(\varpi_{\tilde{\Gamma}}^{\mathrm{KdV}})^{(i)}(z) = \sum_{i_e} \operatorname*{Res}_{z_e\to\beta_{i_e}} \left[\frac{\mathrm{d}\zeta_i(z)}{(\alpha_i)^2} \sum_{d\geqslant 2} \frac{\phi_{0,1}\left[{j \atop 2d}\right]}{2d+1} \left\{ \frac{\langle\psi_1^2\rangle_{1,2}(5)!!(1)!!}{\zeta_i^6(z)} \frac{\zeta_j^{2d+1}(z_e)\,\mathrm{d}\zeta_i(z_e)}{\zeta_i^2(z_e)} \right.\right.$$
$$\left.\left. + \frac{\langle\psi_1\psi_2\rangle_{1,2}(3)!!(3)!!}{\zeta_i^4(z)} \frac{\zeta_j^{2d+1}(z_e)\,\mathrm{d}\zeta_i(z_e)}{\zeta_i^4(z_e)} + \frac{\langle\psi_2^2\rangle_{1,2}(1)!!(5)!!}{\zeta_i^2(z)} \frac{\zeta_j^{2d+1}(z_e)\,\mathrm{d}\zeta_i(z_e)}{\zeta_i^6(z_e)} \right\} \right]$$
$$= \frac{\langle\psi_2^2\rangle_{1,2}}{(\alpha_i)^2} \frac{\mathrm{d}\zeta_i(z)}{\zeta_i^2(z)} (1)!!(5)!! \sum_{d\geqslant 2} \frac{\phi_{0,1}\left[{i \atop 4}\right]}{2d+1} \delta_{i,j}\delta_{d,2} = \delta_{i,j} \frac{\langle\psi_2^2\rangle_{1,2}}{(\alpha_i)^2} \phi_{0,1}\left[{i \atop 4}\right](3) \frac{\mathrm{d}\zeta_i(z)}{\zeta_i^2(z)} . \tag{2.134}$$

Collecting all contributions calculated above, one finds

$$\tilde{\omega}_{1,1}^{(i)}(z) = \sum_{\Gamma\in \mathrm{Bip}_{1,1}^{\boxed{\mathrm{KdV}}}} \varpi_\Gamma^{\mathrm{KdV}} = \left(\varpi_{\Gamma_1+\tilde{\Gamma}_1}^{\mathrm{KdV}} + \varpi_{\Gamma_2+\tilde{\Gamma}_2}^{\mathrm{KdV}}\right)^{(i)} + \left(\varpi_{\Gamma_3}^{\mathrm{KdV}} + \varpi_{\Gamma_4}^{\mathrm{KdV}}\right)^{(i)} + (\varpi_{\Gamma_5}^{\mathrm{KdV}})^{(i)}$$
$$= -\frac{\langle\psi\rangle_{1,1}}{\alpha_i}\,\mathrm{d}\xi_{i,1}(z_1) + \left(\frac{\langle\psi_2^2\rangle_{1,2}}{(\alpha_i)^2}\phi_{0,1}\left[{i \atop 4}\right] - \frac{\langle 1\rangle_{0,3}}{\alpha_i}\phi_{0,2}\left[{i,i \atop 0,0}\right] \right) \mathrm{d}\xi_{i,0}(z_1)$$
$$+ \sum_{k\geqslant 0} \phi_{1,1}\left[{i \atop 2k}\right] \zeta_i^{2k}(z_1)\,\mathrm{d}\zeta_i(z_1) . \tag{2.135}$$

At last consider the set $\mathrm{Bip}_{\mathbf{0,4}}^{\boxed{\mathrm{KdV}}}$***.*** *The graphs are depicted in Figure 2.2.10. The crossed vertex on leaves indicates a contribution by a holomorphic and polar part as it was described above in the case of* $\mathrm{Bip}_{1,1}^{\boxed{\mathrm{KdV}}}$*, see also Remark 2.2.4.2. Note that depending on the specific expansion point structure, not all the combinations of holomorphic and polar leaves appear. This will be seen again below.*
Here the graphs in the first line of the figure are the ones that are already present in ordinary topological recursion, while those in the second line contain higher blobs of topological types $(0,3)$ *and* $(0,4)$*, respectively. Note also that the graphs come with non-trivial multiplicity.*
The first graph, Γ_1^0*, that one might think of is*

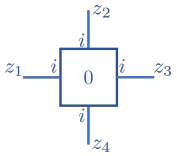

,

which is just the pure KdV contribution. One readily obtains

$$\left[\frac{\varpi_{\Gamma_1^0}^{\mathrm{KdV}}(Z)}{\mathrm{d}\zeta(Z)}\right]^{(i,i,i,i)} = \frac{\langle\psi\rangle_{0,4}}{(\alpha_i)^2}(3!!) \left[\frac{1}{\zeta_i^4(z_1)} \frac{1}{\zeta_i^2(z_2)\zeta_i^2(z_3)\zeta_i^2(z_4)} + \mathrm{symm}(z_1,z_2,z_3,z_4) \right] , \tag{2.136}$$

using the notation

$$\left[\frac{\varpi(Z)}{\mathrm{d}\zeta(Z)}\right]^{(i_1,i_2,i_3,i_4)} = \frac{\varpi^{(i_1,i_2,i_3,i_4)}(z_1,z_2,z_3,z_4)}{\mathrm{d}\zeta_{i_1}(z_1)\,\mathrm{d}\zeta_{i_2}(z_2)\,\mathrm{d}\zeta_{i_3}(z_3)\,\mathrm{d}\zeta_{i_4}(z_4)} . \tag{2.137}$$

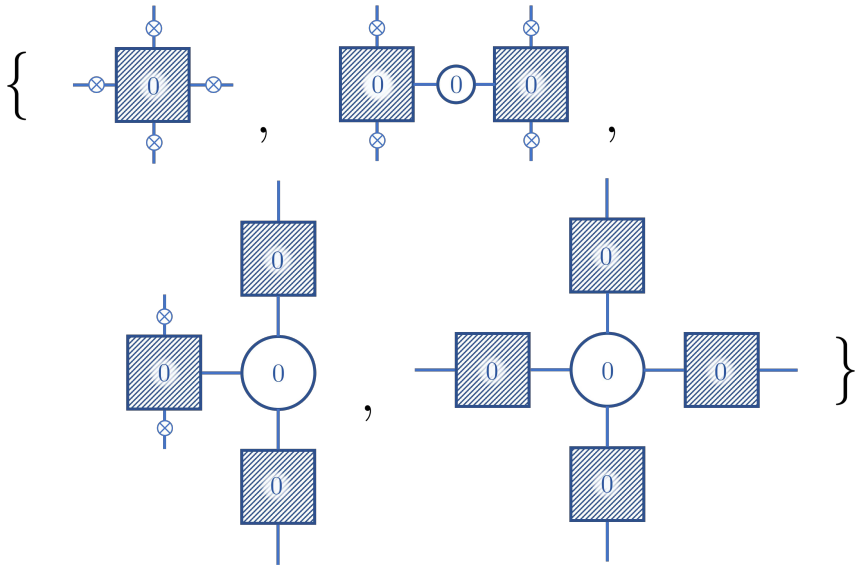

Figure 2.2.10: A list of the graphs present in $\mathrm{Bip}^{\boxed{\mathrm{KdV}}}_{0,4}$. While the hatched squares represent blossomed KdV-vertices and the circles represent Φ-vertices, the crossed vertices are equivalent to a leave plus a leave attached to a KdV-vertex which is attached to a Φ-vertex of type $(0,2)$.

Note that due to its index structure this graph only appears when computing $\omega_{0,4}^{(j_1,j_2,j_3,j_4)}$ *with* $j_1 = j_2 = j_3 = j_4 = i$ *is computed. Attaching one* $(0,2)$*-blob one obtains the graph* Γ_1^1 *given by*

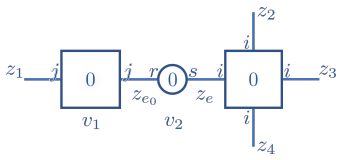

Again computation according to Equation (2.114) yields

$$\frac{[\varpi^{\mathrm{KdV}}_{\Gamma_1^1}(Z)/\,\mathrm{d}\zeta(Z)]^{(j,i,i,i)}}{\langle\psi\rangle_{0,4}/(\alpha_i)^2} = \sum_k \zeta_j^{2k}(z_1)\left[\frac{\phi_{0,2}\left[\begin{smallmatrix} j,i \\ 2k,2\end{smallmatrix}\right]}{\zeta_i^2(z_2)\zeta_i^2(z_3)\zeta_i^2(z_4)}\right. \tag{2.138}$$
$$\left. + 3\phi_{0,2}\left[\begin{smallmatrix} j,i \\ 2k,0\end{smallmatrix}\right]\left(\frac{1}{\zeta_i^4(z_2)\zeta_i^2(z_3)\zeta_i^2(z_4)} + \mathrm{symm}(z_2,z_3,z_4)\right)\right].$$

This graph is present in the case $(j_1,j_2,j_3,j_4) = (j,i,i,i)$*, which includes the two sectors* $j = i$ *as well as* $j \neq i$*.*

In a similar fashion one also obtains the contributions iteratively attaching two, Γ_1^2*, three,* Γ_1^3*, and four,* Γ_1^4*, blobs of type* $(0,2)$ *at the leaves*

$$\frac{[\varpi^{\mathrm{KdV}}_{\Gamma_1^2}(Z)/\,\mathrm{d}\zeta(Z)]^{(j_1,j_2,i,i)}}{\langle\psi\rangle_{0,4}/(\alpha_i)^2} = \sum_{k_1,k_2} \zeta_{j_1}^{2k_1}(z_1)\zeta_{j_2}^{2k_2}(z_2)\left[\frac{\phi_{0,2}\left[\begin{smallmatrix} j_1,i \\ 2k_1,2\end{smallmatrix}\right]\phi_{0,2}\left[\begin{smallmatrix} j_2,i \\ 2k_2,0\end{smallmatrix}\right] + \mathrm{symm}(1,2)}{\zeta_i^2(z_3)\zeta_i^2(z_4)}\right.$$
$$\left. + 3\phi_{0,2}\left[\begin{smallmatrix} j_1,i \\ 2k_1,0\end{smallmatrix}\right]\phi_{0,2}\left[\begin{smallmatrix} j_2,i \\ 2k_2,0\end{smallmatrix}\right]\left(\frac{1}{\zeta_i^4(z_3)\zeta_i^2(z_4)} + \mathrm{symm}(z_3,z_4)\right)\right], \tag{2.139}$$

$$\frac{[\varpi^{\mathrm{KdV}}_{\Gamma_1^3}(Z)/\,\mathrm{d}\zeta(Z)]^{(j_1,j_2,j_3,i)}}{\langle\psi\rangle_{0,4}/(\alpha_i)^2} = \sum_{k_1,k_2,k_3} \zeta_{j_1}^{2k_1}(z_1)\zeta_{j_2}^{2k_2}(z_2)\zeta_{j_3}^{2k_3}(z_3) \times \left[\frac{\phi_{0,2}\left[\begin{smallmatrix} j_1,i \\ 2k_1,2\end{smallmatrix}\right]\phi_{0,2}\left[\begin{smallmatrix} j_2,i \\ 2k_2,0\end{smallmatrix}\right]\phi_{0,2}\left[\begin{smallmatrix} j_3,i \\ 2k_3,0\end{smallmatrix}\right] + \mathrm{symm}(1,2,3)}{\zeta_i^2(z_4)} + \frac{3\phi_{0,2}\left[\begin{smallmatrix} j_1,i \\ 2k_1,0\end{smallmatrix}\right]\phi_{0,2}\left[\begin{smallmatrix} j_2,i \\ 2k_2,0\end{smallmatrix}\right]\phi_{0,2}\left[\begin{smallmatrix} j_3,i \\ 2k_3,0\end{smallmatrix}\right]}{\zeta_i^4(z_4)}\right], \tag{2.140}$$

and

$$[\varpi^{\mathrm{KdV}}_{\Gamma_1^4}(Z)/\,\mathrm{d}\zeta(Z)]^{(j_1,j_2,j_3,j_4)} = \sum_i \frac{\langle\psi\rangle_{0,4}}{(\alpha_i)^2} \sum_{k_1,k_2,k_3,k_4} \zeta_{j_1}^{2k_1}(z_1)\zeta_{j_2}^{2k_2}(z_2)\zeta_{j_3}^{2k_3}(z_3)\zeta_{j_4}^{2k_4}(z_4) \times \left[\phi_{0,2}\left[\begin{smallmatrix} j_1,i \\ 2k_1,2\end{smallmatrix}\right]\phi_{0,2}\left[\begin{smallmatrix} j_2,i \\ 2k_2,0\end{smallmatrix}\right]\phi_{0,2}\left[\begin{smallmatrix} j_3,i \\ 2k_3,0\end{smallmatrix}\right]\phi_{0,2}\left[\begin{smallmatrix} j_4,i \\ 2k_4,0\end{smallmatrix}\right] + \mathrm{symm}(1,2,3,4)\right], \tag{2.141}$$

It should be pointed out here, that the (external) index structure of $\varpi^{\mathrm{KdV},\,(j_1,j_2,j_3,j_4)}_{\Gamma_1^4}$ *does not fix the (internal) index* i*, see the construction of* $\mathrm{Bip}^{\boxed{\mathrm{KdV}}}_{0,3}$*, because at all leaves* $(0,2)$*-blobs have been attached. Thus, in order to get the correct weight for the graph* Γ_1^4*, the index should be summed over all ramification points.*

Turning to the second graph in Figure 2.2.10 one first computes the weight of Γ_2^0*, that is*

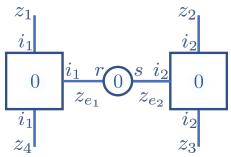

.

This graph represents curves of topological type $(0,4)$ *that degenerated to two components of type* $(0,3)$*. One obtains*

$$(\varpi^{\mathrm{KdV}}_{\Gamma_2^0})^{(i_1,i_2,i_2,i_1)}(Z) = \frac{\mathrm{d}\zeta_{i_1}(z_1)\,\mathrm{d}\zeta_{i_2}(z_2)}{\zeta_{i_1}^2(z_1)\zeta_{i_2}^2(z_2)}\frac{\langle 1\rangle_{0,3}}{\alpha_{i_1}}\phi_{0,2}\left[\begin{smallmatrix} i_1,i_2 \\ 0,0\end{smallmatrix}\right]\frac{\langle 1\rangle_{0,3}}{\alpha_{i_2}}\frac{\mathrm{d}\zeta_{i_2}(z_3)\,\mathrm{d}\zeta_{i_1}(z_4)}{\zeta_{i_2}^2(z_3)\zeta_{i_1}^2(z_4)}, \tag{2.142}$$

and by attaching $(0,2)$*-blobs at the leaves*

$$\frac{[\varpi^{\mathrm{KdV}}_{\Gamma_2^1}(Z)/\,\mathrm{d}\zeta(Z)]^{(j,i_2,i_2,i_1)}}{\phi_{0,2}\left[\begin{smallmatrix} i_1,i_2 \\ 0,0\end{smallmatrix}\right](\langle 1\rangle_{0,3}{}^2)/(\alpha_{i_1}\alpha_{i_2})} = \sum_k \phi_{0,2}\left[\begin{smallmatrix} j,i_1 \\ 2k,0\end{smallmatrix}\right]\frac{\zeta_j^{2k}(z_1)}{\zeta_{i_2}^2(z_2)\zeta_{i_2}^2(z_3)\zeta_{i_1}^2(z_4)}, \tag{2.143}$$

$$\frac{[\varpi^{\mathrm{KdV}}_{\Gamma_2^2}(Z)/\,\mathrm{d}\zeta(Z)]^{(j_1,j_2,i_2,i_1)}}{\phi_{0,2}\left[\begin{smallmatrix} i_1,i_2 \\ 0,0\end{smallmatrix}\right](\langle 1\rangle_{0,3}{}^2)/(\alpha_{i_1}\alpha_{i_2})} = \sum_{k_1,k_2} \phi_{0,2}\left[\begin{smallmatrix} j_1,i_1 \\ 2k_1,0\end{smallmatrix}\right]\phi_{0,2}\left[\begin{smallmatrix} j_2,i_2 \\ 2k_2,0\end{smallmatrix}\right]\frac{\zeta_{j_1}^{2k_1}(z_1)\zeta_{j_2}^{2k_2}(z_2)}{\zeta_{i_2}^2(z_3)\zeta_{i_1}^2(z_4)}, \tag{2.144}$$

as well as

$$\left[\frac{\varpi_{\Gamma_2^3}^{\mathrm{KdV}}(Z)}{\mathrm{d}\zeta(Z)}\right]^{(j_1,j_2,j_3,i_1)} = \sum_{i_2} \phi_{0,2}\left[\begin{smallmatrix} i_1,i_2 \\ 0,0 \end{smallmatrix}\right] \frac{\left(\langle 1\rangle_{0,3}{}^2\right)}{\alpha_{i_1}\alpha_{i_2}} \sum_{k_1,k_2,k_3} \phi_{0,2}\left[\begin{smallmatrix} j_1,i_1 \\ 2k_1,0 \end{smallmatrix}\right] \phi_{0,2}\left[\begin{smallmatrix} j_2,i_2 \\ 2k_2,0 \end{smallmatrix}\right] \phi_{0,2}\left[\begin{smallmatrix} j_3,i_2 \\ 2k_3,0 \end{smallmatrix}\right] \times \frac{\zeta_{j_1}^{2k_1}(z_1)\zeta_{j_2}^{2k_2}(z_2)\zeta_{j_3}^{2k_3}(z_3)}{\zeta_{i_1}^2(z_4)}\,, \tag{2.145}$$

$$\left[\frac{\varpi_{\Gamma_2^4}^{\mathrm{KdV}}(Z)}{\mathrm{d}\zeta(Z)}\right]^{(j_1,j_2,j_3,j_4)} = \sum_{i_1,i_2} \phi_{0,2}\left[\begin{smallmatrix} i_1,i_2 \\ 0,0 \end{smallmatrix}\right] \frac{\left(\langle 1\rangle_{0,3}{}^2\right)}{\alpha_{i_1}\alpha_{i_2}} \sum_{k_1,k_2,k_3,k_4} \phi_{0,2}\left[\begin{smallmatrix} j_1,i_1 \\ 2k_1,0 \end{smallmatrix}\right] \phi_{0,2}\left[\begin{smallmatrix} j_2,i_2 \\ 2k_2,0 \end{smallmatrix}\right] \phi_{0,2}\left[\begin{smallmatrix} j_3,i_2 \\ 2k_3,0 \end{smallmatrix}\right] \phi_{0,2}\left[\begin{smallmatrix} j_4,i_1 \\ 2k_4,0 \end{smallmatrix}\right] \times \zeta_{j_1}^{2k_1}(z_1)\zeta_{j_2}^{2k_2}(z_2)\zeta_{j_3}^{2k_3}(z_3)\zeta_{j_4}^{2k_4}(z_4)\,. \tag{2.146}$$

Note, again, that the (external) index structure of the weight of graph Γ_2^3 and Γ_2^4 does not fix the (internal) indices i_2 and i_1, i_2, respectively. The correct weight is obtained by summing over the corresponding indices.

In order to shorten the discussion here, the weights of the graphs

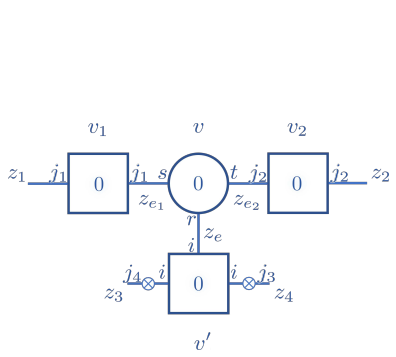

,

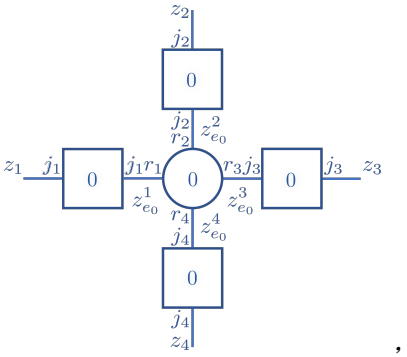

,

which correspond to the third and fourth graph in Figure 2.2.10, are only cited here and not explained in detail. Their computation proceeds analogously. For the former one finds

$$\left[\frac{\varpi_{\Gamma_3^0}^{\mathrm{KdV}}(Z)}{\mathrm{d}\zeta(Z)}\right]^{(j_1,j_2,i,i)} = -\frac{\langle 1\rangle_{0,3}}{\alpha_i} \sum_{l,m} \phi_{0,3}\left[\begin{smallmatrix} i,j_1,j_2 \\ 0,2l,2m \end{smallmatrix}\right] \frac{\zeta_{j_1}^{2l}(z_1)\zeta_{j_2}^{2m}(z_2)}{\zeta_i^2(z_3)\zeta_i^2(z_4)}\,, \tag{2.147}$$

$$\left[\frac{\varpi_{\Gamma_3^1}^{\mathrm{KdV}}(Z)}{\mathrm{d}\zeta(Z)}\right]^{(j_1,j_2,j_3,i)} = -\frac{\langle 1\rangle_{0,3}}{\alpha_i} \sum_{l,m} \sum_{k} \phi_{0,3}\left[\begin{smallmatrix} i,j_1,j_2 \\ 0,2l,2m \end{smallmatrix}\right] \phi_{0,2}\left[\begin{smallmatrix} i,j_3 \\ 0,2k \end{smallmatrix}\right] \frac{\zeta_{j_1}^{2l}(z_1)\zeta_{j_2}^{2m}(z_2)\zeta_{j_3}^{2k}(z_3)}{\zeta_i^2(z_4)}\,, \tag{2.148}$$

$$\left[\frac{\varpi_{\Gamma_3^2}^{\mathrm{KdV}}(Z)}{\mathrm{d}\zeta(Z)}\right]^{(j_1,j_2,j_3,j_4)} = -\sum_{i} \frac{\langle 1\rangle_{0,3}}{\alpha_i} \sum_{l,m} \sum_{k_1,k_2} \phi_{0,3}\left[\begin{smallmatrix} i,j_1,j_2 \\ 0,2l,2m \end{smallmatrix}\right] \phi_{0,2}\left[\begin{smallmatrix} i,j_3 \\ 0,2k_1 \end{smallmatrix}\right] \phi_{0,2}\left[\begin{smallmatrix} i,j_4 \\ 0,2k_2 \end{smallmatrix}\right] \times \zeta_{j_1}^{2l}(z_1)\zeta_{j_2}^{2m}(z_2)\zeta_{j_3}^{2k_1}(z_3)\zeta_{j_4}^{2k_2}(z_4)\,, \tag{2.149}$$

while for the latter there is only the contribution

$$\left[\frac{\varpi_{\Gamma_4}^{\mathrm{KdV}}(Z)}{\mathrm{d}\zeta(Z)}\right]^{(j_1,j_2,j_3,j_4)} = \sum_{k,l,m,n} \phi_{0,4}\left[\begin{smallmatrix} j_1,j_2,j_3,j_4 \\ 2k,2l,2m,2n \end{smallmatrix}\right] \zeta_{j_1}^{2k}(z_{e_1})\zeta_{j_2}^{2l}(z_{e_2})\zeta_t^{2m}(z_{e_3})\zeta_t^{2m}(z_{e_4})\,. \tag{2.150}$$

Note that the former graphs contain vertices of topological type $(0,3)$ *corresponding to the collapse of a component of type* $(0,3)$ *in the curve. This generalizes the picture of curves degenerating by shrinking cycles to components of higher topological type. On the resulting curve intersection numbers are then only computed on the remaining component, which is here of type* $(0,3)$*. This can be seen in the corresponding weights by the appearence of* $(\langle 1\rangle_{0,3}/\alpha_i)$ *associated to the one remaining component. The latter graphs correspond to curves, where the entire curve of topological type* $(0,4)$ *collapsed and only the external structure remains as well as the associated blob.*

All graphs considered above are build from the non-renormalized KdV-vertices. In order to obtain the entire $\widetilde{\omega}_{0,4}$ *blossoming of* $(0,1)$*-blobs must be considered. The only non-vanishing contributions come from*

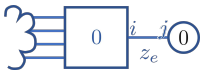

This subgraph has the weight

$$(\varpi^{\mathrm{KdV}}_{\tilde{\Gamma}})^{(i,i,i,i)}(Z) = -\frac{\langle\psi^2\rangle_{0,5}}{(\alpha_i)^3}\phi^{[j]}_{[4]}\frac{\mathrm{d}\zeta_i(z_1)\,\mathrm{d}\zeta_i(z_2)\,\mathrm{d}\zeta_i(z_3)\,\mathrm{d}\zeta_i(z_4)}{\zeta_i^2(z_1)\zeta_i^2(z_2)\zeta_i^2(z_3)\zeta_i^2(z_4)}\,. \tag{2.151}$$

Replacing the KdV-vertex of topological type $(0,4)$ *in graphs* $\{\Gamma_1^k\}_k$ *with this subgraph one obtains*

$$\left[\frac{\varpi^{\mathrm{KdV}}_{\tilde{\Gamma}_1^0}(Z)}{\mathrm{d}\zeta(Z)}\right]^{(i,i,i,i)} = -\frac{\langle\psi^2\rangle_{0,5}}{(\alpha_i)^3}\phi^{[j]}_{[4]}\frac{1}{\zeta_i^2(z_1)\zeta_i^2(z_2)\zeta_i^2(z_3)\zeta_i^2(z_4)}\,, \tag{2.152}$$

$$\left[\frac{\varpi^{\mathrm{KdV}}_{\tilde{\Gamma}_1^1}(Z)}{\mathrm{d}\zeta(Z)}\right]^{(j_1,i,i,i)} = -\frac{\langle\psi^2\rangle_{0,5}}{(\alpha_i)^3}\phi^{[j]}_{[4]}\sum_k \phi^{\left[j_1,i\right]}_{\left[2k,0\right]}\frac{\zeta_{j_1}^{2k}(z_1)}{\zeta_i^2(z_2)\zeta_i^2(z_3)\zeta_i^2(z_4)}\,, \tag{2.153}$$

$$\left[\frac{\varpi^{\mathrm{KdV}}_{\tilde{\Gamma}_1^2}(Z)}{\mathrm{d}\zeta(Z)}\right]^{(j_1,j_2,i,i)} = -\frac{\langle\psi^2\rangle_{0,5}}{(\alpha_i)^3}\phi^{[j]}_{[4]}\sum_{k_1,k_2} \phi^{\left[j_1,i\right]}_{\left[2k_1,0\right]}\phi^{\left[j_2,i\right]}_{\left[2k_2,0\right]}\frac{\zeta_{j_1}^{2k_1}(z_1)\zeta_{j_2}^{2k_2}(z_2)}{\zeta_i^2(z_3)\zeta_i^2(z_4)}\,, \tag{2.154}$$

$$\left[\frac{\varpi^{\mathrm{KdV}}_{\tilde{\Gamma}_1^3}(Z)}{\mathrm{d}\zeta(Z)}\right]^{(j_1,j_2,j_3,i)} = -\frac{\langle\psi^2\rangle_{0,5}}{(\alpha_i)^3}\phi^{[j]}_{[4]}\sum_{k_1,k_2,k_3} \phi^{\left[j_1,i\right]}_{\left[2k_1,0\right]}\phi^{\left[j_2,i\right]}_{\left[2k_2,0\right]}\phi^{\left[j_3,i\right]}_{\left[2k_3,0\right]}\frac{\zeta_{j_2}^{2k_1}(z_1)\zeta_{j_2}^{2k_2}(z_2)\zeta_{j_3}^{2k_3}(z_3)}{\zeta_i^2(z_4)}\,, \tag{2.155}$$

$$\left[\frac{\varpi^{\mathrm{KdV}}_{\tilde{\Gamma}_1^4}(Z)}{\mathrm{d}\zeta(Z)}\right]^{(j_1,j_2,j_3,j_4)} = -\sum_i \frac{\langle\psi^2\rangle_{0,5}}{(\alpha_i)^3}\phi^{[j]}_{[4]}\sum_{k_1,k_2,k_3,k_4} \phi^{\left[j_1,i\right]}_{\left[2k_1,0\right]}\phi^{\left[j_2,i\right]}_{\left[2k_2,0\right]}\phi^{\left[j_3,i\right]}_{\left[2k_3,0\right]}\phi^{\left[j_4,i\right]}_{\left[2k_4,0\right]} \times \zeta_{j_2}^{2k_1}(z_1)\zeta_{j_2}^{2k_2}(z_2)\zeta_{j_3}^{2k_3}(z_3)\zeta_{j_4}^{2k_4}(z_4)\,. \tag{2.156}$$

Concluding, in order to find the expansion of $\omega_{0,4}$ *at the KdV solution in a sector specified by the indices* $(j_1,\ldots,j_4)$ *one needs to add the weights of all graphs contributing in this sector.*

2.2.6 Application to Quartic Kontsevich Model

In this subsection the information of both examples in this section, Examples 2.2.5 and 2.2.6, are combined to find explicit expressions for the blobs $\phi_{g,n}$ in low topologies and order.

Recapitulate the definition of the blobs in Equation (2.105)

$$\phi_{g,n}(z_1,\dots,z_n) = (\mathcal{H}_1\cdots\mathcal{H}_n)\,\widetilde{\omega}_{g,n}(z_1,\dots,z_n) \tag{2.157}$$

This formula can be interpreted in two different manners. Either, from the persepctive of Example 2.2.5, one projects the correlators that are obtained through the recursion to their holomorphic part in all variables. Alternatively, one can first construct the correlators first abstractly using the graphical language. These expressions are parametrized by the expansion components $\phi_{g',n'}\left[\begin{smallmatrix} i_1,\dots,i_n \\ d_1,\dots,d_n \end{smallmatrix}\right]$ for $(g',n') \leqslant (g,n)$, which are defined in Equation (2.106) as

$$\phi_{g',n'}(z_1,\dots,z_{n'}) \overset{z_\bullet\to i_\bullet}{\sim} \sum_{d_1,\dots,d_n\geqslant 0} \phi_{g',n'}\left[\begin{smallmatrix} i_1,\dots,i_n \\ d_1,\dots,d_n \end{smallmatrix}\right] \prod_{k=1}^{n'} (\zeta_{i_k}(z_k))^{d_k}\,\mathrm{d}\zeta_{i_k}(z_k)\ . \tag{2.158}$$

Starting from the blobs of topological types $(g,n)\in\{(0,1),(0,2)\}$, which are given as the initial data of the recursion, one can iteratively deduce blobs of topological type (g,n) from the correlator of type (g,n) as all blobs of lower type are determined by then.
To illustrate how one proceeds the blobs in low topological types are determined in the following for the Quartic Kontsevich Model. Therefore, first expand

$$\omega_{0,1}^{\mathrm{QKM}}(z) = -R(-z)R'(z)\,\mathrm{d}z \tag{2.159}$$

in $\zeta_i(z) = \sqrt{2(R(z)-R(\beta_i))}$ as

$$\begin{aligned}(\phi_{0,1}^{\mathrm{QKM}})^{(i)}(z) &= (\omega_{0,1}^{\mathrm{QKM}})^{(i)}(z)\\ &= \mathrm{d}\zeta_i(z)\Bigg(-R(-\beta)\zeta_i(z) - \frac{y_{i,0}}{x_{i,0}^{1/2}}\zeta_i^2(z) + \frac{y_{i,0}}{x_{i,0}}\frac{x_{i,1}-3y_{i,1}}{6}\zeta_i^3(z)\\ &\qquad + \frac{y_{i,0}}{x_{i,0}^{3/2}}\frac{5x_{i,1}^2-3x_{i,2}+12x_{i,1}y_{i,1}+12y_{i,2}}{72}\zeta_i^4(z)+\mathcal{O}(\zeta_i^5)\Bigg)\end{aligned} \tag{2.160}$$

as well as

$$\omega_{0,2}^{\mathrm{QKM}}(z_1,z_2) = \frac{\mathrm{d}z_1\,\mathrm{d}z_2}{(z_1-z_2)^2} + \frac{\mathrm{d}z_1\,\mathrm{d}z_2}{(z_1+z_2)^2} \tag{2.161}$$

to yield

$$
\begin{aligned}
\phi_{0,2}\left[\begin{smallmatrix} i,i \\ 0,0 \end{smallmatrix}\right] &= \frac{1}{x_{i,0}}\left[\frac{1}{4\beta_i^2}+\frac{1}{24}(x_{i,1}^2-x_{i,2})\right], \\
\phi_{0,2}\left[\begin{smallmatrix} i,i \\ 2,0 \end{smallmatrix}\right] &= \frac{1}{x_{i,0}^2}\Bigg[\frac{3}{16\beta_i^2}+\frac{x_{i,1}}{8\beta_i^3}+\frac{5x_{i,1}^2-3x_{i,2}}{96\beta_i^2}+\frac{1}{5760}\big(175x_{i,1}^4-350x_{i,1}^2x_{i,2}+75x_{i,2}^2 \\
&\qquad +120x_{i,1}x_{i,3}-24x_{i,4}\big)\Bigg] \\
&= \phi_{0,2}\left[\begin{smallmatrix} i,i \\ 0,2 \end{smallmatrix}\right], \\
\phi_{0,2}\left[\begin{smallmatrix} i,i \\ 2,2 \end{smallmatrix}\right] &= \frac{1}{x_{i,0}^3}\Bigg[\frac{15}{8\beta_i^6}+\frac{15x_{i,1}}{8\beta_i^5}+\frac{117x_{i,1}^2-45x_{i,2}}{12\beta_i^4}+\frac{440x_{i,1}^3-405x_{i,1}x_{i,2}+63x_{i,3}}{80\beta_i^3} \\
&\qquad +\frac{1}{17280\beta_i^2}\left(3715x_{i,1}^4-5670x_{i,1}^2x_{i,2}+855x_{i,2}^2+1404x_{i,1}x_{i,3}-180x_{i,4}\right) \\
&\qquad +\frac{1}{1555200}\big(361625x_{i,1}^6-1084875x_{i,1}^4x_{i,2}+411660x_{i,1}^3x_{i,3} \\
&\qquad +741825x_{i,1}^2x_{i,2}^2-116100x_{i,1}^2x_{i,4}-327240x_{i,1}x_{i,2}x_{i,3}-22680x_{i,1}x_{i,5} \\
&\qquad -65475x_{i,2}^3-21546x_{i,3}^2-36720x_{i,2}x_{i,4}+2430x_{i,6}\big)\Bigg] \qquad (2.162)
\end{aligned}
$$

and for $i \neq j$

$$
\begin{aligned}
\phi_{0,2}\left[\begin{smallmatrix} i,j \\ 0,0 \end{smallmatrix}\right] &= \frac{1}{(x_{i,0}x_{j,0})^{1/2}}\left[\frac{1}{(\beta_i-\beta_j)^2}+\frac{1}{(\beta_i+\beta_j)^2}\right], \\
\phi_{0,2}\left[\begin{smallmatrix} i,j \\ 2,0 \end{smallmatrix}\right] &= \frac{1}{(x_{i,0}x_{j,0})^{1/2}}\frac{1}{x_{i,0}}\left[3\left(\frac{1}{(\beta_i-\beta_j)^4}+\frac{1}{(\beta_i+\beta_j)^4}\right)+x_{j,1}\left(\frac{1}{(\beta_i-\beta_j)^3}-\frac{1}{(\beta_i+\beta_j)^3}\right)\right. \\
&\quad \left.+\frac{5x_{i,1}^2-3x_{i,2}}{24}\left(\frac{1}{(\beta_i-\beta_j)^2}+\frac{1}{(\beta_i+\beta_j)^2}\right)\right] \\
&= \phi_{0,2}\left[\begin{smallmatrix} j,i \\ 0,2 \end{smallmatrix}\right], \\
\phi_{0,2}\left[\begin{smallmatrix} i,j \\ 2,2 \end{smallmatrix}\right] &= \frac{1}{(x_{i,0}x_{j,0})^{1/2}}\frac{1}{x_{i,0}x_{j,0}}\left[30\left(\frac{1}{(\beta_i-\beta_j)^6}+\frac{1}{(\beta_i+\beta_j)^6}\right)\right. \\
&\quad -6x_{j,1}\left(\frac{1}{(\beta_i-\beta_j)^5}-\frac{1}{(\beta_i+\beta_j)^5}\right)+6x_{i,1}\left(\frac{1}{(\beta_i-\beta_j)^5}+\frac{1}{(\beta_i+\beta_j)^5}\right) \\
&\quad +\frac{5x_{i,1}^2-3x_{i,2}+5x_{j,1}^2-3x_{j,2}}{8}\left(\frac{1}{(\beta_i-\beta_j)^4}+\frac{1}{(\beta_i+\beta_j)^4}\right) \\
&\quad +\frac{x_{i,1}x_{j,1}}{2}\left(\frac{1}{(\beta_i-\beta_j)^4}-\frac{1}{(\beta_i+\beta_j)^4}\right)-\frac{(5x_{i,1}^2-3x_{i,2})x_{j,1}}{24} \\
&\quad \times\left(\frac{1}{(\beta_i-\beta_j)^3}-\frac{1}{(\beta_i+\beta_j)^3}\right)+\frac{x_{i,1}(5x_{j,1}^2-3x_{j,2})}{24}\left(\frac{1}{(\beta_i-\beta_j)^3}+\frac{1}{(\beta_i+\beta_j)^3}\right) \\
&\quad \left.+\frac{(5x_{i,1}^2-3x_{i,2})(5x_{j,1}^2-3x_{j,2})}{576}\left(\frac{1}{(\beta_i-\beta_j)^2}+\frac{1}{(\beta_i+\beta_j)^2}\right)\right]. \qquad (2.163)
\end{aligned}
$$

Using this data one can proceed to the next higher **topological type** $(0,3)$. Then

the above is inserted in what was in Example 2.2.6 found for $\omega_{0,3}^{\text{QKM}}$. The resulting expression is order by order in the variables equated with the results of Example 2.2.5. The coefficients of negative orders match exactly, while in positive orders there is one free parameter, the blob of that order. Solving for these one finds

$$\begin{aligned}\phi_{0,3}\left[\begin{smallmatrix}i,i,i\\0,0,0\end{smallmatrix}\right] = \frac{1}{4}\Bigg[&-\frac{1}{16\beta_i^6}+\frac{3}{2\beta_i^5}+\frac{1}{\beta_i^4}\left(-\frac{x_{i,1}^2}{48}+\frac{x_{i,2}}{48}-\frac{5y_{i,1}}{4}+\frac{5}{4}\right)+\frac{1}{\beta_i^3}\left(y_{i,1}^2+\frac{y_{i,2}}{2}\right.\\&\left.-\frac{x_{i,1}}{2}-y_{i,1}+1\right)+\frac{1}{\beta_i^2}\left(-\frac{x_{i,1}^4}{576}+\frac{x_{i,2}x_{i,1}^2}{288}-\frac{x_{i,2}^2}{576}-y_{i,1}^3-y_{i,1}y_{i,2}-\frac{y_{i,3}}{6}\right.\\&\left.+\frac{x_{i,2}}{6}+\frac{x_{i,1}y_{i,1}}{2}+y_{i,1}^2+\frac{y_{i,2}}{2}-x_{i,1}-y_{i,1}+1\right)\Bigg]\frac{1}{y_{i,0}x_{i,0}}\frac{1}{x_{i,0}^{3/2}}\\&+\sum_j\left[\frac{1}{(\beta_i+\beta_j)^6}+\frac{2}{(\beta_i+\beta_j)^4(\beta_i-\beta_j)^2}+\frac{1}{(\beta_i+\beta_j)^2(\beta_i-\beta_j)^4}\right]\frac{1}{y_{j,0}x_{j,0}}\frac{1}{x_{i,0}^{3/2}},\end{aligned} \tag{2.164}$$

$$\begin{aligned}\phi\left[\begin{smallmatrix}i,j,j\\0,0,0\end{smallmatrix}\right] = &\left[\frac{10}{(\beta_i+\beta_j)^6}+\frac{1}{(\beta_i+\beta_j)^5}\left(2x_{i,1}-4y_{i,1}\right)+\frac{1}{(\beta_i+\beta_j)^4}\left(\frac{x_{i,1}^2}{4}-\frac{x_{i,2}}{6}-\frac{x_{i,1}y_{i,1}}{2}\right.\right.\\&\left.\left.+y_{i,1}^2+\frac{y_{i,2}}{2}+\frac{1}{4\beta_i^2}\right)+\frac{1}{2\beta_i^2(\beta_i-\beta_j)^2(\beta_i+\beta_j)^2}\right]\frac{1}{y_{i,0}x_{i,0}}\frac{1}{x_{i,0}^{1/2}x_{j,0}}\\&+\left[\frac{3}{2\beta_j^2\left(\beta_i+\beta_j\right)^4}+\frac{1}{\left(\beta_i+\beta_j\right)^3}\left(\frac{1}{\beta_j^2}\left(\frac{x_{j,1}}{2}-\frac{y_{j,1}}{2}\right)+\frac{1}{\beta_j^3}\right)\right.\\&+\frac{1}{\left(\beta_i+\beta_j\right)^2}\left(\frac{1}{\beta_j^3}\left(\frac{x_{j,1}}{4}-\frac{y_{j,1}}{2}\right)+\frac{1}{\beta_j^2}\left(-\frac{x_{j,1}y_{j,1}}{4}+\frac{x_{j,1}^2}{8}-\frac{x_{j,2}}{12}+\frac{y_{j,1}^2}{2}+\frac{y_{j,2}}{4}\right)\right.\\&\left.\left.+\frac{7}{16\beta_j^4}\right)+\frac{1}{16\beta_j^4\left(\beta_i-\beta_j\right)^2}\right]\frac{1}{y_{j,0}x_{j,0}}\frac{1}{x_{i,0}^{1/2}x_{j,0}}\\&+\left\{\frac{1}{(\beta_i+\beta_t)^2(\beta_t+\beta_t)^4}+\frac{1}{(\beta_i-\beta_t)^2(\beta_t+\beta_t)^4}+\frac{2}{(\beta_i+\beta_t)^2(\beta_t-\beta_t)^2(\beta_t+\beta_t)^2}\right\}\\&\qquad\times\frac{1}{y_{t,0}x_{t,0}}\frac{1}{x_{i,0}^{1/2}x_{j,0}},\end{aligned} \tag{2.165}$$

and

$$\begin{aligned}\phi\left[\begin{smallmatrix}i,j,h\\0,0,0\end{smallmatrix}\right] = &\left(\left[\frac{3}{\left(\beta_h+\beta_i\right)^4\left(\beta_i+\beta_j\right)^2}+\frac{3}{\left(\beta_h+\beta_i\right)^2\left(\beta_i+\beta_j\right)^4}+\frac{4}{\left(\beta_h+\beta_i\right)^3\left(\beta_i+\beta_j\right)^3}\right.\right.\\&+\frac{x_{i,1}-2y_{i,1}}{\left(\beta_h+\beta_i\right)^2\left(\beta_i+\beta_j\right)^3}+\frac{x_{i,1}-2y_{i,1}}{\left(\beta_h+\beta_i\right)^3\left(\beta_i+\beta_j\right)^2}+\frac{1}{\left(\beta_h+\beta_i\right)^2\left(\beta_i+\beta_j\right)^2}\left(\frac{x_{i,1}^2}{4}\right.\\&\left.-\frac{x_{i,2}}{6}-\frac{x_{i,1}y_{i,1}}{2}+y_{i,1}^2+\frac{y_{i,2}}{2}+\frac{1}{4\beta_i^2}\right)+\frac{1}{4\beta_i^2\left(\beta_h-\beta_i\right)^2\left(\beta_i+\beta_j\right)^2}\\&\left.+\frac{1}{4\beta_i^2\left(\beta_h+\beta_i\right)^2\left(\beta_i-\beta_j\right)^2}\right]\frac{1}{y_{i,0}x_{i,0}}\frac{1}{(x_{i,0}x_{j,0}x_{h,0})^{1/2}}+\text{symm}(i,j,h)\Bigg)\end{aligned}$$

$$+\left[\frac{1}{(\beta_i-\beta_t)^2(\beta_j+\beta_t)^2(\beta_h+\beta_t)^2}+\frac{1}{(\beta_i+\beta_t)^2(\beta_j-\beta_t)^2(\beta_h+\beta_t)^2}\right.$$
$$\left.+\frac{1}{(\beta_i+\beta_t)^2(\beta_j+\beta_t)^2(\beta_h-\beta_t)^2}+\frac{1}{(\beta_i+\beta_t)^2(\beta_j+\beta_t)^2(\beta_h+\beta_t)^2}\right]$$
$$\times\frac{1}{y_{t,0}x_{t,0}}\frac{1}{(x_{i,0}x_{j,0}x_{h,0})^{1/2}} \tag{2.166}$$

Analogously one finds for the blob of **topological type** $(1,1)$ the expression

$$\frac{\phi_{1,1}[^i_0]}{\mathrm{d}\zeta_i(z)/x_{i,0}^{1/2}}=\frac{1}{(x_0^{[0]})^2}\underbrace{\left[\frac{x_1^{[0]}}{16a_i^2}-\frac{1}{8\beta_i^3}\right]}_{\substack{\text{do not know}\\ \text{which int.numbers}}}-\frac{1}{y_{i,0}x_{i,0}}\left[-\frac{1}{\beta_i^4}\left(-\frac{\langle 1\rangle_{0,3}}{32}+\frac{3\langle\psi\rangle_{1,1}}{16}\right)\right.$$
$$\left.-\frac{1}{\beta_i^3}\frac{\langle\psi\rangle_{1,1}x_{i,1}}{8}+\frac{1}{\beta_i^2}\left(\underbrace{\frac{x_{i,2}}{288}-\frac{x_{i,1}^2}{288}}_{\substack{\text{do not know}\\ \text{which int.numbers}}}+\frac{\langle\psi^2\rangle_{1,2}}{8}x_{i,1}y_{i,1}+\frac{\langle\psi^2\rangle_{1,2}}{8}y_{i,2}\right)\right]$$
$$-\sum_{j\neq i}\frac{1}{y_{j,0}x_{j,0}}\left[-\frac{3\langle\psi\rangle_{1,1}}{(\beta_i+\beta_j)^4}-\frac{\langle\psi\rangle_{1,1}x_{j,1}}{(\beta_i+\beta_j)^3}+\frac{1}{(\beta_i+\beta_j)^2}\left(\frac{\langle 1\rangle_{0,3}}{48}x_{j,2}\right.\right.$$
$$-x_{j,1}^2\left(\frac{5\langle\psi\rangle_{1,1}-\langle\psi^2\rangle_{1,2}}{24}+\frac{\langle 1\rangle_{0,3}}{48}\right)+\frac{\langle\psi^2\rangle_{1,2}}{2}x_{j,1}y_{j,1}+\frac{\langle\psi^2\rangle_{1,2}}{2}y_{j,2}$$
$$\left.\left.-\frac{\langle 1\rangle_{0,3}}{8\beta_j^2}\right)+\frac{\frac{x_{j,1}^2}{144}}{(\beta_i-\beta_j)^2}\right]. \tag{2.167}$$

In the cases above only the blobs of topological type $(0,2)$ were used. Going further in the computation of blobs, for example to type $(0,4)$, also higher blobs occur and need to be included, in that case the blobs of type $(0,3)$ as they appear in the graphical expansion.

Note here that close examination of the respective expressions in Examples 2.2.5 and 2.2.6 enables to write down the blob in terms of intersection numbers for the most part (see caveat in the expression above). It does not give the blobs in terms of intersection numbers in general due to ambiguities in the origin of certain terms inherent in the method of matching the expressions. In these cases the coefficients of the data $\{x_{i,k}\}_k$ is a difference of a number and several intersection numbers. In that case only the numerical result of that difference is given.

In this chapter it has been shown how algebro-geometric data of the moduli space of curves expressed in intersection numbers is inherently encoded in limits of toy models of quantum field theories on non-commutative space. To be precise the results for the expansion of the LSZ model as well as that of the Quartic Kontsevich Model including

the novel data of the blobs of low topological type were presented.
In the next chapter a specific sector of intersection numbers is investigated in the light of its combinatorial structure.

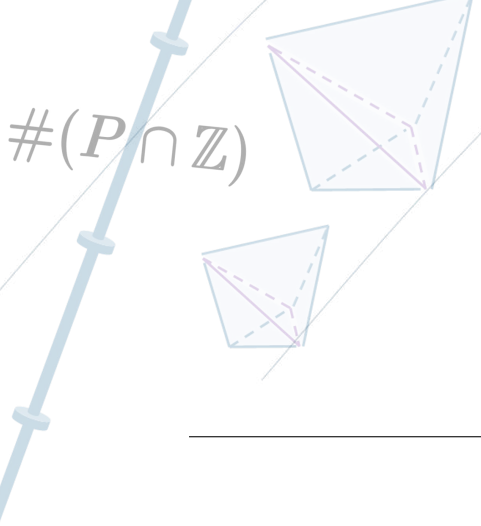

Chapter 3

logarithmic concavity

The moduli space of curves, which is introduced in the previous Chapter 2, has been a fruitful subject of fascinating studies since its construction and compactification by Deligne and Mumford in [DM69, Mum83]. Beyond its relation to field theories, which was iterated on in the previous part of this thesis, a particular interesting perspective was uncovered by Adam Afandi in [Afa22]. The author showed that intersection numbers on the moduli space of complex curves of type

$$\int_{\overline{\mathcal{M}}_{g+m,n+1}} \frac{\psi_1^{d_1} \cdots \psi_n^{d_n}}{1-\psi_{n+1}}$$

are tied to evaluations of Ehrhart polynomials of partial polytopal complexes. This relates the algebro-geometric investigation of the top degree of the tautological ring of the moduli space of complex curves to the combinatorial Ehrhart theory.
After introducing relevant Ehrhart theory, this chapter investigates the particular case of this relation for

$$(d_1, \ldots, d_n) = (1, \ldots, 1) \tag{3.1}$$

in greater detail. As for $n \geqslant 3$ an explicit construction quickly becomes infeasible, the class of polytopal objects corresponding to intersection numbers of this type is characterized through the Ehrhart-theoretic data of f^*- and h^*-vectors. These are determined from the polynomial description in the context of Ehrhart theory and enumerate building blocks of the geometric objects. In the course of this the specific representation the data collected in sequences, here exemplary denoted $(a_k)_k \subset \mathbb{Z}$, allows to reveal a remarkable combinatorial structure

$$a_k^2 \geqslant a_{k+1} a_{k-1}\,, \qquad \text{for all } k\,, \tag{3.2}$$

which is referred to as logarithmic concavity. Logarithmic concavity is shared by many important sequences in various fields in mathematics and often signifies deep structures. While connections to a wide range of disciplines have shed some light on the property and have given rise to methods of proving it, it is oftentimes a hard task to establish that a specific sequence exhibits logarithmic concavity.

In the first section basic facts about Ehrhart theory are reviewed, followed by a discussion of the relation with intersection numbers in the second section. The latter also presents the central Theorems 3.2.4 and 3.2.5, which give explicit so-called f^*- and h^*-expansions of the subset of the Ehrhart polynomials encoding intersection numbers.

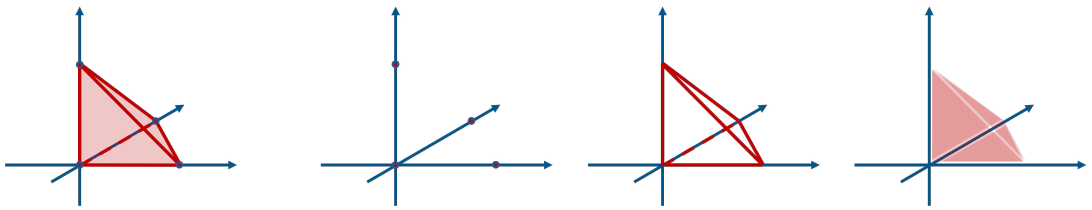

Figure 3.1.1: This depicts the standard simplex Δ_3 in $d = 3$ dimensions (left) as well as its faces of dimensions zero, one, and two, respectively.

As a short digression, in Section 3.3 relevant combinatorial objects are introduced, which are investigated with respect to their logarithmic concavity in the following Section 3.4. The chapter is concluded by the proofs of the theorems about the f^*- and h^*-expansions of the Ehrhart functions, which together with Theorem 3.4.6 show logarithmic concavity of the Ehrhart polynomials considered here. Conjecture 3.2.7 in Section 3.2 claims that this generalizes to all intersection numbers.

3.1 Short exposition of Ehrhart theory

In the following the reader finds a short exposition introducing to Ehrhart theory, which is tailored to the content of this thesis. A far broader presentation of the body of the theory can be found for example in [BR07], which a large portion of this presentation follows.

The basic objects in Ehrhart theory are *polytopes*. Polytopes have two dual descriptions in terms of vertices as well as hyperplanes that are equivalent, which is, in fact, a non-trivial remark[†]. In order to define a polytope using vertices, let $\{v_1, \ldots, v_n\}$ be a set of vectors that span $\mathbb{R}^d$. A polytope P is defined as the convex hull

$$P = \mathrm{Conv}(v_1, \ldots, v_n) := \{\textstyle\sum_{k=1}^n \lambda_k v_k | \ \forall k \ \lambda_k \geqslant 0 \text{ such that } \sum_{k=1}^n \lambda_k = 1\} \ . \tag{3.3}$$

Approaching this object from the perspective of polyhedra, a polytope is described as the bounded intersection of finitely many half-spaces defined by hyperplanes.
Given a polytope P in any description, a general hyperplane is called supporting, if P lies entirely in one closed half-space defined by it. Then, a *face* of P is given by the intersection of P with a supporting hyperplane.

Example 3.1.1. *An important example of a polytope is the standard simplex Δ_d in d dimensions defined by the unit vectors and the origin (see Figure 3.1.1). A general simplex in d dimensions has exactly $(d+1)$ arbitrary vertices. The hyperplanes that correspond to this vertex description of the standard simplex are $\{x \in \mathbb{R}^d \colon x_i = 0\}_{i \in [\![1,d]\!]}$ and $\{x \in \mathbb{R}^d \colon \sum_i x_i = 1\}$. The faces of dimension zero are the vertices, that is the*

[†] see Appendix A of [BR07], which is based on Lecture 1 of [Zie95]

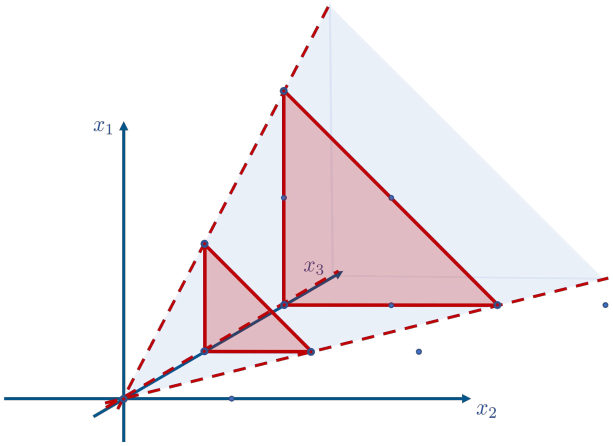

Figure 3.1.2: This illustrates the cone (shaded blue) over the standard 2-simplex. Depicted in shaded red are at $x_3 = 1$ the standard 2-simplex as well as at $x_3 = 2$ second dilate.

origin and the points $\{(\delta_{ij})_{j\in[\![1,d]\!]}\}_{i\in[\![1,d]\!]}$. *Specifying to* $d = 3$, *the faces of dimension one, the edges, are the line segments connecting any two vertices. The facets, which are in general faces of dimension* $d-1$, *are the triangles defined by three vertices. The unique face of dimension three is the simplex itself. In fact the empty set is a face of* P *as well. In many applications it is useful to set its dimension to minus one.*

One can construct a cone over a polytope P by embedding P into $\mathbb{R}^{d+1}$. In the vertex description of the polytope, one constructs the vertices of the cone via $v_i \mapsto w_i = (v_i, 1)$, for all $i \in [\![1, n]\!]$, and sets

$$\operatorname{cone}(P) = \operatorname{cone}(w_1, \ldots, w_n) \coloneqq \{\textstyle\sum_{k=1}^{n} \lambda_k w_k | \ \forall k \ \lambda_k \geqslant 0\} \ . \tag{3.4}$$

Then, the *g-th dilate* of the polytope P, for $g \in \mathbb{N}$, is given by the intersection of the cone with the hyperplane at

$$gP \coloneqq \operatorname{cone}(P) \cap \{x \in \mathbb{R}^d \colon x_{d+1} = g\} \, , \tag{3.5}$$

see Figure 3.1.2. If its vertices are in $\mathbb{Z}^d$, the polytope and its dilates are called integral. Furthermore, an open polytope is the relative interior of a polytope. In the following two definitions the concept of a polytope is generalized.

Definition 3.1.1. An *integral polytopal complex* $\mathcal{P}$ is a finite collection of integral polytopes containing the empty polytope, such that

a) if Q is a face of $P \in \mathcal{P}$, then $Q \in \mathcal{P}$,
b) if $P, Q \in \mathcal{P}$, then $P \cap Q$ is a face of both P and Q.

The elements of $\mathcal{P}$, which are of maximal dimension d, are called faces.

Definition 3.1.2. An *integral partial polytopal complex* $\mathcal{P}$ of dimension d is the disjoint finite union of open integral polytopes. Again, the elements of $\mathcal{P}$ are called faces and are of maximal dimension d.

Remark 3.1.0.1. There are three remarks concerning these definitions. First, the notions introduced above are in fact generalizations of the class of integral polytopes. Every polytope can be thought of as a partial polytopal complex, that is as the disjoint union of the interior of its faces. Then, there is a bijection between the faces of the polytope and the partial polytopal complex. To be precise, the faces of the polytope are the relative closures of the faces of the partial polytopal complex.
Secondly, it should be noted that due to the definitions above, in contrast to polytopal complexes, partial polytopal complexes are not closed under passing to faces, as some relatively open faces might be absent.
Thirdly, results in Ehrhart theory for integral polytopes can often be translated to rational polytopes by clearing denominators. Beyond this domain, regarding irrational polytopes in general dimension few is known. In dimension three and lower, one can in fact transform irrational polytopes into rational ones. This fails in larger dimensions (see [BR07, chapter 3 note 8 and open problem 3.47 as well as chapter 5 note 3]).

Example 3.1.2. *An example for a partial polytopal complex can be constructed starting from the standard simplex Δ_d, discussed in Example 3.1.1. Removing k open facets, that is faces of co-dimension one, one defines Δ_d^k, for $k \in [\![0, d+1]\!]$. In fact, for $k \neq 0$, these objects are neither polytopes nor polytopal complexes by construction, but can be obtained from open polytopes. The corresponding complexes are comprised of the open d simplex, the vertices plus the relative closure of those facets that were not removed, as well as the relative interior of all faces of these objects.*

The task undertaken by Ehrhart theory is to count the lattice points contained in the dilates gP. This count is usually encoded in a function $L_P(g)$ named in honor of Ehrhart, who initiated and developed the theory [Ehr62, Ehr74]. As already mentioned above, for a presentation of results obtained in Ehrhart theory and its methods the reader is kindly referred to [Afa22, BR07] and references therein. The first central theorem, which is cited here, was uncovered by Ehrhart himself for polytopes [Ehr62] and then generalized.

Theorem 3.1.1 (Ehrhart)**.** *The Ehrhart function $L_{\mathcal{P}}(g)$ associated to an integral partial polytopal d-complex $\mathcal{P}$ is a rational polynomial in g of degree d.*

Note that the theorem also received generalization to rational polytopes due to Ehrhart himself. In that case L is a quasi-polynomial with period that divides the lowest common multiple of the denominators of the vertices.
Theorem 3.1.1 allows applying the methods of rational polynomials to Ehrhart theory. The Ehrhart polynomial $L_{\mathcal{P}}(g)$ of an integral partial polytopal d-complex $\mathcal{P}$ can be expanded into binomial bases $\{\binom{g-1}{k}\}_{k\in[\![0,d]\!]}$ or $\{\binom{g+d-k}{d}\}_{k\in[\![0,d]\!]}$, that is

$$L_{\mathcal{P}}(g) =: \sum_{k=0}^{d} f_k^* \binom{g-1}{k}, \qquad \text{and} \qquad L_{\mathcal{P}}(g) =: \sum_{k=0}^{d} h_k^* \binom{g+d-k}{d}. \tag{3.6}$$

The associated coefficients are collected in the vectors $f^*, h^* \in \mathbb{Q}^{d+1}$, respectively. These vectors are the subject of intensive studies in Ehrhart theory and beyond, as information about the partial polytopal complex is encoded in them. A pivotal example of this is Stanley's non-negativity theorem (see [Sta80]) for the h^*-vector.
In order to give an interpretation for the numbers $\{f_k^*\}$ and $\{h_k^*\}$, a few more notions are needed. A partial polytopal complex $\mathcal{P}$ is simplicial, if all of its faces are simplices. A triangulation of $\mathcal{P}$ is a simplicial complex whose support is $\mathcal{P}$. Such a triangulation of $\mathcal{P}$ is unimodular, if the simplices of it can be mapped to the standard simplex by an affine automorphism of $\mathbb{Z}^d$.

Theorem 3.1.2 ([Bre12, Section 2.3] building on [BR07])**.** *For a unimodular triangulation of a polytopal complex $\mathcal{P}$ the f_k^* associated to $\mathcal{P}$ count the k-dimensional open simplices Δ_k^{k+1} in the triangulation.*
If the triangulation, furthermore, is a disjoint union of unimodular half-open[‡] simplices of dimension d, then the h_k^* count the k-dimensional relatively open unimodular simplices Δ_d^k.

Note that not every integral polytopal complex enjoys a unimodular triangulation. In that case the interpretation of the expansion coefficients given in Theorem 3.1.2 does not hold. However, the expansion of $L_{\mathcal{P}}(g)$ in terms of the binomial basis of $\mathbb{Q}[g]$ remains valid.
The following result further characterizes the Ehrhart functions mentioned to be integer-valued. Beyond this it allows to classify Ehrhart polynomials of partial polytopal complexes.

Theorem 3.1.3 (Breuer [Bre12])**.** *Let L be an integer-valued polynomial of degree d and $\mathcal{P}$ is a partial polytopal complex. Then,*

$$L(g) = \#(g\mathcal{P} \cap \mathbb{Z}^d) \quad \Longleftrightarrow \quad f_k^*(L) \geqslant 0 \text{ for all } k \in [\![1, d]\!]\,. \tag{3.7}$$

In the next part of this section the expansion coefficients collected in the f^*- and h^*-vector are related.

3.1.1 Relation of f^*- and h^*-vector

The f^*- and h^*-coefficients of an integer-valued polynomial $p \in \mathbb{Q}[n]$ of degree d as defined in Equation (3.6) are generated by

$$\sum_{n\geqslant 0} p(n)z^n = \frac{\sum_{k=0}^d h_k^* z^k}{(1-z)^{d+1}} =: H^*(z)\,, \quad \text{and} \quad \sum_{n\geqslant 1} p(n)z^n = \sum_{k=0}^d f_k^* \frac{z^{k+1}}{(1-z)^{k+1}} =: F^*(z)\,. \tag{3.8}$$

This can be seen as follows.

[‡]A *half-open* polytope is a set of the form $P \setminus \cup_{i=1}^l p_i$, where P is a polytope and p_i are faces of P. Note that every such polytope is supported by a partial polytopal complex.

***h**-expansion** First, expand the denominator and use the reflection relation and symmetry of binomial coefficients to find

$$\frac{\sum_{k=0}^{d} h_k^* z^k}{(1-z)^{d+1}} = \sum_{k=0}^{d} h_k^* z^k \sum_{n\geqslant 0} \binom{d+n}{n} z^n = \sum_{k=0}^{d} \sum_{n\geqslant k} h_k^* \binom{d+n-k}{d} z^n \,, \tag{3.9}$$

where in the last step one shifts $n \mapsto n-k$. As the sum over k does not change when starting at zero, then interchange the two sums to find the desired form

$$\sum_{k\geqslant 0} z^k \sum_{l=0}^{d} h_l^* \binom{k+d-l}{d} = \sum_{k\geqslant 0} z^k p(k) \,. \tag{3.10}$$

***f**-expansion** In a parallel fashion one shows the expression for the f^*-vector using

$$\frac{z^{k+1}}{(1-z)^{k+1}} = \sum_{n\geqslant 1} \binom{n-1}{k} z^n \,. \tag{3.11}$$

Remark 3.1.3.1. The expressions (3.8) can already be found in [Bre12][‡]. There, the definitions are different to the present work. This concerns in particular the binomial coefficient $\binom{n}{m}$ beyond the classical domain $n \geqslant 0$ and $0 \leqslant m \leqslant n$. The fact that the combinatorial interpretation breaks down for negative n suggests $\binom{n}{m} = 0$ for all $n < 0$. This is in conflict with the continuation of the binomial coefficient using the Γ-function to negative arguments. In order to adapt to this, the sum in (3.8) begins at $k = 1$.

Using the two generating series defined in equation (3.8) one can relate the f^*- and h^*-coefficients via $H^*(z) = p(0) + F^*(z)$. Therefore,

$$\sum_{k=0}^{d} h_k^* z^k = p(0)(1-z)^{n+1} + \sum_{k=0}^{d} f_k^* z^{k+1} (1-z)^{d-k} \,, \tag{3.12}$$

which can be interpreted as artificially adding the term $f_{-1}^* = p(0)$.

3.1.2 Ehrhart theory background

This section should serve the interested reader by providing some background on Ehrhart theory motivating some definitions and giving settings in which classical results can be proved. For the understanding of the following text, this is not crucial and one can readily skip it. This section mostly builds on [BR07].

In general a cone is a set

$$K = \{a + \textstyle\sum_k \lambda_k w_k | \ \forall k \ \lambda_k \geqslant 0\} \tag{3.13}$$

[‡]The h^*-expression is a classical result by Stanley, while the idea of generating functions for the f^*- and h^*-vector goes already back to Ehrhart.

specified by its apex and generators $a, w_k \in \mathbb{R}^d$, respectively. The dimension of K is the dimension of the affine space spanned by its generators. A cone of dimension d is called simplicial, if $\{w_k\}_k$ is a basis of its span. Similar to polytopes, also cones can alternatively be described in terms of half-spaces.
For a rational cone K, Ehrhart theory defines the lattice point counting function

$$\rho_K(z) \equiv \rho_K(z_1, \ldots, z_d) \coloneqq \sum_{m \in K \cap \mathbb{Z}^d} z^m \,, \tag{3.14}$$

where $z^m = z_1^{m_1} \cdots z_d^{m_d}$ is understood. The lattice point count ρ obtains its name due to its bounded analogue. If $\tilde{K}$ was a bounded object,

$$\rho_{\tilde{K}}(1, \ldots, 1) = \#(\tilde{K} \cap \mathbb{Z}^d) \,. \tag{3.15}$$

At this point ρ is only a generating function, but later one can show that it is rather a meromorphic function, to which already the following short example alludes to.

Example 3.1.3. *Consider the one-dimensional cone $K = [0, \infty)$. Then*

$$\rho_{[0,\infty)}(z) \equiv \rho_{[0,\infty)}(z_1) = \sum_{m_1 \in [0,\infty) \cap \mathbb{Z}} z_1^{m_1} = \sum_{m \in \mathbb{N}} z_1^{m_1} = \frac{1}{1 - z_1} \,. \tag{3.16}$$

In case of the general rational cone K one tiles the cone with the fundamental parallelepiped

$$\Pi_K \coloneqq \{\textstyle\sum_k \lambda_k w_k | \; \forall k \; 1 > \lambda_k \geqslant 0\} \,, \tag{3.17}$$

to find the lattice point count

$$\rho_K(z) = \frac{\rho_{a + \Pi_K}(z)}{(1 - z^{w_1}) \cdots (1 - z^{w_d})} \,. \tag{3.18}$$

For a proof see [BR07], theorem 3.5. Considering cones as objects originating from polytopes via the process described in Equation (3.4), one finds

$$\begin{aligned} \rho_{\mathrm{cone}(P)}(z_1, \ldots, z_d, z_{d+1})\Big|_{\substack{z_1 = \cdots = z_d = 1 \\ z_{d+1} = z}} &= 1 + \sum_{g \geqslant 1} \sigma_{gP}(z_1, \ldots, z_d)\, z_{d+1}^g \Big|_{\substack{z_1 = \cdots = z_d = 1 \\ z_{d+1} = z}} \\ &=: 1 + \sum_{g \geqslant 1} L_P(g) z^g =: \mathrm{ehr}_P(z) \end{aligned} \tag{3.19}$$

defining the *Ehrhart function* L_P, which is invariant under unimodular transformations of the polytope, and associated the Ehrhart series ehr_P. Using Equation (3.18), one computes

$$\mathrm{ehr}_P(z) = \frac{f(z)}{(1 - z)^{d+1}} \,, \tag{3.20}$$

and identifies $f(z) = \sum_k h_k^* z^k$ as well as analogously for the f^*-vector.

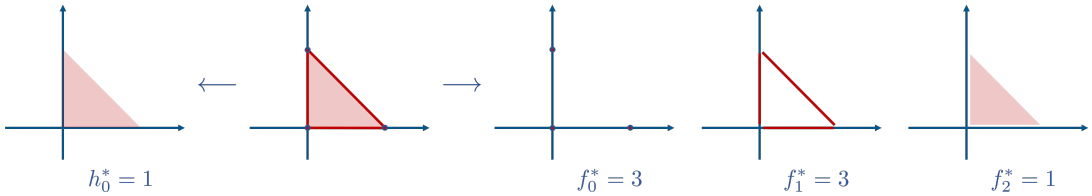

Figure 3.1.3: This counts the (relatively) open simplices Δ_k^{k+1} (panels to the right) and Δ_d^k (panels to the left) of a unimodular triangulation of $\Delta_{d=2} = \Delta$ (second panel) by dimension.

Example 3.1.4. *Consider the cone over the standard simplex $\Delta_2 = \Delta$ of Example 3.1.1, see Figure 3.1.2. This cone has the generators w_k obtained from the vertices v_k of Δ, for $k \in [\![1,3]\!]$, with*

$$\{v_k\}_k = \{(1,0),\,(0,1),\,(0,0)\} \quad \mapsto \quad \{w_k\}_k = \{(1,0,1),(0,1,1),(0,0,1)\}\,. \tag{3.21}$$

Consequently, $\rho_{\Pi_\Delta} = 1$, as the lattice point count of the fundamental parallelepiped associated to these generators only includes the origin. Tiling (see Equation (3.18)) the cone by Π_Δ one finds

$$\rho_\Delta(z_1,z_2,z_3) = \frac{\rho_{\Pi_\Delta}(z_1,z_2,z_3)}{(1-z^{w_1})(1-z^{w_2})(1-z^{w_3})} = \frac{1}{(1-z_1z_3)(1-z_2z_3)(1-z_3)} \tag{3.22}$$

and by specifying to $z_1 = z_2 = 1$ (see Equation (3.19))

$$\mathrm{ehr}_\Delta(z) = (1-z)^{-3} = 1 + \sum\nolimits_{g\geqslant 1} L_\Delta(g) z^t\,. \tag{3.23}$$

Upon inspection this yields $L_\Delta(g) = 1 + (3/2)g + (1/2)g^2$, which gives the vectors

$$f^* = (3,3,1)\,, \qquad \textit{and} \qquad h^* = (1,0,0)\,. \tag{3.24}$$

Going back this reproduces the result cited in Theorem 3.1.2, see Figure 3.1.3. Note also that the coefficients in the monomial basis are rational, while those in the binomial are integral.

In this setup one can build the theory. This includes the results highlighted at the beginning of this section as well as determinations such as

$$h_0^* = 1\,, \qquad \text{and} \qquad h_1^* = L_P(1) - (d+1)\,, \tag{3.25}$$

or results that connect the discrete realm to continuous objects such as the volume

$$\mathrm{vol}(P) = \lim_{g\to\infty} \frac{\#(gP \cap \mathbb{Z}^d)}{g^d} = \sum_k \frac{h_k^*}{d!}\,, \tag{3.26}$$

both cited from [BR07]. Furthermore, although the domain of L might at first sight only be the positive integers, there is a plethora of results reaching from extending this to the negative integers to rather recent research investigating $\mathbb{R}$ as the domain, see references in [BR07]. Applications of these results can be found in various fields including computer science or the moduli space of curves. The latter, which was recently demonstrated in [Afa22], will be portrayed in the following.

3.2 Ehrhart theory and intersection numbers on the moduli space of curves

As already stated above, it is shown in [Afa22] that the information about ψ-class intersection numbers is entirely determined by the family of maps

$$\left\{ \begin{array}{ccc} \mathbb{N}^n & \to & \mathrm{Ehr} \\ (d_i)_i & \mapsto & L_{(d_i)_i}(g+m) \end{array} \right\}_{n\in\mathbb{N}},$$

where Ehr denotes the space of Ehrhart polynomials in g. These maps encode the intersection numbers specified by the array $(d_1,\dots,d_n)$ in the shifted Ehrhart polynomial $L_{(d_i)_i}(g+m)$ of a partial polytopal complex. This result provides an intriguing perspective on tautological intersection numbers and naturally raises the question about what types of partial polytopal complexes correspond to various moduli space data. A partial answer to this for the case of $(d_1,\dots,d_n)=(1,\dots,1)$ is provided in this section in terms of a combinatorial interpretation by the f^*- and h^*-vector.

The theorem of [Afa22] providing the connection encoded in these maps states the following.

Theorem 3.2.1 (Afandi [Afa22])**.** *Let $n\in\mathbb{N}^\times$ as well as $(d_1,\dots,d_n)\in\mathbb{N}^n$. Then there exists a partial polytopal complex $\mathcal{P}_{(d_i)_i}$ of dimension $\sum_i d_i$ with associated integer-valued Ehrhart polynomial $L_{\mathcal{P}_{(d_i)_i}}(g)$ such that*

$$24^{g+m}(g+m)!\,C(\{d_i\}_i)\int_{\overline{\mathcal{M}}_{g+m,n+1}}\frac{\psi_1^{d_1}\cdots\psi_n^{d_n}}{1-\psi_{n+1}} = L_{\mathcal{P}_{(d_i)_i}}(g)\,. \tag{3.27}$$

The constant C and the shift m are given by

$$C(\{d_i\}_i)=\prod_{i=1}^{n}(2d_i+1)!! \qquad \textit{and} \qquad m(\{d_i\}_i)=\left\lceil\Big(-(n+1)+\sum_{i=1}^{n}d_i\Big)/3\right\rceil. \tag{3.28}$$

The quotient of ψ-classes in the theorem should be understood as a geometric series. By the notation of intersection numbers this reduces to only one term with the appropriate power of ψ_{n+1}. Then, the shift m in the genus ensures that

$$\int_{\overline{\mathcal{M}}_{g+m,n+1}}\frac{\psi_1^{d_1}\cdots\psi_n^{d_n}}{1-\psi_{n+1}}\neq 0 \qquad\Longleftrightarrow\qquad g-1\geqslant 0\,, \tag{3.29}$$

which is required to make the connection to Ehrhart theory, which is, at least classically, concerned with (positive) integer dilates of polytopes.
The proof of the theorem provided in the original work, relies on the recursive structure of the moduli space of curves encoded in the Virasoro constraints on the intersection numbers, see Section 2.1.2. These are translated to equations for the Ehrhart functions encoding the corresponding intersection numbers. Using these the property of being

an integer-valued function with non-negative f^*-vector is recursively checked starting from initial cases. By Theorem 3.1.3 due to Breuer this shows the correspondence of intersection numbers and Ehrhart theory.

In the following, the Ehrhart polynomial associated to intersection numbers with

$$(d_1, \dots, d_n) = (1, \dots, 1) \tag{3.30}$$

such that $\sum_i d_i = n$ is further investigated, for which

$$C_{(1,\dots,1)} = 3^n \qquad \text{and} \qquad m(1, \dots, 1) = 0\,. \tag{3.31}$$

In this context denote

$$L_n(g) \coloneqq L_{\mathcal{P}_{(1,\dots,1)}}(g)\,. \tag{3.32}$$

First, an explicit representation is given.

Proposition 3.2.2. *In the setting of Theorem 3.2.1 specify to $(d_i)_i = (1, \dots, 1)$. Then,*

$$L_n(g) = 3^n \prod_{k=1}^{n} (2(g-1)+k) = \prod_{k=1}^{n} (6g + (3k-6)) \tag{3.33}$$

Proof. This proposition is achieved iteratively using the Dilaton equation, see Theorem 2.1.3, as

$$\begin{aligned} L_n(g) &= 24^g (g!)\, 3^n \int_{\overline{\mathcal{M}}_{g,n+1}} \frac{\psi_1 \psi_2 \cdots \psi_n}{1 - \psi_{n+1}} \\ &= 24^g (g!) 3^n (2(g-1)+n) \int_{\overline{\mathcal{M}}_{g,n}} \frac{\psi_2 \cdots \psi_n}{1 - \psi_{n+1}} \\ &= 3(2(g-1)+n) L_{n-1}(g)\,. \end{aligned} \tag{3.34}$$

Removing the ψ-classes step by step one produces in each step one factor of the product in the proposition. The result is completed through the base case $\int_{\overline{\mathcal{M}}_{g,1}} \psi^{3(g-1)+1}$, which equates to $1/(g! 24^g)$, see [Wit90] between equations (2.26) and (2.27). □

In order to find an enumerative interpretation in terms of the f^*- and h^*-vector of the Ehrhart polynomials $L_n(g)$, an appropriate normalization is provided. Using the representation of $L_n(g)$ found from the algebro-geometric interpretation, define $\mathcal{L}_n$ so that

$$L_n(g) = 3^n (n!) \mathcal{L}_n(g)\,. \tag{3.35}$$

Proposition 3.2.3. *The normalized Ehrhart polynomial $\mathcal{L}_n(g)$ defined through Equation (3.35) is an integer-valued polynomial.*

Proof. Note that the coefficients of the polynomial in a monomial basis are in general not divisible by $n!$ contrary to the f_i^*. Therefore, it is suggestive to find an expression in terms of binomial coefficients. This is provided by considering

$$3^{-n}L_n(g) = \prod_{k=1}^{n}(2(g-1)+k) = \frac{(2(g-1)+n)!}{(2(g-1))!}$$
$$= n! \cdot \frac{(2(g-1)+n)!}{n!(2(g-1)+n-n)!} = n!\binom{2(g-1)+n}{n}. \quad (3.36)$$

□

The constructive proof of this proposition explicitly gives

$$\mathcal{L}_n(g) = \binom{2(g-1)+n}{n}. \quad (3.37)$$

This sets the stage to analysing the polynomials from the *combinatorial perspective* of f^*- and h^*-vectors, which is what the next sections constitute. Theorems 3.2.4 and 3.2.5 below give the h^*- and f^*-vectors of the normalized Ehrhart polynomials $\{\mathcal{L}_n(g)\}$ associated to the type of ψ-class intersection numbers described above.
The first of these is treating the f^*-expansion.

Theorem 3.2.4. *The f^*-vector of the normalized Ehrhart polynomial $\mathcal{L}_n(g)$ associated to ψ-class intersection numbers of powers $(d_i)_i = (1,\dots,1) \in \mathbb{N}^n$ computes the number of order-consecutive partition sequences of $(n+1)$ objects into $(k+1)$ parts, that is*

$$\mathcal{L}_n(g) = \sum_{k=0}^{n} f_k^* \binom{g-1}{k}, \quad \textit{with} \quad f_k^* = \mathrm{OCPS}^{(n+1)}(k+1) = \sum_{l=0}^{k}(-1)^{k+l}\binom{2l+n}{n}\binom{k}{l}. \quad (3.38)$$

The h^*-expansion is treated in the second.

Theorem 3.2.5. *Let $2 \leqslant n \in \mathbb{N}$. The normalized Ehrhart polynomial $\mathcal{L}_n(g)$, which computes intersection numbers of ψ-classes with powers $(d_i)_i = (1,\dots,1) \in \mathbb{N}^n$, enjoys the h^*-expansion*

$$\mathcal{L}_n(g) = \sum_{k=0}^{n} h_k^* \binom{g+n-k}{n} \qquad \textit{with} \qquad h_k^* = \binom{n+1}{2(k-1)}. \quad (3.39)$$

The latter theorem mentions the numbers $\mathrm{OCPS}^{(n)}(p)$. These numbers, which count combinatorial objects named *order-consecutive partition sequences*, will be defined just below in Section 3.3. They share with the binomial numbers computed by the h^*-vector the fact that they are *logarithmically concave*. This enticing property as well as the proof of it for $\mathrm{OCPS}^{(n)}(p)$ will be the topic of Section 3.4. After establishing logarithmic concavity of these numbers the proof of Theorems 3.2.4 and 3.2.5 will be given.
The following corollary explicitly summarizes this result.

Corollary 3.2.6. *The normalized Ehrhart polynomials $\mathcal{L}_n(g)$ which correspond to intersection numbers specified by the vector*

$$(d_1, \dots, d_n) = (1, \dots, 1) \tag{3.40}$$

have logarithmically concave f^*- and h^*-expansions.

Proof. This is a direct implication of Theorems 3.2.4 and 3.2.5 above together with Theorem 3.4.6. □

Logarithmic concavity of f^*- and h^*-expansion of all $\mathcal{L}_{\mathcal{P}_d}$
Even further, numerical data strongly suggests that expanding the general Ehrhart polynomials $\mathcal{L}_{\mathcal{P}_d}$ according to the f^*- and h^*-bases the property of logarithmic concavity persists.

Conjecture 3.2.7. *The Ehrhart polynomial $L_{\mathcal{P}_{(d_i)_i}}$ of a partial polytopal complex $\mathcal{P}_{(d_i)_i}$ associated to ψ-class intersection numbers specified by $(d_1, \dots, d_n) \in \mathbb{N}^n$ for $n \in \mathbb{N}$ given by*

$$L_{\mathcal{P}_{(d_i)_i}}(g) = 24^{g+m}(g+m)!C(\{d_i\}_i) \int_{\overline{\mathcal{M}}_{g,n+1}} \frac{\psi_1^{d_1} \cdots \psi_n^{d_n}}{1 - \psi_{n+1}} \tag{3.41}$$

enjoys logarithmically concave f^*- and h^*-expansions.

In Appendix B.2 data is offered supporting this statement for $(d_i)_i$ beyond the case $(d_i)_i = (1, \dots, 1)$.

3.3 Combinatorial definitions

This section provides the definitions of the combinatorial objects – *order-consecutive partition sequences* – which appear in Theorem 3.2.4 above. These were first investigated in [COR85, HM95], which this section mainly follows.
Start with a (linearly) ordered set $N_n = (1, \dots, n) \subset \mathbb{N}$ of n elements and a *partition* $S_p^n = \{s_1, \dots, s_p\}$ of it, for some $p \in [\![1, n]\!]$. The family of sets S_p^n is such that it does not contain the empty set, and it covers N_n in a disjoint manner. The elements s_k of a partition are called parts.
The classical counting result states that there are

$$\mathrm{P}^{(n)}(p) = \left\{ {n \atop p} \right\} \tag{3.42}$$

p-part partitions of N_n referring to the Sterling numbers of the second kind [Sti30, Sta97, Sta99]. This can be seen by considering the recurrence relation of these numbers

$$\left\{ {n+1 \atop p+1} \right\} = \left\{ {n \atop p} \right\} + (p+1) \left\{ {n \atop p+1} \right\}. \tag{3.43}$$

Then, note that the element $(n+1) \in N_n$ can be a singleton of the partition or not. If so, there are n remaining elements that are partitioned into the remaining p parts, giving the first summand above. If $(n+1)$ is not a singleton, then such partitions can be constructed by first partitioning the other n elements into $(p+1)$ parts and then adding $(n+1)$ in one of these $(p+1)$ parts, thus yielding the second summand.
A consecutive partition consists of parts that form consecutive sets, that is two subsequent elements of a part differ by one. In this case the count reduces to

$$\mathrm{CP}^{(n)}(p) = \binom{n-1}{p-1} \tag{3.44}$$

essentially counting the ways of inserting $(p-1)$ characters into the $(n-1)$ spaces between elements in N_n and thereby specifying the parts s_k.
The techniques exemplified above will occur in the following sections at various instances.

Definition 3.3.1. Let $n, p \in \mathbb{N}^\times$. A partition S_p^n of the ordered set N_n is a *partition sequence*, if the parts s_k of S_p^n have a fixed order, denoted by $(s_1, \ldots, s_p)$.

Definition 3.3.2. In the setting of Definition 3.3.1 a partition sequence is *order-consecutive*, if for all $k \in [\![1, p]\!]$ the union $\cup_{l=1}^{k} s_l$ is consecutive.

Example 3.3.1. *In order to illustrate the definition above, consider $N_5 = (1, \ldots, 5)$ partitioned into three parts by the partition sequence $S = (s_1, s_2, s_3)$ such that*

$$s_1 = (2)\,, \qquad s_2 = (3, 4)\,, \qquad s_3 = (1, 5)\,. \tag{3.45}$$

One readily verifies that S is order-consecutive, see the left panel of Figure 3.3.1. In contrast to this, $\tilde{S} = (\tilde{s}_1, \tilde{s}_2, \tilde{s}_3)$ defined by

$$\tilde{s}_1 = (2)\,, \qquad \tilde{s}_2 = (3, 5)\,, \qquad \tilde{s}_3 = (1, 4)\,, \tag{3.46}$$

serves as a counterexample. This partition sequence is not order-consecutive, which can be inspected in the right panel of Figure 3.3.1. As indicated there, $\tilde{s}_1 \cup \tilde{s}_2 = (2, 3, 5)$ is not consecutive.

Finally, the counting result about order-consecutive partition sequences is cited.

Theorem 3.3.1 (Hwang-Mallows [HM95, Theorem 7])**.** *Let $n, p \in \mathbb{N}^\times$. Then the number of order-consecutive partition sequences of an ordered set with n elements into p parts is*

$$\mathrm{OCPS}^{(n)}(p) = \sum_{k=0}^{p-1} (-1)^{p-1-k} \binom{p-1}{k} \binom{n-1+2k}{2k}\,. \tag{3.47}$$

Sketch of proof. The proof, which is presented in the original work by Hwang and Mallows, is sketched here. It relies on a different notation for order-consecutive partition sequences using commas and slashes.

$$\begin{array}{r|ccccc} s_1 & & 2 & & & \\ s_1 \cup s_2 & & 2 & 3 & 4 & \\ s_1 \cup s_2 \cup s_3 & 1 & 2 & 3 & 4 & 5\,. \end{array} \qquad \rightarrow \qquad \begin{array}{r|ccccc} \tilde{s}_1 & & 2 & & & \\ \tilde{s}_1 \cup \tilde{s}_2 & & 2 & 3 & \_ & 5 \\ \tilde{s}_1 \cup \tilde{s}_2 \cup \tilde{s}_3 & 1 & 2 & 3 & 4 & 5\,. \end{array}$$

Figure 3.3.1: This inspects the partition sequences S and $\tilde{S}$ of Example 3.3.1. It shows that the former is order-consecutive (left panel) while the latter is not (right panel). This lack, due to the set $\tilde{s}_1 \cup \tilde{s}_2$ not being consecutive, is highlighted in the second line on the right panel in red.

Encoding an order-consecutive partition sequence S_p^n is achieved by inserting $2(p-1)$ characters, alternating commas and slashes, into the spaces between the elements of N_n (the space after the last element is allowed to contain a slash). One requires that if the slashes are ignored, the commas yield a p-part partition. The parts of the partition are obtained part-by-part considering the sequence of numbers between two commas (in front of 1 and after n there are obligatory commas which are not included in the $2(p-1)$ characters). The slash separates a sequence. Having part s_k the next part s_{k+1} contains the consecutive sequence of numbers directly prior to the lowest number of s_k as well as directly after the highest number of the same. The length of both of these is determined by the lengths of the sequences separated by the slash, respectively. This is best illustrated going back to Example 3.3.1. The order-consecutive partition sequence $S = ((2),(3,4),(1,5))$ of Example 3.3.1 is encoded by $1,/23,4/5$ as

$$\begin{array}{ll} ,/1, & s_1 \text{ has one element,} \\ ,/23, & s_2 \text{ has two elements to the right of (larger than) } s_1\,, \\ ,4/5, & s_3 \text{ has one element to the left (smaller) and} \\ & \quad \text{one to the right of (larger than) } s_1 \cup s_2 \end{array}$$

Using this approach one counts order-consecutive partition sequences by an inclusion-exclusion argument, see Figure 3.3.2. Therefore, first count all ways of inserting the characters into N_n to be

$$\binom{(n-1)+2(p-1)}{2(p-1)} = \binom{n+2p-3}{2p-2}\,. \tag{3.48}$$

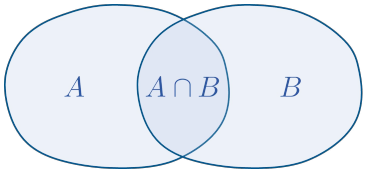

$$|A \cup B| = |A| + |B| - |A \cap B|$$

Figure 3.3.2: This illustrates the simplest case of an inclusion-exclusion counting argument. Counting the elements in the union of the sets A and B, one counts the elements of these sets themselves and subtracts the count of their intersection. This is because the latter is accounted for twice as it is included in the counting of A and B.

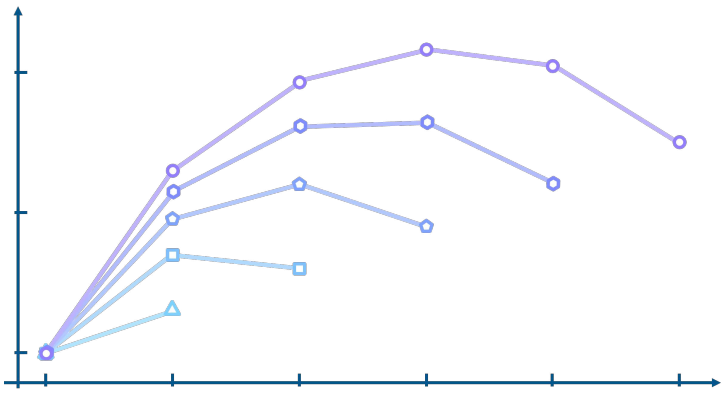

Figure 3.3.3: This plots the values of $(\log \mathrm{OCPS}^{(n)}(p))_{p\in[\![2,n]\!]}$ for $n \in [\![1,6]\!]$ (from light blue to purple and with increasing number of angles). One recognizes the concave shape, see Section 3.4.

This ignores the requirements one the commas and slashes introducing parts of length zero. Therefore, remove all arrangements, where the j-th part is empty for all $j \in [\![1,p]\!]$. In the language of commas and slashes these are the arrangements in which there is no element of N_n between the j-th and $(j+1)$-st comma. By deleting one of these commas and the in-between slash one obtains one of the arrangements counted by

$$\binom{(n-1)+2(p-1-1)}{2(p-1-1)} = \binom{n+2p-5}{2p-4}. \tag{3.49}$$

Proceeding iteratively, the theorem is shown by reversing the order in the sum. □

Logarithmic concavity of these numbers is shown in the following Section 3.4. Computing the first few $\mathrm{OCPS}^{(n)}(p)$ one gets the values

n \ p	1	2	3
1	1		
2	1	2	
3	1	5	4

n \ p	1	2	3	4	5	6
4	1	9	16	8		
5	1	14	41	44	16	
6	1	20	85	146	112	32

see also Figure 3.3.3.

3.4 Logarithmic concavity

This section introduces and discusses the property of logarithmic concavity, which is referred to in Section 3.2 in Corollary 3.2.6 and Conjecture 3.2.7.

Logarithmic concavity and different generalizations have been found in various fields in pure and applied mathematics reaching from applications in control theory, finance

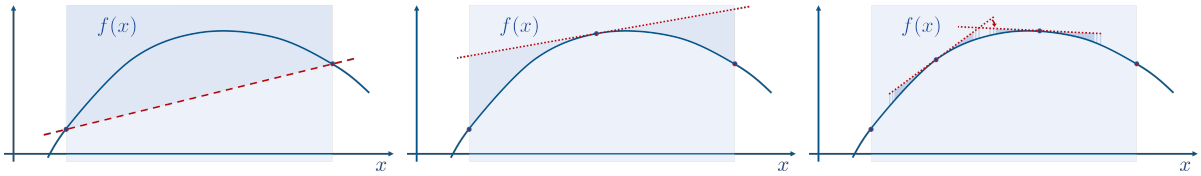

Figure 3.4.1: This shows the graph of a concave function f illustrating the conditions given in Equations (3.50) and (3.51). The secant is an under-estimator of the function, corresponding to the original condition. Furthermore, the first order condition is fullfilled as the tangents to the graph are over-estimators. The slope of the tangents decreases with x suggesting that it obeys the second order condition.

mathematics and use in various algorithms to applications inspired by quantum mechanics or results in matroid theory.
The analysis of concave functions has been substantially studied showing their well-behavedness. An example is the fact that on sufficiently nice domains concave functions can only have singular behavior on the relative boundary. Introducing concavity following [BV04] and the dual concept of convexity[4] as a property of functions, which can then be discretized to apply to sequences, a function $f\colon \mathbb{R} \to \mathbb{R}$ is called concave, if between two points $x, y \in \mathbb{R}$ the secant is always below the value of the function, that is

$$f(tx + (1-t)y) \geqslant tf(x) + (1-t)f(y)\,, \qquad \text{for } t \in [0,1]\,, \tag{3.50}$$

see Figure 3.4.1. In that regard the requirement of concavity is a restriction to the growth rate of a function without referring to differentiability. If f is differentiable this condition can be translated to a condition on its derivatives. One can show that

$$(3.50) \quad \Leftrightarrow \quad f(x) \leqslant f(y) + f'(y)(x-y) \quad \Leftrightarrow \quad f''(x) \leqslant 0\,, \tag{3.51}$$

which is illustrated in Figure 3.4.1. Examples for concave functions are $f(x) = x^a$ for $a \in [0,1]$ or the logarithm $f(x) = \log(x)$ or, generalizing to $\mathbb{R}^n$, the logarithmic determinant $f(X) = \log\det M$ on the set of symmetric positive-definite matrices, while the exponential function $f(x) = \exp(x)$ is convex. Linear functions are both concave and convex.
For many problems it is convenient to generalize to the class to logarithmically or even quasi-concave functions, of which the former is discussed here. Logarithmically concave functions f obey Equation (3.50) only with $\log f$. This can be translated to

$$f(tx + (1-t)y) \geqslant (f(x))^t (f(y))^{(1-t)}\,, \qquad \text{for } t \in [0,1]\,, \tag{3.52}$$

turning the arithmetic comparison in Equation (3.50) to a geometric one. Analogously, the second-order condition yields

$$f(x)f''(x) \leqslant (f'(x))^2\,. \tag{3.53}$$

[4] A function f is convex if $(-f)$ is concave.

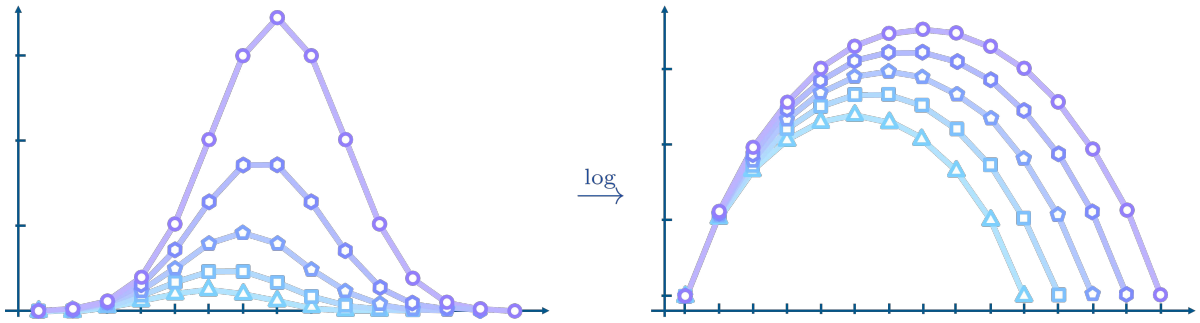

Figure 3.4.2: This plots the sequences $(\binom{n}{k})_{k\in[\![0,n]\!]}$ for $n \in [\![10, 14]\!]$ (from light blue to purple and with increasing number of angles) on linear (left panel) and logarithmic scale (right panel).

The application of the logarithm, see Figure 3.4.2, induces that the exponential function $f(x) = \exp(ax + b)$ now takes the role of linear functions in that they are both logarithmically concave and convex. Other examples for logarithmic concavity are the determinant on symmetric positive-definite matrices or the normal distribution $f(x) = (2\pi a)^{-1/2} \exp(-x^2/a)$.
In order to discretize the property to apply to sequences one maps the derivative $\partial_x f(x)$ to the finite difference $\Delta_x f(x) = (f(x+h) - f(x))/h$ for some finite value $h \in \mathbb{R}^\times$. From Equation (3.52) one finds

$$(f(x+1))^2 \geqslant f(x+2)f(x)\,, \tag{3.54}$$

for $h = 1$. This motivates the following definition.

Definition 3.4.1. A sequence of real numbers $(a_k)_{k\in\mathbb{N}}$ is *logarithmically concave*, if for all $k \in \mathbb{N}^\times$

$$(a_k)^2 \geqslant a_{k+1}a_{k-1}\,, \qquad \text{and} \qquad (a_0)^2 \geqslant 0\,. \tag{3.55}$$

Remark 3.4.0.1. Occasionally the definition of logarithmic concavity of a sequence $(a_k)_k$ includes requiring positiveness $a_k \geqslant 0$ for all $k \in \mathbb{N}$ and the absence of internal zeros. An internal zero is an a_k with $a_k = 0$ such that there exist $\check{k} < k$ and $\hat{k} > k$ such that $a_{\check{k}} \neq 0 \neq a_{\hat{k}}$. In this thesis these additional conditions are separated from logarithmic concavity in order to properly include them in the discussion.

Logarithmic concavity (often also log-concavity) is a distinguished property of sequences. In the past many important sequences have been shown to have this property with examples throughout various fields, see reviews by Richard P. Stanley [Sta89], Francesco Brenti [Bre94] and Petter Brändén [Brä14].
Referring back to the examples above the binomial coefficients $\{\binom{n}{k}\}_{k\in[\![0,n]\!]}$ for some fixed $n \in \mathbb{N}$ constitute the pivotal example for logarithmically concave sequences, see Figure 3.4.2. In this case the proof is an immediate consequence of the definition.

Having no internal zeros in their classical domain $0 \leqslant k \leqslant n$ one readily calculates

$$\binom{n}{k}^2 \Big/ \binom{n}{k+1}\binom{n}{k-1} = \frac{\left(\frac{n!}{(n-k)!k!}\right)^2}{\frac{n!}{(n-k-1)!(k+1)!}\frac{n!}{(n-k+1)!(k-1)!}} = \frac{k+1}{k}\frac{n-k+1}{n-k} > 1 \tag{3.56}$$

for $1 \leqslant k \leqslant n-1$ and additionally notes $\binom{n}{0} = \binom{n}{n} = 1 \geqslant 0$. Beyond this and similar simple examples it proves to be a substantial challenge to establish logarithmic concavity. A ubiquitous technique in its investigation is the formation of generating series for sequences $(a_k)_{k\in\mathbb{N}} \subset \mathbb{R}$ by

$$\mathbb{R}[[x]] \ni \sum\nolimits_{k\in\mathbb{N}} a_k x^k \,, \tag{3.57}$$

which are polynomials if the sequence is eventually vanishing. Important properties of sequences such as the fact that the element-wise product of two logarithmically concave sequences is logarithmically concave are inherited by their generating series. Amongst these many important properties of the generating series, here *real-rootedness* is highlighted. A polynomial $f(x) \in \mathbb{R}[x]$, and by extension the associated sequence, is said to be real-rooted, if

$$f(x) = 0 \qquad \Longrightarrow \qquad x \in \mathbb{R} \,. \tag{3.58}$$

It turns out that real-rootedness of the generating polynomial is a stronger property than logarithmic concavity of the associated sequence, which is a classic result, which can for example be found in [Sta89]. A proof will be sketched in Theorem 3.4.8 below.

Theorem 3.4.1 (Stanley)**.** *Let $(a_k)_{k\in\mathbb{N}}$ be an eventually vanishing sequence with non-negative elements. If $(a_k)_k$ is real-rooted, then it is logarithmically concave and has no internal zeros.*

This result will be used in Section 3.4.2 to prove logarithmic concavity of the counts of order-consecutive partition sequences. Furthermore, real-rootedness implies an additional natural property called *unimodality*. A general sequence $(a_k)_{k\in\mathbb{N}}$ is unimodal if there exists an index $k_0 \in \mathbb{N}$, called the mode, such that

$$a_0 \leqslant a_1 \leqslant \ldots \leqslant a_{k_0-1} \leqslant \; a_{k_0} \; \geqslant a_{k_0+1} \geqslant \ldots \tag{3.59}$$

A characterization of positive, real-rooted sequences can be found in [Bre88], which are called Pólya frequency sequences. This is used in an alternative proof of logarithmic concavity of the counts of order-consecutive partition sequences formulated in Section 3.4.3. To define the Pólya frequency condition, consider the sequence of real numbers $(a_k)_{k\in\mathbb{N}}$ and associate the (possibly infinite) Toeplitz matrix $M = (M_{k,l})_{k,l}$ to it with

$$M_{k,l} = a_{l-k} \,. \tag{3.60}$$

This matrix is a lower-triangular matrix with diagonals given by the elements of $(a_k)_k$. The deciding objects are, in fact, the signs of the minors of M. If all minors of a specific rank up to some rank have the same sign, then one can construct a sequence $\epsilon = (\epsilon_r)_r$ formed by the signs of the minors of the rank specified by the index.

Definition 3.4.2. A sequence $(a_k)_{k\in\mathbb{N}}$ is a *Pólya frequency sequence of order* r, denoted $\mathfrak{P}_r$, if the sign sequence of M starts with at least r ones. If $(a_k)_{k\in\mathbb{N}}$ is $\mathfrak{P}_r$ for all $r \geqslant 0$, then it is called $\mathfrak{P}$.

Note that $\mathfrak{P}_1$ sequences are just sequences with non-negative elements.

Remark 3.4.1.1. Non-negative sequences are those, which are of interest in combinatorics as they can be associated to counting problems.

The definition above implies a theorem due to Brenti [Bre88].

Theorem 3.4.2 (Brenti)**.** *An eventually vanishing sequence with non-negative elements is real-rooted if and only if it is* $\mathfrak{P}$.

Relating Pólya frequency sequences to logarithmic concavity, there is a stronger result in terms of $\mathfrak{P}_2$, which will be discussed in Section 3.4.3 related to the proof of logarithmic concavity of the numbers $\mathrm{OCPS}^{(n)}(p)$ in Theorem 3.4.6. Furthermore, the theory of Pólya frequency sequences implies that the sequences found in this thesis in the context of intersection theory on the moduli space of curves are unimodal. This is because logarithmically concave combinatorial sequences are unimodal if and only if they are $\mathfrak{P}_2$.

In the following, a proof of a recurrence relation for the count of order-consecutive partition sequences is presented in order to deduce the generating function. Then, the zeros of this generating function are located by applying an appropriate change of variables, which in turn verifies logarithmic concavity by Theorem 3.4.1 cited above. The section is concluded with the discussion of an alternative proof using the theory of Pólya frequency sequences, see Definition 3.4.2 above.

3.4.1 Generating function for OCPS

Arrange the numbers $\mathrm{OCPS}^{(n+1)}(p+1)$ counting order-consecutive partition sequences, see Definitions 3.3.1 and 3.3.2 and Theorem 3.3.1, into the generating function

$$G(x,y) \coloneqq \sum_{n,p\in\mathbb{N}} \mathrm{OCPS}^{(n+1)}(p+1)\; x^n y^p\,, \tag{3.61}$$

with coefficients

$$g_n(y) \coloneqq \frac{1}{n!}\,\frac{\partial^n G(x,y)}{\partial x^n}\bigg|_{x=0} = \sum_{p\in\mathbb{N}} \mathrm{OCPS}^{(n+1)}(p+1)\; y^p\,. \tag{3.62}$$

Remark 3.4.2.1. Constructed in this way $G(x,y) \in \mathbb{R}[[x]][y]$ as it is a power series in x and each coefficient of this power series, given by $g_n(y)$, is a polynomial in y. This is because as long as $p > n$ the coefficient of $x^n y^p$ in $G(x,y)$, that is $\mathrm{OCPS}^{(n+1)}(p+1)$, vanishes.

The following propositions, 3.4.3 and 3.4.5, provide a closed expression for G and for g_n, respectively.

Proposition 3.4.3. *The rational generating function for the numbers of order-consecutive partition sequences* $\mathrm{OCPS}^{(n+1)}(p+1)$ *for* $n, p \in \mathbb{N}$ *is*

$$G(x,y) = \frac{1-x}{1-2x-2xy+x^2+x^2y}\,. \tag{3.63}$$

This rational function expands into

$$G(x,y) \overset{x\to 0}{\sim} 1 + (1+2y)\,x + \left(1+5y+4y^2\right)x^2 + \mathcal{O}\left(x^3\right). \tag{3.64}$$

Remark 3.4.3.1. This generating function was conjectured before in [BDGP17] (in Section 9 on page 26) but no proof was given. In that work, the numbers of order-consecutive partition sequences appeared in the context of a combinatorial approach to lacunary series of generalized Laguerre polynomials.

Theorem 3.4.3 is shown in two steps by

- first finding a recurrence relation (Lemma below) and
- then deducing the generating function from there.

Lemma 3.4.4. *The double-indexed sequence* $\left(\mathrm{OCPS}^{(n+1)}(p+1)\right)_{n,p\in\mathbb{N}^\times}$ *of numbers of order-consecutive partition sequences is determined by the recursion*

$$(n)\mathrm{OCPS}^{(n+1)}(p+1) = (2p)\mathrm{OCPS}^{(n)}(p) + (n+2p)\mathrm{OCPS}^{(n)}(p+1)\,. \tag{3.65}$$

Proof. This can be seen by explicit calculation

$$\begin{aligned}
&\mathrm{OCPS}^{(n+1)}(p+1) - \binom{2p}{n}\mathrm{OCPS}^{(n)}(p) - \binom{n+2p}{n}\mathrm{OCPS}^{(n)}(p+1)\\
&= \sum_{k=0}^{p-1}(-1)^{p-k}\binom{p}{k}\left[\binom{n+2k}{2k} - \left(\frac{n+2p}{n} - \frac{2p}{n}\frac{p-k}{p}\right)\binom{n+2k-1}{2k}\right]\\
&\qquad\qquad + (-1)^{p-p}\binom{p}{p}\left[\binom{n+2p}{2p} - \frac{n+2p}{n}\binom{n+2p-1}{2p}\right]\\
&= \sum_{k=0}^{p-1}(-1)^{p-k}\binom{p}{k}\binom{n+2k}{2k}\left[1-\left(\frac{n+2k}{n}\frac{n}{n+2k}\right)\right] + \left[1-\frac{n+2p}{n}\frac{n}{n+2p}\right] = 0\,,
\end{aligned} \tag{3.66}$$

where the binomial relation $\binom{a-1}{b} = \frac{a-b}{b}\binom{a}{b}$ was employed several times. □

Using this lemma Proposition 3.4.3 can be proved.

Proof of Prop. 3.4.3. From the recurrence relation given in the lemma above a partial differential equation is deduced that the generating function must satisfy. It reads

$$x\left[1+(-1+x)\partial_x+2y\left(1+(1+y)\partial_y\right)\right]h(x,y)=0\,. \tag{3.67}$$

To see this, note that by taking the general ansatz $\sum_{n,p} a_{n,p}x^n y^p$ the recursion of Theorem 3.4.4 is recovered for the coefficients $a_{n,p}$.
It can easily be verified that the proposed rational function $G(x,y)$ of Equation (3.63) satisfies this differential equation. Hence, with the correct initial conditions it generates the numbers of order-consecutive partition sequences. □

Based on the above determination of $G(x,y)$ its coefficients $g_n(y)$, see Equation (3.62), are deduced in the following.

Proposition 3.4.5. *For a fixed $n\in\mathbb{N}$, the generating polynomial for the numbers of order-consecutive partition sequences $\mathrm{OCPS}^{(n+1)}(p+1)$ for $p\in\mathbb{N}$ is*

$$g_n(y)=\frac{(1+y)^{\frac{n-1}{2}}}{2}\left[\left(\sqrt{1+y}+\sqrt{y}\right)^{n+1}+\left(\sqrt{1+y}-\sqrt{y}\right)^{n+1}\right]. \tag{3.68}$$

It is emphasized here, that $g_n(y)$ is in fact a polynomial for each $n\in\mathbb{N}$ (see Remark 3.4.2.1).

Proof. The proof presented here uses relations of special functions named after Chebyshev. The author wants to thank Raimar Wulkenhaar for pointing out this elegant approach. Alternatively, the proposition can be shown using elementary methods via a rather tedious induction in n.
The generating polynomial $g_n(y)$ is the coefficient of x^n in the series $G(x,y)$. In order to extract this coefficient rewrite

$$G(x,y)=\frac{1-x}{1-2x(1+y)+x^2(1+y)}=\frac{1-x}{1-2\sqrt{1+y}\left(x\sqrt{1+y}\right)+\left(x\sqrt{1+y}\right)^2}\,. \tag{3.69}$$

This can be expanded into

$$G(x,y)=(1-x)\sum\nolimits_{n=0}^{\infty}\mathscr{U}_n\Big(\sqrt{1+y}\Big)(1+y)^{n/2}x^n\,, \tag{3.70}$$

where $\mathscr{L}_n(z)=\mathscr{C}_n^{(1)}(z)$ for $n\in\mathbb{N}$ are Chebyshev polynomials of the second kind, a special case of Gegenbauer polynomials C_n^λ [SW16, Čeb53]. These polynomials have explicit representations, which will be employed here. For $|z|\leqslant 1$, let $z=\cos\vartheta$, then

$$\mathscr{U}_n(\cos\vartheta)=\frac{\sin((n+1)\vartheta)}{\sin\vartheta}\,. \tag{3.71}$$

Using this as well as trigonometric relations, one calculates

$$\begin{aligned}
[x^n]G(x, z^2-1) &= z^n \mathscr{U}_n(t) - z^{n-1}\mathscr{U}_{n-1}(z) \\
&= \frac{\sin((n+1)\vartheta)}{\sin\vartheta}\cos^n\vartheta - \frac{\sin(n\vartheta)}{\sin\vartheta}\cos^{n-1}\vartheta \\
&= \left[\frac{\sin(n\vartheta)}{\sin\vartheta}\cos^2\vartheta + \cos\vartheta\cos(n\vartheta) - \frac{\sin(n\vartheta)}{\sin\vartheta}\right]\cos^{n-1}\vartheta \\
&= [\cos\vartheta\cos(n\vartheta) - \sin\vartheta\sin(n\vartheta)]\cos^{n-1}\vartheta \\
&= \cos((n+1)\vartheta)\cos^{n-1}\vartheta = z^{n-1}\mathscr{T}_{n+1}(z)\,, \qquad (3.72)
\end{aligned}$$

where $\{\mathscr{T}_n\}_{n\in\mathbb{N}}$ are the Chebyshev polynomials of first kind [Čeb53]. These, in turn, can be written as

$$\mathscr{T}_n(z) = \frac{1}{2}\left[\left(z+\sqrt{z^2-1}\right)^n + \left(z-\sqrt{z^2-1}\right)^n\right]. \qquad (3.73)$$

Passing back to $z^2-1=y$ one finds

$$g_n(y) = \frac{(1+y)^{\frac{n-1}{2}}}{2}\left[\left(\sqrt{1+y}+\sqrt{y}\right)^{n+1} + \left(\sqrt{1+y}-\sqrt{y}\right)^{n+1}\right]. \qquad (3.74)$$

Note that for $|z| \geqslant 1$, there are equivalent relations of the Chebyshev polynomials in terms of hyperbolic trigonometric functions giving the same result for g_n here. This concludes the proof. □

3.4.2 Proof of logarithmic concavity of OCPS

The combinatorial Theorem 3.4.6 below states that the numbers of order-consecutive partition sequences form logarithmically concave sequences. Thereby, it establishes that the f^*-vector of the Ehrhart polynomial associated to ψ-class intersection numbers of powers one is logarithmically concave.

Theorem 3.4.6. *For every $n \in \mathbb{N}^\times$ the sequence $(\mathrm{OCPS}^{(n)}(p))_{p\in[\![1,n]\!]}$ is logarithmically concave.*

Proof. In this proof, the results of the previous sections are used. According to Theorem 3.4.5 the generating function

$$g_n(y) = \frac{(1+y)^{\frac{n-1}{2}}}{2}\left[\left(\sqrt{1+y}+\sqrt{y}\right)^{n+1} + \left(\sqrt{1+y}-\sqrt{y}\right)^{n+1}\right] \qquad (3.75)$$

for a fixed $n \in \mathbb{N}$ generates the sequence of numbers $(\mathrm{OCPS}^{(n+1)}(p+1))_{p\in[\![1,n]\!]}$. Thus, to obtain the logarithmic concavity for these sequences, one needs to show for all $n \in \mathbb{N}$ that $g_n(y)$ has only *real* zeros. This implies by Theorem 3.4.1 about real rooted generating polynomials the assertion. In order to do this, note that due to the first

factor of its closed expression in the equation above g_n has a zero of order $\lceil (n-1)/2 \rceil$ at $y = -1$. The remaining $\lceil n/2 \rceil$ zeros are determined by

$$\left(\sqrt{1+y} + \sqrt{y}\right)^{n+1} + \left(\sqrt{1+y} - \sqrt{y}\right)^{n+1} = 0\,. \tag{3.76}$$

This is solved by $y_k \in \mathcal{Y}_0$, such that

$$\mathcal{Y}_0 \coloneqq \left\{ \frac{\tan^2\left(\frac{\pi}{2}\frac{2k+1}{n+1}\right)}{1+\tan^2\left(\frac{\pi}{2}\frac{2k+1}{n+1}\right)} \right\}_{k\in\mathbb{Z}}\,. \tag{3.77}$$

To see this note that Equation (3.76) is equivalent to

$$\sqrt{1+y_k} + \sqrt{y_k} = e^{\frac{\pi \mathrm{i}}{n+1} + \frac{2\pi \mathrm{i} k}{n+1}} \left(\sqrt{1+y_k} - \sqrt{y_k}\right)\,, \tag{3.78}$$

for all $k \in \mathbb{Z}$. Rearranging this yields

$$\sqrt{\frac{1+y_k}{y_k}} = \frac{\exp\left(\mathrm{i}\pi\frac{2k+1}{n+1}\right)-1}{\exp\left(\mathrm{i}\pi\frac{2k+1}{n+1}\right)+1} = \frac{\exp\left(\frac{\mathrm{i}\pi}{2}\frac{2k+1}{n+1}\right)-\exp\left(-\frac{\mathrm{i}\pi}{2}\frac{2k+1}{n+1}\right)}{\exp\left(\frac{\mathrm{i}\pi}{2}\frac{2k+1}{n+1}\right)+\exp\left(-\frac{\mathrm{i}\pi}{2}\frac{2k+1}{n+1}\right)} = \mathrm{i}\tan\left(\frac{\pi}{2}\frac{2k+1}{n+1}\right)\,. \tag{3.79}$$

In the last step Euler's formula $\exp(\mathrm{i}z) = \cos(z) + \mathrm{i}\sin(z)$ was employed to reduce the numerator and denominator to a sine and cosine, respectively, giving a tangent. Finally, solving for y_k gives the desired result

$$y_k = \frac{\left(\mathrm{i}\tan\left(\frac{\pi}{2}\frac{2k+1}{n+1}\right)\right)^2}{\left(\mathrm{i}\tan\left(\frac{\pi}{2}\frac{2k+1}{n+1}\right)\right)^2 - 1} = \frac{\tan^2\left(\frac{\pi}{2}\frac{2k+1}{n+1}\right)}{\tan^2\left(\frac{\pi}{2}\frac{2k+1}{n+1}\right)+1}\,. \tag{3.80}$$

By closely examining this expression one realizes that symmetries of the tangent translate to the identification $y_k = y_{-k-1}$. Thus, the number of different values in $\mathcal{Y}_0$ reduces by half, to be precise to $\lceil n/2 \rceil$.
This calculation gives the set of solutions $\mathcal{Y}_0$. Adding up the numbers of zeros and taking their order into account, one finds $\lceil n/2 \rceil + \lceil (n-1)/2 \rceil = n$. This verifies that all zeros of g_n are found, since $g_n(y)$ is a polynomial of degree n (see Remark 3.4.2.1), concluding the proof since

$$\{y \in \mathbb{C} \colon g_n(y) = 0\} = \{-1\} \cup \mathcal{Y}_0 \subset \mathbb{R}\,. \tag{3.81}$$

□

3.4.3 Abstract theory of Pólya frequency sequences

It is mentioned above that the result of logarithmic concavity of the number of order-consecutive partition sequences can also be inferred from abstract theory of Pólya frequency sequences, see Definition 3.4.2. In [Bre88], amongst others this family of

properties is investigated including its relation to other properties such as unimodularity and logarithmic concavity as well as different operations that preserve it.
Referring back to Definition 3.4.1, the defining equation of logarithmic concavity is quadratic in the elements of the sequence, see Equation (3.55). This suggests that logarithmic concavity is related to $\mathfrak{P}_2$, which is concerned with minors of the form

$$\det\begin{pmatrix} a_k & a_l \\ a_{k-1} & a_{l-1} \end{pmatrix}. \tag{3.82}$$

It turns out that one is able to show that the property $\mathfrak{P}_2$ is invariant under binomial transformations. To be precise, if $(q_k)_{k\in\mathbb{N}}$ is a finite $\mathfrak{P}_2$ sequence, then so is $(p_k)_{k\in\mathbb{N}}$ with $p_k = \sum_{l\geqslant 0}\binom{l}{k}q_l$ [Bre88]. Remark that this transformation does, in general, not preserve logarithmic concavity. A direct consequence of this fact is the following theorem of [Bre88].

Theorem 3.4.7 ([Bre88], Theorem 2.5.8)**.** *Let $P(x)$ be a polynomial of degree $d \in \mathbb{N}$. Then the expansion coefficients in terms of $\{\binom{x}{k}\}_{k\in[\![0,d]\!]}$ form a $\mathfrak{P}_2$ sequence if the expansion coefficients in terms of $\{\binom{x+d-k}{d}\}_{k\in[\![0,d]\!]}$ do.*

In terms of the notation of Section 3.1 of this thesis Brenti's result can be translated to the implication

$$h^* \text{ is a } \mathfrak{P}_2 \text{ sequence} \qquad \Longrightarrow \qquad f^* \text{ is a } \mathfrak{P}_2 \text{ sequence.} \tag{3.83}$$

In order to relate this result to logarithmic concavity, first note that from the definitions it is obvious that $\mathfrak{P}_2$ implies logarithmic concavity, see Definitions 3.4.1 and 3.4.2 and Equation (3.82). Additionally, due to its definition $\mathfrak{P}_2$ implies $\mathfrak{P}_1$.
The inverse relation, which is provided by [Bre88] where it is stated as Theorem 2.5.1, requires additionally that $a_k \geqslant 0$ and that there are no internal zeros. That these conditions are necessary can be seen by modifying the sequence $(1, 1, 1, 1, 0, \dots)$, which is both a logarithmically concave and $\mathfrak{P}_2$ sequence. If the third of these ones changes sign, then the sequence remains logarithmically concave as one can check, but calculating minors of order two of the associated matrix M one realizes

$$\det\begin{pmatrix} M_{2,3} & M_{2,5} \\ M_{3,3} & M_{3,5} \end{pmatrix} = 1\times(-1) - 1\times 1 = -2 < 0\,. \tag{3.84}$$

Similarly, if the two internal ones, that is the second and third, are changed to zero, then

$$\det\begin{pmatrix} M_{2,3} & M_{2,5} \\ M_{3,3} & M_{3,5} \end{pmatrix} = 0\times 0 - 1\times 1 = -1 < 0\,, \tag{3.85}$$

but logarithmic concavity remains valid. The following result of [Bre88] is a re-stating of Theorem 3.4.1 in the language of Pólya frequency sequences.

Theorem 3.4.8 ([Bre88], Theorem 2.5.1)**.** *An eventually vanishing sequence is a $\mathfrak{P}_2$ sequence if and only if it is a $\mathfrak{P}_1$ sequence that is logarithmically concave without internal zeros.*

Sketch of proof. In order to show that a $\mathfrak{P}_1$ sequence without internal zeros which obeys logarithmic concavity is, in fact, a $\mathfrak{P}_2$ sequence, one propagates the defining equation of logarithmic concavity

$$0 \leqslant a_{k+1}^2 - a_{k+2}a_k = \det\begin{pmatrix} a_{k+1} & a_{k+2} \\ a_k & a_{k+1} \end{pmatrix} \tag{3.86}$$

to arbitrary minors of order two. This can be done by repeatedly applying operations of the form

$$\begin{aligned} &a_{k+2}\det\begin{pmatrix} a_{k+2} & a_{k+3} \\ a_k & a_{k+1} \end{pmatrix} \\ &= a_{k+2}(a_{k+2}a_{k+1} - a_{k+3}a_k) \geqslant a_{k+2}\left(\frac{a_{k+3}a_{k+1}^2}{a_{k+2}} - a_{k+3}a_k\right) \\ &\qquad = a_{k+3}(a_{k+1}^2 - a_{k+2}a_k)\,, \end{aligned} \tag{3.87}$$

using logarithmic concavity as well as the fact that internal elements of the sequence do not vanish. □

As a consequence of the results in this section, the result of this work in Theorem 3.4.6 can be shown in a different fashion.

Alternative proof of Theorem 3.4.6. The theorem states the logarithmic concavity of the numbers $(\mathrm{OCPS}^{(n)}(p))_{p\in[\![1,n]\!]}$ for all $n \in \mathbb{N}^\times$. Using the theory of Pólya frequency sequences, one deduces this from the fact that they are the f^*-vectors of polynomials that have as h^*-vector the sequence of numbers of type $\{\binom{n}{p}\}_{p\in[\![0,n-1]\!]}$ for some n, due to Theorem 3.2.5 proved in Section 3.5.2. Note, that the latter is calculated from the explicit representation of the f^*-vector. This sequence of binomial coefficients is the prime example for $\mathfrak{P}$ sequences and is, in particular, $\mathfrak{P}_2$. Thus, by Theorem 3.4.7 also the f^*-vector, being the numbers of order-consecutive partition sequences, is, which proves the theorem. □

3.5 Proof of Theorems 3.2.4 and 3.2.5

Owing to the explicit determination of the Ehrhart polynomial associated to the intersection numbers described in Section 3.2, Theorems 3.2.4 and 3.2.5 explicitly calculate the f^* and h^*-vector of these polynomials.
Beyond their value by themselves, these are, in fact, interesting counting results as the vectors are the numbers of combinatorial objects which enjoy properties such as logarithmic concavity as shown in the previous section. Here the proofs of the theorems are presented starting with the determination of the f^*-vector followed the by h^*-vector, which is deduced from the former.

3.5.1 f^*-expansion

This section proves the combinatorial significance of the f^*-vector of the normalized Ehrhart polynomial $\mathcal{L}_n(g)$ in terms of order-consecutive partition sequences (see theorem below).

Theorem (see above, Theorem 3.2.4)**.** *The f^*-vector of the normalized Ehrhart polynomial $\mathcal{L}_n(g)$ associated to ψ-class intersection numbers of powers $(d_i)_i = (1,\dots,1) \in \mathbb{N}^n$ computes the number of order-consecutive partition sequences of $[\![1, n+1]\!]$ into $(k+1)$ parts, that is*

$$\mathcal{L}_n(g) = \sum_{k=0}^{n} f_k^* \binom{g-1}{k}, \quad \textit{with} \quad f_k^* = \mathrm{OCPS}^{(n+1)}(k+1) = \sum_{l=0}^{k} (-1)^{k+l} \binom{2l+n}{n} \binom{k}{l}. \tag{3.88}$$

Proof. Equipped with the definitions of the combinatorial objects provided by Section 3.3, the theorem can now be proved by applying the *Gregory-Newton interpolation formula* [Fra20]. The classical relation states that an integer-valued polynomial $p(t)$ in t of degree d can uniquely be expressed in terms of binomials via

$$p(t) = \sum_{r=0}^{d} a_r \binom{t}{r}, \qquad \text{with} \qquad a_r = \sum_{s=0}^{r} (-1)^{r-s} \binom{r}{s} p(s). \tag{3.89}$$

In the present context $\mathcal{L}_n(g+1) = \binom{2g+n}{n}$ takes the role of $p(g)$, and its coefficients are defined via

$$\binom{2g+n}{n} =: \sum_{k=0}^{n} a_k^{(n)} \binom{g}{k}. \tag{3.90}$$

By the interpolation formula the expansion coefficients are calculated as

$$a_k^{(n)} = \sum_{l=0}^{k} (-1)^{k-l} \binom{2l+n}{n} \binom{k}{l} = \sum_{l=0}^{k} (-1)^{k-l} \binom{n+2l}{2l} \binom{k}{l}, \tag{3.91}$$

using a symmetry of the binomial coefficients. This implies

$$\sum_{r=0}^{n} \left[\sum_{l=0}^{k} (-1)^{k-l} \binom{n+2l}{2l} \binom{k}{l} \right] \binom{g}{k} = \binom{2g+n}{n} = \mathcal{L}_n(g+1). \tag{3.92}$$

One obtains the assertion of the theorem by shifting $g \mapsto (g-1)$ and identifying $\mathrm{OCPS}^{(n+1)}(k+1)$ in the above due to Hwang-Mallow's theorem. □

For the first few sequences of these numbers enumerating order-consecutive partition sequences see Figure 3.3.3 in Section 3.3.

3.5.2 h^* expansion

After proving the combinatorial meaning of the f^*-coefficients, the same is aspired for the h^*-coefficients here. At first, the cases $\mathcal{L}_0$ and $\mathcal{L}_1$ are set aside and will be discussed separately further below, see Equation (3.99).

Theorem (see above, Theorem 3.2.5)**.** *Let $n \in \mathbb{N}$ with $n \geqslant 2$. The normalized Ehrhart polynomial $\mathcal{L}_n(g)$, which computes the intersection numbers of ψ-classes with powers $(d_i)_i = (1, \dots, 1) \in \mathbb{N}^n$, enjoys the h^*-expansion*

$$\mathcal{L}_n(g) = \sum_{k=0}^{n} h_k^* \binom{g+n-k}{n} \qquad \textit{with} \qquad h_k^* = \binom{n+1}{2(k-1)}. \tag{3.93}$$

Proof. The h^*-expansion is deduced from the f^*-expansion provided in Theorem 3.2.4 via their algebraic relation (3.12) of Section 3.1.1.
Referring to Theorem 3.2.2 the constant term of $\mathcal{L}_n(g)$ is given by $\prod_{k=1}^{n}(k-2)$ which vanishes as long as $n \geqslant 2$. This is the technical reason for the restriction of the theorem to $n \geqslant 2$. Then, by expanding the right-hand side of Equation (3.12) one finds

$$\sum_{k=0}^{n} f_k^* \frac{z^{k+1}}{(1-z)^{k-n}} = \sum_{k=0}^{n} \sum_{l=0}^{n-k} (-1)^l f_k^* \binom{n-k}{l} z^{k+l+1}. \tag{3.94}$$

Due to Theorem 3.2.4 providing the f^*-vector, the h^*-vector of $\mathcal{L}_n(g)$ is given by the coefficients of

$$H^*(z) = \sum_{k=0}^{n} h_k^* z^k = \sum_{k=0}^{n} \sum_{l=0}^{n-k} \sum_{m=0}^{k} (-1)^{l+k+m} \binom{n+2m}{2m} \binom{k}{m} \binom{n-k}{l} z^{k+l+1}, \tag{3.95}$$

which yields by reordering of the sums

$$\begin{aligned} h_{k+1}^* &= \sum_{l=0}^{k} \sum_{m=0}^{l} (-1)^{k-m} \binom{n+2m}{2m} \binom{l}{m} \binom{n-l}{k-l} \\ &= \sum_{m=0}^{k} (-1)^{k-m} \binom{n+2m}{2m} \sum_{l=0}^{k-m} \binom{l+m}{m} \binom{n-m-l}{k-m-l}. \end{aligned} \tag{3.96}$$

The inner sum can be treated by the Chu-Vandermonde relation in the transformed form $\sum_{K=0}^{N} \binom{X+K}{K} \binom{Y+N-K}{N-K} = \binom{X+Y+N+1}{N}$, with $N = k-m$, $X = m$ and $Y = n-k$. It can be deduced from the more-common version by the relation $(-1)^v \binom{u}{v} = \binom{-u+v-1}{v}$. Thus,

$$h_{k+1}^* = \sum_{m=0}^{k} (-1)^{k-m} \binom{n+2m}{2m} \binom{n+1}{k-m}. \tag{3.97}$$

Rewriting in terms of the Γ-function, one has

$$h_{k+1}^* = \frac{\Gamma(-n-1+2k)}{\Gamma(-n-1)\Gamma(2k+1)}. \tag{3.98}$$

This computes the desired result which can be seen using the reflection identity of the Γ-function $\frac{\Gamma(-u+v+1)}{\Gamma(-u)} = (-1)^{v+1} \frac{\Gamma(u+1)}{\Gamma(u-v)}$, with $u = n+1$ and $v = 2k-1$. □

At this point a remark on the restriction of the theorem above to $n \geqslant 2$ is appropriate. As mentioned in the proof, this is due to the fact that as long as $n \notin \{0,1\}$, the Ehrhart polynomial $\mathcal{L}_n(g)$ has no constant term. For the two exceptional cases

$$\mathcal{L}_0(g) = 1\,, \qquad \text{and} \qquad \mathcal{L}_1(g) = 2g - 1\,, \tag{3.99}$$

one calculates by hand

$$n = 0: \quad h_0^* = 1\,, \qquad \text{and} \qquad n = 1: \quad h_0^* = -1\,,\ h_1^* = 3\,. \tag{3.100}$$

This distinction of $n \in \{0,1\}$ can conceptually be motivated using the algebro-geometric origin of the Ehrhart polynomials. Recalling that L_n computes ψ-class intersection numbers on $\overline{\mathcal{M}}_{g,n+1}$, the Ehrhart polynomials indexed by $n \in \{0,1\}$ cover the realm of unstable topologies of positive Euler characteristic $\chi_{g,n}$. Here intersection numbers are classically not well-defined.

Properties Parallel to the f^*-vector, the h^*-vector has nice properties, which can directly be read off from the representation in Theorem 3.2.5 such as the fact that the sequences $\{(h_k^*)_{k\in[\![0,n]\!]}\}_{n\in\mathbb{N}}$ have no internal zeros and are logarithmically concave, see Section 3.4. Furthermore, it is notable that starting from $n = 2$ the h^*-vector is non-negative and h_0^* always vanishes.

To summarize, for the first few $\mathcal{L}_n$ the $\{h_k^*\}_{k\in[\![0,n]\!]}$ are given by

n \ i	0	1	2
1	1		
2	−1	3	
3	0	1	3

n \ i	0	1	2	3	4	5
4	0	1	6	1		
5	0	1	10	5	0	
6	0	1	15	15	1	0

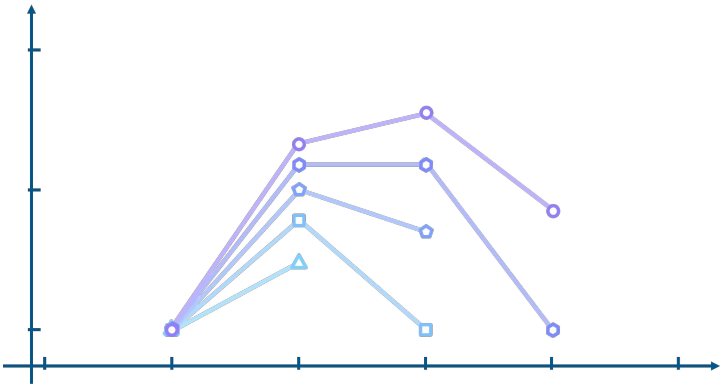

Figure 3.5.1: This plots the values of $(\log \binom{n+1}{2(p-1)})_{p\in[\![1,n]\!]}$ for $n \in [\![3,7]\!]$ (from light blue to purple and with increasing number of angles), which highlights the concave shape.

Conclusions

Since the scientific revolution science devoloped into the main catalizing force driving societal progress and fueling human curiosity. In that process the character of the sciences changed in many ways. As human knowledge diversified and refined advances become more and more driven by collaborative, interdisciplinary as well as gradual steps. The author of this thesis hopes to contribute to this quest within the respective fields of research the work is embedded in while realizing his own personal pursuit.

The moduli space of complex curves has been a classical algebro-geometric subject of studies for decades. The explicit calculations presented in this thesis in Chapter 2 quantify its relation to the Quartic Kontsevich Model as well as the related LSZ model, which are related to the quest of finding a non-trivial interacting quantum field theory that describes the world we live in. This is set to aid future research in a deeper understanding of the physical model especially towards its integrability.
These results are prepared in Chapters 1 and 2 with short introductions to the specific models as well as the theory of intersection numbers on the moduli space of curves. On that basis the explicit expressions are presented as examples for the universal structure of topological recursion, which governs, amongst many other mathematical and physical phenomena, the Quartic Kontsevich Model and the calculation of intersection numbers. This framework is used for calculating how intersection numbers are convoluted in the physical models for the first correlators. While the LSZ model, the complex counterpart to the Quartic Kontsevich Model being a hermitian matrix model, is governed by ordinary topological recursion, the latter requires a broader framework, called blobbed topological recursion. The additional structures, which are encoded in the loop equations constraining the model, are determined for the first correlators. Therefore, the graphical representation of the theory is exploited. That process not only yields new data which will provide valuable insight for future research, but it also unifies notation of various parts in the literature and fixes it for concrete applications.

Building on the structure of the moduli space, or more specifically that of its intersection numbers explained in the dedicated sections, a different perspective on intersection numbers is investigated in detail in Chapter 3. This work is rooted in a recently developed relation between the algebraic theory of intersection numbers with Ehrhart theory, which is a combinatorial approach to counting lattice points in polytopal objects. In the study of this relation, not only natural questions after the class of polytopal objects corresponding to these types of collections of intersection numbers and their properties are approached. But in significant structures within this relation also interesting phenomena are observed such as logarithmic concavity of special expansion data – a desirable property for sequences that can be found throughout a variety of different fields in mathematical research.

To be more precise, it is found that the expansion data of the Ehrhart theoretic objects corresponding to a subclass of intersection numbers has, in fact, a combinatorial interpretation in terms of a count of a specific kind of partitions. These partitions, which are called order-consecutive partition sequences, are counted by sequences of numbers that obey logarithmic concavity. Although different approaches to logarithmic concavity all provide different perspectives on it, it is generally a hard task to establish it in explicit examples. Here, the deduction is presented in two different ways either by computations via special functions and via abstract theory of Pólya frequency sequences, while the author is aware of an additional elementary proof via induction. This reflects the deep structure that this class of polytopal objects have, which ultimately ties back to that of the moduli space of curves.
Together with strong numerical evidence the origin in the moduli space suggests that using its recursive structure the property of having logarithmically concave expansion data generalizes from the class of intersection numbers investigated here. Using the framework of topological recursion a proof of this conjecture constitutes an interesting avenue for future research.

In this sense this thesis combines motivations, results and methods within the fields of mathematical physics, algebraic geometry and combinatorics to provide a mutual benefits to the respective questions that are approached. These include explicit computations for matrix models relating them to invariants of algebraic geometry as well as a combinatorial investigation of these invariants revealing interesting new properties.

Scientific Appendices

SCIENTIFIC APPENDICES A

Complementary definitions

A.1 Hermitian and self-adjoint operators

Let $\mathcal{H}$ be a Hilbert space and $\langle \cdot, \cdot \rangle$ the inner product on it. On $\mathcal{H}$ there acts a not necessarily bounded operator A with dense domain $\mathrm{Dom}(A) \subseteq \mathcal{H}$. Note here that A need not be defined on the entire $\mathcal{H}$. If this is however the case, then the notions of symmetric and self-adjoint operators, that are explained below, will coincide. As this can often be assumed, in many cases it is only referred to Hermitian operators. Note also that this is automatic if $\mathcal{H}$ is finite-dimensional, as then $\mathrm{Dom}(A) = \mathcal{H}$. [DS88]
The action of the operator A^* adjoint to A is prescribed by

$$\langle Ax, y \rangle = \langle x, A^* y \rangle \,, \tag{A.1}$$

for $y \in \mathrm{Dom}(A^*)$ for all $x \in \mathrm{Dom}(A)$.

Definition A.1.1. A is called *symmetric*, if $\mathrm{Dom}(A) \subset \mathrm{Dom}(A^*)$ and on $x \in \mathrm{Dom}(A)$ $Ax = A^* x$.

In that case

$$\langle Ax, y \rangle = \langle x, Ay \rangle \,, \qquad \text{for } x, y \in \mathrm{Dom}(A) \,. \tag{A.2}$$

In the physical context it is often desired to have a real pairing in order to define observables. This can be achieved if an additional requirement is considered.

Definition A.1.2. A is called *self-adjoint*, if it is symmetric and $\mathrm{Dom}(A) = \mathrm{Dom}(A^*)$.

For such operators A also A^* is symmetric and

$$\langle Ax, x \rangle = \langle x, Ax \rangle \in \mathbb{R} \,, \tag{A.3}$$

for $x \in \mathrm{Dom}(A)$.
In this thesis, such real symmetric, that is self-adjoint operators defined on a Hilbert space are called Hermitian.

A.2 Singular homology and cohomology

In this appendix *singular homology* and the associated *cohomology groups* of connected, smooth, complete varieties X over $\mathbb{C}$, or better its underlying manifold of $\mathbb{C}$-valued points $X(\mathbb{C})$, will be discussed following (classical) references such as [Har77, Hir66, Sch20, Zvo12].

Therefore, from singular simplices in the space X, that is continuous function from the standard n-simplex to X, in the familiar way, which follows from the abstract axiomatic definition, homology $H_*(X) \coloneqq H_*(X(\mathbb{C}), \mathbb{Q})$ and cohomology $H^*(X) \coloneqq H^*(X(\mathbb{C}), \mathbb{Q})$ are constructed, where $X(\mathbb{C})$ are the of $\mathbb{C}$-points of X equipped with the complex topology. An example for this is provided below. In cohomology one can introduce a natural product, the *cup-product*, which respects the grading by

$$H^p(X) \times H^q(X) \longrightarrow H^{p+q}(X)\,, \qquad (\alpha, \beta) \mapsto \alpha \smile \beta\,, \tag{A.4}$$

introducing a ring structure. Complementary to this, in homology one defines the *cap-product* by

$$H_p(X) \times H^q(X) \longrightarrow H_{p-q}(X)\,, \qquad (\alpha, \beta) \mapsto \alpha \frown \beta\,, \tag{A.5}$$

which is also referred to as partial integration. Note that these products are compatible satisfying $\sigma \frown (\alpha \smile \beta) = (\sigma \frown \alpha) \smile \beta$. Using these one can introduce a pairing by setting $p - q = 0$, that is

$$H_p(X) \times H^p(X) \longrightarrow H_0(X) \simeq \mathbb{Q}\,. \tag{A.6}$$

The isomorphism to $\mathbb{Q}$ is induced by the *degree map* of a zero-cycle $D = \sum_k a_k[x_k]$ defined by $\deg(D) \coloneqq \sum_k a_k$, reflecting that all points $x_k \in X(\mathbb{C})$ are homologically equivalent, since the considered spaces X are connected. This, in turn, induces the *Poincaré duality* via the pairing in cohomology by setting $p + q = 2d$

$$H^p(X) \times H^{2d-p}(X) \longrightarrow H^{2d}(X) \simeq \mathbb{Q}\,, \tag{A.7}$$

where the degree map is composed with multiplication with the pairing with the *fundamental class* $[X] \in H^0(X)$ of X,

$$\int_X \eta \coloneqq \deg([X] \frown \eta)\,, \tag{A.8}$$

to obtain the isomorphism to $\mathbb{Q}$ for $\eta \in H^{2d}(X)$. This suggests $H^p(X) \simeq H_{2d-p}(X)$ based on the assumption that X is also a compact complex mani- or orbifold, which is called Poincaré duality.

Remark A.2.0.1. The integral notation introduced here is used throughout this text recurrently and its convenience can even be increased by extending its applicability to classes beyond the top cohomological group H^{2d} on X. Therefore, one writes

$$\int_X \tilde{\eta} \coloneqq \begin{cases} \deg([X] \frown \tilde{\eta})\,, & \text{for } k = 2d\,, \\ 0\,, & \text{otherwise}\,, \end{cases} \tag{A.9}$$

provided a cohomological class $\tilde{\eta} \in H^k(X)$.

Due to this insight one can interpret the products in a geometrical manner. At least in the smooth setting, for $A, B \subset X$ closed oriented submanifolds of co-dimension cd_A and cd_B, which intersect transversely, one can form the product of their fundamental classes $[A] \in H^{\mathrm{cd}_A}(X)$, $[B] \in H^{\mathrm{cd}_B}(X)$ and calculate

$$[A] \smile [B] = [A \cap B] H^{\mathrm{cd}_A + \mathrm{cd}_B}(X)\,, \tag{A.10}$$

for a suitable orientation of the submanifold $A \cap B$. This gives rise to the term *intersection theory*.

Pushforward and pullback Relating connected, proper, smooth varieties (or orbifolds) X and Y of dimension d_X and d_Y by a morphism $m\colon X \to Y$ induces maps in homology and cohomology

$$m_*\colon H_k(X) \longrightarrow H_k(Y)\,, \qquad\qquad m^*\colon H^k(Y) \longrightarrow H^k(X)\,, \tag{A.11}$$

denoted *pushforward* and *pullback*, respectively. Note that the pullback is compatible with the cup-product and both are functorial for compositions of morphisms. Using Poincaré duality the pushforward can also be interpreted as a map on cohomology, i.e.

$$m_*\colon H^k(X) \longrightarrow H^{k+2(d_Y - d_X)}(Y)\,. \tag{A.12}$$

Composing both induced maps, it can be shown, that they satisfy

$$m_*(m^*\beta \smile \alpha) = \beta \smile m_*\alpha\,, \tag{A.13}$$

the *projection formula*.

Chern classes Of pivotal importance in this text are elements of cohomology called *Chern classes* $c_k(\mathcal{E}) \in H^{2k}(\mathcal{E})$ of a complex vector bundle $\mathcal{E}$. The sum $c(\mathcal{E}) = \sum_k c_k(\mathcal{E})$, the total Chern class, which collects all Chern classes, is uniquely determined by requiring naturality and additivity and setting $c = 1 + c_1$ for a complex line bundle. Naturality concerns behavior under pullback to a different base $m\colon B \to \tilde{B}$ and refers to

$$c_k(m^*\mathcal{E}) = m^* c_k(\mathcal{E})\,. \tag{A.14}$$

Additivity relates total Chern classes of vector bundles forming a short exact sequence

$$0 \to \mathcal{E}' \to \mathcal{E} \to \mathcal{E}'' \to 0 \qquad \Longrightarrow \qquad c(\mathcal{E}) = c(\mathcal{E}') \smile c(\mathcal{E}'')\,. \tag{A.15}$$

Using these axioms one can construct[†] the higher Chern classes from the total Chern class $c = 1 + c_1$ of a line bundle.

[†]Therefore, exhaust the vector bundle V by line bundles, introducing the Chern roots $\mathfrak{r}_i$ by Remark A.2.0.2. Then $c(V) = \prod_i (1 + \mathfrak{r}_i)$.

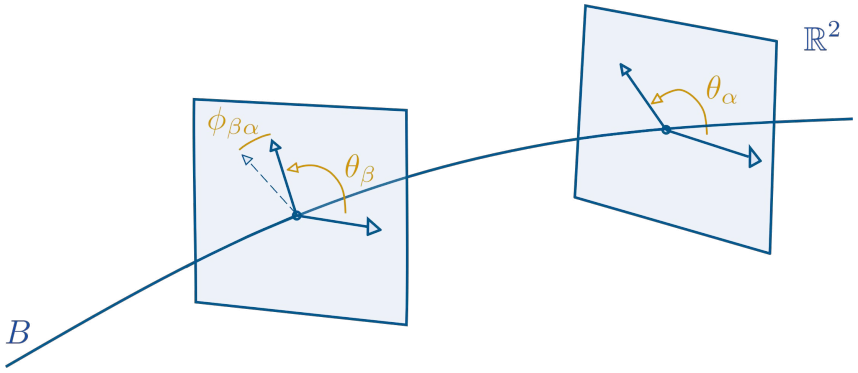

Figure A.2.1: This illustrates the construction for defining the Euler class

Remark A.2.0.2. Given a complex holomorphic line bundle over the base B, let s be a nonzero meromorphic section and $[Z]$, and $[P]$ the divisors associated to the set of zeroes and the set of poles. Then $[Z] - [P] \in H^2(B)$ is the *first Chern class* of the line bundle.

This is well posed, as it can be shown that this definition does not depend on the specific section s chosen.
Alternatively, in terms of de Rham cohomology with real coefficients the first Chern class of a line bundle $\mathcal{E}$ can instructively be defined as the *Euler class* $e(\mathcal{E}_\mathbb{R})$ of the associated oriented real vector bundle. This class can be constructed in local coordinates. Therefore, choose charts $\{U_k\}_k$ on the base that locally trivialize $\mathcal{E}$. As $\mathcal{E}$ is oriented one can choose polar coordinates $\{(r_k, \vartheta_k)\}$ over U_k, see Figure A.2.1. Denote the transition functions of the angles by $\phi_{kl} \colon U_k \cap U_l \to \mathbb{R}$. Using a smooth partition of unity $\{e_k\}_k$ associated to $\{U_k\}_k$ one can glue the one forms $\mathrm{d}\varphi_{nk}$ to a global two form

$$e|_{U_k} \coloneqq \mathrm{d}\gamma_k \ , \qquad \text{with } \gamma_k \coloneqq \frac{1}{2\pi} \sum\nolimits_n g_n \, \mathrm{d}\varphi_{nk} \ , \tag{A.16}$$

which is the Euler class of $\mathcal{E}$. This construction suggests the geometrical interpretation of the first Chern class. In the case one can define the curvature form, c_1 is directly proportional to it. This section is concluded with an example of the construction of homology and cohomology.

Example A.2.1. *In order to illustrate the construction of homology and cohomology in a short example the cellular homology and cohomology groups of a cell complex are constructed, following [Hat02]. Note that the notions of cellular and singular groups canonically agree for cell complexes. The latter generalizes the cellular setting by considering maps from simplices to the space and thus solve various issues with orientation as well as rigidity of the theory. This identification is induced by sending each simplex to its characteristic map $\Delta_n \to X$, which is used to define singular cohomology.*
For computing the cellular homology H_* over $\mathbb{Z}$ of the spaces X_1, X_2, and X_3 depicted in

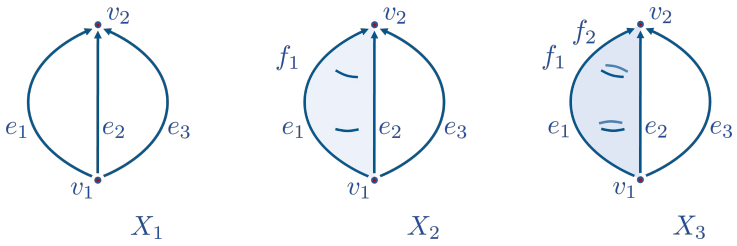

Figure A.2.2: This depicts the cell complexes X_1, X_2, and X_3 that are considered in Example A.2.1. The complex X_1 has two vertices and three edges, while X_2 and X_3 extend X_1 by a one and two faces, respectively.

Figure A.2.2, first the generators of the cell groups are listed.

	X_1	X_2	X_3
C_0	$\{v_1, v_2\}$	$\{v_1, v_2\}$	$\{v_1, v_2\}$
C_1	$\{e_1, e_2, e_3\}$	$\{e_1, e_2, e_3\}$	$\{e_1, e_2, e_3\}$
C_1	$-$	$\{f_1\}$	$\{f_1, f_2\}$

(A.17)

The boundary maps between these such that

$$\{0\} \xrightarrow{\partial_3} C_2 \xrightarrow{\partial_2} C_1 \xrightarrow{\partial_1} C_0 \xrightarrow{\partial_0} \{0\} \tag{A.18}$$

are given by

$$\partial_0(v_1) = \partial_0(v_2) = 0\,, \qquad \partial_1(e_1) = \partial_1(e_2) = v_2 - v_1\,, \qquad \partial_3(0) = 0\,, \tag{A.19}$$

equally for all spaces considered and for X_1, X_2, and X_3, respectively, and

$$\partial_2(0) = 0\,, \qquad \partial_2(f_1) = e_2 - e_1\,, \qquad \partial_2(f_1) = \partial_2(f_2) = e_2 - e_1\,. \tag{A.20}$$

Homology *Noting the crucial relation $\partial^2 = 0$, the homology groups are from here defined for all $p \in \mathbb{N}$ as*

$$H_p(X) = \ker(\partial_p)/\operatorname{im}(\partial_{p+1})\,. \tag{A.21}$$

The zeroth homology is, thus given by

$$H_0(X_i) = \operatorname{span}_{\mathbb{Q}}\{v_1, v_2\}/\operatorname{span}_{\mathbb{Q}}\{v_2 - v_1\} \simeq \mathbb{Q}\,, \tag{A.22}$$

for all spaces X_1, X_2, and X_3 identically. Note that in general the number of summands in H_0 counts the connected components of the space of which it is computed. The higher homologies similarly count the numbers of independent cycles of the respective dimension. For identifying the first homology, the kernel of ∂_1 and the image of ∂_2 need to be computed. Therefore,

$$\begin{aligned} \partial_1(e_1 - e_2) &= (v_2 - v_1) - (v_2 - v_1) = 0 \\ &= \partial_1(e_1 - e_3) = \partial_1(e_2 - e_3)\,. \end{aligned} \tag{A.23}$$

Thus, $\ker(\partial_1) = \mathrm{span}_{\mathbb{Q}}\{e_1 - e_2, e_1 - e_3\}$. *The map* ∂_2 *varies for the different spaces. Its image is given for* X_1 *by* $\{0\}$ *and for* X_2 *and* X_3 *by* $\mathrm{span}_{\mathbb{Q}}\{e_2 - e_1\}$. *The homology is therefore*

$$H_1(X_1) = \mathrm{span}_{\mathbb{Q}}\{e_1 - e_2, e_1 - e_3\} \simeq \mathbb{Q} \oplus \mathbb{Q}\,, \tag{A.24}$$

$$H_1(X_k) = \mathrm{span}_{\mathbb{Q}}\{e_1 - e_2, e_1 - e_3\}/\,\mathrm{span}_{\mathbb{Q}}\{e_2 - e_1\} = \mathrm{span}_{\mathbb{Q}}\{e_1 - e_3\} \simeq \mathbb{Q}\,, \tag{A.25}$$

for $k \in \{2, 3\}$. *This reflects the fact that while in* X_1 *there are still two independent one-cycles, the introduction of the face* f_1 *collapses the cycle* $e_1 - e_2$. *In order to compute the second homology the kernel of* ∂_2 *is given by elements* f *of* C_2 *such that* $\partial_2(f) = 0$. *This can only be achieved in* X_3, *because there*

$$\partial_2(f_1 - f_2) = (e_2 - e_1) - (e_2 - e_1) = 0\,. \tag{A.26}$$

Hence, for $k \in \{1, 2\}$

$$H_2(X_i) = \{0\} \qquad \textit{and} \qquad H_2(X_3) = \mathrm{span}_{\mathbb{Q}}\{f_1 - f_2\} \simeq \mathbb{Q}\,. \tag{A.27}$$

Cohomology *The associated cohomology is constructed by taking* $\hom(-, \mathbb{Q})$ *of the chain sequence obtaining the associated co-chain sequence formed by the* Δ_p *and the co-boundary maps* $\delta_p \colon \Delta_{p-1} \to \Delta_p$. *Analogously to homology* $\delta^2 = 0$ *yields the co-homology*

$$H^p = \ker(\delta_{p+1})/\,\mathrm{im}(\delta_p)\,. \tag{A.28}$$

The zeroth cohomology is equal for all spaces considered as their structure in dimension zero and one agree. The spaces Δ_0 *and* Δ_1 *are generated by dual generators* $\{v_0^*, v_1^*\}$ *and* $\{e_1^*, e_2^*, e_3^*\}$, *respectively. Using the relation*

$$\delta_p \alpha = \alpha \partial_p \tag{A.29}$$

between the boundary and co-boundary maps for some $\alpha \in \Delta_{k-1}$, *one computes*

$$\delta_1 v_1^*(e_1) = v_1^*(\partial_1 e_2) = v_1^*(v_2 - v_1) = -1\,, \tag{A.30}$$

which is the same as $\delta_1 v_1^*$ *applied to the other edges. Analogously, one finds*

$$\delta_1 v_2^*(e_1) = \delta_1 v_2^*(e_2) = \delta_1 v_2^*(e_3) = 1\,. \tag{A.31}$$

One realizes that $\delta_1 v_2^* = -\delta_1 v_1^*$, *and thus* $\ker(\delta_1) = \mathrm{span}_{\mathbb{Q}}\{v_1^* - v_2^*\}$ *and*

$$H^0(X_k) = \mathrm{span}_{\mathbb{Q}}\{v_1^* - v_2^*\} \simeq \mathbb{Q}\,, \tag{A.32}$$

for all $k \in [\![1, 3]\!]$. *The first cohomology is given by the quotient of the kernel of* δ_2 *and the image of* δ_1. *The former is for* X_1 *the entire space* Δ_3. *For* X_2 *and* X_3 *a general linear combination*

$$\delta_2(k_1 e_1^* + k_2 e_2^* + k_3 e_3^*)(f) = (k_1 e_1^* + k_2 e_2^* + k_3 e_3^*)(e_2 - e_1) \tag{A.33}$$

for $f \in \Delta_2$ vanishes only if $k_1 = k_2$. Hence, $\ker(\delta_2) = \operatorname{span}_{\mathbb{Q}}\{e_1^*, e_2^*, e_3^*\}/\operatorname{span}_{\mathbb{Q}}\{e_1^* - e_2^*\}$. *The map δ_1 is the same for all spaces that are considered here. Its image is given by* $\operatorname{im}(\delta_1) = \operatorname{span}_{\mathbb{Q}}\{\delta_1 v_1^*, \delta_1 v_1^*\}/\operatorname{span}_{\mathbb{Q}}\{\delta_1 v_1^* + \delta_1 v_1^*\}$. *This can be seen by computing $\delta_1 v_1^*(e)$ and $\delta_1 v_2^*(e)$ for $e \in C_1$ and realizing $\delta_1 v_1 = -\delta_1 v_2$. Consequently,*

$$H^1(X_1) = \operatorname{span}_{\mathbb{Q}}\{e_1^*, e_2^*, e_3^*\}/(\operatorname{span}_{\mathbb{Q}}\{\delta_1 v_1^*, \delta_1 v_1^*\}/\operatorname{span}_{\mathbb{Q}}\{\delta_1 v_1^* + \delta_1 v_1^*\}) \simeq \mathbb{Q}^2\,, \tag{A.34}$$

$$\begin{aligned} H^1(X_k) &= (\operatorname{span}_{\mathbb{Q}}\{e_1^*, e_2^*, e_3^*\}/\operatorname{span}_{\mathbb{Q}}\{e_1^* - e_2^*\})/(\operatorname{span}_{\mathbb{Q}}\{\delta_1 v_1^*, \delta_1 v_1^*\}/\operatorname{span}_{\mathbb{Q}}\{\delta_1 v_1^* + \delta_1 v_1^*\}) \\ &\simeq \mathbb{Q}\,, \end{aligned} \tag{A.35}$$

for $k \in \{2, 3\}$. This can be interpreted geometrically as well as algebraically as described in the below. Furthermore, in physics force fields that are in cohomology are of special significance and are called conservative. In general for a 2-simplex β bounded by the edges α_1, α_2, and α_3 one has $\delta\psi(\beta) = \psi(\alpha_1) + \psi(\alpha_2) - \psi(\alpha_3)$ for some $\psi \in \Delta_1$. This measures the deviation of ψ from being additive with respect to the paths $\alpha_1\alpha_2$ and α_3. Alternatively, consider the equation $\psi = \delta\varphi$ for some $\phi \in \Delta_0$. If such ϕ exists, then $\delta\psi = 0$ due to $\delta^2 = 0$. Thus, $\delta\psi$ can be regarded as a local obstruction to finding such ϕ. If this local obstruction vanishes, then (according to the definition of cohomology) $[\psi] \in H^1$ and, further, it vanishes if $\psi = \delta\phi$ has a solution. As the boundary map of this class vanishes due to its construction it can be seen as the global obstruction to solving $\psi = \delta\phi$.
At last the second cohomology is given. As $\Delta_3 = 0$ for all spaces considered the kernel of δ_3 is $\operatorname{span}_{\mathbb{Q}}\{f^* |\ f \in C_2\}$. *The image of δ_2 is* $\operatorname{span}_{\mathbb{Q}}\{\delta_2 e_1^*, \delta_2 e_2^*\}/\operatorname{span}_{\mathbb{Q}}\{\delta_2 e_1^* + \delta_2 e_2^*\}$ *for X_2 and X_3. This is due to the fact that e_3^* is in the kernel of δ_2 and that*

$$\delta_2 e_1^*(f) = -1\,, \qquad \textit{and} \qquad \delta_2 e_2^*(f) = 1\,, \tag{A.36}$$

for $f \in C_2$. Computing the cohomology yields

$$H_2(X_1) = \{0\}\,, \tag{A.37}$$

$$H_2(X_2) = \operatorname{span}_{\mathbb{Q}}\{f_1^*\}/(\operatorname{span}_{\mathbb{Q}}\{\delta_2 e_1^*, \delta_2 e_2^*\}/\operatorname{span}_{\mathbb{Q}}\{\delta_2 e_1^* + \delta_2 e_2^*\}) \simeq \{0\}\,, \tag{A.38}$$

$$H_2(X_3) = \operatorname{span}_{\mathbb{Q}}\{f_1^*, f_2^*\}/(\operatorname{span}_{\mathbb{Q}}\{\delta_2 e_1^*, \delta_2 e_2^*\}/\operatorname{span}_{\mathbb{Q}}\{\delta_2 e_1^* + \delta_2 e_2^*\}) \simeq \mathbb{Q}\,. \tag{A.39}$$

Concluding,

$$H_*(X_1) = \begin{cases} \mathbb{Q} \\ \mathbb{Q} \oplus \mathbb{Q} \\ \{0\} \end{cases}, \qquad H_*(X_2) = \begin{cases} \mathbb{Q} \\ \mathbb{Q} \\ \{0\} \end{cases}, \qquad H_*(X_3) = \begin{cases} \mathbb{Q} \\ \mathbb{Q} \\ \mathbb{Q} \end{cases}, \tag{A.40}$$

$$H^*(X_1) = \begin{cases} \mathbb{Q} \\ \mathbb{Q}^2 \\ \{0\} \end{cases}, \qquad H^*(X_2) = \begin{cases} \mathbb{Q} \\ \mathbb{Q} \\ \{0\} \end{cases}, \qquad H^*(X_3) = \begin{cases} \mathbb{Q} \\ \mathbb{Q} \\ \mathbb{Q} \end{cases}. \tag{A.41}$$

Calculations and data

B.1 Expansion data in topological recursion

In this appendix for different sets of expansion data related to the spectral curve of topological recursion, see Section 2.2, explicit relations as well as tables are provided.

B.1.1 Closed expression for $\mathfrak{z}_{\beta,p,l}$ in terms of $x_{\beta,n}$

In the following a closed expression for the expansion coefficients $\{\mathfrak{z}_{\beta,p,l}\}_{p,l\in\mathbb{N}}$ is provided. First, note that

$$\mathfrak{z}_{\beta,0,l} = \delta_{l=0} \tag{B.1}$$

trivially. Then, consider $\mathfrak{z}_{\beta,p,l}$ for $p = 1$ and write $\mathfrak{z}_{1,l} \coloneqq \mathfrak{z}_{\beta,1,l}$, dropping the index indicating the ramification point. By recalling the definition one computes

$$\begin{aligned}\zeta(z) = \sqrt{2}\sqrt{x(z)-x(a)} &= \sqrt{x_0}(z-\beta)\sqrt{1+\sum_{n=1}^{\infty}\frac{x_n}{(n+2)!}(z-\beta)^n} \\ &= \sqrt{x_0}(z-\beta)\sum_{k=0}^{\infty}\binom{1/2}{k}\left(\sum_{n=1}^{\infty}\frac{x_n}{(n+2)!}(z-\beta)^n\right)^k ,\end{aligned} \tag{B.2}$$

where the square-root was expanded. Assuming absolute convergence of the inner sum, one can iteratively use the Cauchy product formula for sums as

$$\left(\sum_{n=1}^{\infty}\frac{x_n}{(n+2)!}(z-\beta)^n\right)^k = \sum_{n=0}^{\infty}\left[\sum_{\substack{r_1+\cdots+r_k=n\\ r_i\geqslant 1}}\prod_{i=1}^{k}\frac{x_{r_i}}{(r_i+2)!}\right](z-\beta)^n . \tag{B.3}$$

Due to the fact that $r_i \geqslant 1$ the sum over k gives only non-zero contributions as long as $k \leqslant n$. Reordering one finds

$$\zeta(z) = \sqrt{x_0}\sum_{n=0}^{\infty}\left[\delta_{n=0}+\delta_{n\geqslant 1}\sum_{k=1}^{n}\binom{1/2}{k}\sum_{\substack{r_1+\cdots+r_k=n\\ r_i\geqslant 1}}\prod_{i=1}^{k}\frac{x_{r_i}}{(r_i+2)!}\right](z-\beta)^{n+1} , \tag{B.4}$$

that is

$$\mathfrak{z}_{\beta,1,l} = \begin{cases}\sqrt{x_{\beta,0}}\,, & l=1\,,\\ \sqrt{x_{\beta,0}}\sum_{k=1}^{l-1}\binom{1/2}{k}\sum_{\substack{r_1+\cdots+r_k=l-1\\ r_i\geqslant 1}}\prod_{i=1}^{k}\frac{x_{\beta,r_i}}{(r_i+2)!}\,, & l\geqslant 2\,.\end{cases} \tag{B.5}$$

In order to compute $\mathfrak{z}_{\beta,p,n}$ when $p \geqslant 1$ one raises the above expression to the p-th power and again expands using the Cauchy product formula according to

$$(\zeta(z))^p = \left(\sum_{n=0}^{\infty} \mathfrak{z}_{1,n+1}(z-\beta)^{n+1}\right)^p = \sum_{n=0}^{\infty}\left[\sum_{\substack{s_1+\cdots+s_p=n\\ s_j\geqslant 0}} \prod_{j=1}^{p} \mathfrak{z}_{1,s_j+1}\right](z-\beta)^{n+p}\,. \tag{B.6}$$

Thus,

$$\mathfrak{z}_{\beta,p,l} = \sum_{\substack{s_1+\cdots+s_p=l\\ s_j\geqslant 1}} \prod_{j=1}^{p} \mathfrak{z}_{\beta,1,s_j}\,, \qquad \text{for } l \geqslant p \geqslant 1\,. \tag{B.7}$$

For negative $p = -q < 0$ one needs to invert the power series (B.6). This yields the recursive formula

$$\mathfrak{z}_{\beta,-q,l} = \begin{cases} (\mathfrak{z}_{\beta,q,q})^{-1}\,, & l = -q\,,\\ -\frac{1}{\mathfrak{z}_{\beta,q,q}} \sum_{i=1}^{l+q} \mathfrak{z}_{\beta,q,i+q}\,\mathfrak{z}_{\beta,-q,l-i}\,, & l > -q\,. \end{cases} \tag{B.8}$$

All other coefficients $\mathfrak{z}_{\beta,p,l}$ vanish.

B.1.2 Closed expression for $y_{\beta,n}$ and $x_{\beta,n}$ in terms of $t_{\beta,k}$ and $\mathfrak{z}_{\beta,k,l}$

Reversely to the previous section, here a closed expressions for the moduli of the spectral curve $y_{\beta,n}$ and $x_{\beta,n}$ in terms of $t_{\beta,k}$ and $\mathfrak{z}_{\beta,k,l}$ are deduced. Therefore, consider first

$$y(z) = \sum_{k\geqslant 0} t_{\beta,k+2}(\zeta_a(z))^k = \sum_{k\geqslant 0} t_{\beta,k+2}\left[\sum_{l\geqslant k} \mathfrak{z}_{\beta,k,l}(z-\beta)^l\right]\,. \tag{B.9}$$

With the convention $\mathfrak{z}_{\beta,k,l} = 0$ if $l \geqslant k$ the sums can be exchanged as

$$\sum_{k\geqslant 0} t_{\beta,k+2}\left[\sum_{l\geqslant k} \mathfrak{z}_{\beta,k,l}(z-\beta)^l\right] = \sum_{l\geqslant 0}\sum_{k\geqslant 0} t_{\beta,k+2}\mathfrak{z}_{\beta,k,l}(z-\beta)^l = \sum_{l\geqslant 0}\left[\sum_{k\leqslant l} t_{\beta,k+2}\mathfrak{z}_{\beta,k,l}\right](z-\beta)^l\,. \tag{B.10}$$

Reading off yields

$$y_{\beta,n} = \begin{cases} t_{\beta,3}\mathfrak{z}_{\beta,1,1}\,, & n = 0\,,\\ (n+1)!\sum_{k\leqslant n+1} \frac{t_{\beta,k+2}}{t_{\beta,3}}\frac{\mathfrak{z}_{\beta,k,n+1}}{\mathfrak{z}_{\beta,1,1}}\,, & n \geqslant 1\,, \end{cases} \tag{B.11}$$

as $\mathfrak{z}_{\beta,k,1} = 0$ for $k \geqslant 1$ Secondly, similarly to the above, one can also express the $x_{\beta,n}$ in terms of the $\mathfrak{z}_{\beta,k,l}$. Note, however, that this is in practice not particularly helpful, as in

order to obtain the $\mathfrak{z}_{\beta,k,l}$ one already needs $x(z)$. Nevertheless, for the sake of symmetry consider using the product formula for infinite sums

$$x(z)-x(a)=(\zeta_a(z))^2=\left[\sum_{l\geqslant 1}\mathfrak{z}_{\beta,1,l}(z-\beta)^l\right]^2=\sum_{l\geqslant 1}\left[\sum_{r+s=l}\mathfrak{z}_{\beta,1,r}\mathfrak{z}_{\beta,1,s}\right](z-\beta)^l\,. \tag{B.12}$$

Therefore,

$$x_{\beta,n}=\begin{cases}\mathfrak{z}_{\beta,1,1}\mathfrak{z}_{\beta,1,1} & =2\mathfrak{z}_{\beta,2,2}\,, & n=0\,,\\ \frac{(n+2)!}{2}\sum\limits_{r+s=l+2}\frac{\mathfrak{z}_{\beta,1,r}\mathfrak{z}_{\beta,1,s}}{\mathfrak{z}_{\beta,1,s}\mathfrak{z}_{\beta,1,s}} & =\frac{(n+2)!}{2}\frac{\mathfrak{z}_{\beta,2,n+2}}{\mathfrak{z}_{\beta,2,2}}\,, & n\geqslant 1\,.\end{cases} \tag{B.13}$$

B.1.3 First $t_{\beta,k}$ and $\hat{t}_{\beta,k}$ in terms of $x_{\beta,n}$ and $y_{\beta,k}$

Using the algorithm described in Section 2.2.3, the Tables B.1.1 and B.1.2 give the first few coefficients $t_{\beta,k}$ and $\hat{t}_{\beta,k}$ in terms of $x_{\beta,n}$ and $y_{\beta,k}$.

k	$t_{\beta,k}$
3	$\frac{y_0}{x_0^{1/2}}$
4	$\frac{y_0}{6x_0}(-x_1+3y_1)$
5	$\frac{y_0}{72x_0^{3/2}}\big(-12x_1y_1+5x_1^2-3x_2+12y_2\big)$
6	$\frac{y_0}{1080x_0^2}\big(90x_1^2y_1-90x_1y_2-45x_2y_1-40x_1^3+45x_2x_1-9x_3+45y_3\big)$
7	$\frac{y_0}{17280x_0^{5/2}}\big(-840x_1^3y_1+840x_1^2y_2+840x_2x_1y_1-480x_1y_3-144x_3y_1-360x_2y_2+385x_1^4-630x_2x_1^2+168x_3x_1$ $+105x_2^2-24x_4+144y_4\big)$
8	$\frac{y_0}{136080x_0^3}\big(4200x_1^4y_1-4200x_1^3y_2-6300x_2x_1^2y_1+2520x_1^2y_3+1512x_3x_1y_1+3780x_2x_1y_2-945x_1y_4+945x_2^2y_1-189x_4y_1$ $-567x_3y_2-945x_2y_3-1960x_1^5+4200x_2x_1^3-1260x_3x_1^2-1575x_2^2x_1+252x_4x_1+378x_2x_3-27x_5+189y_5\big)$
9	$\frac{y_0}{43545600\sqrt{2}x_0^3}\big(-900900x_1^5y_1+900900x_1^4y_2+1801800x_2x_1^3y_1-554400x_1^3y_3-498960x_3x_1^2y_1-1247400x_2x_1^2y_2$ $+226800x_1^2y_4-623700x_2^2x_1y_1+90720x_4x_1y_1+272160x_3x_1y_2+453600x_2x_1y_3-60480x_1y_5$ $+136080x_2x_3y_1-8640x_5y_1+170100x_2^2y_2-30240x_4y_2-60480x_3y_3-75600x_2y_4+425425x_1^6$ $-1126125x_2x_1^4+360360x_3x_1^3+675675x_2^2x_1^2-83160x_4x_1^2-249480x_2x_3x_1+12960x_5x_1-51975x_2^3$ $+13608x_3^2+22680x_2x_4-1080x_6+8640y_6\big)$

Table B.1.1: This lists the first expansion coefficients or times $t_{\beta,k}$ of $y(z)$ at the ramification point $z=\beta$ expressed in terms of the parameters $x_n\equiv x_{\beta,n}$ and $y_n\equiv y_{\beta,n}$.

k	$\hat{t}_{\beta,k}$	
0	$\log \frac{1}{8\sqrt{2}t_{\beta,3}}$	$\log\left(\frac{\sqrt{x_0}}{8\sqrt{2}y_0}\right)$
1	$-\frac{3t_{\beta,5}}{t_{\beta,3}}$	$\frac{1}{24x_0}\left(12x_1y_1-5x_1^2+3x_2-12y_2\right)$
2	$\frac{9t_{\beta,5}^2}{2t_{\beta,3}^2}$ $-\frac{15t_{\beta,7}}{t_{\beta,3}}$	$\frac{1}{48x_0^2}\big(30x_1^3y_1+6x_1^2y_1^2-30x_1^2y_2-32x_2x_1y_1-12x_1y_1y_2+20x_1y_3+6x_3y_1+12x_2y_2-15x_1^4+25x_2x_1^2$ $-7x_3x_1-4x_2^2+x_4+6y_2^2-6y_4\big)$
3	$-\frac{9t_{\beta,5}^3}{t_{\beta,3}^3}$ $+\frac{15t_{\beta,7}t_{\beta,5}}{t_{\beta,3}^2}$ $-\frac{35t_{\beta,9}}{8t_{\beta,3}}$	$\frac{1}{5760x_0^3}\big(10800x_1^5y_1+1800x_1^4y_1^2-10800x_1^4y_2+240x_1^3y_1^3-22200x_2x_1^3y_1-3600x_1^3y_1y_2+7200x_1^3y_3$ $-1920x_2x_1^2y_1^2+1800x_1^2y_2^2+6360x_3x_1^2y_1-720x_1^2y_1^2y_2+15000x_2x_1^2y_2+1200x_1^2y_1y_3$ $-3000x_1^2y_4+360x_3x_1y_1^2+720x_1y_1y_2^2+7920x_2^2x_1y_1-1200x_4x_1y_1-3360x_3x_1y_2$ $+2640x_2x_1y_1y_2-6000x_2x_1y_3-1200x_1y_2y_3-360x_1y_1y_4+840x_1y_5-720x_2y_2^2$ $-1800x_2x_3y_1+120x_5y_1-1920x_2^2y_2+360x_4y_2-360x_3y_1y_2+840x_3y_3+960x_2y_4$ $-5525x_1^6+14775x_2x_1^4-4830x_3x_1^3-8900x_2^2x_1^2+1130x_4x_1^2+3360x_2x_3x_1-180x_5x_1$ $+660x_2^3-189x_3^2-300x_2x_4+15x_6-240y_2^3+360y_2y_4-120y_6\big)$

Table B.1.2: This lists the first expansion coefficients or dual times $\hat{t}_{\beta,k}$ of the Laplace transform of $\mathrm{d}y(z)$ at the ramification point $z=\beta$ in terms of the parameters $x_n \equiv x_{\beta,n}$ and $y_n \equiv y_{\beta,n}$. These coefficients are dual to the times $t_{\beta,k}$ (see Table B.1.1) and their relation is provided in the second column.

B.2 Data supporting conjecture about logarithmic concavity of all normalized Ehrhart polynomials associated to intersection numbers

In Section 3.2 it is conjectured that logarithmic concavity of the f^*- and h^*-vector of the Ehrhart polynomial associated to intersection numbers of the form

$$\int_{\overline{\mathcal{M}}_{g,n+1}} \frac{\psi_1^{d_1}\cdots\psi_n^{d_n}}{1-\psi_{n+1}} \tag{B.14}$$

holds true for general $(d_i)_i \in \mathbb{N}^n$ for $n \in \mathbb{N}$ beyond the case of $(1,\ldots,1)$, which is treated in Theorems 3.1.2 and 3.2.5 proved in Sections 3.5.1 and 3.5.2. Here, the numerical data supporting this conjecture is collected.
Table B.2.1 lists the f^*- and h^*-vectors of the Ehrhart polynomials corresponding to intersection numbers specified through $(d_i)_i \in T$ for

$$T = \{(2,1,1),\ (2,2,1),\ (2,2,2),\ (5,1,1),\ (5,5,1),\ (5,5,5)\}\,. \tag{B.15}$$

In the logarithmic plots in Figure B.2.1, one can observe the concave shape of the f^*- and h^*-vectors associated to these. In order to verify log-concavity numerically, that is if

$$a_i^2 \geqslant a_{i-1}a_{i+1}\,, \tag{B.16}$$

for $a \in \{f^*, h^*\}$, define

$$\gamma_i^{(a)} \coloneqq a_{i-1}a_{i+1}/a_i^2 \qquad \text{for } i \in \mathbb{N}\,. \tag{B.17}$$

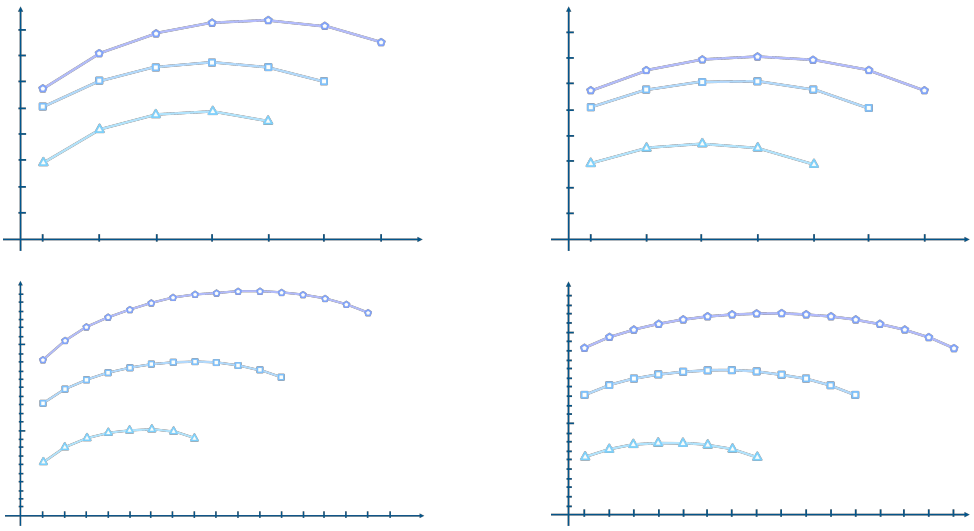

Figure B.2.1: This depicts the on the left the f^*-, i.e. $(f_i^*)_{i\in[\![0,i_*]\!]}$, and on the right the absolute value of the h^*-coefficients, i.e. $(h_i^*)_{i\in[\![0,i_*]\!]}$, associated to vectors d listed in Equation (B.15) on a logarithmic scale. The upper panels depict the coefficients corresponding to $(2,1,1)$ (light blue triangles), $(2,2,1)$ (dark blue squares), and $(2,2,2)$ (purple pentagon) – the lower panels those to $(5,1,1)$ (light blue triangles), $(5,5,1)$ (dark blue squares), and $(5,5,5)$ (purple pentagon).

This ratio is well-defined as long as $a_i \neq 0$. As the sequences considered here have no internal zeros, one can therefore calculate $\gamma_i^{(a)}$ as long as $i = 0, \ldots, i_*$, where i_* is the highest i such that $a_i \neq 0$. In order to define γ_i at the beyond the classical domain, set $\gamma_i^{(a)} = 0$ for negative i and if $i > i_*$.
If the sequence $(a_i)_{i\in\mathbb{N}}$ is log-concave, then $\gamma_i^{(a)} \leqslant 1$ for all $i \in \mathbb{N}$. See Table B.2.2 for a verification of this for all vectors $(d_i)_i \in T$.

d	f^*	h^*
$(2,1,1)$	$(810, 14850, 56808, 73872, 31104)$	$(810, -3240, 4860, -3240, 810)$
$(2,2,1)$	$(113400, 1043280, 3363768,$ $4984416, 3483648, 933120)$	$(113400, -567000, 1134000,$ $-1134000, 567000, -113400)$
$(2,2,2)$	$(567000, 12312000, 70201080,$ $175718160, 220838400, 137168640,$ $33592320)$	$(567000, -3402000, 8505000,$ $-11340000, 8505000, -3402000,$ $567000)$
$(5,1,1)$	$(1871100, 111068496,$ $1181882988, 4917186648,$ $10150059456, 11142852480,$ $6248171520, 1410877440)$	$(1871100, -13097700,$ $39293100, -65488500,$ $65488500, -39293100,$ $13097700, -1871100)$
$(5,5,1)$	$(12795710447520,$ $545672898650880,$ $7514237614403520,$ $51028612339985280,$ $203286770565167520,$ $517792118624161920,$ $880212456654612480,$ $1013640585479262720,$ $783018965116846080,$ $389338243761438720,$ $112781704966963200,$ $14481697524940800)$	$(12795710447520,$ $-140752814922720,$ $703764074613600,$ $-2111292223840800,$ $4222584447681600,$ $-5911618226754240,$ $5911618226754240,$ $-4222584447681600,$ $2111292223840800,$ $-703764074613600,$ $140752814922720,$ $-12795710447520)$
$(5,5,5)$	$(1935093730525956000,$ $313789090270595940000,$ $11148733407647723025600,$ $1709150243289446743632000,$ $145716123879093951746640000,$ $78484758523387438428360000,$ $28721323128140529351696000,$ $7459206460286291925984000,$ $1410242113281583903749120000,$ $196484612524240769351884800,$ $20191423809281138594611200,$ $1513318167083870460149760000,$ $80505819140360989468262400,$ $28821324615457982172364800,$ $6230468372491573552742400,$ $614848852548510547968000)$	$(1935093730525956000,$ $-29026405957889340000,$ $203184841705225380000,$ $-880467647389309980000,$ $2641402942167929940000,$ $-5811086472769445868000,$ $9685144121282409780000,$ $-12452328155934526860000,$ $12452328155934526860000,$ $-9685144121282409780000,$ $5811086472769445868000,$ $-2641402942167929940000,$ $880467647389309980000,$ $-203184841705225380000,$ $29026405957889340000,$ $-1935093730525956000)$

Table B.2.1: Here the f^*- and h^*-vectors associated to vectors $d \in T$ listed in Equation (B.15) are presented.

d	$\gamma^{(f^*)}$	$\gamma^{(h^*)}$
$(2,1,1)$	$(0, 0.2087, 0.0003, 7.9 \cdot 10^{-8}, 0)$	$(0, 0.375, 0.4444, 0.375, 0)$
$(2,2,1)$	$(0, 0.3505, 0.0001, 9.1 \cdot 10^{-9}, 4.5 \cdot 10^{-13}, 0)$	$(0., 0.4, 0.5, 0.5, 0.4, 0)$
$(2,2,2)$	$(0., 0.2626, 3.0 \cdot 10^{-4}, 7.0 \cdot 10^{-10}, 6.4 \cdot 10^{-15}, 3.7 \cdot 10^{-20}, 0)$	$(0., 0.4167, 0.5333, 0.5625, 0.5333, 0.4167, 0.)$
$(5,1,1)$	$(0, 0.1793, 6.1 \cdot 10^{-7}, 2.5 \cdot 10^{-13}, 2.6 \cdot 10^{-20}, 1.3 \cdot 10^{-27}, 4.5 \cdot 10^{-35}, 0)$	$(0, 0.4286, 0.5556, 0.6, 0.6, 0.5556, 0.4286, 0)$
$(5,5,1)$	$(0, 0.3229, 6.4 \cdot 10^{-9}, 1.1 \cdot 10^{-17}, 3.1 \cdot 10^{-27}, 2.2 \cdot 10^{-37}, 6.4 \cdot 10^{-48}, 1.1 \cdot 10^{-58}, 1.5 \cdot 10^{-69}, 2.5 \cdot 10^{-80}, 6.2 \cdot 10^{-91}, 0)$	$(0, 0.4545, 0.6, 0.6667, 0.7, 0.7143, 0.7143, 0.7, 0.6667, 0.6, 0.4545, 0)$
$(5,5,5)$	$(0., 0.2191, 3.3 \cdot 10^{-12}, 1.8 \cdot 10^{-24}, 7.2 \cdot 10^{-38}, 3.7 \cdot 10^{-52}, 3.6 \cdot 10^{-67}, 1.0 \cdot 10^{-82}, 1.1 \cdot 10^{-98}, 6.7 \cdot 10^{-115}, 2.5 \cdot 10^{-131}, 9.6 \cdot 10^{-148}, 4.7 \cdot 10^{-164}, 3.9 \cdot 10^{-180}, 6.6 \cdot 10^{-196}, 0)$	$(0, 0.4667, 0.6190, 0.6923, 0.7333, 0.7576, 0.7714, 0.7778, 0.7778, 0.7714, 0.7576, 0.7333, 0.6923, 0.6190, 0.4667, 0)$

Table B.2.2: Here the ratios $\gamma^{(f^*)}$ and $\gamma^{(h^*)}$ defined in Equation (B.17) associated to vectors $d \in T$ listed in Equation (B.15) are presented.

B.2.1 Numerical methods

The data presented in the previous section was generated and analyzed using the software `mathematica` [Wol20]. Therefore, an object was defined, that allows to extract the data of the f^*-vector, which is defined in Equation (3.6), from an arbitrary polynomial *poly* of given degree *n*. The source code is provided in the following.

```
(*Define the function fvecfunc, which takes a polynomial in g and an integer n
    returns its f^*-vector up to f^*_n)

Clear[fvecfunc, pol, fvec, i, k]
fvecfunc[poly_, n_] :=
    Module[
        {pol = poly,
        fvec = {poly /. g -> 1}},
        For[i = 1, i <= n, i++,
            fveclower = AppendTo[ fvec, (poly/.g->i+1) - Sum[Binomial[i, k] fvec[[k
                +1]], {k, 0, i-1}]]
        ];
        fvec
    ]
```

Formal Appendices

Formal Appendix D

Illustration note

The illustrations on the top of pages on which chapters start are inspired from various sources and figures.

Introduction:
https://www.researchgate.net/publication/303697433_Solitons/figures,
https://www.artspace.com/augustus-goertz/uncertainty-principle-from-the-quantum-series.

Chapter 1 - Field theories on non-commutative space:
https://events.theory.nipne.ro/gap/index.php/18-student-circle/math-resources/92-noncommutative-geometry-a-la-connes.

Chapter 2 - The moduli space of curves and topological recursion:
https://upload.wikimedia.org/wikipedia/commons/b/bf/A_triangulation_of_the_torus%2C_with_bounding_box_fixed.svg.

Conclusions:
https://en.wikipedia.org/wiki/Drawing_Hands

List of Figures

Bibliography

[AC96] Enrico Arbarello and Maurizio Cornalba, Combinatorial and Algebro-Geometric Cohomology Classes on the Moduli Spaces of Curves, Journal of Algebraic Geometry **5** (1996), no. 4, 705–749.

[ACG11] Enrico Arbarello, Maurizio Cornalba, and Phillip A. Griffiths, Geometry of Algebraic Curves: Volume II with a Contribution by Joseph Daniel Harris, Grundlehren Der Mathematischen Wissenschaften, vol. 268, Springer, Berlin, Heidelberg, 2011.

[AD21] Michael Aizenman and Hugo Duminil-Copin, Marginal Triviality of the Scaling Limits of Critical 4D Ising and $\lambda\phi_4^4$ Models, Annals of Mathematics **194** (2021), no. 1, 163–235.

[Afa22] Adam Afandi, An Ehrhart Theory For Tautological Intersection Numbers, no. arXiv:2209.14131.

[Aiz81] Michael Aizenman, Proof of the Triviality of ${{\ensuremath{\phi}}_{d}}^{4}$ Field Theory and Some Mean-Field Features of Ising Models for $d>4$, Physical Review Letters **47** (1981), no. 1, 1–4.

[Bac05] Francis Bacon, Advancement of Learning, 1605.

[Bac20] ———, Parasceve Ad Historiam Naturalem et Experimentalem, 1620.

[Bac23] ———, De Augmentis Scientiarum, 1623.

[Bac11] ———, The Works of Francis Bacon: Volume 1: Philosophical Works 1, Cambridge Library Collection - Philosophy, vol. 1, Cambridge University Press, Cambridge, 2011.

[BCEG23] Raphaël Belliard, Séverin Charbonnier, Bertrand Eynard, and Elba Garcia-Failde, Topological Recursion for Generalised Kontsevich Graphs and R-Spin Intersection Numbers, no. arXiv:2105.08035.

[BDGP17] Danilo Babusci, Giuseppe Dattoli, Katarzyna Gorska, and Karol Penson, Lacunary Generating Functions for the Laguerre Polynomials, Séminaire Lotharingien de Combinatoire **76** (2017).

[BH23] Johannes Branahl and Alexander Hock, Complete Solution of the LSZ Model via Topological Recursion, Communications in Mathematical Physics **401** (2023), no. 3, 2845–2899.

[BHW22] Johannes Branahl, Alexander Hock, and Raimar Wulkenhaar, Blobbed Topological Recursion of the Quartic Kontsevich Model I: Loop Equations and Conjectures, Communications in Mathematical Physics **393** (2022), no. 3, 1529–1582.

[BM18] Harald Bohr and Johannes Mollerup, Lærebog i Matematisk Analyse. 3dje Afsnit, Lærebog i Matematisk Analyse, Jul. Gjellerups Forlag, København, 1918.

[Boc32] Salomon Bochner, Vorlesungen über Fouriersche Integrale, Akadearticlehe Verlagsgesellschaft, Leipzig, 1932.

[Bou77] Joseph Boussinesq, Essai sur la théorie des eaux courantes, Impr. naionale, Paris, 1877.

[BR07] Matthias Beck and Sinai Robins, Computing the Continuous Discretely: Integer-Point Enumeration in Polyhedra, Undergraduate Texts in Mathematics, Springer New York, 2007.

[Brä14] Petter Brändén, Unimodality, Log-concavity, Real-rootedness and Beyond, Handbook of Enumerative Combinatorics (2014).

[Bra22] Johannes Branahl, The Recursive Structure of the Quartic Kontsevich Model, Ph.D. thesis, University of Münster, 2022.

[Bre88] Francesco Brenti, Unimodal, Log-Concave and Pólya Frequency Sequences in Combinatorics, Thesis, Massachusetts Institute of Technology, 1988.

[Bre94] ———, Log-Concave and Unimodal Sequences in Algebra, Combinatorics, and Geometry: An Update, Contemporary Mathematics **178** (1994), 71–89.

[Bre12] Felix Breuer, Ehrhart F*-Coefficients of Polytopal Complexes Are Non-Negative Integers, Electronic Journal of Combinatorics **19** (2012), 16.

[BS51] Stefan Bergman and Menahem M. Schiffer, Kernel Functions and Conformal Mapping, Compositio Mathematica **8** (1951), 205–249.

[BS58] Armand Borel and Jean-Pierre Serre, Le théorème de Riemann-Roch, Bulletin de la Société Mathématique de France **86** (1958), 97–136.

[BS17] Gaëtan Borot and Sergey Shadrin, Blobbed Topological Recursion: Properties and Applications, Mathematical Proceedings of the Cambridge Philosophical Society **162** (2017), no. 1, 39–87.

[BV04] Stephen Boyd and Lieven Vandenberghe, Convex Optimization, Cambridge University Press, Cambridge, March 2004.

[Čeb53] Pafnutij L'vovič Čebyšev, Théorie des mécanismes connus sous le nom de parallélogrammes, Imprimerie de l'Académie impériale des sciences, 1853.

[CEO06] Leonid Chekhov, Bertrand Eynard, and Nicolas Orantin, Free Energy Topological Expansion for the 2-Matrix Model, Journal of High Energy Physics **2006** (2006), no. 12, 053.

[Con94] Alain Connes, Noncommutative Geometry, Academic Press, Inc., San Diego, CA, 1994.

[Con95] ———, Noncommutative Geometry and Reality, Journal of Mathematical Physics **36** (1995), no. 11, 6194–6231.

[Con96] ———, Gravity Coupled with Matter and the Foundation of Non-Commutative Geometry, Communications in Mathematical Physics **182** (1996), no. 1, 155–176.

[COR85] Amiya K. Chakravarty, James B. Orlin, and Uriel G. Rothblum, Consecutive Optimizers for a Partitioning Problem with Applications to Optimal Inventory Groupings for Joint Replenishment, Operations Research **33** (1985), no. 4, 820–834.

[DGMR07] Margherita Disertori, Razvan Gurau, Jacques Magnen, and Vincent Rivasseau, Vanishing of Beta Function of Non-Commutative ϕ_4^4 Theory to All Orders, Physics Letters B **649** (2007), no. 1, 95–102.

[DM69] Pierre Deligne and David Mumford, The Irreducibility of the Space of Curves of given Genus, Publications Mathématiques de l'Institut des Hautes Études Scientifiques **36** (1969), no. 1, 75–109.

[Dra57] Stillman Drake, Discoveries and Opinions of Galileo, 1957.

[DS88] Nelson Dunford and Jacob T. Schwartz, Linear Operators, Part 1: General Theory, John Wiley & Sons, February 1988.

[EGBV89] Ricardo Estrada, José M. Gracia-Bondía, and Joseph C. Várilly, On Asymptotic Expansions of Twisted Products, Journal of Mathematical Physics **30** (1989), no. 12, 2789–2796.

[Ehr62] Eugène Ehrhart, Sur Les Polyèdres Rationnels Homothétiques à n Dimensions, Comptes Rendus Hebdomadaires des Séances de l'Académie des Sciences, Paris **254** (1962).

[Ehr74] ———, Polynômes arithmétiques et méthode des polyèdres en combinatoire, Institut de recherche mathématique avancée, 1974.

[EO07] B. Eynard and N. Orantin, Invariants of Algebraic Curves and Topological Expansion, Communications in Number Theory and Physics **1** (2007), no. 2, 347–452.

[Eyn11a] B. Eynard, Invariants of Spectral Curves and Intersection Theory of Moduli Spaces of Complex Curves, no. arXiv:1110.2949.

[Eyn11b] Bertrand Eynard, Intersection Numbers of Spectral Curves, no. arXiv:1104.0176.

[Eyn11c] ———, Recursion Between Mumford Volumes of Moduli Spaces, Annales Henri Poincaré **12** (2011), no. 8, 1431–1447.

[Eyn16] B. Eynard, Counting Surfaces, Progress in Mathematical Physics, vol. 70, Springer, 2016.

[Fan01] Barbara Fantechi, Stacks for Everybody, European Congress of Mathematics (Basel) (Carles Casacuberta, Rosa Maria Miró-Roig, Joan Verdera, and Sebastià Xambó-Descamps, eds.), Birkhäuser, 2001, pp. 349–359.

[FP11] Carel Faber and Rahul Pandharipande, Tautological and Non-Tautological Cohomology of the Moduli Space of Curves, no. arXiv:1101.5489.

[Fra20] Duncan C. Fraser, Newton's Interpolation Formulas, Journal of the Institute of Actuaries (1886-1994) **52** (1920), no. 2, 117–135.

[Gal23] Galileo di Vincenzo Bonaiuti de' Galilei, Il Saggiatore, Nel Quale Con Bilancia Esquisita e Giusta Si Ponderano Le Cose Contenute Nella Libra Astronomica e Filosofica Di Lotario Sarsi Sigensano, Rome, 1623.

[GBV88] José M. Gracia-Bondía and Joseph C. Várilly, Algebras of Distributions Suitable for Phase-space Quantum Mechanics. I, Journal of Mathematical Physics **29** (1988), no. 4, 869–879.

[GHW19] Harald Grosse, Alexander Hock, and Raimar Wulkenhaar, Solution of All Quartic Matrix Models, no. arXiv:1906.04600.

[GJ87] James Glimm and Arthur Jaffe, Quantum Physics, Springer, New York, NY, 1987.

[GW05] Harald Grosse and Raimar Wulkenhaar, Renormalisation of Φ4-Theory on Non-Commutative$$\mathbb{R}^{4}$$to All Orders, Letters in Mathematical Physics **71** (2005), no. 1, 13–26.

[Har77] Robin Hartshorne, Algebraic Geometry, Springer New York, 1977.

[Hat02] Allen Hatcher, Algebraic Topology, Cambridge University Press, 2002.

[HB21] John Harnad and Ferenc Balogh, Tau Functions and Their Applications, Cambridge Monographs on Mathematical Physics, Cambridge University Press, Cambridge, 2021.

[Hir66] Friedrich Hirzebruch, Topological Methods in Algebraic Geometry, Grundlehren Der Mathematischen Wissenschaften, Springer, Berlin, Heidelberg, 1966.

[Hir71] Ryogo Hirota, Exact Solution of the Korteweg—de Vries Equation for Multiple Collisions of Solitons, Physical Review Letters **27** (1971), no. 18, 1192–1194.

[HK12] June Huh and Eric Katz, Log-Concavity of Characteristic Polynomials and the Bergman Fan of Matroids, Mathematische Annalen **354** (2012), no. 3, 1103–1116.

[HM95] Frank K. Hwang and Colin L. Mallows, Enumerating Nested and Consecutive Partitions, Journal of Combinatorial Theory, Series A **70** (1995), no. 2, 323–333.

[HM98] Joe Harris and Ian Morrison, Moduli of Curves, Graduate Texts in Mathematics, vol. 187, Springer-Verlag, New York, 1998.

[Hoc23a] Alexander Hock, Laplace Transform of the $x-Y$ Symplectic Transformation Formula in Topological Recursion, Communications in Number Theory and Physics **17** (2023), no. 4, 821–845.

[Hoc23b] ———, A Simple Formula for the X-y Symplectic Transformation in Topological Recursion, Journal of Geometry and Physics **194** (2023), 105027.

[Huh12] June Huh, Milnor Numbers of Projective Hypersurfaces and the Chromatic Polynomial of Graphs, Journal of the American Mathematical Society **25** (2012), no. 3, 907–927.

[Huh15] ———, H-Vectors of Matroids and Logarithmic Concavity, Advances in Mathematics **270** (2015), 49–59.

[Hur93] Adolf Hurwitz, Ueber Algebraische Gebilde Mit Eindeutigen Transformationen in Sich, Mathematische Annalen **41** (1893), 403–442.

[HW21] Alexander Hock and Raimar Wulkenhaar, Blobbed Topological Recursion of the Quartic Kontsevich Model II: Genus=0, no. arXiv:2103.13271.

[HW23] ———, Blobbed Topological Recursion from Extended Loop Equations, no. arXiv:2301.04068.

[Kac49] Mark Kac, On Distributions of Certain Wiener Functionals, Transactions of the American Mathematical Society **65** (1949), no. 1, 1–13.

[Kac90] Victor G. Kac, Infinite-Dimensional Lie Algebras, 3 ed., Cambridge University Press, Cambridge, 1990.

[KDV95] Diederik Johannes Korteweg and Gustav De Vries, On the Change of Form of Long Waves Advancing in a Rectangular Canal, and on a New Type of Long Stationary Waves, The London, Edinburgh, and Dublin Philosophical Magazine and Journal of Science **39** (1895), no. 240, 422–443.

[KK66] Takako Kōmura and Yukio Kōmura, Über die Einbettung der nuklearen Räume in (s)A, Mathematische Annalen **162** (1966), no. 2, 284–288.

[Knu83] Finn F. Knudsen, The Projectivity of the Moduli Space of Stable Curves, II: The Stacks Mgn, Mathematica Scandinavica **52** (1983), 161–199.

[Kon92] Maxim Kontsevich, Intersection Theory on the Moduli Space of Curves and the Matrix Airy Function, Communications in Mathematical Physics **147** (1992), no. 1, 1–23.

[KP70] Boris B. Kadomtsev and Vladimir I. Petviashvili, On the Stability of Waves in Weakly Dispersive Media, Soviet Physics Doklady **15** (1970), 539–541.

[Kre99] Andrew Kresch, Cycle Groups for Artin Stacks, Inventiones mathematicae **138** (1999), no. 3, 495–536.

[Kün23] Hermann Künneth, Über die Bettischen Zahlen einer Produktmannigfaltigkeit, Mathematische Annalen **90** (1923), no. 1, 65–85.

[Lan82] Serge Lang, Introduction to Algebraic and Abelian Functions, Graduate Texts in Mathematics, vol. 89, Springer, New York, NY, 1982.

[LS02] Edwin Langmann and Richard J. Szabo, Duality in Scalar Field Theory on Noncommutative Phase Spaces, Physics Letters B **533** (2002), no. 1, 168–177.

[LSZ04] Edwin Langmann, Richard J. Szabo, and Konstantin Zarembo, Exact Solution of Quantum Field Theory on Noncommutative Phase Spaces, Journal of High Energy Physics **2004** (2004), no. 01, 017.

[LX09] Kefeng Liu and Hao Xu, A Proof of the Faber Intersection Number Conjecture, Journal of Differential Geometry **83** (2009), no. 2, 313–335.

[Min59] Robert Adol'fovich Minlos, Generalized Random Processes and Their Extension in Measure, GIFML **8** (1959), 497–518.

[Mir07a] Maryam Mirzakhani, Simple Geodesics and Weil-Petersson Volumes of Moduli Spaces of Bordered Riemann Surfaces, Inventiones mathematicae **167** (2007), no. 1, 179–222.

[Mir07b] ———, Weil-Petersson Volumes and Intersection Theory on the Moduli Space of Curves, Journal of the American Mathematical Society **20** (2007), no. 1, 1–23.

[MS06] Motohico Mulase and Brad Safnuk, Mirzakhani's Recursion Relations, Virasoro Constraints and the KdV Hierarchy, no. arXiv:math/0601194.

[Mum83] David Mumford, Towards an Enumerative Geometry of the Moduli Space of Curves, Arithmetic and Geometry: Papers Dedicated to I.R. Shafarevich on the Occasion of His Sixtieth Birthday. Volume II: Geometry (Michael Artin and John Tate, eds.), Birkhäuser, Boston, MA, 1983, pp. 271–328.

[OS73] Konrad Osterwalder and Robert Schrader, Axioms for Euclidean Green's Functions, Communications in Mathematical Physics **31** (1973), no. 2, 83–112.

[OS75] ———, Axioms for Euclidean Green's Functions II, Communications in Mathematical Physics **42** (1975), no. 3, 281–305.

[Pan16] Rahul Pandharipande, A Calculus for the Moduli Space of Curves, no. arXiv:1603.05151.

[Pes18] Michael E. Peskin, An Introduction To Quantum Field Theory, CRC Press, Boca Raton, January 2018.

[Pic99] Georg A. Pick, Geometrisches zur Zahlenlehre (Geometric resuts on number theory), Sitzungsberichte des deutschen naturwissenschaftlich-medizinischen Vereines für Böhmen „Lotos“ in Prag (Prag), 1899, pp. 311–319.

[Pól21] Georg Pólya, Über eine Aufgabe der Wahrscheinlichkeitsrechnung betreffend die Irrfahrt im Straßennetz, Mathematische Annalen **84** (1921), no. 1, 149–160.

[Rie57] Bernhard Riemann, Theorie der Abel'schen Functionen., Journal für die reine und angewandte Mathematik **54** (1857), 115–155.

[Rie68] ———, Über die Hypothesen, welche der Geometrie zu Grunde liegen. (Mitgetheilt durch R. Dedekind), Abhandlungen der Königlichen Gesellschaft der Wissenschaften in Göttingen **13** (1868), 133–152.

[Riv07] Vincent Rivasseau, Non-Commutative Renormalization, Quantum Spaces: Poincaré Seminar 2007 (Vincent Rivasseau and Bertrand Duplantier, eds.), Birkhäuser, Basel, 2007, pp. 19–107.

[Sch59a] Samuel Schechter, On the Inversion of Certain Matrices, Mathematical Tables and Other Aids to Computation **13** (1959), no. 66, 73–77.

[Sch59b] Julian Schwinger, Euclidean Quantum Electrodynamics, Physical Review **115** (1959), no. 3, 721–731.

[Sch13] Matthew D. Schwartz, Quantum Field Theory and the Standard Model, Cambridge University Press, Cambridge, 2013.

[Sch20] Johannes Schmitt, The Moduli Space of Curves, https://www.math.uni-bonn.de/people/schmitt/moduli_of_curves, 2020.

[Spe83] T. P. Speed, Cumulants and Partition Lattices, Australian Journal of Statistics **25** (1983), no. 2, 378–388.

[ST20] Leonardo Santilli and Miguel Tierz, Complex (Super)-Matrix Models with External Sources and q-Ensembles of Chern–Simons and ABJ(M) Type, Journal of Physics A: Mathematical and Theoretical **53** (2020), no. 42, 425201.

[Sta80] Richard P. Stanley, Decompositions of Rational Convex Polytopes, Annals of Discrete Mathematics (J. Srivastava, ed.), Combinatorial Mathematics, Optimal Designs and Their Applications, vol. 6, Elsevier, January 1980, pp. 333–342.

[Sta89] ———, Log-Concave and Unimodal Sequences in Algebra, Combinatorics, and Geometry, Annals of the New York Academy of Sciences **576** (1989), no. 1, 500–535.

[Sta97] ———, Enumerative Combinatorics, Cambridge Studies in Advanced Mathematics, vol. 1, Cambridge University Press, Cambridge, 1997.

[Sta99] ———, Enumerative Combinatorics, Cambridge Studies in Advanced Mathematics, vol. 2, Cambridge University Press, Cambridge, 1999.

[Sti30] James Stirling, Methodus differentialis, 1730.

[SW85] Graeme Segal and George Wilson, Loop Groups and Equations of KdV Type, Publications Mathématiques de l'Institut des Hautes Études Scientifiques **61** (1985), no. 1, 5–65.

[SW89] Raymond F. Streater and Arthur S. Wightman, PCT, Spin and Statistics, and All That, Princeton University Press, 1989.

[SW16] Elias M. Stein and Guido Weiss, Introduction to Fourier Analysis on Euclidean Spaces, Princeton University Press, June 2016.

[SW23] Jörg Schürmann and Raimar Wulkenhaar, An Algebraic Approach to a Quartic Analogue of the Kontsevich Model, Mathematical Proceedings of the Cambridge Philosophical Society **174** (2023), no. 3, 471–495.

[Sza03] Richard J. Szabo, Quantum Field Theory on Noncommutative Spaces, Physics Reports **378** (2003), no. 4, 207–299.

[tH74] Gerard 't Hooft, A Planar Diagram Theory for Strong Interactions, Nuclear Physics B **72** (1974), no. 3, 461–473.

[Tod67] Morikazu Toda, Vibration of a Chain with Nonlinear Interaction, Journal of the Physical Society of Japan **22** (1967), no. 2, 431–436.

[Vis89] Angelo Vistoli, Intersection Theory on Algebraic Stacks and on Their Moduli Spaces, Inventiones mathematicae **97** (1989), no. 3, 613–670.

[Vog00] Dietmar Vogt, Lectures on Fréchet Spaces, https://www2.math.uni-wuppertal.de/~vogt/vorlesungen/fs.pdf (2000).

[Wei] Eric W. Weisstein, Pólya's Random Walk Constants, https://mathworld.wolfram.com/.

[Wey11] Hermann Weyl, Ueber die asymptotische Verteilung der Eigenwerte, Nachrichten von der Gesellschaft der Wissenschaften zu Göttingen, Mathematisch-Physikalische Klasse **1911** (1911), 110–117.

[Wey13] ———, Die Idee der Riemannschen Fläche, B.G. Teubner, Leipzig, 1913.

[Wig56] Arthur S. Wightman, Quantum Field Theory in Terms of Vacuum Expectation Values, Physical Review **101** (1956), no. 2, 860–866.

[Wit90] Edward Witten, Two-Dimensional Gravity and Intersection Theory on Moduli Space, Surveys in Differential Geometry **1** (1990), no. 1, 243–310.

[Wit92] ———, On the Kontsevich Model and Other Models of Two Dimensional Gravity, Differential Geometric Methods in Theoretical Physics (Sultan Catto and Alvany Rocha, eds.), January 1992, pp. 176–216.

[Wol11] Scott A. Wolpert, Lectures and Notes: Mirzakhani's Volume Recursion and Approach for the Witten-Kontsevich Theorem on Moduli Tautological Intersection Numbers, no. arXiv:1108.0174.

[Wol20] Wolfram Research Inc., Mathematica, Version 12.3, 2020.

[Wul06] Raimar Wulkenhaar, Field Theories on Deformed Spaces, Journal of Geometry and Physics **56** (2006), no. 1, 108–141.

[Wul19] ———, Quantum Field Theory on Noncommutative Spaces, Advances in Noncommutative Geometry: On the Occasion of Alain Connes' 70th Birthday (Ali Chamseddine, Caterina Consani, Nigel Higson, Masoud Khalkhali, Henri Moscovici, and Guoliang Yu, eds.), Springer International Publishing, Cham, 2019, pp. 607–690.

[Zie95] Günter M. Ziegler, Lectures on Polytopes, Graduate Texts in Mathematics, vol. 152, Springer, New York, NY, 1995.

[Zvo12] Dimitri Zvonkine, An Introduction to Moduli Spaces of Curves and Their Intersection Theory, IRMA Lectures in Mathematics and Theoretical Physics (Athanase Papadopoulos, ed.), vol. 17, EMS Press, 1 ed., June 2012, pp. 667–716.